DOE/NV/0003590-60

# Tonopah Test Range Air Monitoring: CY2019 Meteorological, Radiological, and Wind Transported Particulate Observations

Prepared by

Jenny Chapman, George Nikolich, John Goreham, Greg McCurdy,
Julianne J. Miller, and Austin Chapman

Submitted to

U.S. Department of Energy
Environmental Management Nevada Program
Las Vegas, Nevada

March 2021

**Publication No. 45296**

***Nevada System of Higher Education***

DOE/NV/0003590-60

# Tonopah Test Range Air Monitoring: CY2019 Meteorological, Radiological, and Wind Transported Particulate Observations

Prepared by

Jenny Chapman, George Nikolich, John Goreham, Greg McCurdy,
Julianne J. Miller, and Austin Chapman

Desert Research Institute
Nevada System of Higher Education

Publication No. 45296

Submitted to

U.S. Department of Energy
Environmental Management Nevada Program
Las Vegas, Nevada

March 2021

The work upon which this report is based was supported by the U.S. Department of Energy under Contract #DE-NA0003590. Approved for public release; further dissemination unlimited.

**THIS PAGE INTENTIONALLY LEFT BLANK**

## EXECUTIVE SUMMARY

In 1963, the U.S. Department of Energy (DOE) (formerly the Atomic Energy Commission [AEC]), implemented Operation Roller Coaster on the Tonopah Test Range (TTR) and an adjacent area of the Nevada Test and Training Range (NTTR) (formerly the Nellis Air Force Range). This operation resulted in radionuclide-contaminated soils at the Double Tracks site and Clean Slate I, II, and III sites. This report documents observations made during ongoing monitoring of radiological, meteorological, and dust conditions at stations installed adjacent to the Clean Slate sites and at the TTR Sandia National Laboratories (SNL) Range Operations Center (ROC). The main objectives of the monitoring effort are to support the DOE Environmental Management Nevada Program (EM NV) in the safe remediation of the environmental legacy of nuclear device development and testing by determining if wind blowing across the Clean Slate sites is transporting particles of radionuclide-contaminated soil beyond the physical and administrative boundaries of the sites, and providing information for designing long-term monitoring of the sites.

The monitoring program in 2019 included five stations. Station 400, located within TTR Area 3 and near the ROC, monitors conditions near the local workforce center. Stations 401 and 403 are located on the northern and southeastern perimeter fence lines, respectively, of the Clean Slate III site. Stations 404 and 405 are along the northern and eastern boundary fence, respectively, at Clean Slate II. The stations are generally downwind of the contaminated areas during either northwesterly or southerly winds, which are the predominant wind directions.

The stations—which are similar in design to the Community Environmental Monitoring Program (CEMP) stations operating at locations surrounding the Nevada National Security Site and TTR—include meteorological instruments and continuous-flow, low-volume air samplers. Three pressurized ionization chambers for measuring gamma energy are in use at Stations 400, 401, and 403. Saltation sensors and saltation traps are deployed at the stations adjacent to the Clean Slate sites. Detailed meteorological data are recorded on data loggers, with periodic uploads via a satellite system to the Western Regional Climate Center (WRCC) at Desert Research Institute (DRI), to monitor instrument and site conditions. Air filter samples are collected every two weeks and the deposits in the saltation traps are collected when a sufficient sample mass for analysis has accumulated (generally a six- to eight-month interval).

Monitoring at TTR in calendar year (CY) 2019 provided surveillance of ambient conditions and of ground disturbance associated with remediation activities at Clean Slate III and revegetation activities at both Clean Slate II and III. Ambient conditions prevailed at Station 400 throughout the year, and for the first nine months at the Clean Slate II Stations 404 and 405. Data collected from the first of the year until the end of August at Stations 401 and 403 at Clean Slate III occurred during remediation activities at that site. Revegetation work, including ripping the soil surface and reseeding, occurred in October and in mid-December 2019 at Clean Slate II and between the first of October and first few days of December 2019 at Clean Slate III.

Dust transport by suspension and saltation is strongly dependent on wind speed. Concentrations of $PM_{10}$ (particulate matter of aerodynamic diameter ≤10 micrometers [µm], a size fraction of small particles that are suspended in the air and can be easily inhaled) remain low until winds exceed 24 kilometers per hour (km/hr) to 32 km/hr (15 miles per hour [mph] to 20 mph). Saltation particle counts (which measure larger particles of 50 µm to 500 µm in size that bounce along the ground surface) also increase above the same general threshold wind speed. Wind speeds in excess of 24 km/hr (15 mph) occur less than 10 percent of the time at the sites, and winds in excess of 32 km/hr (20 mph) occur less than 3 percent of the time.

Station 401 is located closest to the Clean Slate III remediation area and is downwind of the area when winds are from the south. Throughout the year, plutonium-239+240 ($^{239+240}$Pu) was above the detection limit in particulate samples collected on filters at Station 401, and americium-241 ($^{241}$Am) was detected on four of the samples collected in two-week intervals, and plutonium-238 ($^{238}$Pu) was detected on three samples. The highest plutonium and gross alpha concentrations at Station 401 occurred in the first half of the year, with $^{239+240}$Pu of $301.75 \times 10^{-16}$ microcuries per milliliter (µCi/ml) and gross alpha of $19.19 \times 10^{-15}$ µCi/ml. Radionuclide concentrations were lower at Station 403 than at Station 401, which is consistent with Station 403 being a greater distance from the contamination area than Station 401. Peaks in gross alpha concentration at one site are often paired with relatively low concentrations at the other monitoring station, when high winds are predominantly from one direction, placing one station upwind and the other downwind of the contamination area.

The radionuclide content of material that saltated into the passive Big Spring Number Eight (BSNE) traps at the Clean Slate III monitoring stations was generally higher in 2019 than in 2018, by more than ten times at some traps and particle sizes. Although radionuclide concentrations of saltated material are usually higher at the station closer to the contaminated area, a significant exception occurred for the February to September collection in 2019, when the largest size fraction at the traps at Station 403 contained much higher concentrations of all measured radionuclides compared with Station 401.

Remediation work at Clean Slate II was completed in 2018, so Stations 404 and 405 monitored undisturbed conditions for most of 2019 until reseeding activities in the autumn. Nevertheless, other than a couple of samples from each station in the summer, most of the air filters analyzed by alpha spectroscopy measured $^{239+240}$Pu above the detection limit. The highest $^{239+240}$Pu concentration measured at Clean Slate II in CY2019 was $17.62 \times 10^{-16}$ µCi/ml at Station 404 in May. The highest gross alpha at Station 404 was measured in March, with a concentration of $3.82 \times 10^{-15}$ µCi/ml. Radionuclide concentrations for material collected in the saltation traps at Clean Slate II generally declined in 2019 compared with those measured in 2018.

Revegetation of the remediation areas at both Clean Slate II and III occurred late in 2019 and involved additional ground disturbance as the soil was ripped and seeded. This activity increased airborne dust at both sites, but radionuclide concentrations on suspended soil were most notably affected at Clean Slate III. A slight increase in $^{239+240}$Pu concentrations is observed at Clean Slate II Stations 404 and 405 during the reseeding timeframe, but it is not as high as the concentrations measured earlier in the year during ambient conditions, nor as high as the concentrations observed at Stations 401 and 403 during reseeding at Clean Slate III. The year between remediation and reseeding may have allowed for stabilization of the surface that had not occurred in the month between remediation and reseeding at Clean Slate III.

Radiological monitoring at Station 400—which is located at the ROC, and therefore the closest regularly staffed work location to the Clean Slate sites—recorded a lower mean gross alpha activity for dust collected on air filters than in the previous year. Gamma spectroscopy of all air filters from Station 400 identified only naturally occurring radionuclides, with no detection of $^{241}Am$ (which is used as an indicator of plutonium-241[$^{241}Pu$]). Alpha spectrometry of selected air filters collected at Station 400 did not detect $^{238}Pu$ or $^{239+240}Pu$ above the analytical detection limit. No saltation traps are deployed at Station 400.

Mean annual gross beta concentrations of air filter samples collected at all monitoring stations are lower than those measured at CEMP sites in the region. The mean gamma exposure rate (measured at Stations 400, 401, and 403) was similar to the mean for the Warm Springs Summit CEMP location, although the maximum values were greater than the maximum plus two standard deviations at the regional CEMP sites in 2019. At the Clean Slate III stations, there was a cluster of higher gamma rate measurements in October and November, during the reseeding time period, unassociated with rainfall (rainfall can cause higher gamma rates by deposition of dust from the atmosphere onto the instruments).

Strong winds are the driver for both suspension and saltation of dust and soil. The recorded wind speed and $PM_{10}$ during remediation activities at Clean Slate III identified discrete wind events lasting approximately two to nine hours each, which accounted for the greatest $PM_{10}$ concentrations at the monitoring stations. These events captured the effect of winds from the northwest and from the south. The observed differences in dust loading and radionuclide concentrations for the monitoring stations when they were either upwind or downwind of the contamination area identify the remediation area as a source of plutonium-contaminated dust. The increase in concentration of dust and radionuclides during the remediation activities, compared with measurements under previous ambient conditions, highlights the effect of land disturbance on wind-borne contaminant transport from the Clean Slate test areas.

The meteorological and particulate matter monitoring indicate that the soil and atmospheric conditions for wind-borne contaminant movement exist at the Clean Slate sites, and that transport of radionuclide-contaminated soil by both suspension and saltation occurred under ambient conditions and accelerated when the sites were disturbed. The monitoring also indicates that the disturbed land surface may restabilize to the previous ambient transport conditions within a year after disturbance. Monitoring activities during CY2020 will confirm site stabilization conditions.

**THIS PAGE INTENTIONALLY LEFT BLANK**

**CONTENTS**

## LIST OF FIGURES

## LIST OF TABLES

## LIST OF ACRONYMS

| | |
|---|---|
| AEC | Atomic Energy Commission |
| $^{241}Am$ | americium-241 |
| BSNE | Big Spring Number Eight |
| CAU | Corrective Action Unit |
| CEMP | Community Environmental Monitoring Program |
| CSI | Clean Slate I |
| CSII | Clean Slate II |
| CSIII | Clean Slate III |
| CY | calendar year |
| DL | detection limit |
| DOE | Department of Energy |
| DRI | Desert Research Institute |
| EM NV | Environmental Management Nevada Program |
| EPA | Environmental Protection Agency |
| GOES | Geostationary Operational Environmental Satellite |
| GZ | ground zero |
| MDC | minimum detectable concentration |
| NNSS | Nevada National Security Site |
| NTTR | Nevada Test and Training Range |
| PIC | pressurized ionization chamber |

| | |
|---|---|
| $PM_{2.5}$ | particulate matter of aerodynamic diameter ≤2.5 micrometers |
| $PM_{10}$ | particulate matter of aerodynamic diameter ≤10 micrometers |
| PST | Pacific Standard Time |
| $^{230+240}Pu$ | plutonium-230+240 |
| $^{238}Pu$ | plutonium-238 |
| $^{239+240}Pu$ | plutonium-239+240 |
| $^{241}Pu$ | plutonium-241 |
| ROC | Range Operations Center |
| RSL | Radioanalytical Services Laboratory |
| SNL | Sandia National Laboratories |
| TDR | time-domain reflectometry |
| TTR | Tonopah Test Range |
| VWC | volumetric water content |
| WRCC | Western Regional Climate Center |

## INTRODUCTION

In May and June of 1963, the U.S. Department of Energy (DOE) (formerly the Atomic Energy Commission [AEC]) implemented Operation Roller Coaster to evaluate the dispersal of radionuclides when nuclear devices were subjected to chemical explosions while in storage or transit (Dick *et al.*, 1963; Johnson and Edwards, 1996). The operation consisted of four tests: Double Tracks, conducted in Stonewall Flat on the Nevada Test and Training Range (NTTR); and Clean Slate I, II, and III, conducted in Cactus Flat on the Tonopah Test Range (TTR). The Clean Slate sites, located southeast of Tonopah, Nevada, in Nye County (Figures 1 and 2) are the focus of this report.

The Clean Slate tests involved one device containing plutonium and several simulated weapons containing uranium (Dick *et al.*, 1963; Johnson and Edwards, 1996). For each test, data collection was conducted along arcs within a wedge-shaped area that extended from the test ground zero (GZ) along a radius to the south or southeast (Dick *et al.*, 1963; Johnson and Edwards, 1996), which were the expected downwind directions. Data collection during the tests focused on plutonium and uranium because of the radiological toxicity (Dick *et al.*, 1963). Subsequent surveys to characterize radionuclide-contaminated soils focused on the detection of plutonium by measuring the plutonium daughter product, americium-241 ($^{241}$Am; Proctor and Hendricks, 1995). Americium-241 emits gamma rays that are more readily measured than the alpha-emitting plutonium isotopes.

Immediate post-shot remediation at each test involved disposing of contaminated debris in a pit at GZ, scraping the surface soil around GZ to a depth of several inches, and placing the soil in the disposal pit or mounding it over the contaminated debris. The mound of contaminated materials was covered with additional uncontaminated soil, compacted, and then watered down (Johnson and Edwards, 1996). Fences were constructed around the contaminated area at each site. Based on soil survey data collected during 1973, a second fence was constructed at the approximate limit of 40 picocuries per gram (pCi/g) of plutonium in soil (Duncan *et al.*, 2000).

Aerial surveys of Operation Roller Coaster contamination areas were conducted in 1977 (EG&G, 1979) and 1993 (Proctor and Hendricks, 1995). These surveys used gamma detectors to measure $^{241}$Am. Based on the 1977 survey, the total area of diffuse plutonium for all Operation Roller Coaster sites was estimated to be approximately 20 km$^2$ (4,900 acres) (SNL, 2014). The 1993 survey estimated the maximum radiation level at the Clean Slate I GZ to be between 200 pCi/g and 400 pCi/g. At Clean Slate II and III, the maximum concentrations at GZ were reported to be in excess of 2,000 pCi/g. Contamination was reported outside the outer perimeter fence at all three Clean Slate sites. At Clean Slate III, plutonium concentration outside of the fence did not exceed 200 pCi/g. However, the concentrations reported outside the fences at Clean Slate I and II were greater than 200 pCi/g but less than 400 pCi/g (Proctor and Hendricks, 1995).

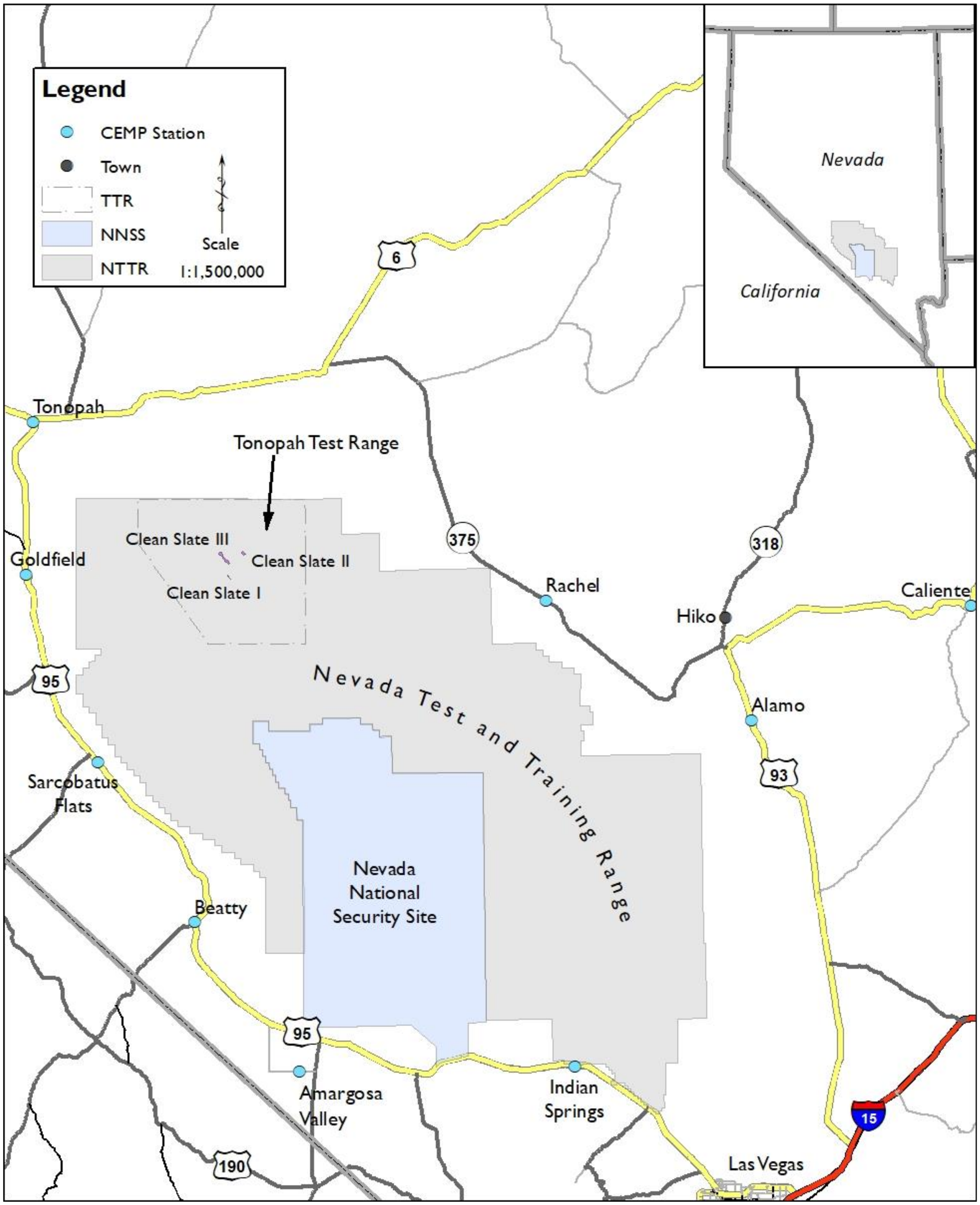


Figure 1. Location of Clean Slate sites at the Tonopah Test Range (TTR) in the north end of the Nevada Test and Training Range (NTTR) in southern Nevada. The current and former Community Environmental Monitoring Program (CEMP) stations, for which monitoring data are available, are also shown.

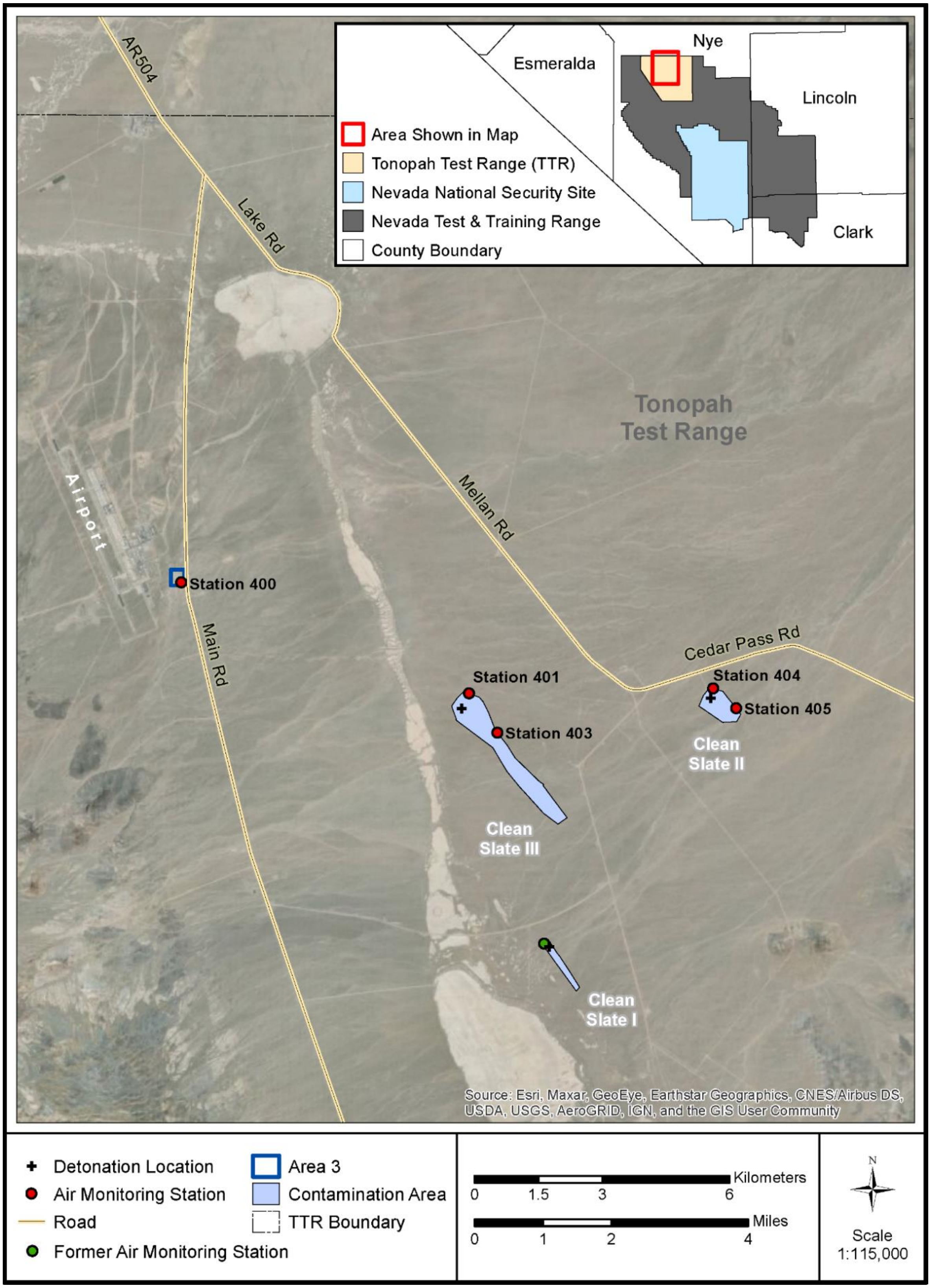


Figure 2. The TTR environmental monitoring stations relative to the Clean Slate sites.

Soil contamination at Clean Slate I was remediated in 1997 to a transuranic radiation level of ≤400 pCi/g (SNL, 2012). The DOE Environmental Management Nevada Program (EM NV) began remediation of the Clean Slate II site during the autumn of 2017 and concluded in the summer of 2018 (Table 1). Soil disturbing remediation activities at Clean Slate III began during September 2018 and concluded at the end of August 2019. Revegetation of both sites, which involved ripping and preparing the soil and seeding, inside and outside the contamination area, occurred between October and December 2019 (Table 1).

In 2008, at the request of DOE, Desert Research Institute (DRI) constructed and deployed two portable environmental monitoring stations at the TTR as part of the Environmental Restoration Project, Soils Activity. Additional stations were subsequently added (Tables 2 and 3). These stations provide data supporting the DOE EM NV mission of safely cleaning up the environmental legacy remaining from nuclear device development and testing. The primary objective of the monitoring stations is to evaluate whether there is wind transport of radiological contaminants, specifically plutonium, from the Soils Corrective Action Units (CAUs) associated with Operation Roller Coaster and if so, under what weather conditions such transport occurs. Plutonium particles tend to attach to small soil particles, so wind-suspended dust and rainfall runoff are the likely mechanisms for transporting radiological contaminants. Inhalation of plutonium-contaminated dust particles is the most likely mechanism for human exposure. The objectives of this annual report are to document the operation of the TTR monitoring stations during calendar year (CY) 2019, present the data collected, interpret the results in the context of the monitoring objectives stated above, and provide recommendations as needed.

Table 1. Dates of remediation and revegetation activities at Clean Slate II and III.

| | **Clean Slate II** | **Clean Slate III** |
|---|---|---|
| Start of Remediation | 10/31/2017 | 9/6/2018 |
| Hiatus in Remediation | none | 12/20/2018 to 1/8/2019 |
| End of Remediation | 7/26/2018 | 8/26/2019 |
| Start of Revegetation | 10/7/2019 | 10/1/2019 |
| Hiatus in Revegetation | 10/24/2019 to 12/9/2019 | none |
| End of Revegetation | 12/18/2019 | 12/3/2019 |

## MONITORING STATION LOCATIONS AND CAPABILIITIES

Five monitoring stations are in operation at TTR. Stations 400 and 401 were installed in May and June 2008, respectively. Stations 403, 404, and 405 were installed in April 2017. Former Station 402 was installed in May 2011 and ceased operation in April 2017. Wind direction, access, and power availability were key considerations in selecting the specific monitoring station locations. The predominant wind directions in the area are from the northwest and south-southeast (Engelbrecht *et al.*, 2008).

Station 400 is located within the Sandia National Laboratories (SNL) TTR Area 3, and adjacent to the Range Operations Center (ROC). Table 2 provides station coordinates. Tonopah Test Range Area 3, which is adjacent to the TTR airfield, is downwind of the Clean Slate contamination areas when winds are from the south-southeast. At a distance of eight to nine kilometers (km) (five to six miles [mi]), this area is the closest, regularly manned work location to the Clean Slate sites. Therefore, Station 400 facilitates the characterization of radiological conditions in the TTR work areas that may result from wind transport of radionuclide-contaminated soils from the Clean Slate sites and provides data to compare radiological conditions at TTR Area 3 with conditions at the Clean Slate sites. Station 400 is approximately 90 meters (m) (300 feet [ft]) south of the ROC near the southeast corner of TTR Area 3 (Figure 2). Sandia National Laboratories provides line power to operate the equipment at Station 400, which consists of a meteorological tower and air sampling equipment installed on a 2.1 m x 4.3 m (7 ft x 14 ft) trailer (Figure 3). The wind measurement instruments are located approximately 4.5 m (15 ft) above ground surface.

Table 2. Location coordinates (with respect to the WGS84 reference system) and elevations for the TTR air monitoring stations.

| Station | Latitude | Longitude | Elevation |
|---|---|---|---|
| Station 400 | 37° 47’ 10” N | 116° 45’ 21” W | 5,515 ft |
| Station 401 | 37° 45’ 39” N | 116° 40’ 58” W | 5,421 ft |
| Station 402 (former station) | 37° 42’ 33” N | 116° 39’ 32” W | 5,389 ft |
| Station 403 | 37° 45’ 14” N | 116° 40’ 17.30” W | 5,419 ft |
| Station 404 | 37°45’ 47” N | 116° 36’ 49.81” W | 5,526 ft |
| Station 405 | 37°45’ 32” N | 116° 36’ 27.78” W | 5535 ft |

Figure 3. Station 400 is a trailer-mounted radiological and meteorological measurement system located near the Range Operations Center (ROC) in the Sandia National Laboratories (SNL) compound on the TTR.

Station 401 is located at the demarcation fence on the northern perimeter of the Clean Slate III contamination area (it was moved slightly during 2018 to facilitate remediation logistics) and Station 403 is located on the eastern perimeter, which is southeast of the Clean Slate III detonation area (Figure 2). The locations of Stations 401 and 403 were selected for their proximity to the downwind side of the higher contaminated zone (detonation area) during either of the predominant wind directions (south and northwest). Similarly, Stations 404 and 405 are north and southeast, respectively, of the Clean Slate II fenced contamination area. Solar-charged batteries power all stations other than Station 400. The air samplers, solar panels, and batteries are on trailers. This configuration requires the meteorological towers to be installed on freestanding tripods that are separate from the trailer (see Appendix B for station photos). The wind monitors on the tripod towers are approximately 3 m (10 ft) above ground surface.

The fundamental design of these stations is similar to those used in the Community Environmental Monitoring Program (CEMP) (NSTec, 2013). The Quality Assurance Program is also patterned after that used by CEMP (Appendix A). The equipment deployed provides data on radiological, meteorological, and environmental conditions. Table 3 lists the parameters measured and the approximate date of the initial data collection at each of the monitoring stations.

Continuous-flow, low-volume air samplers (Hi-Q Environmental Products, San Diego, California) are used to collect airborne particulate matter for radiological analysis. Glass-fiber filters with an effective pore size of 0.3 micrometers (μm) and diameter of 10 centimeters (cm) (4 inches [in]) were used for the first two filter deployments of CY2019 (from December 19, 2018, to January 2, 2019, and January 2, 2019, to January 16, 2019). Five-centimeter (2 in) diameter filters composed of the same glass-fiber material were used for the remainder of CY2019. The Hi-Q air sampling equipment draws ambient air through the 5 cm diameter filters at a rate of approximately 50 L/min (1.75 $ft^3$/min) and is designed to maintain the same flow rate with increased filter loadings. This flow rate is reduced from the 56.6 L/min (2 $ft^3$/min) flow rate used for the 10 cm (4 in) diameter filters to avoid the tunneling of material through the filter. The total volume of ambient air drawn through the filter and the total hours of operation are recorded every two weeks when filters are collected from the monitoring stations. Filters are weighed before and after deployment to determine the mass of particulate matter collected. The filters are then submitted to the Radioanalytical Services Laboratory (RSL) at the University of Nevada, Las Vegas, for gross alpha, gross beta, and gamma spectroscopy analyses. If $^{241}$Am is detected by the gamma spectroscopy analysis, then alpha spectrometry is performed at Eurofins TestAmerica Laboratories Inc. to confirm and determine the quantity of plutonium isotopes. Alpha spectrometry is also performed quarterly for select air filters. Alpha spectrometry is more sensitive than gamma spectroscopy because it can measure a narrower window of energy specific to plutonium isotopes and because plutonium is chemically extracted from the sample prior to analysis.

Stations 400, 401, and 403 measure gamma energy using a pressurized ionization chamber (PIC) (Reuter Stokes, Youngstown, Ohio). The PICs measure gamma radiation exposure every three seconds. These measurements are averaged and maximum/minimum values are determined every 10 minutes before being recorded in the database.

Suspension and transport of contaminated dust are controlled by local meteorological and environmental conditions, such as wind speed and soil moisture content. Meteorological data are also important for interpreting natural variations in radiation exposure rates. At low atmospheric pressures, more natural radioactive gases, such as radon, are released from the Earth’s surface. Precipitation can also wash naturally occurring radioactive particles and wind-suspended radionuclide-contaminated particles from the atmosphere, contributing to radiation exposure at the surface. Weather instruments at the stations record air temperature, humidity, wind speed and direction, solar radiation, barometric pressure, soil temperature, and precipitation data. In addition to meteorological sensors, soil volumetric water content (VWC) is monitored in the top 5 cm (2 in) of soil using time domain reflectometry (TDR) probes installed at a shallow angle below ground surface. The TDR probes provide an estimate of soil water content based on the direct measurement of electrical soil conductivity.

Table 3. Radiological, meteorological, and environmental sensors deployed at the TTR air monitoring stations. The dates refer to the first occurrence of data collection for that parameter at the given station. Data collection ended at Station 402 on April 25, 2017.

| **Instrument/ Measurement** | **Station 400** | **Station 401** | **Station 402** | **Station 403** | **Station 404** | **Station 405** |
|---|---|---|---|---|---|---|
| Wind speed | 5/27/2008 | 6/10/2008 | 5/18/2011 | 4/25/2017 | 4/25/2017 | 4/25/2017 |
| Wind direction | 5/27/2008 | 12/22/2009 | 5/18/2011 | 4/25/2017 | 4/25/2017 | 4/25/2017 |
| Precipitation | 5/27/2008 | 12/22/2009 | 5/18/2011 | 4/25/2017 | 4/25/2017 | 4/25/2017 |
| Air temperature | 5/27/2008 | 6/10/2008 | 5/18/2011 | 4/25/2017 | 4/25/2017 | 4/25/2017 |
| Relative humidity | 5/27/2008 | 6/10/2008 | 5/18/2011 | 4/25/2017 | 4/25/2017 | 4/25/2017 |
| Solar radiation | 5/27/2008 | N/A | 5/18/2011 | 4/25/2017 | 4/25/2017 | 4/25/2017 |
| Barometric pressure | 5/27/2008 | N/A | 5/18/2011 | 4/25/2017 | 4/25/2017 | 4/25/2017 |
| Soil temperature | 5/27/2008 | 12/22/2009 | 5/18/2011 | 4/25/2017 | 4/25/2017 | 4/25/2017 |
| Soil moisture content | 5/27/2008 | 12/22/2009 | 5/18/2011 | 4/25/2017 | 4/25/2017 | 4/25/2017 |
| Airborne particle size profiler | 5/27/2008 | 6/10/2008 | 5/18/2011 | 4/25/2017 | 4/25/2017 | 4/25/2017 |
| Airborne particle collector | 5/27/2008 | 7/30/2008 | 8/23/2011 | 4/25/2017 | 4/25/2017 | 4/25/2017 |
| Saltation sensor | N/A | 8/9/2011 | 8/9/2011 | 4/25/2017 | 4/25/2017 | 4/25/2017 |
| Gamma rad. PIC | 5/27/2008 | 12/22/2009 | 12/15/2011 | 4/25/2017 | N/A | N/A |
| MiniVol[1] | 5/27/2008 | N/A | N/A | N/A | N/A | N/A |
| Data logger | 5/27/2008 | 6/10/2008 | 5/18/2011 | 4/25/2017 | 4/25/2017 | 4/25/2017 |
| Satellite transmitter | 5/27/2008 | 12/22/2009 | 5/18/2011 | 4/25/2017 | 4/25/2017 | 4/25/2017 |
| Saltation traps | N/A | 4/01/2014 | 4/01/2014 | 4/25/2017 | 4/25/2017 | 4/24/2017 |

[1] Samples have never been collected from the MiniVol collectors.
N/A = not applicable.

Electronic sensors measure meteorological and other environmental conditions every three seconds. These measurements are averaged or totaled every 10 minutes, as appropriate, and stored in the on-site data logger. The maximum and minimum values of each parameter are also saved on the data logger and used to assess data quality. The data loggers are downloaded every two weeks, during site visits. To assess instrument performance and provide rapid updates of conditions at the monitoring sites, observations are transmitted to the Western Regional Climate Center (WRCC) via the Geostationary Operational Environmental Satellite (GOES) system every hour. At the WRCC, data are quality checked and archived for later interpretation.

Aerosol concentrations are measured directly at the stations with a Met One Ambient Particulate Profiler (Model 212, Met One Instruments, Inc., Grants Pass, Oregon). These instruments are well suited for operation in harsh climates and remote locations where line power is not available. The Met One instruments are mounted so that the inlet of the instrument is between 1.5 m (4.9 ft) and 1.7 m (5.6 ft) above ground level, which is considered the respiratory zone for adult humans. The Met One Ambient Particulate Profiler

Model 212 is a nephelometer-type instrument that detects suspended aerosol particles based on 90-degree light scattering, which is affected by particle size, shape, color, and chemical composition. The instrument is not a U.S. Environmental Protection Agency (EPA) Federal Reference Method instrument approved for regulatory monitoring of $PM_{10}$ (particulate matter of aerodynamic diameter ≤10 micrometers [µm]) and $PM_{2.5}$ (particulate matter of aerodynamic diameter ≤2.5 µm), but such instruments have been shown to have a good correlation with gravimetric methods and have an excellent signal-to-noise ratio (Moosmüller *et al.*, 2001; Wang *et al.*, 2011).The Met One detects and records the suspended particle count in eight different size bins within the range of 0.5 µm (0.00002 in) to 10 µm (0.00039 in) in diameter. Particle counts are reported every minute and the average for each 10-minute interval is recorded on the data logger. These particle counts are used to estimate $PM_{10}$ and $PM_{2.5}$ mass concentrations by converting the particulate counts in the eight size bins to a mass concentration by assuming the mineral dust particles are spherical with a uniform density of 2.6 grams per cubic meter ($g/m^3$).

The Sensit H11-LIN (Sensit, Inc., Redlands, California) records impacts from saltating particles. The sensing area of the Sensit is set 10 cm (4 in) above the ground surface, wraps completely around the vertically oriented instrument, and is capable of registering impacts from all directions. The sensing area is made of piezoelectric material that converts particle impacts to electrical impulses that are registered and summed over 10-minute intervals, and subsequently stored on the station data logger. The saltation sensor is located in proximity to the meteorological tower at each station in areas that are free of recent soil surface disturbance and vegetation, which might interfere with instrument operation. Windblown plant debris, such as tumbleweed, is cleared from the sensor area as needed. Raindrop impacts dislodge soil particles and eject particles, which may result in spurious impact counts on the saltation sensors during precipitation events. Therefore, saltation sensor data that coincide with precipitation are excluded from the data analyses.

The Sensit piezoelectric instruments record real-time saltation activity that can be used to identify transport events when analyzed in conjunction with wind speed data. One of the drawbacks of the Sensit instrument is that it provides count information but not the transport mass flux. Big Spring Number Eight (BSNE; Custom Products and Consulting LLC, Big Spring, Texas) traps are used to estimate integrated transport mass flux and provide physical samples for size and radiological analyses. The BSNEs are wind-aspirated samplers that collect sand that enters the opening (Figure 4). The inlet height is set at 15 cm (6 in) to collect the near-ground erodible soil material transported by saltation. Two collectors are installed at each mounting rod (Figure 5). One collector is pointed toward the contaminated area to collect material likely to have been transported from either Clean Slate II or III. The other collector is pointed in the opposite direction (“away”) and is used to collect the material moving toward the sites. This physical setup and orientation allow the net movement of soil material from the Clean Slate II and III sites to be estimated for the area near the monitoring stations.

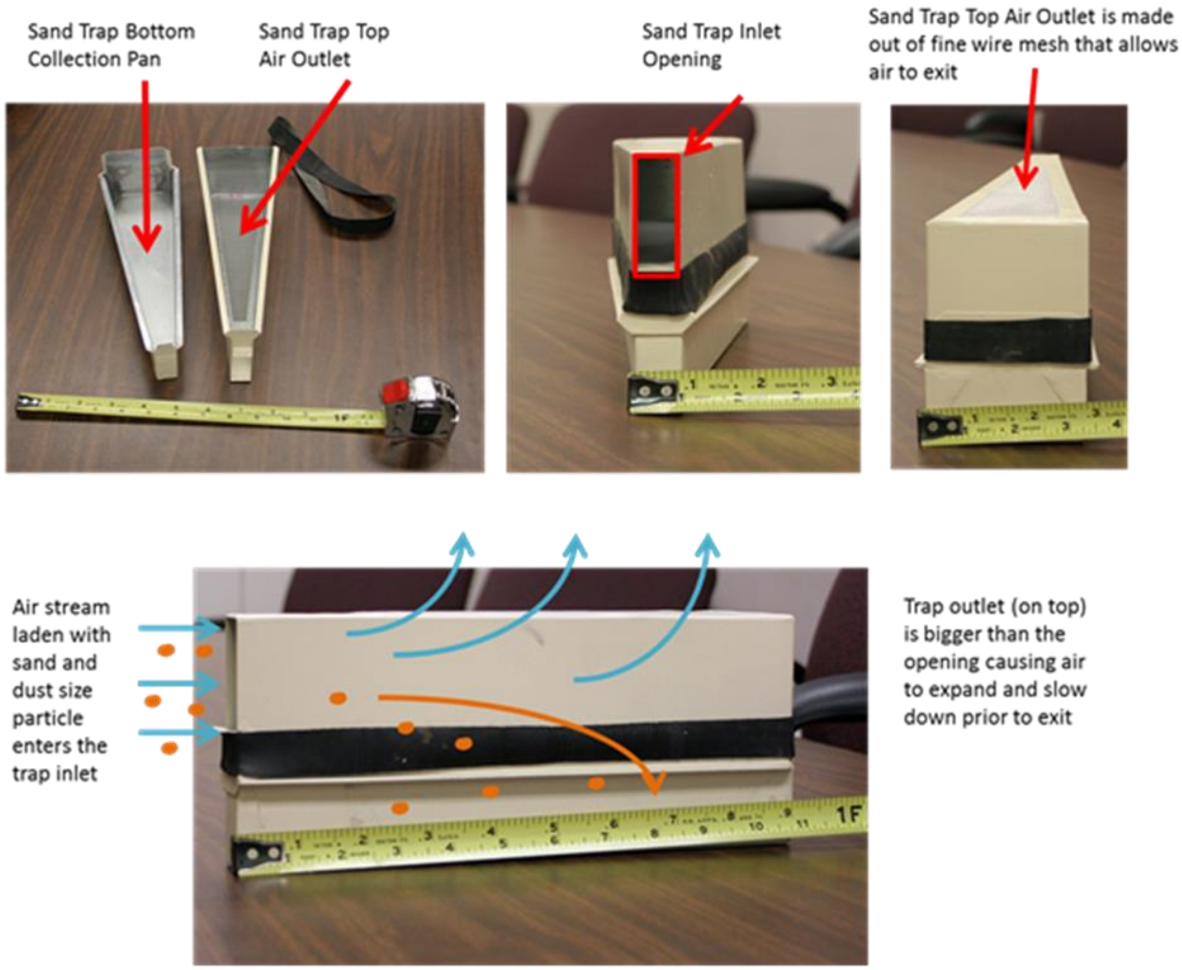


Figure 4. Sand particles are carried into the BSNE sand trap by fast-moving air. As the air slows down in the chamber, momentum is lost and the particles settle on the bottom of the collection pan. However, dust particles may be small enough to be carried out through the wire mesh at the top of the trap by air.

Figure 5. Northeast view at Station 401 prior to station relocation. In the foreground is one of three BSNE sand trap installations at this station. The Clean Slate III boundary fence is to the right. Behind the sand trap is the Sensit saltation sensor (highlighted by the red box) and a meteorological station with additional sand traps (not visible) is located along the fence line.

Three replicate BSNE samplers with two collectors each are part of each sampler installation (Figures 6 and 7) along a fence line. The samplers are checked by field operators during biweekly field visits. When sufficient mass is collected for analysis, the traps are retrieved and the replacement traps are deployed.

There are a total of 48 BSNE collectors that can be deployed at Stations 401, 403, 404, and 405. All the odd-numbered traps are oriented with the collector facing toward the contaminated area (collecting material moving from/downwind of the contaminated area) and the even-numbered traps are oriented with the collector opening facing away from the contaminated area (collecting material moving from the area upwind of the contaminated area) (Figures 6 and 7). Two sets of traps are used in rotation as sample collection occurs.

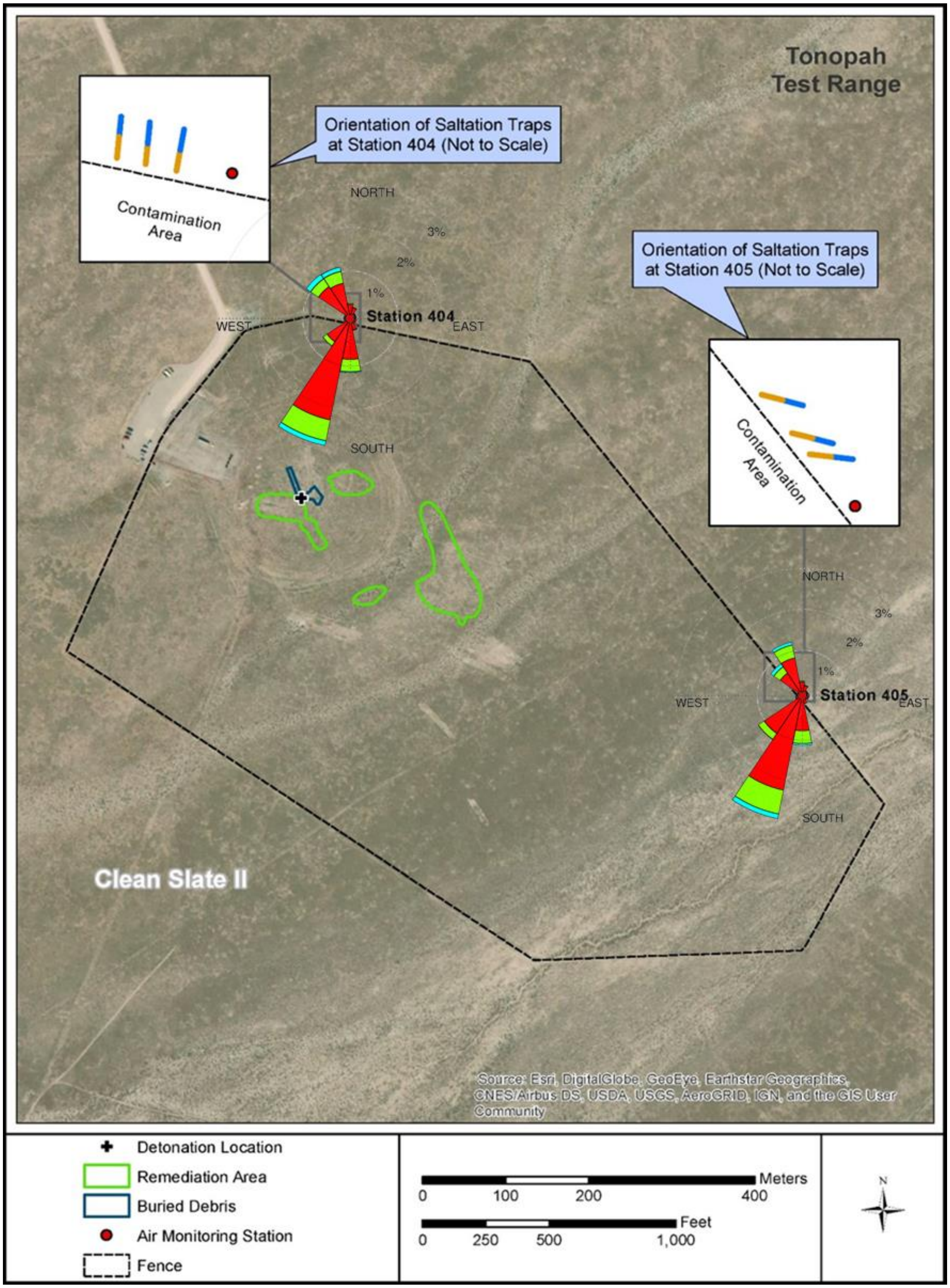


Figure 6. BSNE sampler locations and orientations at Clean Slate II. For reference, wind roses indicate the direction of winds greater than 24 kilometers per hour (km/hr) (15 miles per hour [mph]) measured at the stations during the sampling period.

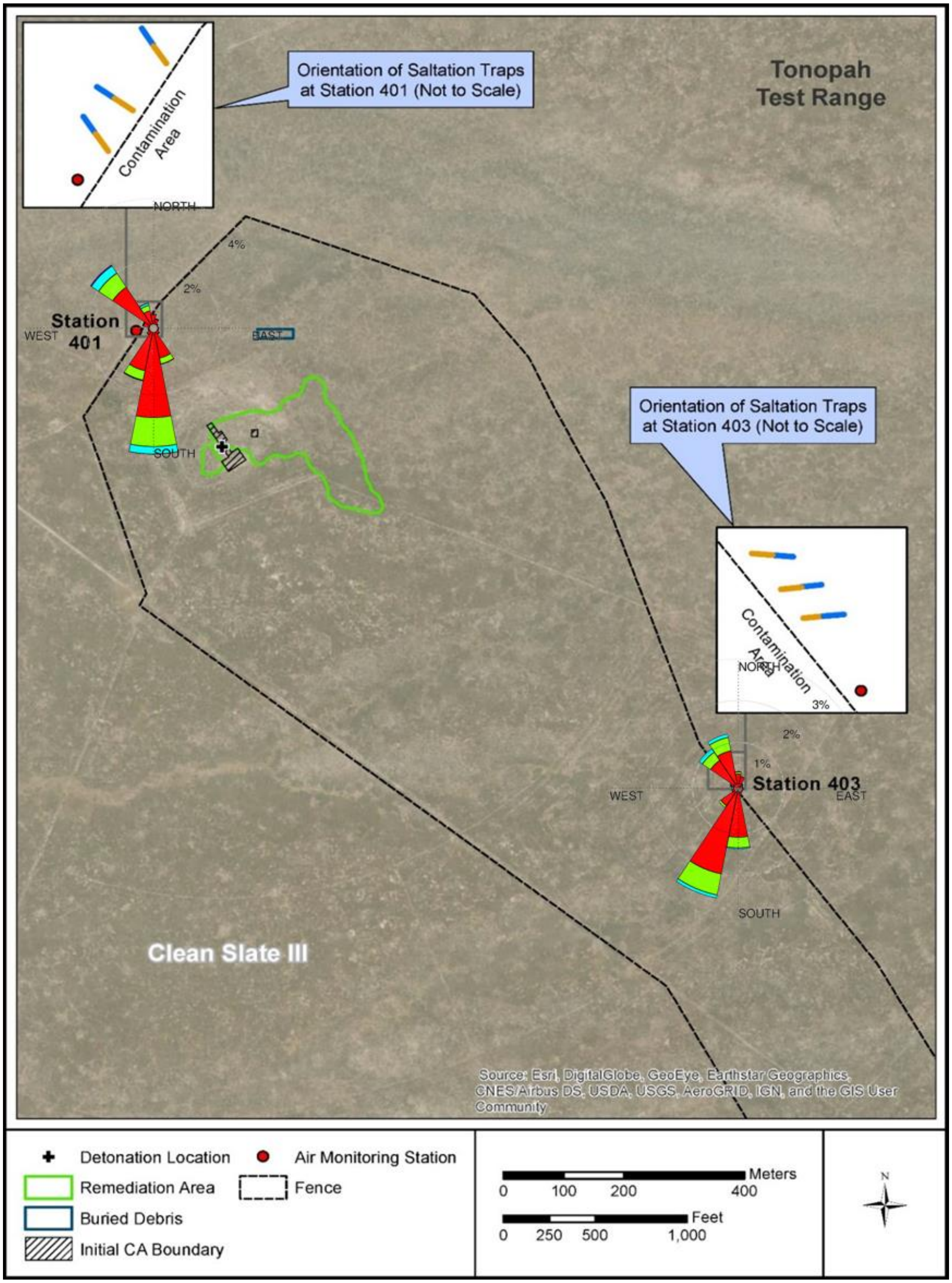


Figure 7. BSNE sampler locations and orientations at Clean Slate III. For reference, wind roses indicate the direction of winds greater than 24 km/hr (15 mph) measured at the stations during the sampling period.

Because of the small amount of material collected by each sampler, the material from the three odd-numbered BSNEs at each station location are combined into a 0.5 L plastic bottle for laboratory analysis. The same procedure is followed for the even-numbered BSNEs at each location, which results in the collection of two composite samples for each station for each collection period. In the laboratory, the samples are sieved into three size ranges for analysis: ≥250 µm, 63 to 250 µm, and ≤63 µm in diameter.

In addition to the sensors and collectors described above, one MiniVol (Air Metrics, Springfield, Oregon) is deployed at Station 400. This sampler is intended to be run in the event of a nearby wildfire or during extreme dust storms because it is set up to facilitate analyses that distinguish organic and inorganic constituents. The MiniVol is a manually activated, low-volume air sampler equipped with Teflon-membrane filters. No events resulted in the MiniVol being activated in 2019, so no data were collected from this instrument. Appendix B includes photographs and the instrument layout of each monitoring station.

## WEATHER CONDITIONS AND OTHER ENVIRONMENTAL PARAMETERS

Appendix C presents summary tables of the meteorological data recorded at the stations and Appendix D shows plots of the daily average meteorological and environmental data. These data are summarized and discussed below.

Figure 8 shows the daily summaries of air temperature at Station 400 between January 1, 2019, and December 31, 2019. The three traces shown in the figure depict the maximum, average, and minimum daily temperature based on the 10-minute average measurements. The average air temperature during CY2019 for Station 400 was 10.9 degrees Celsius (°C) (51.6 degrees Fahrenheit [°F]). The maximum air temperature of 35.6 °C (96.1 °F) was recorded on July 22, 2019, and the minimum air temperature of -19.6 °C (-3.3 °F) was recorded on February 11, 2019. The highest average monthly air temperature of 24.6 °C (76.3 °F) was recorded in July and the lowest average monthly air temperature of -1.2 °C (29.8 °F) was recorded in February. Air temperatures at Stations 401, 403, 404, and 405 follow a very similar pattern as observed for Station 400 (Figure 9 and Appendix D). The air temperature sensor used at the monitoring stations has a reported accuracy of ±0.5 °C (±0.9 °F) for temperatures ranging from 5 °C to 40 °C (40 °F to 105 °F).

Figure 10 shows the daily average soil temperatures for all six TTR stations. Soil temperature is measured using thermocouple wire that has been buried at a depth of 10 cm to 13 cm (4 in to 5 in). Generally, there are minor differences in soil temperature readings between the stations. These minor differences may be explained in part by differences in local soil thermal conductivity, soil moisture, vegetation cover, variations in probe burial depth, and sensor accuracy and drift. The correlation between daily soil temperature and air temperature data for Station 401 (Figure 11) shows the close relationship between these parameters, with an $R^2$ value of 0.98.

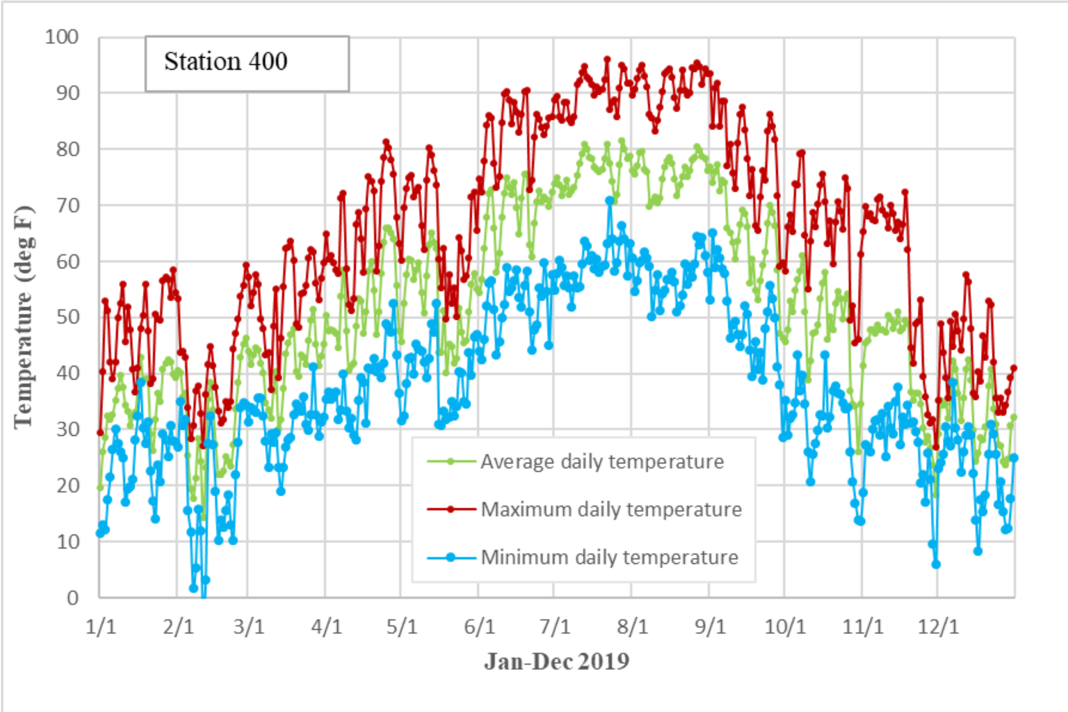


Figure 8. Ambient air temperature for Station 400 for CY2019.

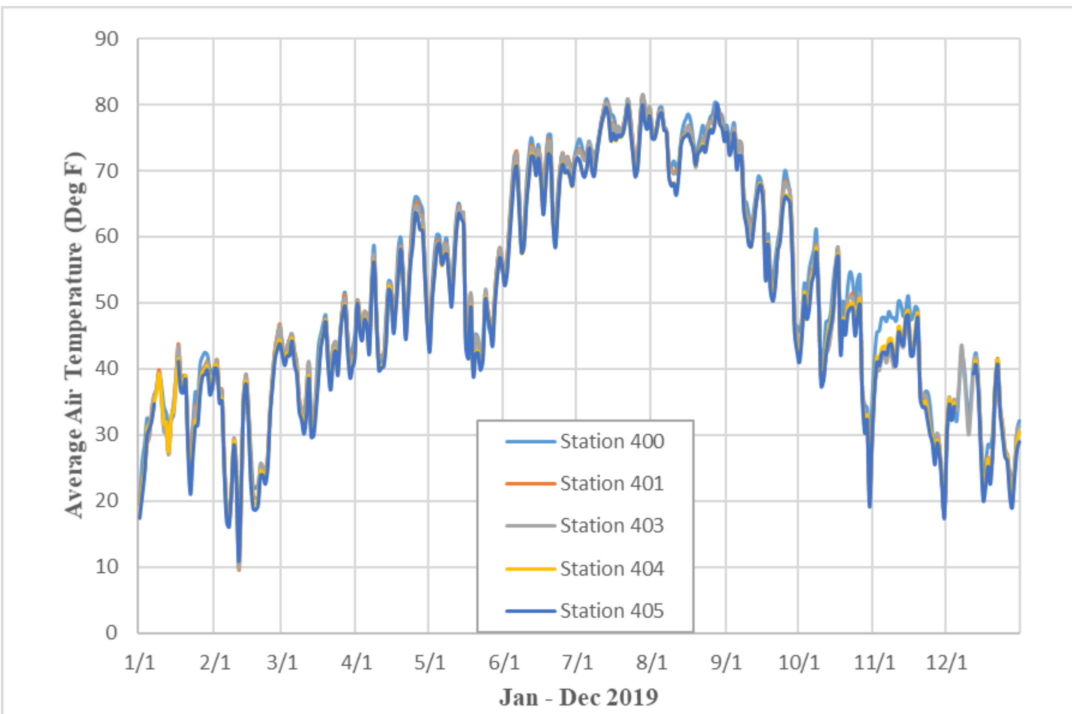


Figure 9. Average daily ambient air temperature for Stations 400, 401, 403, 404, and 405 for CY2019.

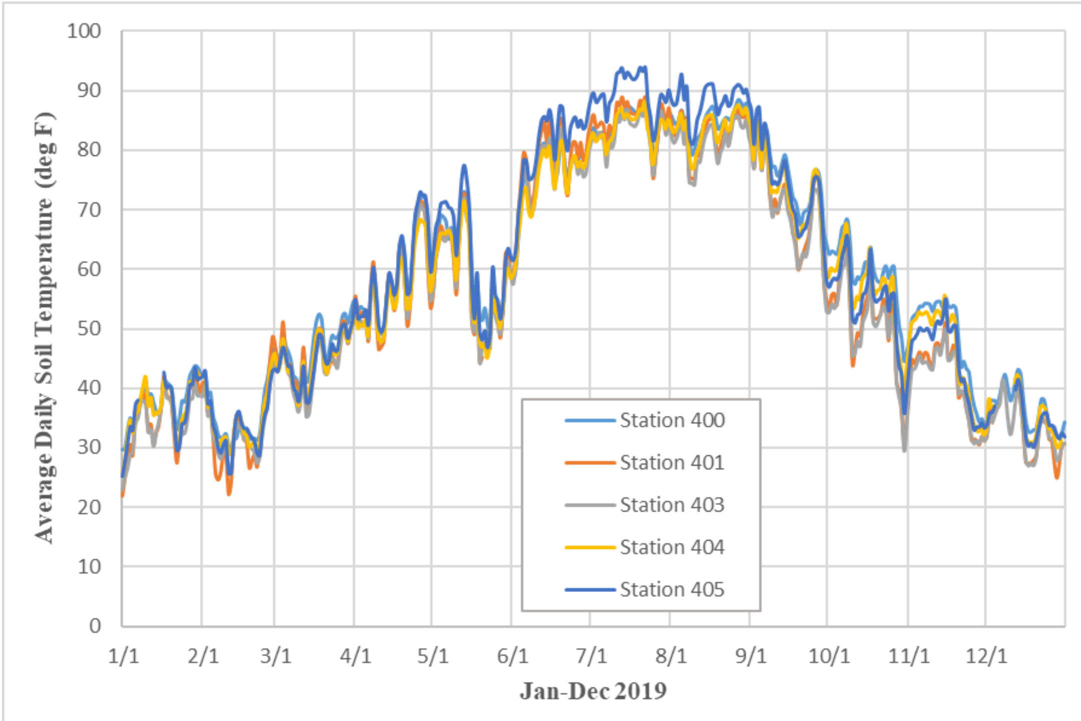


Figure 10. Average ambient soil temperature for Stations 400, 401, 403, 404, and 405 for CY2019.

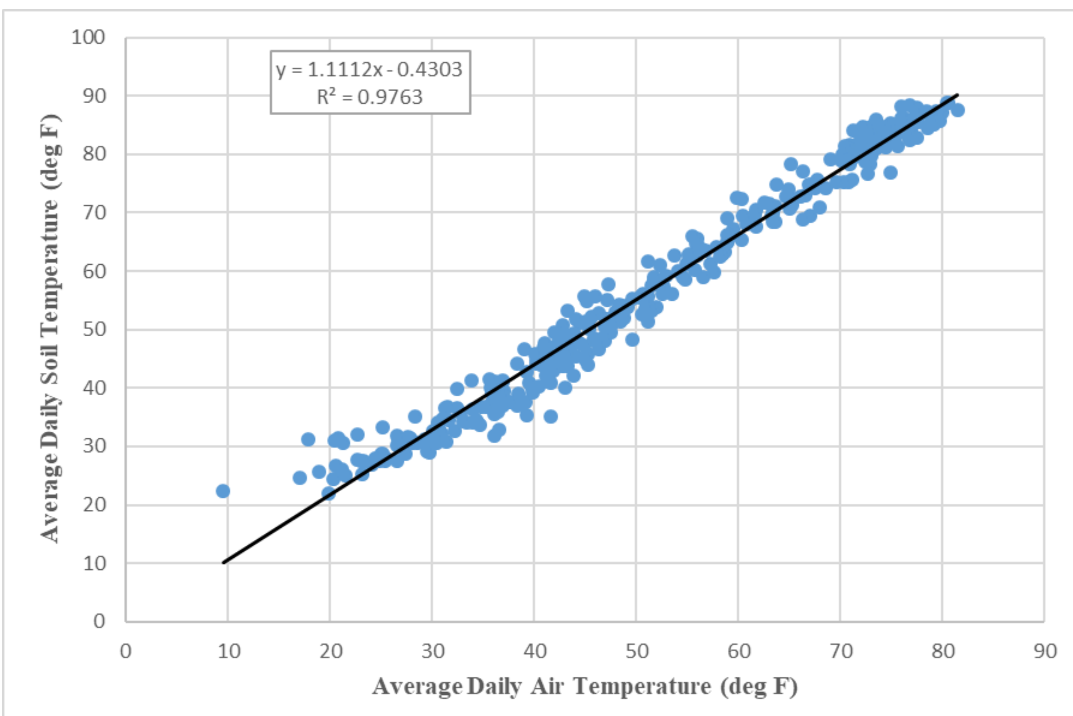


Figure 11. Comparison of average daily air and soil temperatures by regression shows the close relationship between the two parameters at Station 401.

Figure 12 shows the total daily precipitation for the monitoring stations between January 1, 2019, and December 31, 2019. Figure 13 shows the total cumulative precipitation for the same period. Precipitation for CY2019 totaled 152.7 mm (6.01 in) for Station 400, 135.6 mm (5.34 in) for Station 401, 159.0 mm (6.26 in) for Station 403, 162.3 mm (6.39 in) for Station 404, and 161.5 mm (6.36 in) for Station 405.

Most major precipitation events in CY2019 were widespread enough to be recorded by all stations, even though rain intensity varies by station and event. The largest precipitation events occurred in May 2019. The North American Monsoon was weak in the TTR area, with very little rainfall from June through October. The maximum daily precipitation at all stations (400, 401, 403, 404, and 405) occurred in the month of May, with values of 12.7 mm (0.50 in), 15.5 mm (0.61 in), 13.0 mm (0.51 in), 11.7 mm (0.46 in), and 12.2 mm (0.48 in), respectively.

Total annual precipitation in CY2019 for all five stations averaged 154.18 mm (6.07 in). This is higher than the historical average annual precipitation of 129.5 mm (5.10 in) measured at the Tonopah Airport from 1954 through 2019 (https://wrcc.dri.edu/WRCCWrappers.py?sodxtrmts+268170+por+por+pcpn+none+msum+5+01+F, accessed September 21, 2020). The Tonopah Airport also measured more precipitation than the long-term average, with annual precipitation for 2019 of 188.98 mm (7.44 in). Given the lack of summer monsoonal precipitation, the above-average annual precipitation measurements at all of the station gages demonstrate the importance of winter precipitation to the TTR annual record. Because non-heated rain gages are used at the TTR stations and rain gages only measure liquid water, snowfall (and total precipitation) may have been underestimated if the gages froze or if snow was blown or sublimated out of the gage before it melted.

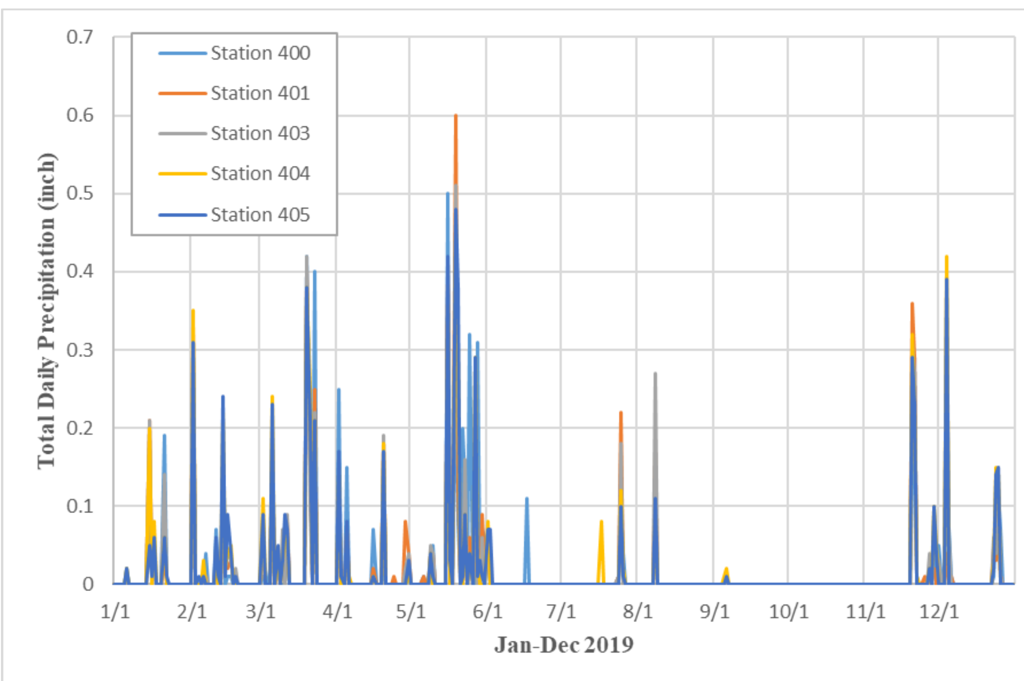


Figure 12. Total daily precipitation for Stations 400, 401, 403, 404, and 405 for CY2019.

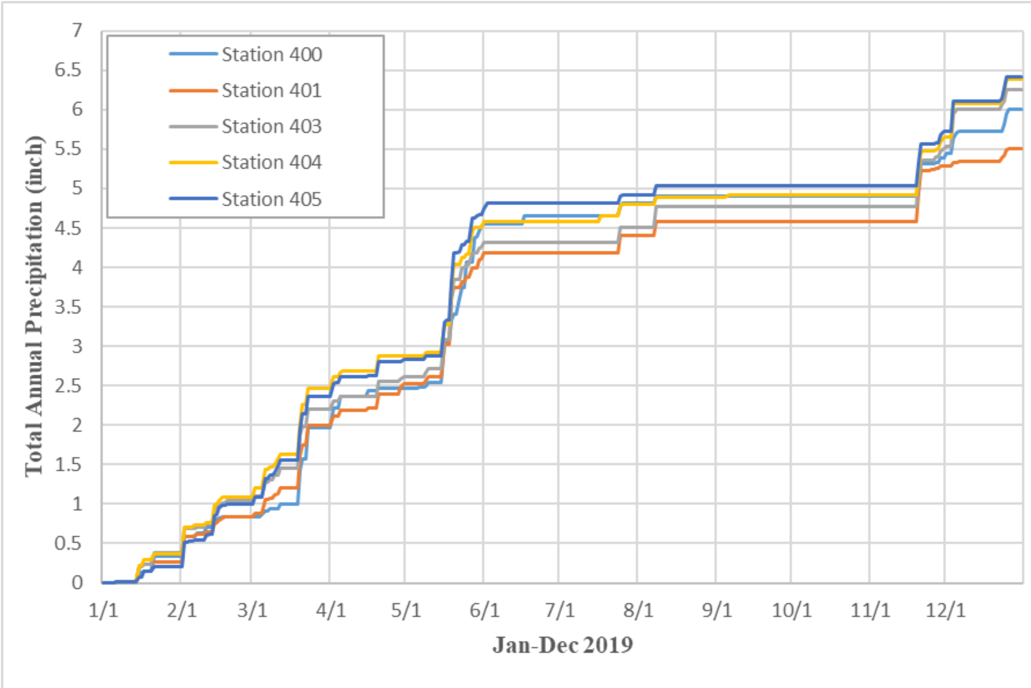


Figure 13. Cumulative precipitation for Stations 400, 401, 403, 404, and 405 for CY2019.

The water content of the top layer of soil is an important factor that affects entrainment of soil by high winds. Sufficiently high soil-moisture content also diminishes the soil material available for wind transport because moisture helps bind the soil particles together. Figure 14 shows the daily average VWC of the top layer of soil at each of the stations in CY2019. Increases in soil VWC coincided with precipitation events and subsequent decreases in VWC corresponded to drying periods. Soil moisture was highest at intermittent periods between February and June 2019, coinciding with rainfall events. The soils were driest in the late summer and autumn.

Figure 15 shows the daily average relative humidity for all stations for the monitoring period between January 1, 2019, and December 31, 2019. During precipitation events, the relative humidity increases to almost 100 percent (Appendix C includes the maximum reported values). During 2019, the lowest monthly average relative humidity was measured in August and varied between 18.25 percent and 20.12 percent at the stations (Appendix C). The highest monthly average relative humidity in 2019 was measured in December and varied between 71.27 percent and 77.35 percent (Appendix C).

Wind is likely the primary mechanism for soil transport at the Clean Slate sites. Wind rose diagrams (Figures 16, 17, and 18) were developed for the monitoring stations. Wind roses classify wind direction into 16 directional classes that occupy 22.5 degrees each, and the different colors indicate different wind speed classes. The frequency (percent of time) of each wind speed class and wind direction is indicated by the size of each band. In keeping with meteorological conventions, the wind direction indicated refers to the direction from which the wind is coming.

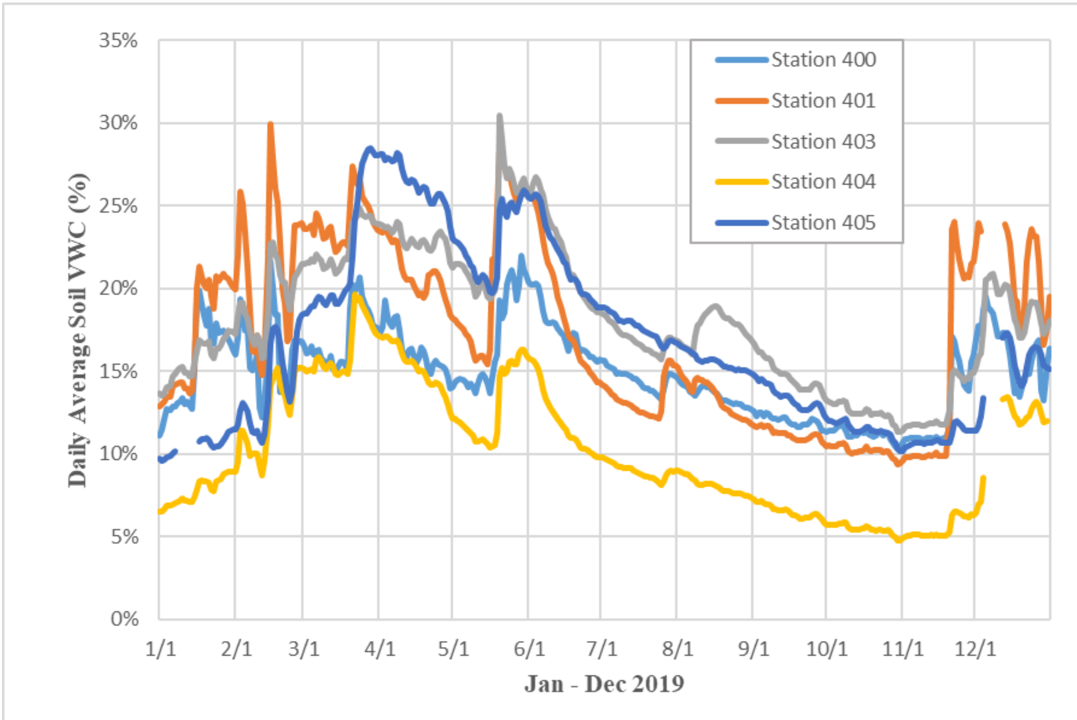


Figure 14. Soil volumetric water content for Stations 400, 401, 403, 404, and 405 for CY2019.

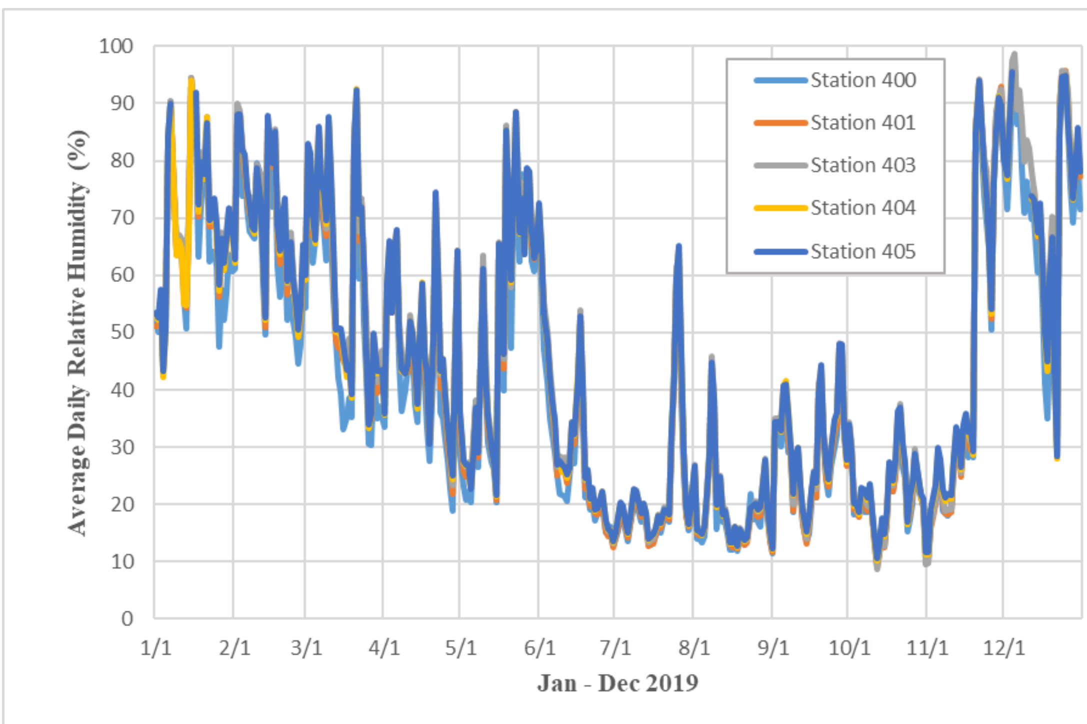


Figure 15. Average daily relative humidity for Stations 400, 401, 403, 404, and 405 for CY2019.

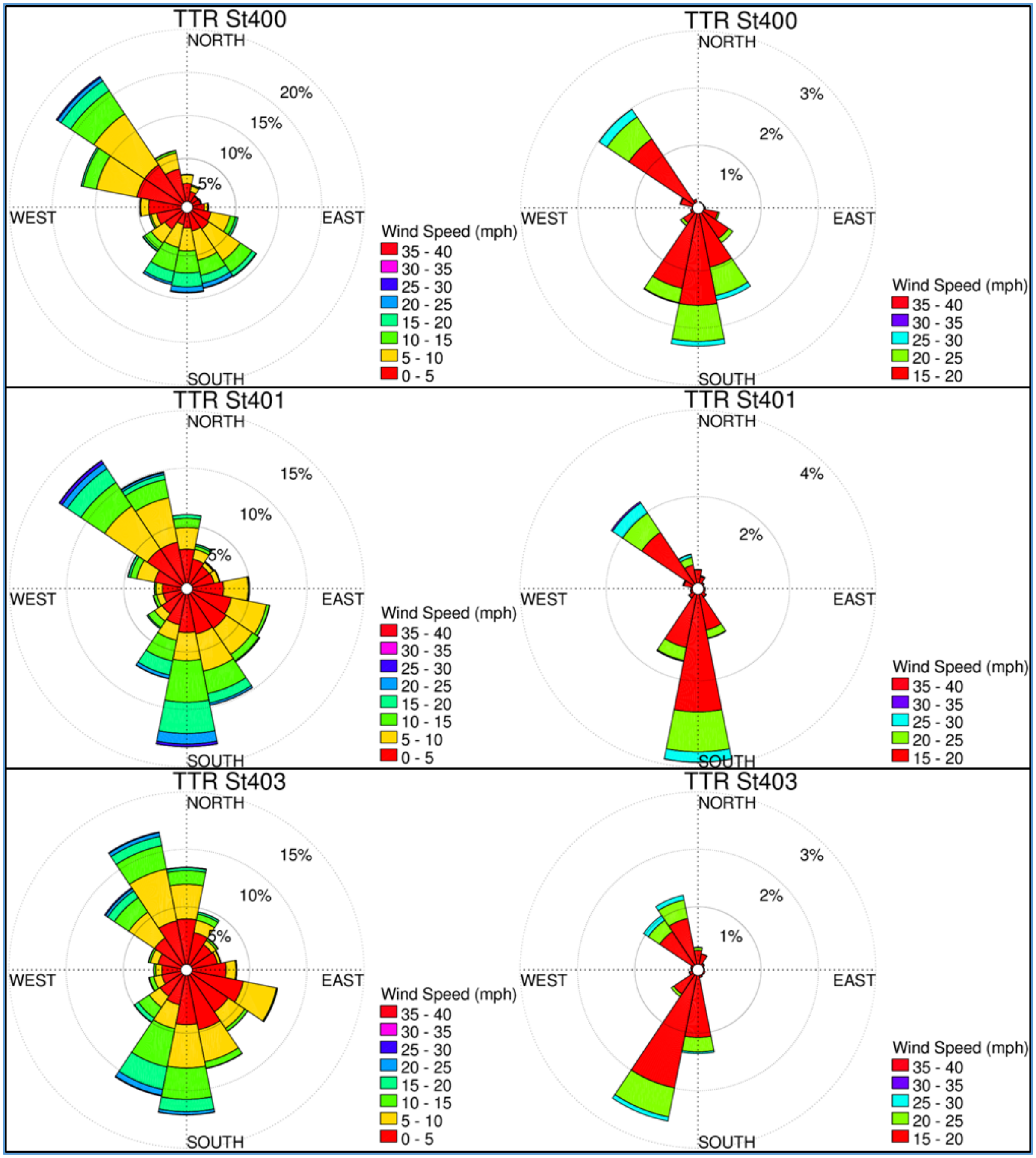


Figure 16. CY2019 annual wind roses for Station 400 at the ROC, and Stations 401 and 403 at Clean Slate III. Left panel: all winds. Right panel: winds greater than 24 km/hr (15 mph).

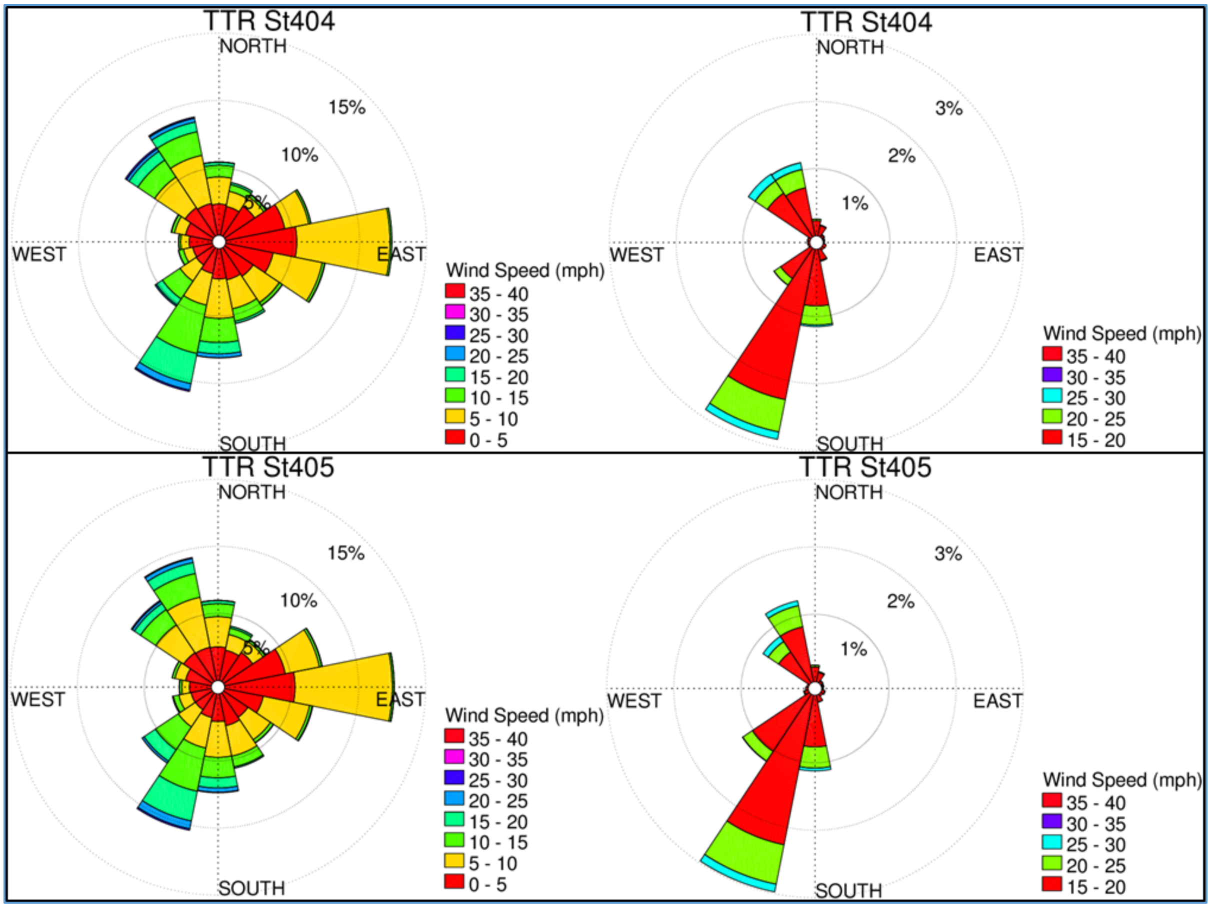


Figure 17. CY2019 annual wind roses for Stations 404 and 405 at Clean Slate II. Left panel: all winds. Right panel: winds greater than 24 km/hr (15 mph).

In Figures 16 and 17, each station has two wind roses for CY2019. The wind rose on the left shows all wind speeds and their contribution to the overall wind rose, whereas the wind rose on the right shows only winds above 24 kilometers per hour (km/hr) (15 miles per hour [mph]) because this is typically the speed above which wind-borne soil erosion has been observed at these sites (Mizell *et al.*, 2014).

In general, winds above 24 km/hr (15 mph) result in elevated $PM_{10}$ concentrations in the air. The $PM_{10}$ concentration is an indicator of small particles that are suspended in the air and can be easily inhaled. As seen in Figures 16 and 17, the most prevalent winds are from the south-southwest or northwest, especially for wind speeds above 24 km/hr (15 mph). Figure 18 shows the geographic context of the wind measurements. Winds out of the southerly and northwesterly directions are predominant and the strongest, and they generally align with the valley topography (Figure 18).

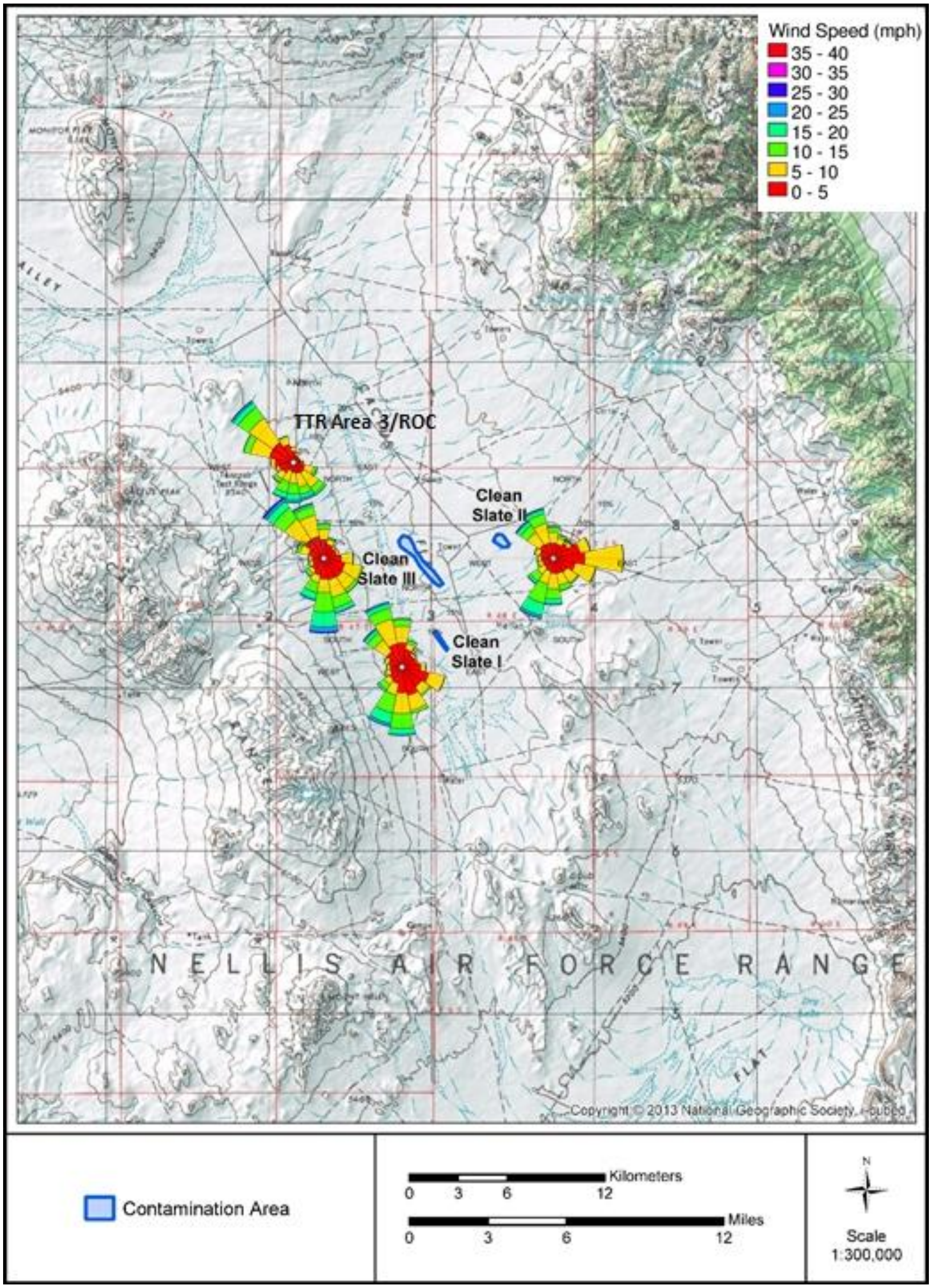


Figure 18. Wind rose diagrams for the TTR stations shown in relation to topography.

The generally southerly winds at Stations 403, 404, and 405 had a southwesterly component, whereas at Stations 400 and 401, the winds from that general direction were more frequently aligned due south. Although southerly and northwesterly winds were dominant, Stations 404 and 405 exhibited a relatively high frequency of moderate-strength winds from the east that was not evident at the other locations.

The time series of average daily wind speed exhibits a similar pattern for all stations (Figure 19). The maximum average monthly wind speed for all stations was recorded in February and ranged from 14.0 km/hr to 16.7 km/hr (8.7 mph and 10.4 mph) (Appendix C).

The highest 10-minute-interval, sustained wind speed of 2019 was 51.7 km/hr (32.1 mph), which was measured in November at Station 401. The highest sustained winds were variously measured in January, April, and May at the other stations. The maximum three-second-interval wind speed gust was recorded in June at Station 405, at a speed of 80.8 km/hr (50.2 mph) (Appendix C).

Figure 20 shows the average daily barometric pressure (atmospheric pressure) for all stations except Station 401, which is not equipped with a barometric pressure sensor. The fluctuations in barometric pressure provide an indicator of the passage of weather fronts that can often cause high winds. Differences between stations reflect variation in barometric pressure with elevation. The readings at the TTR stations are station pressures, not corrected to sea level equivalent. As a result, lower elevation stations have higher pressure readings.

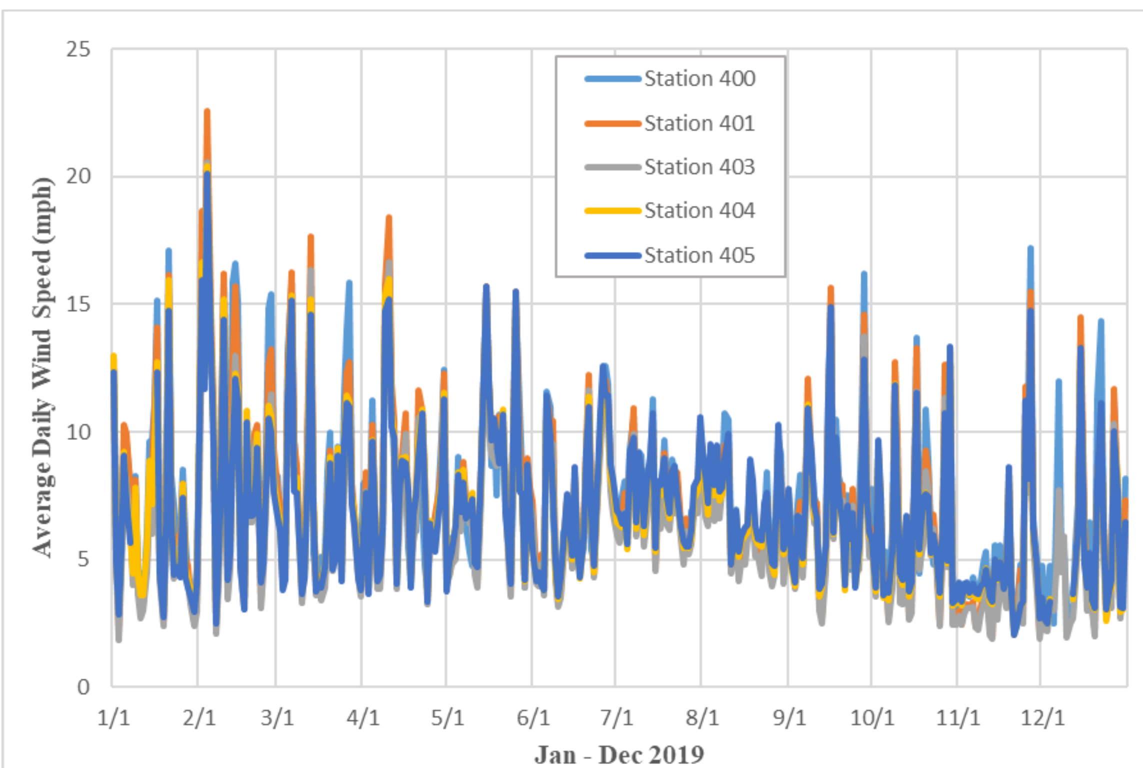


Figure 19. Average daily wind speed for Stations 400, 401, 403, 404, and 405 for CY2019.

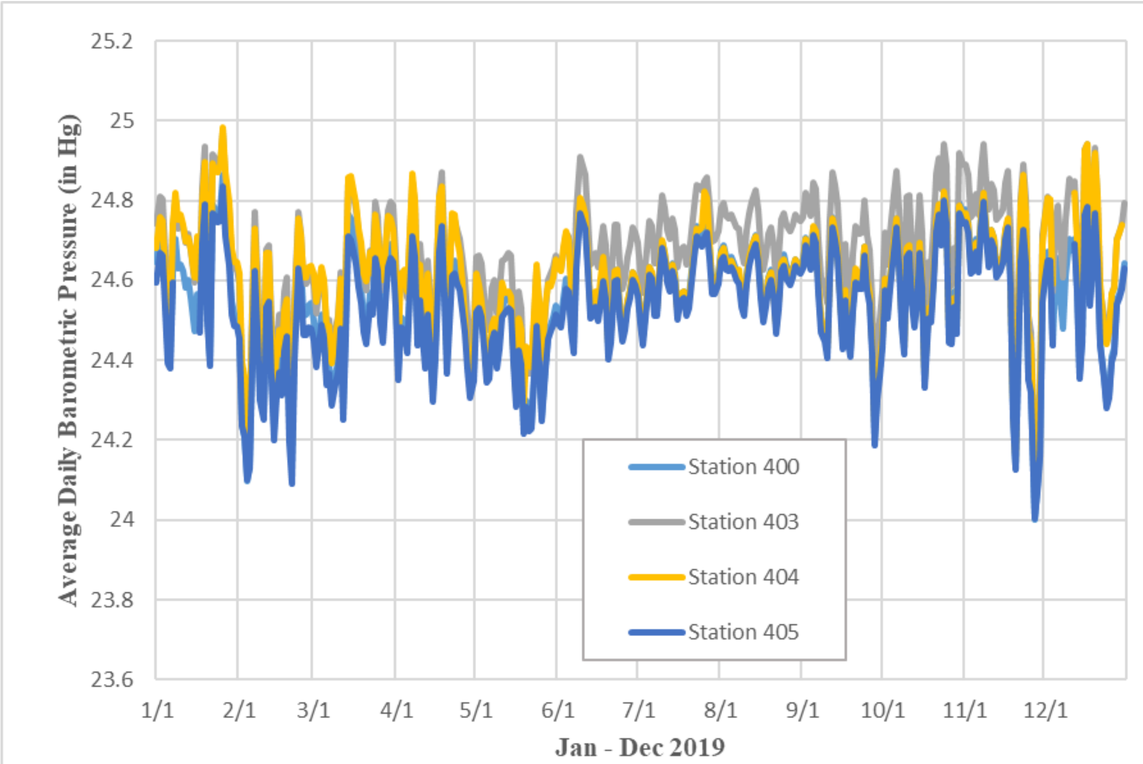


Figure 20. Average daily barometric pressure for Stations 400, 403, 404, and 405 for CY2019.

## SOIL/DUST TRANSPORT BY WIND

Soil movement initiated by wind is characterized as either surface creep, saltation, or suspension (Figure 21). Surface creep is a process by which particles are rolled across the ground surface by wind-generated shear stress and by impacts from saltating particles. Particles moved by creeping are generally over 500 µm (0.02 in) in aerodynamic diameter and are too heavy to be lifted into the air. Saltation is the mechanism by which soil particles in the range of 50 µm (0.002 in) to 500 µm (0.02 in) are transported. These particles are dislodged and carried a short distance in the air before falling back to the ground. Particle transport paths usually follow a parabolic trajectory as the particles bounce across the ground surface. The amount of time the particles are in the air and the distances traveled are functions of wind speed and particle mass. Saltation is important because the impact of saltating particles pushes creeping particles, which dislodge smaller particles that are then ejected into the air and transported via suspension. Suspended particles are usually smaller than 50 µm (0.002 in). Particles less than 20 µm (0.0008 in) in diameter can be entrained in the air by wind or from impacts with saltation-sized particles. Once these particles are suspended in the air, the particles can be transported over long distances. Fine-sized particles, which are particles with an aerodynamic diameter <10 µm (0.0004 in) ($PM_{10}$), are small enough to be inhaled by humans and are called "respirable suspended particles." The Clean Slate stations separately monitor particle movement by suspension and saltation, as described below.

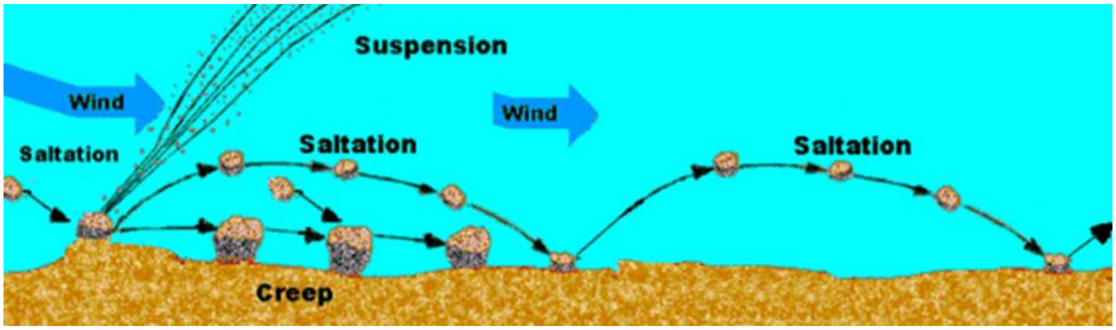

Figure 21. Diagram of the saltation process. The suspension of smaller particles ejected by the impact of a particle landing after saltation is depicted on the left. (The Weather Doctor, http://www.islandnet.com/~see/weather/elements/dustwind.htm, accessed December 7, 2015.)

## Observations of Soil/Dust Transport by Suspension

Suspended particles are counted using a Met One Ambient Particulate Profiler Model 212. Table 4 summarizes wind speed and the corresponding average annual $PM_{10}$ concentration by wind speed class for the monitoring stations. Approximately 90 percent or more of the time, the wind speed at all stations is below 24 km/hr (15 mph) and the corresponding average $PM_{10}$ concentrations are below 15 micrograms per cubic meter ($\mu g/m^3$). The $PM_{10}$ concentrations remain low until winds exceed 24 km/hr to 32 km/hr (15 mph to 20 mph). Although $PM_{10}$ concentrations generally increase as wind speed increases through most of the wind speed range, the average $PM_{10}$ concentration at Station 404, essentially levels off above 40 km/hr (25 mph).

At Station 400, the highest annual average $PM_{10}$ concentration was 69 $\mu g/m^3$ for winds greater than 48 km/hr (>30 mph). Station 400 is surrounded by asphalt and gravel-covered parking areas and the $PM_{10}$ measured at Station 400 is lower than at all the other stations for winds greater than 8 km/hr (5 mph). Both Stations 401 and 403 exhibit larger increases in $PM_{10}$ in the higher wind speed ranges than the other stations, with an average value of 807 $\mu g/m^3$ at Station 401 for winds in excess of 48 km/hr (>30 mph), and an average of 304 $\mu g/m^3$ during winds between 40 and 48 km/hr (25 and 30 mph) at Station 403. The average $PM_{10}$ measured at Stations 404 and 405 for winds greater than 40 km/hr (25 mph) (87 $\mu g/m^3$ and 50 $\mu g/m^3$, respectively) is less than half that measured in CY2018 and CY2017, when remediation of Clean Slate II occurred.

The overall frequency of various wind speeds was similar at all stations (Figure 22), although wind velocity greater than 48 km/hr (30 mph) was more common at Station 401 and absent at Stations 403 and 405. Light winds (0 km/hr to 16 km/hr [0 mph to 10 mph]) were the most common. Wind speeds in excess of 24 km/hr (15 mph) occurred less than 10 percent of the time and wind speeds in excess of 32 km/hr (20 mph) occurred less than 3 percent of the time. Stations 400, 401, and 403 exhibit an increase in average $PM_{10}$ concentration in an approximately exponential pattern with increases in wind speed, as does Station 404 until $PM_{10}$ levels off at wind speeds greater than 48 km/hr (30 mph) (Figure 23). Dust concentrations at Station 405 remained below 15 $\mu g/m^3$ throughout the wind speed range observed. Figure 24 shows similar trends between monitoring stations for annual average $PM_{2.5}$ concentration and corresponding wind speed class.

Table 4. Summary of wind speed and $PM_{10}$ data for monitoring stations during CY2019. $PM_{10}$ is reconstructed from the Met One aerosol particle size instrument.

| Wind Speed Class (mph) | Duration (hours) | Frequency (%) | Cumulative Frequency (%) | Average Wind Speed (mph) | $PM_{10}$* ($\mu g/m^3$) |
|---|---|---|---|---|---|
| **Station 400** | | | | | |
| 0-5 | 3,583.67 | 40.909% | 40.909% | 3.2 | 4.5 |
| 5-10 | 3,014.83 | 34.416% | 75.325% | 7.1 | 3.4 |
| 10-15 | 1,392.83 | 15.900% | 91.225% | 12.3 | 4.6 |
| 15-20 | 564.50 | 6.444% | 97.669% | 17.0 | 5.6 |
| 20-25 | 174.00 | 1.986% | 99.656% | 22.0 | 14.0 |
| 25-30 | 29.67 | 0.339% | 99.994% | 26.3 | 36.7 |
| >30 | 0.50 | 0.006% | 100.000% | 30.8 | 69.4 |
| Total Hours | 8,760.00 | N/A | N/A | N/A | N/A |
| **Station 401** | | | | | |
| 0-5 | 3,896.33 | 45.265% | 45.265% | 2.8 | 7.1 |
| 5-10 | 2,555.00 | 29.682% | 74.947% | 7.1 | 8.4 |
| 10-15 | 1,281.50 | 14.888% | 89.835% | 12.3 | 13.0 |
| 15-20 | 632.67 | 7.350% | 97.185% | 17.1 | 24.1 |
| 20-25 | 185.17 | 2.151% | 99.336% | 21.9 | 84.5 |
| 25-30 | 51.83 | 0.602% | 99.938% | 27.1 | 213.2 |
| >30 | 5.33 | 0.062% | 100.000% | 30.9 | 807.4 |
| Total Hours | 8,607.83 | N/A | N/A | N/A | N/A |
| **Station 403** | | | | | |
| 0-5 | 4,462.33 | 50.940% | 50.940% | 2.8 | 4.1 |
| 5-10 | 2,480.83 | 28.320% | 79.260% | 7.0 | 6.6 |
| 10-15 | 1,202.83 | 13.731% | 92.991% | 12.2 | 6.1 |
| 15-20 | 468.33 | 5.346% | 98.337% | 17.0 | 9.7 |
| 20-25 | 121.00 | 1.381% | 99.718% | 22.0 | 31.0 |
| 25-30 | 24.67 | 0.282% | 100.000% | 26.6 | 304.2 |
| >30 | 0.00 | 0.000% | 100.000% | N/A | N/A |
| Total Hours | 8,760.00 | N/A | N/A | N/A | N/A |
| **Station 404** | | | | | |
| 0-5 | 3,770.00 | 43.308% | 43.308% | 3.1 | 7.2 |
| 5-10 | 3,079.50 | 35.376% | 78.685% | 6.8 | 9.2 |
| 10-15 | 1,200.33 | 13.789% | 92.474% | 12.3 | 7.8 |
| 15-20 | 498.83 | 5.730% | 98.204% | 17.1 | 12.5 |
| 20-25 | 125.50 | 1.442% | 99.646% | 22.0 | 23.5 |
| 25-30 | 30.67 | 0.352% | 99.998% | 26.9 | 86.7 |
| >30 | 0.17 | 0.002% | 100.000% | 30.1 | 83.6 |
| Total Hours | 8,705.00 | N/A | N/A | N/A | N/A |
| **Station 405** | | | | | |
| 0-5 | 3,681.00 | 42.650% | 42.650% | 3.1 | 7.0 |
| 5-10 | 3,108.50 | 36.017% | 78.667% | 6.8 | 7.6 |
| 10-15 | 1,164.17 | 13.489% | 92.156% | 12.3 | 7.0 |
| 15-20 | 509.67 | 5.905% | 98.061% | 17.1 | 11.0 |
| 20-25 | 139.33 | 1.614% | 99.676% | 21.9 | 18.2 |
| 25-30 | 28.00 | 0.324% | 100.000% | 26.5 | 49.5 |
| >30 | 0.00 | 0.000% | 100.000% | N/A | N/A |
| Total Hours | 8,630.67 | N/A | N/A | N/A | N/A |

N/A = not applicable.

Note: mph can be converted to km/hr by multiplying by 1.6.

* Ten-minute average concentrations reconstructed from the Met One aerosol particle size instrument.

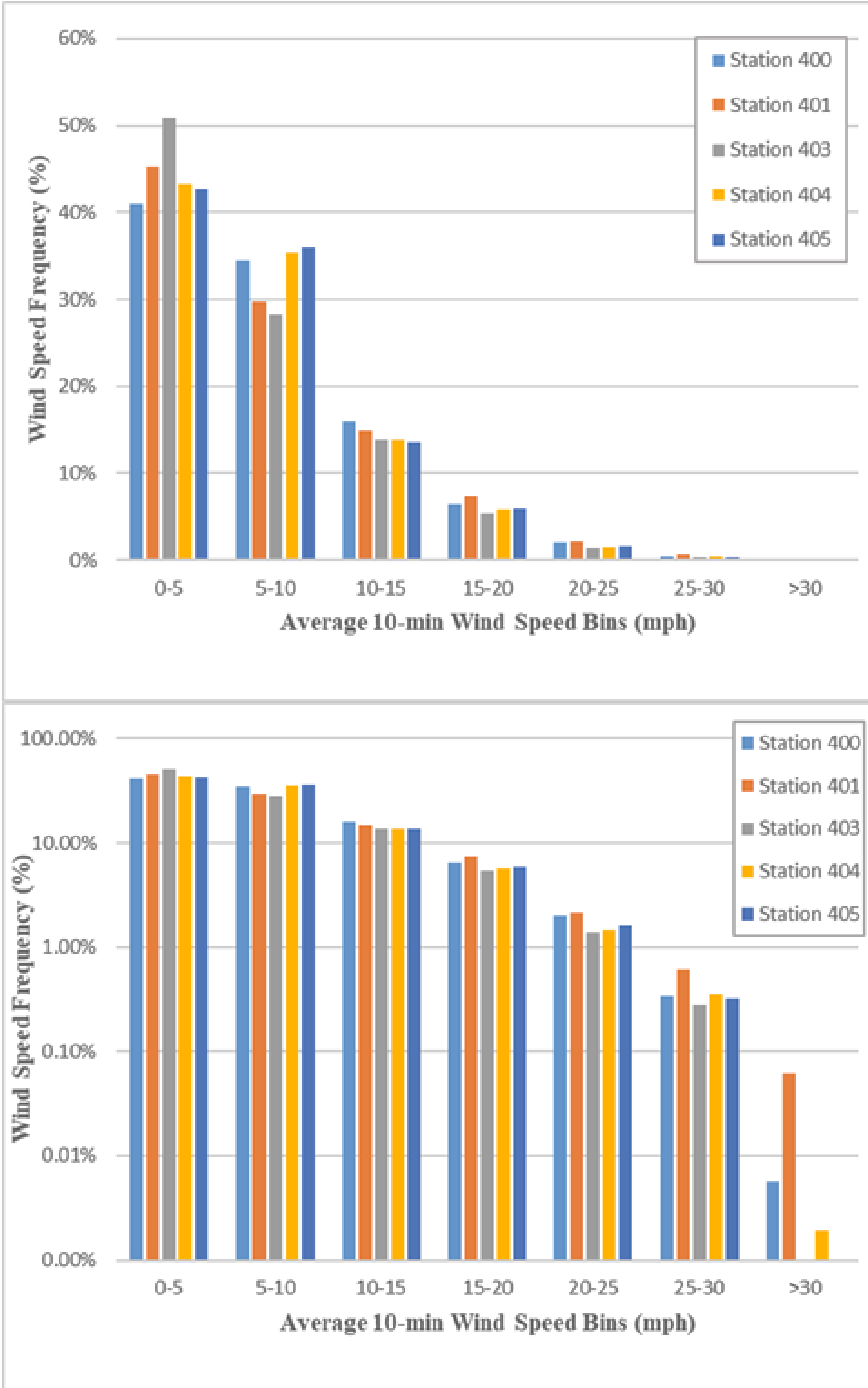


Figure 22. Wind speed frequency (top: linear scale; bottom: logarithmic scale) by wind class for Stations 400, 401, 403, 404, and 405 for CY2019.

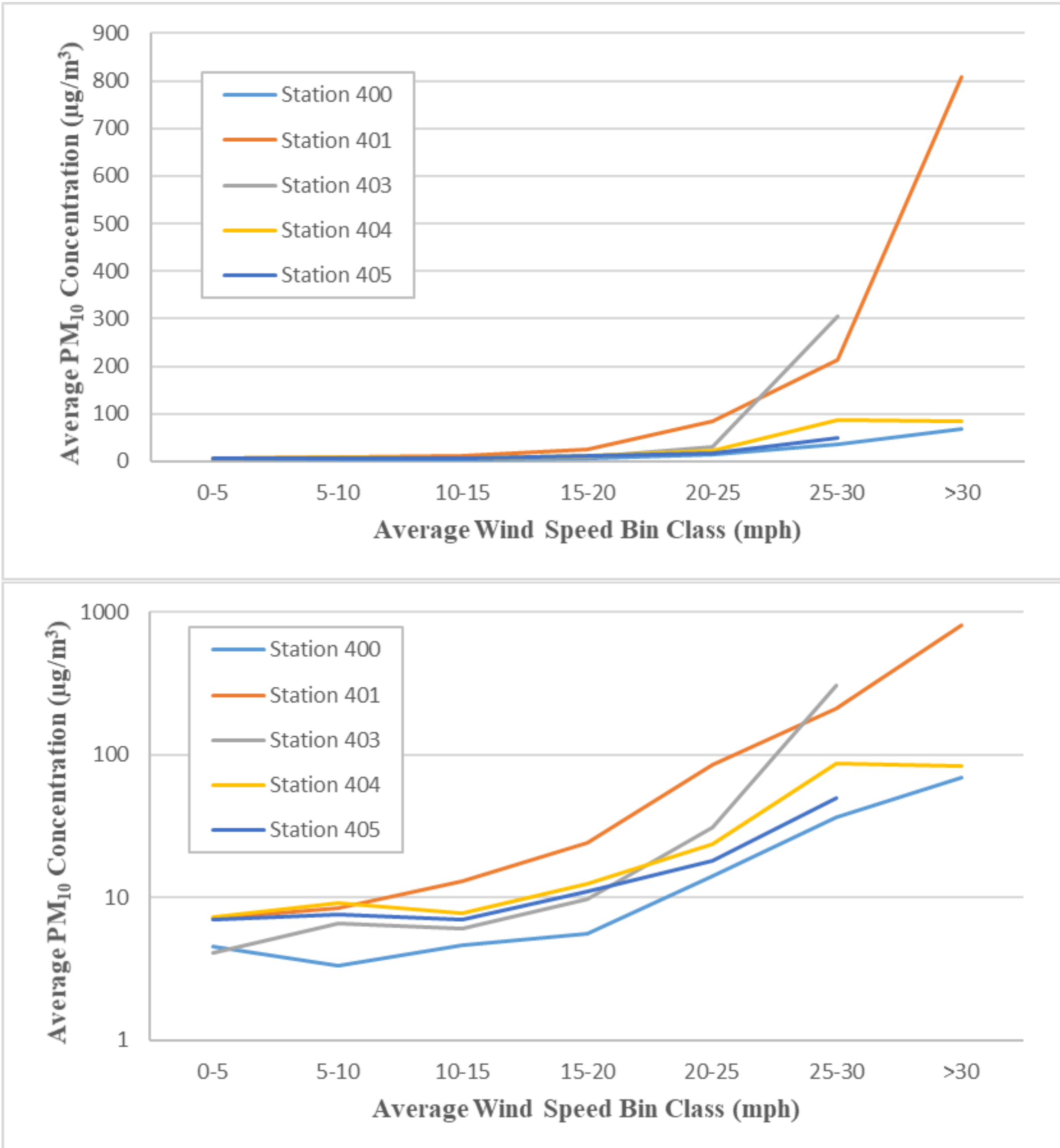


Figure 23. $PM_{10}$ trends as a function of wind speed at the monitoring stations for CY2019. Average $PM_{10}$ concentration is plotted on both a linear scale (top) and logarithmic scale (bottom).

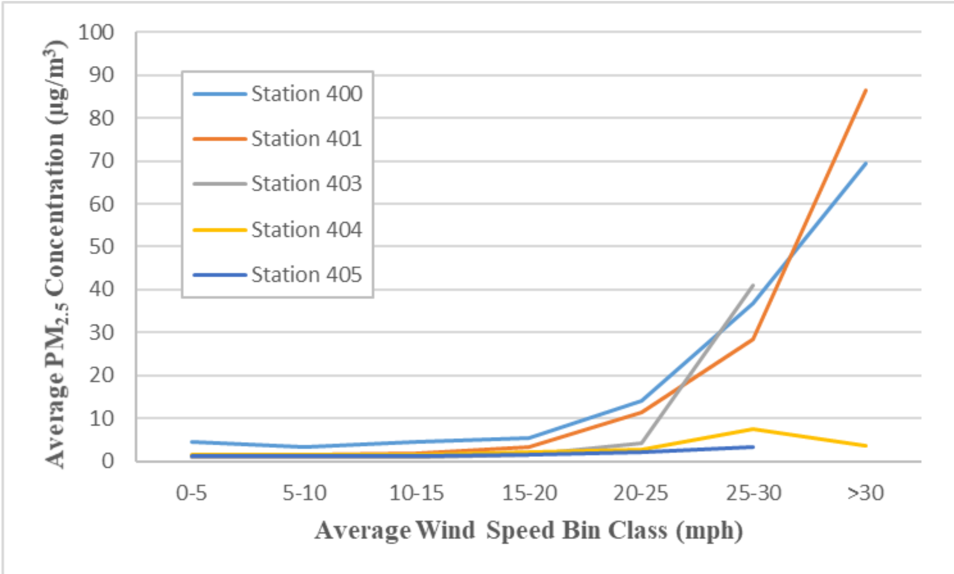


Figure 24. $PM_{2.5}$ trends as a function of wind speed for the monitoring stations for CY2019.

## Comparison of Soil/Dust Transport by Suspension during Northerly and Southerly Winds

The $PM_{10}$ transport was previously evaluated (Mizell *et al.*, 2014; Nikolich *et al.*, 2015) by establishing relationships between different wind speed classes and the corresponding average $PM_{10}$ concentration. The data indicated an exponential-type increase in $PM_{10}$ concentration as wind speeds increased over 24 km/hr (15 mph). Table 5 shows the frequency of winds from the south and northwest compared with all winds based on wind speed class. For all five stations, winds from the south and northwest account for over 85 percent of winds above 24 km/hr (15 mph), which are the winds that generally cause saltation and dust transport.

Table 6 and Figure 25 show the average wind speed and the corresponding average $PM_{10}$ concentration for southerly and northwesterly winds. Southerly winds are defined as a 90 degree range centered on the south axis (from 135 to 225 degrees) and northwesterly winds are defined as between due west and due north (270 to 360 degrees). During 2019, winds over 24 km/hr (15 mph) occurred more frequently out of the south than the northwest. The associated $PM_{10}$ for south and northwest winds slower than 24 km/hr (15 mph) was comparable. At all stations, $PM_{10}$ tended to be higher for winds from the northwest compared with winds from the south for winds greater than 24 km/hr (15 mph). The $PM_{10}$ concentration generally increased with increasing wind speed for all station and wind directions, although a decline in $PM_{10}$ at the highest wind speed was observed for winds from the south at Station 400 and winds from the northwest at Station 404 (Figure 25).

Table 5. Summary of wind speed, duration, and direction data for all stations for CY2019.

| | Wind Speed Class (mph) | Total Duration (hours) | Duration from South (hours) | Duration from Northwest (hours) | Portion of Time from South and Northwest (%) |
|---|---|---|---|---|---|
| **Station 400** | 0-5 | 3,583.67 | 672.33 | 1,578.17 | 62.8% |
| | 5-10 | 3,014.83 | 1,050.67 | 1,271.33 | 77.0% |
| | 10-15 | 1,392.83 | 747.50 | 444.00 | 85.5% |
| | 15-20 | 564.50 | 368.00 | 141.50 | 90.3% |
| | 20-25 | 174.00 | 125.33 | 40.67 | 95.4% |
| | 25-30 | 29.67 | 15.33 | 14.00 | 98.9% |
| | >30 | 0.50 | 0.33 | 0.17 | 100.0% |
| | Total hours | 8,760.00 | 2,979.50 | 3,489.83 | 73.9% |
| **Station 401** | 0-5 | 3,896.33 | 1,133.50 | 1,174.33 | 59.2% |
| | 5-10 | 2,555.00 | 756.33 | 950.17 | 66.8% |
| | 10-15 | 1,281.50 | 685.33 | 431.67 | 87.2% |
| | 15-20 | 632.67 | 404.33 | 182.50 | 92.8% |
| | 20-25 | 185.17 | 118.67 | 61.83 | 97.5% |
| | 25-30 | 51.83 | 22.17 | 28.83 | 98.4% |
| | >30 | 5.33 | 0.67 | 4.33 | 93.8% |
| | Total hours | 8,607.83 | 3,121.00 | 2,833.67 | 69.2% |
| **Station 403** | 0-5 | 4,462.33 | 1,333.17 | 1,079.50 | 54.1% |
| | 5-10 | 2,480.83 | 876.00 | 844.67 | 69.4% |
| | 10-15 | 1,202.83 | 628.00 | 376.17 | 83.5% |
| | 15-20 | 468.33 | 283.33 | 140.00 | 90.4% |
| | 20-25 | 121.00 | 66.00 | 51.67 | 97.2% |
| | 25-30 | 24.67 | 8.50 | 15.33 | 96.6% |
| | >30 | 0.00 | 0.00 | 0.00 | N/A |
| | Total hours | 8,760.00 | 3,195.00 | 2,507.33 | 65.1% |
| **Station 404** | 0-5 | 3,770.00 | 768.33 | 881.00 | 43.7% |
| | 5-10 | 3,079.50 | 825.50 | 734.33 | 50.7% |
| | 10-15 | 1,200.33 | 648.00 | 346.67 | 82.9% |
| | 15-20 | 498.83 | 310.83 | 141.17 | 90.6% |
| | 20-25 | 125.50 | 72.50 | 47.17 | 95.4% |
| | 25-30 | 30.67 | 11.33 | 18.83 | 98.4% |
| | >30 | 0.17 | 0.00 | 0.17 | 100.0% |
| | Total hours | 8,705.00 | 2,636.50 | 2,169.33 | 55.2% |
| **Station 405** | 0-5 | 3,681.00 | 733.00 | 957.33 | 45.9% |
| | 5-10 | 3,108.50 | 769.17 | 741.00 | 48.6% |
| | 10-15 | 1,164.17 | 596.83 | 335.17 | 80.1% |
| | 15-20 | 509.67 | 322.67 | 129.17 | 88.7% |
| | 20-25 | 139.33 | 84.83 | 44.33 | 92.7% |
| | 25-30 | 28.00 | 13.33 | 14.00 | 97.6% |
| | >30 | 0.00 | 0.00 | 0.00 | N/A |
| | Total hours | 8,630.67 | 2,519.83 | 2,221.00 | 54.9% |

Note: mph can be converted to km/hr by multiplying by 1.6.

Table 6. Summary of wind and $PM_{10}$ data for all stations for CY2019.

| | Wind Speed Class* (mph) | South Average Wind Speed (mph) | Northwest Average Wind Speed (mph) | Average $PM_{10}$ ** for South Wind ($\mu g/m^3$) | Average $PM_{10}$ ** for Northwest Wind ($\mu g/m^3$) |
|---|---|---|---|---|---|
| **Station 400** | 0-5 | 3.32 | 3.30 | 4.97 | 4.43 |
| | 5-10 | 7.26 | 7.09 | 3.15 | 3.39 |
| | 10-15 | 12.40 | 12.12 | 3.40 | 6.32 |
| | 15-20 | 17.07 | 16.95 | 4.21 | 9.16 |
| | 20-25 | 21.98 | 22.15 | 6.06 | 37.29 |
| | 25-30 | 26.07 | 26.49 | 5.35 | 66.94 |
| | >30 | 30.83 | 30.62 | 0.72 | 138.09 |
| **Station 401** | 0-5 | 2.80 | 2.58 | 6.39 | 9.33 |
| | 5-10 | 7.36 | 7.21 | 8.48 | 7.93 |
| | 10-15 | 12.45 | 12.17 | 11.60 | 17.36 |
| | 15-20 | 17.15 | 17.05 | 21.06 | 34.15 |
| | 20-25 | 21.89 | 22.07 | 78.37 | 94.56 |
| | 25-30 | 26.82 | 27.27 | 207.53 | 220.00 |
| | >30 | 31.01 | 30.80 | 746.43 | 871.56 |
| **Station 403** | 0-5 | 2.78 | 2.81 | 4.24 | 3.96 |
| | 5-10 | 7.28 | 7.17 | 6.01 | 8.90 |
| | 10-15 | 12.32 | 12.13 | 5.72 | 7.56 |
| | 15-20 | 17.06 | 17.03 | 7.24 | 16.01 |
| | 20-25 | 21.90 | 22.29 | 12.50 | 53.84 |
| | 25-30 | 26.63 | 26.62 | 11.49 | 458.11 |
| | >30 | N/A | N/A | N/A | N/A |
| **Station 404** | 0-5 | 3.06 | 2.70 | 7.45 | 7.28 |
| | 5-10 | 7.31 | 7.23 | 9.60 | 10.92 |
| | 10-15 | 12.37 | 12.11 | 8.33 | 8.14 |
| | 15-20 | 17.09 | 17.16 | 11.50 | 16.06 |
| | 20-25 | 21.87 | 22.25 | 16.81 | 34.01 |
| | 25-30 | 26.80 | 26.92 | 21.45 | 126.05 |
| | >30 | N/A | 30.05 | N/A | 83.61 |
| **Station 405** | 0-5 | 2.97 | 2.51 | 6.78 | 6.44 |
| | 5-10 | 7.30 | 7.24 | 8.62 | 5.95 |
| | 10-15 | 12.38 | 12.14 | 7.45 | 6.58 |
| | 15-20 | 17.16 | 17.13 | 10.07 | 14.93 |
| | 20-25 | 21.94 | 22.08 | 15.18 | 24.46 |
| | 25-30 | 26.47 | 26.57 | 22.85 | 74.80 |
| | >30 | N/A | N/A | N/A | N/A |

Note: mph can be converted to km/hr by multiplying by 1.6.

*Based on 10-minute averages.

** Ten-minute average concentrations reconstructed from the Met One aerosol particle size instrument.

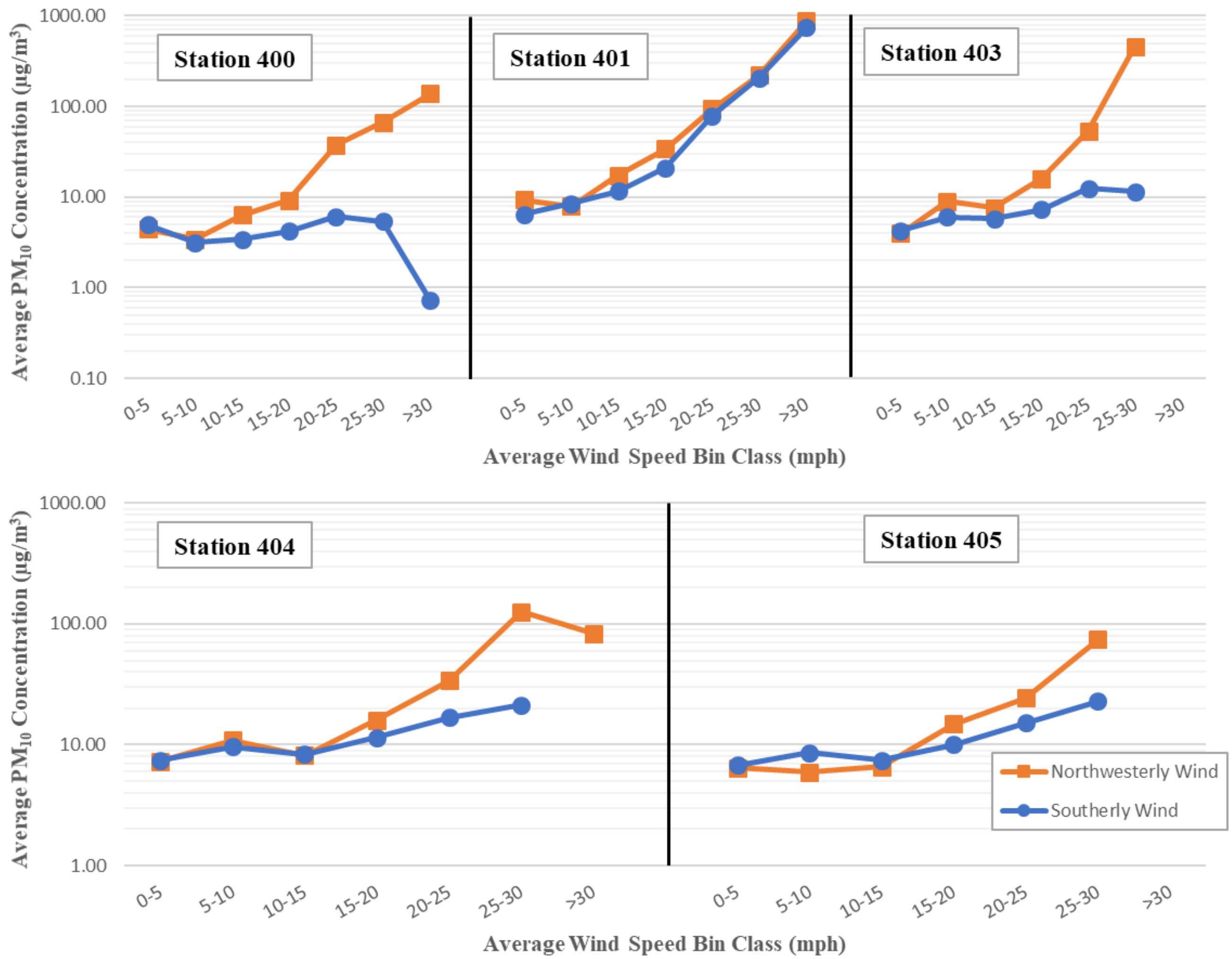


Figure 25. $PM_{10}$ trends as a function of wind speed and direction for CY2019. Average $PM_{10}$ concentration is plotted on a logarithmic scale to show the wide range of $PM_{10}$ concentrations among these sites.

## Effect of Site Remediation on Soil/Dust Transport by Suspension

Site remediation at Clean Slate II and III involved removing contaminated soil and debris from each area, sealing it in containers during transportation, and transporting it to a radioactive waste management facility on the Nevada National Security Site (NNSS). Dust can be generated directly by the soil disturbance associated with contaminant removal activities within the CA and by the associated increased vehicle and equipment movement and traffic in and outside the CA. These activities also increase the potential for the suspension of dust and soil by winds blowing across the disturbed surface, even after the activities conclude. During remediation, disturbed surfaces were sprayed with water to suppress dust. Remediation activities concluded at Clean Slate II on July 26, 2018, almost a half year prior to CY2019, whereas remediation was active at Clean Slate III during 2019 until the end of August (Table 1). The dust concentrations at the Clean Slate II stations (404 and 405) were much lower in 2019 than observed during site remediation activities in previous years. The $PM_{10}$ measured at the Clean Slate III monitoring stations (401 and 403) was higher than that measured at the Clean Slate II monitoring stations in 2019. In the "Discussion" section of this report, discrete wind events recorded by the monitoring stations at Clean Slate II and III are examined for the effect of site remediation on the suspension of soil and dust and radionuclide concentrations.

## Observations of Soil/Dust Transport by Saltation

Real-time sand saltation at Stations 401, 403, 404, and 405 was monitored using the Sensit H11-LIN (Sensit, Inc., Redlands, California) sand movement sensor. Sand particle saltation was strongly dependent on wind speed (Table 7 and Figure 26). The counts of saltation particles increased exponentially with increases in wind speed. Above a threshold wind speed of 32 km/hr to 40 km/hr (20 mph to 25 mph) at Stations 403, 404, and 405 (measured at 3 m [10 ft] above ground level), a significant increase in saltation counts was observed. A similar increase occurs at Station 401 above a threshold of 16 km/hr to 24 km/hr (10 mph to 15 mph). There is a positive correlation between $PM_{10}$ and saltation counts (Figure 27).

The first BSNE saltation samples of CY2019 were collected in February 2019 and consisted of dust and sand that entered into the BSNE traps between September 26, 2018, and February 12, 2019. The second collection period extended from February 13, 2019, until September 25, 2019. Details of the collection process can be found in previous annual monitoring reports (e.g., Chapman *et al*. [2017]). Table 8 provides the individual trap identifiers, the collection period, and the weight of collected material. Table 9 shows the results of laboratory gravimetric analysis based on the particle size fraction for the combined trap sets (all three traps with collectors facing toward a contaminated area were combined, as were all three collectors facing away from a contaminated area). At Clean Slate II and III, odd-numbered BSNEs collect material moving from the contaminated area (the trap faces the site) and even-numbered BSNEs collect material moving toward the contaminated area (the trap faces away from the site).

Table 7. Average saltation particle impact counts by wind speed class during CY2019.

| Wind Speed Class (mph) | Duration (hours) | Average Wind Speed (mph) | Average Particle Counts (count/10-min) |
|---|---|---|---|
| **Station 401** | | | |
| 0-5 | 3,896.17 | 2.80 | 0.00 |
| 5-10 | 2,554.83 | 7.10 | 0.05 |
| 10-15 | 1,281.33 | 12.31 | 0.83 |
| 15-20 | 632.67 | 17.09 | 15.68 |
| 20-25 | 185.17 | 21.92 | 24.87 |
| 25-30 | 51.83 | 27.05 | 16.39 |
| >30 | 5.33 | 30.88 | 30.88 |
| Total Hours | 8,607.33 | N/A | N/A |
| **Station 403** | | | |
| 0-5 | 4,462.33 | 2.80 | 0.01 |
| 5-10 | 2,480.83 | 7.04 | 0.12 |
| 10-15 | 1,202.83 | 12.21 | 0.29 |
| 15-20 | 468.33 | 17.00 | 1.40 |
| 20-25 | 121.00 | 22.04 | 4.07 |
| 25-30 | 24.67 | 26.62 | 15.55 |
| >30 | 0.00 | N/A | N/A |
| Total Hours | 8,760.00 | N/A | N/A |
| **Station 404** | | | |
| 0-5 | 3,770.00 | 3.15 | 3.58 |
| 5-10 | 3,079.50 | 6.83 | 1.15 |
| 10-15 | 1,200.33 | 12.26 | 0.57 |
| 15-20 | 498.83 | 17.09 | 0.99 |
| 20-25 | 125.50 | 21.98 | 4.25 |
| 25-30 | 30.67 | 26.87 | 13.74 |
| >30 | 0.17 | 30.05 | 30.05 |
| Total Hours | 8,705.00 | N/A | N/A |
| **Station 405** | | | |
| 0-5 | 3,681.00 | 3.12 | 0.41 |
| 5-10 | 3,108.33 | 6.84 | 0.03 |
| 10-15 | 1,164.17 | 12.26 | 0.40 |
| 15-20 | 509.67 | 17.09 | 3.09 |
| 20-25 | 139.33 | 21.92 | 3.88 |
| 25-30 | 28.00 | 26.50 | 16.05 |
| >30 | 0.00 | N/A | N/A |
| Total Hours | 8,630.50 | N/A | N/A |

N/A = not applicable.

Note: mph can be converted to km/hr by multiplying by 1.6.

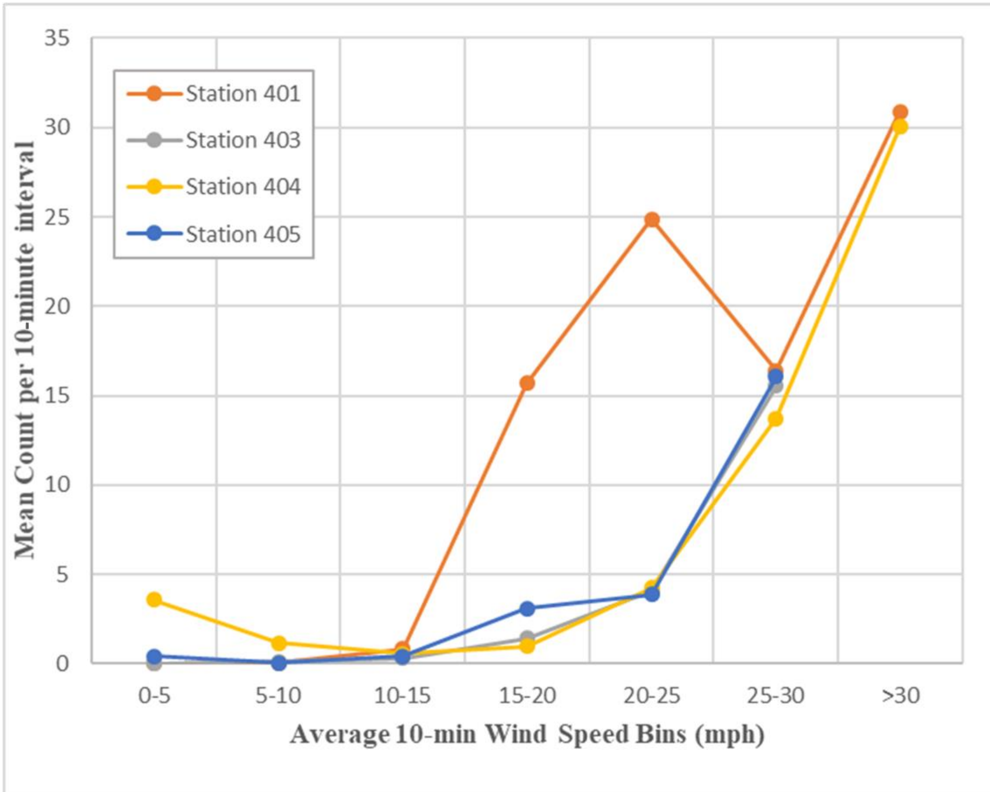


Figure 26. Relationships of particle counts and wind speed.

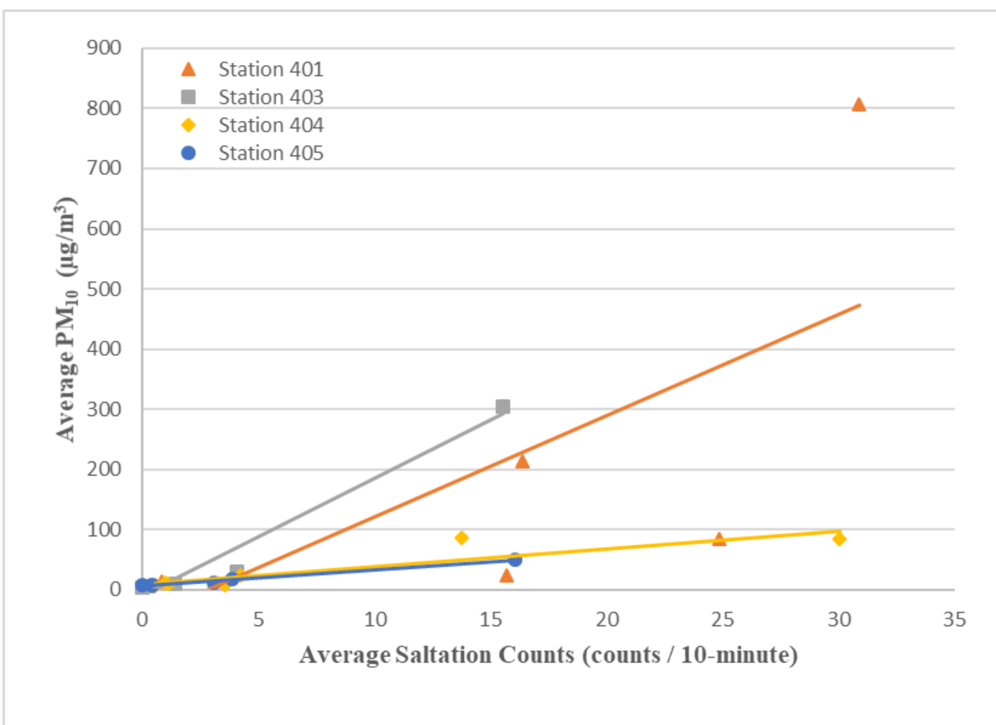


Figure 27. Regression of $PM_{10}$ against saltation counts by wind speed class.

Table 8. Field weights of collected saltation samples and collection dates.

| Site | Station | BSNE # | Orientation Relative to Contaminated Area* | Start Date | End Date | Total Mass (g) |
|---|---|---|---|---|---|---|
| Clean Slate II North | 404 | 61, 63, 65 | toward | 26-Sep-18 | 12-Feb-19 | 1.26 |
| Clean Slate II North | 404 | 62, 64, 66 | away | 26-Sep-18 | 12-Feb-19 | 1.44 |
| Clean Slate II South | 405 | 67, 69, 71 | toward | 26-Sep-18 | 12-Feb-19 | 0.69 |
| Clean Slate II South | 405 | 68, 70, 72 | away | 26-Sep-18 | 12-Feb-19 | 0.51 |
| Clean Slate III North | 401 | 13, 15, 17 | toward | 26-Sep-18 | 12-Feb-19 | 3.51 |
| Clean Slate III North | 401 | 14, 16, 18 | away | 26-Sep-18 | 12-Feb-19 | 2.52 |
| Clean Slate III South | 403 | 19, 21, 23 | toward | 26-Sep-18 | 12-Feb-19 | 0.87 |
| Clean Slate III South | 403 | 20, 22, 24 | away | 26-Sep-18 | 12-Feb-19 | 0.90 |
| Clean Slate II North | 404 | 49, 51, 53 | toward | 13-Feb-19 | 25-Sep-19 | 2.39 |
| Clean Slate II North | 404 | 50, 52, 54 | away | 13-Feb-19 | 25-Sep-19 | 2.53 |
| Clean Slate II South | 405 | 55, 57, 59 | toward | 13-Feb-19 | 25-Sep-19 | 3.57 |
| Clean Slate II South | 405 | 56, 58, 60 | away | 13-Feb-19 | 25-Sep-19 | 1.50 |
| Clean Slate III North | 401 | 1, 3, 5 | toward | 13-Feb-19 | 25-Sep-19 | 6.50 |
| Clean Slate III North | 401 | 2, 4, 6 | away | 13-Feb-19 | 25-Sep-19 | 5.99 |
| Clean Slate III South | 403 | 7, 9, 11 | toward | 13-Feb-19 | 25-Sep-19 | 3.47 |
| Clean Slate III South | 403 | 8, 10, 12 | away | 13-Feb-19 | 25-Sep-19 | 2.75 |

*The opening of the trap collecting saltating material is facing toward the contaminated area for odd-numbered traps and away from the contaminated area for even-numbered traps.

Table 9. Laboratory particle-size analysis of saltation samples collected during CY2019.

| BSNE # | Orientation Relative to Contaminated Area* | Mass < 63 µm (g) | Mass 63-250 µm (g) | Mass > 250 µm (g) | Total Mass Lab (g) |
|---|---|---|---|---|---|
| CSII Traps: 61, 63, 65 | toward | 0.134 | 0.626 | 0.214 | 0.974 |
| CSII Traps: 62, 64, 66 | away | 0.126 | 0.232 | 0.101 | 0.459 |
| CSII Traps: 67, 69, 71 | toward | 0.237 | 0.335 | 0.111 | 0.683 |
| CSII Traps: 68, 70, 72 | away | 0.073 | 0.211 | 0.068 | 0.353 |
| CSIII Traps: 13, 15, 17 | toward | 1.320 | 1.360 | 0.889 | 3.569 |
| CSIII Traps: 14, 16, 18 | away | 0.738 | 1.100 | 0.476 | 2.314 |
| CSIII Traps: 19, 21, 23 | toward | 0.324 | 0.383 | 0.359 | 1.066 |
| CSIII Traps: 20, 22, 24 | away | 0.186 | 0.213 | 0.051 | 0.450 |
| CSII Traps: 49, 51, 53 | toward | 0.755 | 1.140 | 0.240 | 2.135 |
| CSII Traps: 50, 52, 54 | away | 0.755 | 1.160 | 0.395 | 2.310 |
| CSII Traps: 55, 57, 59 | toward | 0.765 | 2.022 | 0.579 | 3.366 |
| CSII Traps: 56, 58, 60 | away | 0.297 | 0.982 | 0.208 | 1.487 |
| CSIII Traps: 1, 3, 5 | toward | 1.590 | 2.730 | 1.610 | 5.930 |
| CSIII Traps: 2, 4, 6 | away | 0.376 | 2.820 | 1.040 | 4.236 |
| CSIII Traps: 7, 9, 11 | toward | 0.826 | 1.410 | 0.850 | 3.086 |
| CSIII Traps: 8, 10, 12 | away | 0.664 | 0.810 | 0.911 | 2.385 |

CS = Clean Slate

*The opening of the trap collecting saltating material is facing toward the contaminated area for odd-numbered traps and away from the contaminated area for even-numbered traps.

Figures 28 and 29 show the results of the soil particle-size analysis for BSNE samples collected at the Clean Slate sites during 2019. A larger mass of particles was leaving the Clean Slate II and III sites for almost every sampling location and period compared with the particle mass moving onto the sites (the BSNE samplers with their openings facing toward the sites collected more mass than those facing the opposite direction). The general size fraction characteristics were similar between all of the sites and stations. Most of the saltating particles by mass are in the 63 µm to 250 µm size fraction (generally more than 50 percent) (Figure 29).

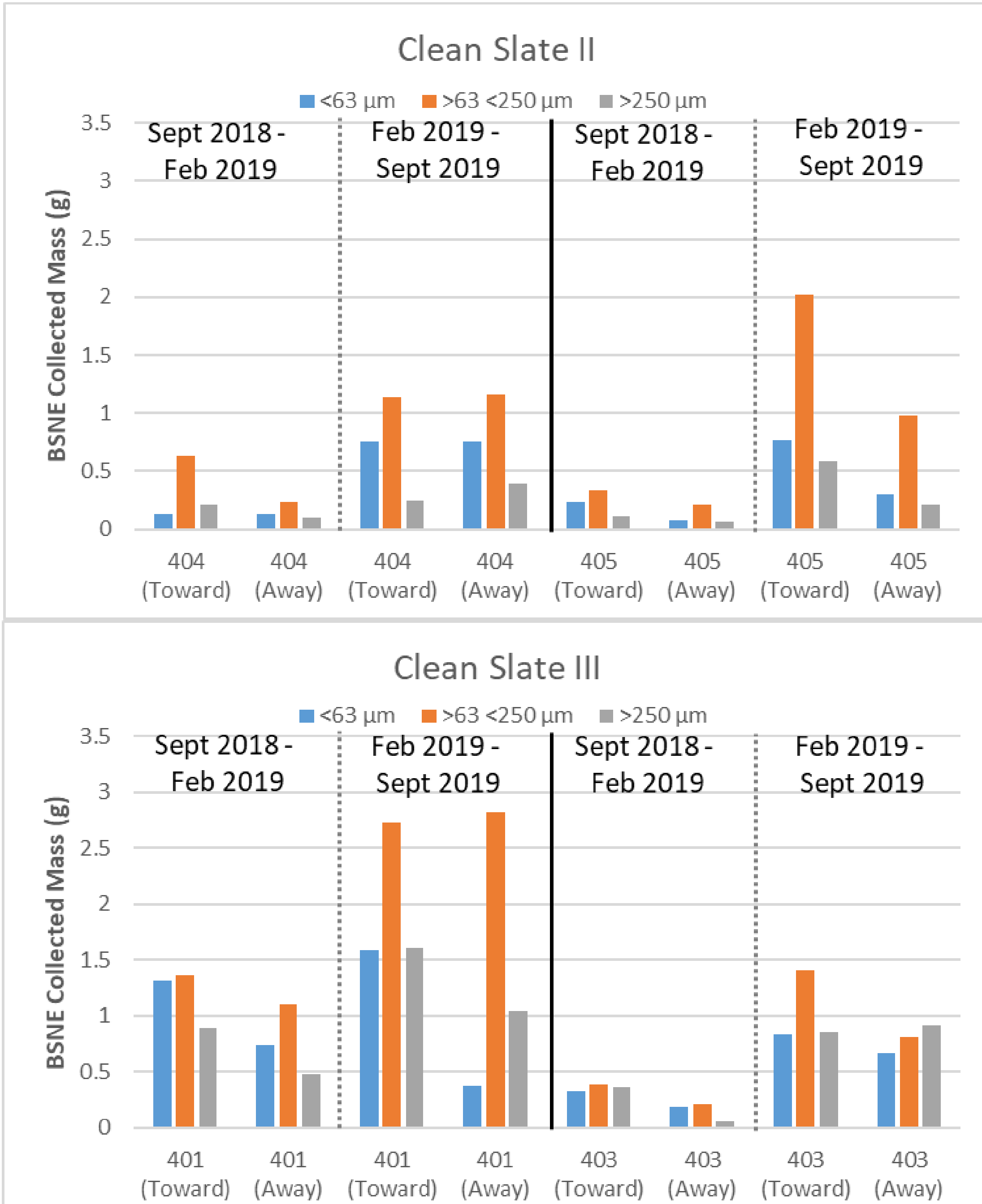


Figure 28. BSNE collected soil mass and sample size distributions for Clean Slate II (top) and III (bottom).

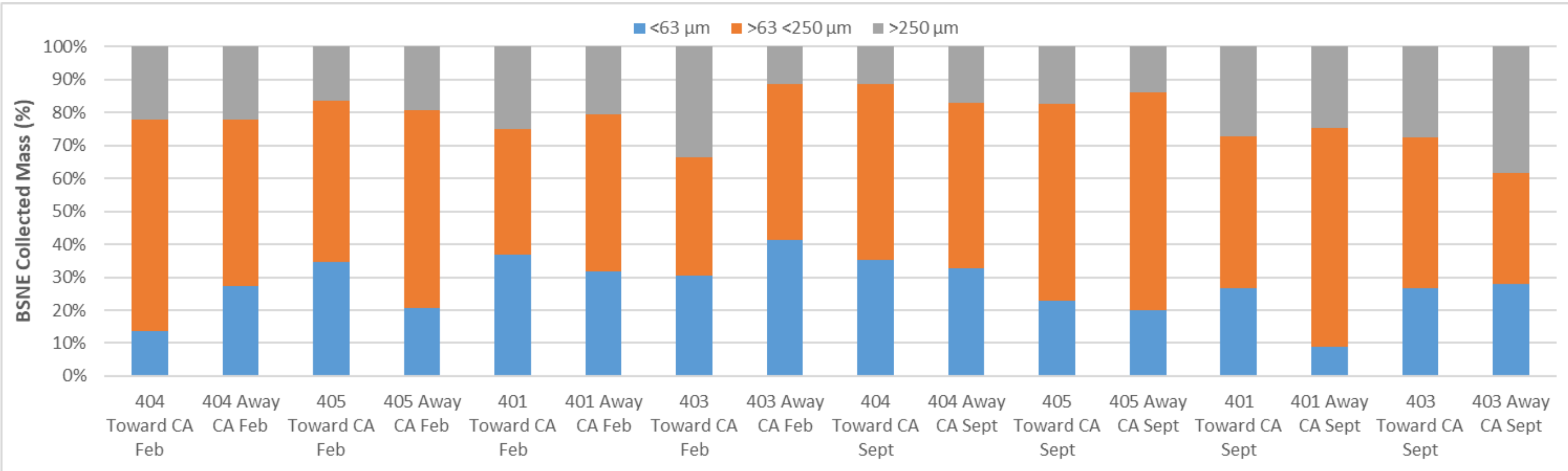


Figure 29. BSNE normalized soil sample size distributions for Clean Slate II and III. The labeled month refers to month of collection, either February or September 2019.

## RADIOLOGICAL ASSESSMENT OF WIND-TRANSPORTED SUSPENDED MATERIAL

Suspended dust particles are collected continuously using Hi-Q samplers located at each of the TTR air monitoring stations. All filter samples are analyzed for gross alpha, gross beta, and gamma spectroscopy. Filters collected during CY2019 were deployed between December 19, 2018, and December 18, 2019. This generated 26 particulate matter filter samples for analysis, although equipment and analytical malfunctions resulted in fewer samples at most sites. Radionuclide concentrations are reported as activity in microcuries (µCi) per volume of airflow through the sampler.

The gross alpha and gross beta measurements for CY2019 are summarized below in Tables 10 and 11, respectively. The mean annual gross alpha activity (Table 10) for the glass-fiber filter samples ranged from $1.75 \times 10^{-15}$ µCi/mL at Station 400 to $4.39 \times 10^{-15}$ µCi/mL at Station 401. The maximum gross alpha measurement for 2019 of $19.19 \times 10^{-15}$ µCi/ml was for the filter collected from Station 401 on February 12, 2019. The mean annual gross beta activity (Table 11) for the glass-fiber filter samples ranged from $1.35 \times 10^{-14}$ µCi/mL at Station 401 to $1.64 \times 10^{-14}$ µCi/mL at Station 404. The maximum gross beta measurement for 2019 of $3.59 \times 10^{-14}$ µCi/mL was recorded for the filter collected at Station 404 on November 20, 2019.

Table 10. Gross alpha activity results for 2019.

| Sampling Location | Number of Samples | Concentration (× $10^{-15}$ µCi/mL [$3.7 \times 10^{-5}$ Becquerel (Bq)/$m^3$]) | | | |
|---|---|---|---|---|---|
| | | Mean | Standard Deviation | Minimum | Maximum |
| Station 400 | 26 | 1.75 | 0.67 | 0.38 | 3.20 |
| Station 401 | 23 | 4.39 | 4.41 | 0.50 | 19.19 |
| Station 403 | 25 | 2.49 | 1.26 | 0.38 | 5.71 |
| Station 404 | 25* | 2.09 | 0.75 | 0.46 | 3.82 |
| Station 405 | 25 | 1.98 | 0.65 | 0.45 | 2.95 |

NOTES: Bq = Becquerel; $m^3$ = cubic meter; µCi/ml = microcuries per milliliter.
*The total number of samples collected from Station 404 is 26, but the gross alpha reported for one of these filters was below the minimum detection limit and is not included in the statistical results.

Table 11. Gross beta activity results for 2019.

| Sampling Location | Number of Samples | Concentration (× $10^{-14}$ µCi/mL [$3.7 \times 10^{-4}$ Becquerel (Bq)/$m^3$]) | | | |
|---|---|---|---|---|---|
| | | Mean | Standard Deviation | Minimum | Maximum |
| Station 400 | 26 | 1.46 | 0.47 | 0.75 | 2.99 |
| Station 401 | 23 | 1.35 | 0.45 | 0.54 | 2.87 |
| Station 403 | 25 | 1.58 | 0.55 | 0.79 | 3.44 |
| Station 404 | 26 | 1.64 | 0.55 | 0.82 | 3.59 |
| Station 405 | 25 | 1.59 | 0.51 | 0.88 | 3.23 |

NOTES: Bq = Becquerel; $m^3$ = cubic meter; µCi/ml = microcuries per milliliter.

Table 12 shows the CY2019 gross alpha and gross beta concentrations reported for CEMP stations surrounding the TTR. Because glass-fiber filters are also used in the air samplers at the CEMP stations, comparisons can be made with the glass-fiber filter samples from the Clean Slate sites. Mean annual gross alpha concentrations from the monitoring stations are higher than the values from the surrounding CEMP stations (Figure 30). The mean annual gross beta measurements for the Clean Slate air filters were lower than the measurements for the surrounding CEMP stations (Figure 31).

Table 12. Mean annual gross alpha and gross beta concentrations for 2019 reported at the CEMP stations surrounding the TTR.

| **Sampling Location** | **Gross Alpha (× $10^{-15}$ µCi/mL)** | | | **Gross Beta (× $10^{-14}$ µCi/mL)** | | |
|---|---|---|---|---|---|---|
| | **Mean** | **Minimum** | **Maximum** | **Mean** | **Minimum** | **Maximum** |
| Alamo | 1.52 | 1.00 | 1.75 | 2.35 | 1.36 | 3.17 |
| Beatty | 1.33 | 0.68 | 1.62 | 2.46 | 1.29 | 3.53 |
| Goldfield | 1.51 | 0.45 | 2.37 | 2.15 | 0.84 | 4.02 |
| Rachel | 1.58 | 0.37 | 2.40 | 2.15 | 1.03 | 2.99 |
| Sarcobatus Flat | 1.71 | 0.59 | 2.39 | 2.30 | 1.40 | 3.68 |
| Tonopah | 1.69 | 0.48 | 2.63 | 2.15 | 1.11 | 3.17 |

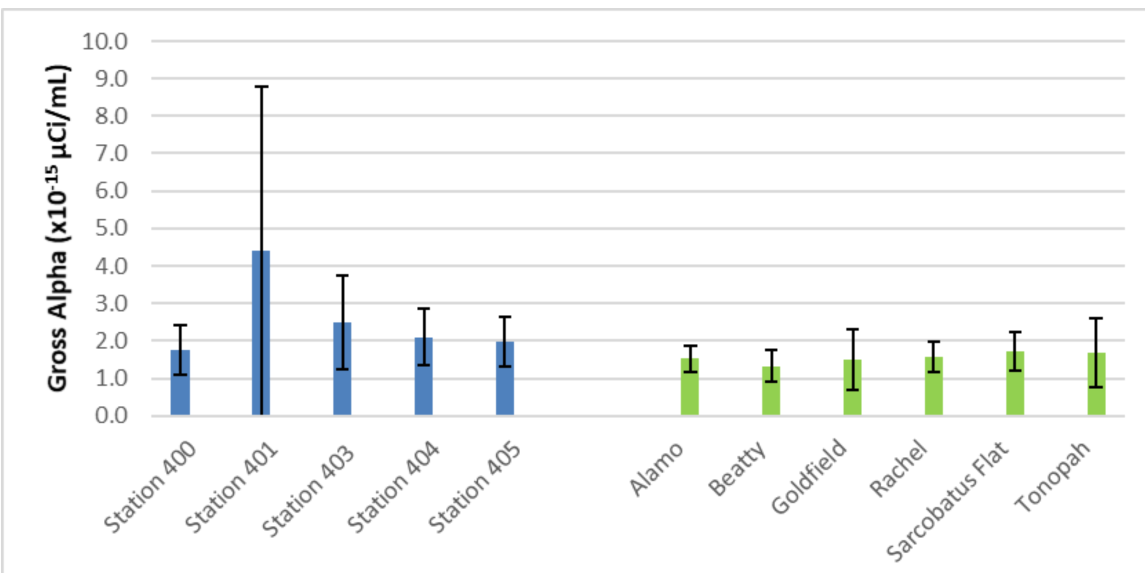


Figure 30. The mean annual gross alpha concentrations for the Clean Slate samples (blue) compared with the mean annual gross alpha concentrations for samples collected at surrounding CEMP stations (green) during 2019. The black bar displays one standard deviation above and below the mean value.

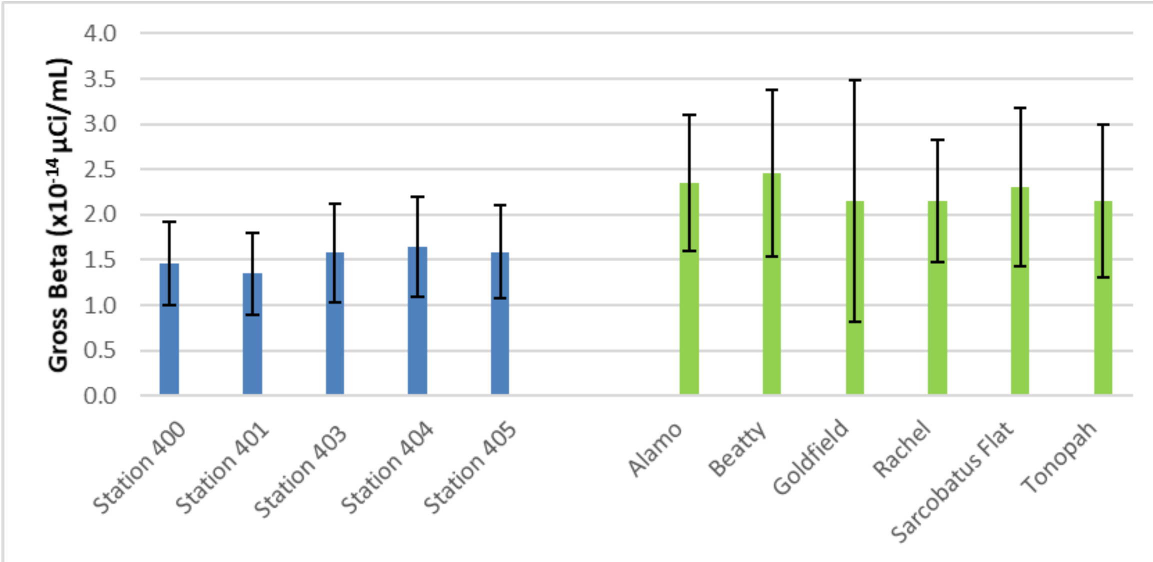


Figure 31. The mean annual gross beta concentrations for the Clean Slate samples (blue) compared with the mean annual gross beta concentrations for samples collected at surrounding CEMP stations (green) during 2019. The black bar displays one standard deviation above and below the mean value.

The mean gross alpha for the filters collected in 2019 was lower for all monitoring stations than that calculated for 2018, with the exception of Station 401. The 2019 mean gross alpha at Station 401 was larger than the mean plus standard deviation measured in 2018, which itself was an increase from 2017. The highest gross alpha measurements for Station 401 occur in the first half of the year (Table 13). All stations record a decrease to very low gross alpha concentrations for the last filter collection period of December 5 to 18, 2019 (Table 13). These results were confirmed by the laboratory by duplicate measurements on a separate measurement date. Additionally, review of laboratory control samples from the measurement dates found them to all be within the range of acceptance values for the standards.

Gamma spectroscopy measured $^{241}$Am (a product of plutonium-241 [$^{241}$Pu] radioactive decay) on four filters during CY2019 at Station 401. The detections occurred for the filters deployed during January 28th to February 12th ($1.58 \times 10^{-15}$ µCi/mL), February 27th to March 13th ($3.21 \times 10^{-15}$ µCi/mL), April 24th to May 9th ($1.01 \times 10^{-15}$ µCi/mL), and October 23rd to November 6th ($1.86 \times 10^{-15}$ µCi/mL). Naturally occurring radionuclides were also identified in the particulate matter samples collected from all TTR stations during CY2019 (Table 14). The detected natural radionuclides occurred with varying frequency, with Beryllium-7 being the most commonly detected.

Table 13. Gross alpha activities for individual filters collected biweekly from the monitoring stations.

| Start Date | End Date | Station 400 | 401 | 403 | 404 | 405 |
|---|---|---|---|---|---|---|
| | | Gross alpha ($\times 10^{-15}$ µCi/mL) | | | | |
| 12/19/2018 | 1/2/2019 | 2.76 | 2.41 | 4.71 | 2.84 | 2.57 |
| 1/2/2019 | 1/16/2019 | 2.08 | 6.55 | 2.09 | 2.83 | 2.63 |
| 1/16/2019 | 1/28/2019 | 3.07 | 2.45 | 3.04 | 2.73 | 2.12 |
| 1/28/2019 | 2/12/2019 | 2.36 | 19.19 | 2.77 | 3.46 | 2.95 |
| 2/12/2019 | 2/27/2019 | 2.20 | 2.91 | 2.65 | N/A | 2.23 |
| 2/27/2019 | 3/13/2019 | 1.90 | 15.19 | 1.87 | 1.99 | 1.89 |
| 3/13/2019 | 3/27/2019 | 3.20 | 3.18 | 2.51 | 3.82 | 2.84 |
| 3/27/2019 | 4/11/2019 | 1.66 | 2.59 | 4.50 | 2.18 | N/A |
| 4/11/2019 | 4/24/2019 | 1.75 | 4.10 | 1.78 | 2.52 | 1.56 |
| 4/24/2019 | 5/9/2019 | 1.88 | 8.83 | 3.50 | 2.45 | 2.58 |
| 5/9/2019 | 5/21/2019 | 1.76 | 2.66 | N/A | 2.21 | 2.43 |
| 5/21/2019 | 6/5/2019 | 1.78 | 2.16 | 1.84 | 1.86 | 1.67 |
| 6/5/2019 | 6/19/2019 | 1.43 | 3.51 | 3.49 | 2.29 | 1.94 |
| 6/19/2019 | 7/3/2019 | 1.69 | N/A | 3.99 | 2.06 | 2.21 |
| 7/3/2019 | 7/17/2019 | 1.42 | N/A | 1.89 | 1.89 | 2.37 |
| 7/19/2019 | 7/31/2019 | 0.89 | N/A | 1.12 | 1.37 | 1.36 |
| 7/31/2019 | 8/14/2019 | 1.48 | 3.47 | 1.82 | 1.91 | 1.78 |
| 8/14/2019 | 8/28/2019 | 1.14 | 2.61 | 1.38 | 1.31 | 1.13 |
| 8/28/2019 | 9/11/2019 | 1.18 | 2.00 | 1.73 | 1.31 | 1.49 |
| 9/11/2019 | 9/25/2019 | 1.36 | 3.94 | 1.54 | 1.55 | 1.45 |
| 9/25/2019 | 10/8/2019 | 2.12 | 2.21 | 2.39 | 2.27 | 2.66 |
| 10/8/2019 | 10/23/2019 | 1.46 | 3.23 | 2.48 | 2.19 | 2.28 |
| 10/23/2019 | 11/6/2019 | 2.09 | 3.27 | 5.71 | 2.14 | 2.47 |
| 11/6/2019 | 11/20/2019 | 1.99 | 2.51 | 2.14 | 1.86 | 1.76 |
| 11/20/2019 | 12/5/2019 | 0.50 | 1.61 | 0.82 | 0.72 | 0.67 |
| 12/5/2019 | 12/18/2019 | 0.38 | 0.50 | 0.38 | 0.46 | 0.45 |

N/A = not available; no sample due to sampler problems.

Alpha spectrometry analysis for plutonium isotopes was conducted on select air filters for comparison with analyses of soil collected from saltation traps (see the “Radiological Assessment of Saltation Material” section). Two filters from each quarter of the year were selected and submitted to Eurofins TestAmerica Laboratories Inc. for alpha spectrometry analysis. These quarterly samples include the sample with the highest gross alpha result plus one random sample from each of the stations, for eight samples per station

Table 14. The number of CY2019 particulate matter samples from TTR air sampling stations in which naturally occurring radionuclides were identified by gamma spectroscopy.

| Radionuclide | Number of Samples | | | | |
|---|---|---|---|---|---|
| | **Station 400** | **Station 401** | **Station 403** | **Station 404** | **Station 405** |
| Beryllium-7 ($^{7}$Be) | 22 | 20 | 22 | 22 | 20 |
| Lead-210 ($^{210}$Pb) | 19 | 19 | 18 | 19 | 21 |
| Potassium-40 ($^{40}$K) | 1 | 0 | 0 | 0 | 0 |
| Lead-212 ($^{212}$Pb) | 2 | 7 | 4 | 4 | 6 |
| Bismuth-214 ($^{214}$Bi) | 10 | 3 | 6 | 3 | 4 |
| Bismuth-210 ($^{210}$Bi) | 0 | 0 | 1 | 0 | 0 |
| Lead-214 ($^{214}$Pb) | 1 | 3 | 1 | 1 | 0 |
| Actinium-228 ($^{228}$Ac) | 0 | 1 | 0 | 0 | 1 |

per year. As noted above, gamma spectroscopy is another factor in sample selection for alpha spectrometry analysis. Any filter that detected $^{241}$Am by gamma spectroscopy triggered alpha spectrometry analysis of the filter, taking the place of the highest gross alpha selection (although, in fact, the samples detecting $^{241}$Am also had the highest gross alpha for the quarter). During the first quarter at Station 401, there were two $^{241}$Am detections and both of these samples were analyzed by alpha spectroscopy so that no random sample was included for the first quarter at Station 401. For the second and fourth quarters when $^{241}$Am was detected in one filter each at Station 401, that filter plus a randomly selected filter were analyzed by alpha spectroscopy.

Tables 15 and 16 summarize the results of alpha spectrometry analyses for plutonium-238 ($^{238}$Pu) and plutonium-239+240 ($^{239+240}$Pu) for filters selected during CY2019. Appendix E provides the analytical results for individual filters. Plutonium-238 was detected above the minimum detectable concentration (MDC) in three samples from Station 401, one sample from Station 403, and one sample from Station 405. All detections occurred during the first half of the year. Plutonium-239+240 was detected at all sampling stations except Station 400. The highest $^{238}$Pu ($1.93 \text{ x } 10^{-16}$ µCi/ml) and $^{239+240}$Pu ($301.75 \times 10^{-16}$ µCi/mL) concentrations were measured in the same filter deployed between February 27, 2019, and March 13, 2019, at Station 401. As stated above, gamma spectroscopy measured $^{241}$Am (a product of $^{241}$Pu radioactive decay) on four filters during 2019 at Station 401 for the filters deployed during January 28th to February 12th ($1.58 \times 10^{-15}$ µCi/mL), February 27th to March 13th ($3.21 \times 10^{-15}$ µCi/mL), April 24th to May 9th ($1.01 \times 10^{-15}$ µCi/mL), and October 23rd to November 6th ($1.86 \times 10^{-15}$ µCi/mL). All of these samples also contained detectable $^{238}$Pu and $^{239+240}$Pu, with the exception of the filter deployed during October 23rd to November 6th, which did not have detectable $^{238}$Pu.

Table 15. Plutonium-238 alpha spectrometry results for 2019 at TTR air sampling stations.

| Station Number | No. Samples Analyzed | No. Samples > MDC $^{238}Pu$ | Quarters with $^{238}Pu$ Detected | $^{238}Pu$ Concentration ($\times 10^{-16}$ µCi/mL [$3.7 \times 10^{-6}$ Bq/m$^3$]) | | | |
|---|---|---|---|---|---|---|---|
| | | | | Mean | Standard Deviation | Min. | Max. |
| 400 | 8 | 0 | none | N/A | N/A | N/A | N/A |
| 401 | 8 | 3 | Q1, Q2 | 1.56 | 0.64 | 0.82 | 1.93 |
| 403 | 8 | 1 | Q1 | 0.35 | N/A | 0.35 | 0.35 |
| 404 | 8 | 0 | none | N/A | N/A | N/A | N/A |
| 405 | 8 | 1 | Q2 | 0.11 | N/A | 0.11 | 0.11 |

Table 16. Plutonium-239+240 alpha spectrometry results for 2019 at TTR air sampling stations.

| Station Number | No. Samples Analyzed | No. Samples > MDC $^{239+240}Pu$ | Quarters with $^{239+240}Pu$ Detected | $^{239+240}Pu$ Concentration ($\times 10^{-16}$ µCi/mL [$3.7 \times 10^{-6}$ Bq/m$^3$]) | | | |
|---|---|---|---|---|---|---|---|
| | | | | Mean | Standard Deviation | Min. | Max. |
| 400 | 8 | 0 | none | N/A | N/A | N/A | N/A |
| 401 | 8 | 8 | Q1, Q2, Q3, Q4 | 110.40 | 120.39 | 2.94 | 301.75 |
| 403 | 8 | 6 | Q1, Q2, Q3, Q4 | 39.26 | 43.79 | 2.20 | 102.72 |
| 404 | 8 | 6 | Q1, Q2, Q4 | 4.32 | 6.62 | 0.60 | 17.62 |
| 405 | 8 | 6 | Q1, Q2, Q4 | 1.95 | 1.65 | 0.72 | 5.09 |

N/A = not applicable; MDC = minimum detectable concentration; MDC $^{238}Pu$ = 0.95 ± 0.34 µCi/mL × $10^{-16}$;
MDC $^{239+240}Pu$ = 0.71 ± 0.29 µCi/mL × $10^{-16}$.

## GAMMA RADIATION OBSERVATIONS

Gamma radiation is measured using a PIC detector. A PIC detector is generally deployed to detect gamma radiation that substantially exceeds ambient radiation levels, which is often ascribed to human activities. In the absence of such activities, ambient gamma radiation rates are recorded. These radiation values vary naturally among locations and reflect differences in altitude and latitude (cosmic radiation) and radioactivity in the soil (terrestrial radiation). Additionally, slight variations in gamma radiation at a single location may be caused by changes in weather (UNSCEAR, 2000), such as precipitation bringing dust down from the atmosphere or the occurrence of higher dust concentrations because of entrainment from the surface by wind.

The PIC data were collected in 2019 for Stations 400, 401, and 403. Stations 404 and 405 do not have PICs. Figure 32 shows the 10-minute average gamma values for CY2019. Tables 17 and 18 provide average annual gamma values measured by PICs at the Clean Slate stations and at CEMP stations in the region, respectively, for comparison purposes. The average gamma exposure rates measured at the regional CEMP stations were lower than the TTR stations, except for the CEMP station at Warm Springs Summit. The mean gamma exposure rate measured at Warm Springs Summit was within one standard deviation of the mean measured for Stations 401 and 403, and within two standard deviations of Station 400, although the maximum values at all of the TTR stations were greater than the maximum plus two standard deviation at Warm Springs Summit (Tables 17 and 18).

Spikes in gamma values higher than the mean plus two standard deviations occurred periodically at all stations (Figure 32). Mizell *et al.* (2014) examined atmospheric conditions coinciding with increases in gamma radiation at TTR and concluded that the observed intervals of increased gamma values were not associated with wind transport of radionuclide-contaminated soil material, but instead were related to weather events such as precipitation. Visual comparison of the CY2019 gamma record for the TTR stations with precipitation events recorded at the stations revealed that some of the short-term gamma increases coincide with precipitation events (Figure 32). The distribution of gamma values collected during precipitation events was significantly skewed to higher values than the distribution of the entire data set for each station (Figure 33). Measurements of gamma radiation greater than the mean plus three standard deviations at one station often coincided with similar measurements at the other stations (Figure 34), which is consistent with the effects of a widespread precipitation event.

Table 17. Gamma exposure rates at the TTR measured in 2019 by the PIC detectors.

| **Sampling Location** | **Average of 10-minute Gamma Exposure Rate (µR/hr)** | | | |
|---|---|---|---|---|
| | **Mean** | **Standard Deviation** | **Minimum** | **Maximum** |
| Station 400 | 19.36 | 0.43 | 15.77 | 24.80 |
| Station 401 | 20.49 | 0.63 | 17.89 | 26.29 |
| Station 403 | 20.39 | 0.63 | 18.71 | 27.20 |

Note: µR/hr = microroentgen per hour.

Table 18. Gamma exposure rates measured with PICs at CEMP stations in the TTR region in 2019.

| **Sampling Location** | **Average of 10-minute Gamma Exposure Rate (µR/hr)** | | | |
|---|---|---|---|---|
| | **Mean** | **Standard Deviation** | **Minimum** | **Maximum** |
| Alamo | 13.10 | 0.34 | 12.2 | 14.0 |
| Beatty | 16.45 | 0.31 | 15.4 | 17.5 |
| Goldfield | 15.10 | 0.44 | 12.1 | 18.1 |
| Rachel | 15.30 | 0.33 | 14.3 | 16.3 |
| Sarcobatus Flat | 16.95 | 0.31 | 16.1 | 17.8 |
| Tonopah | 17.15 | 0.40 | 15.0 | 19.3 |
| Warm Springs Summit | 20.20 | 0.48 | 18.0 | 22.4 |

Note: µR/hr = microroentgen per hour.

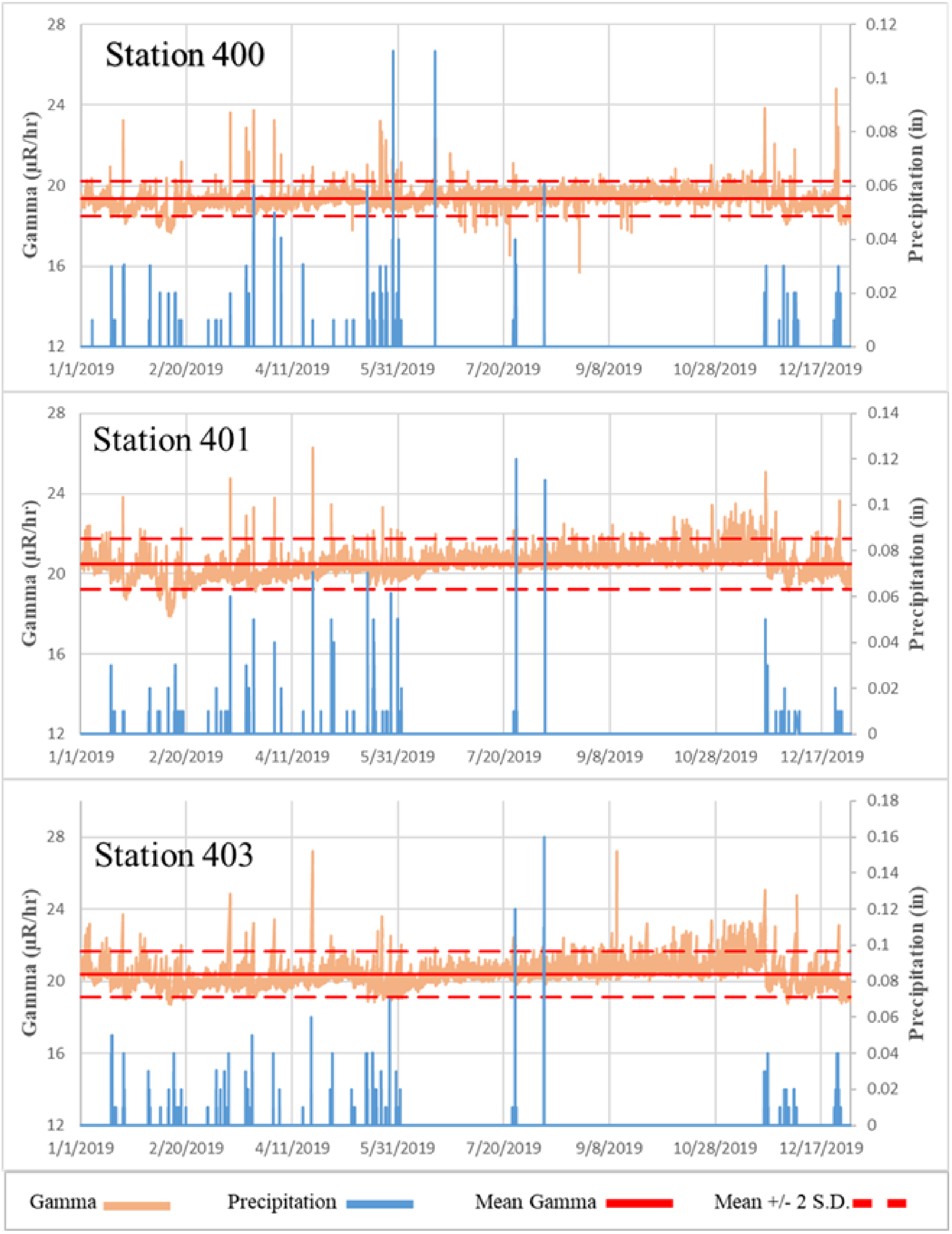


Figure 32. The CY2019 10-minute PIC gamma radiation and 10-minute precipitation data for the TTR monitoring stations.

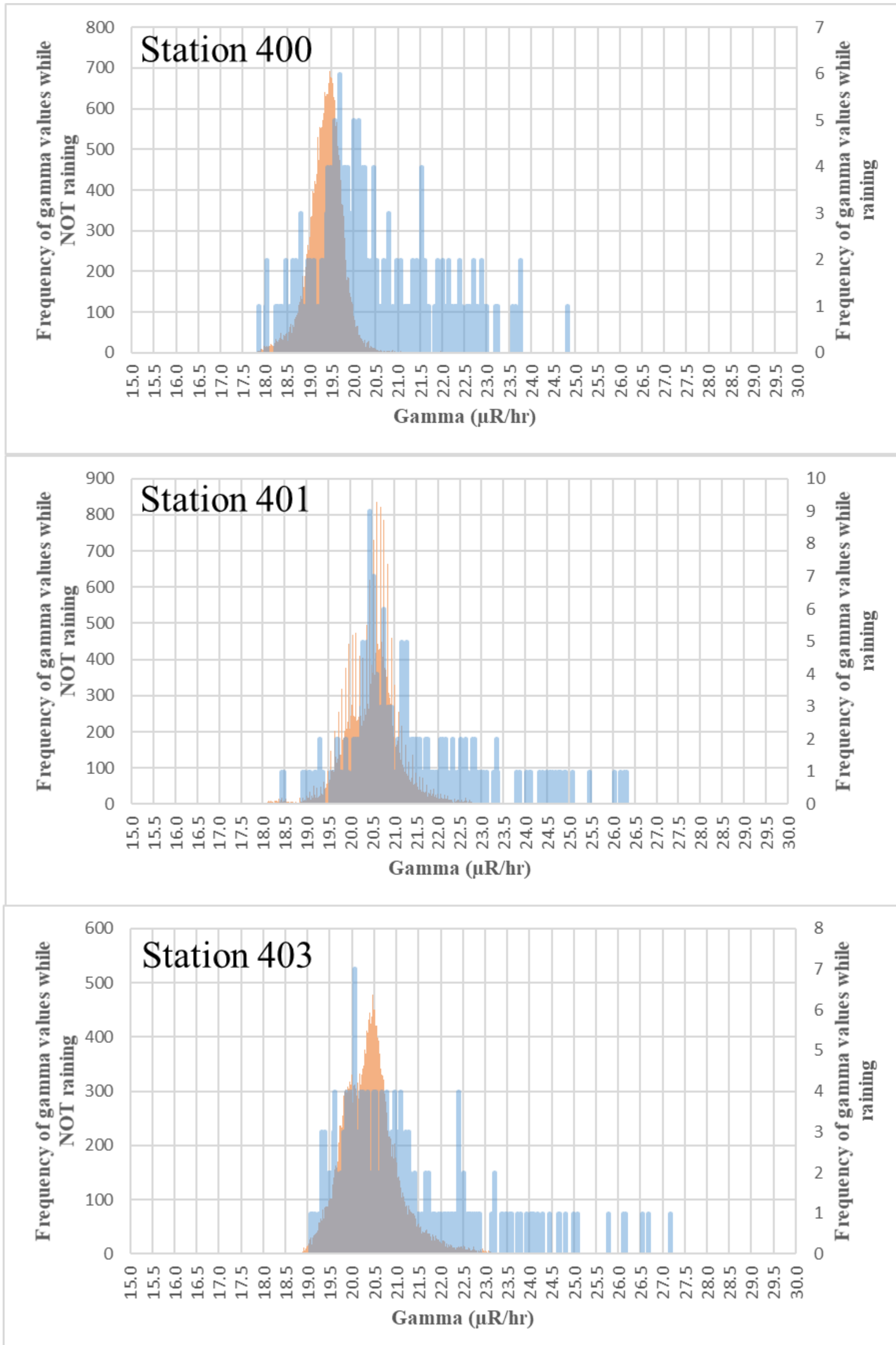


Figure 33. Frequency distributions for gamma exposure rate measurements occurring when there is no measured precipitation during CY2019 for each station (orange, frequency on the left axis) and for only those measurements occurring during measured precipitation (blue, frequency on the right axis).

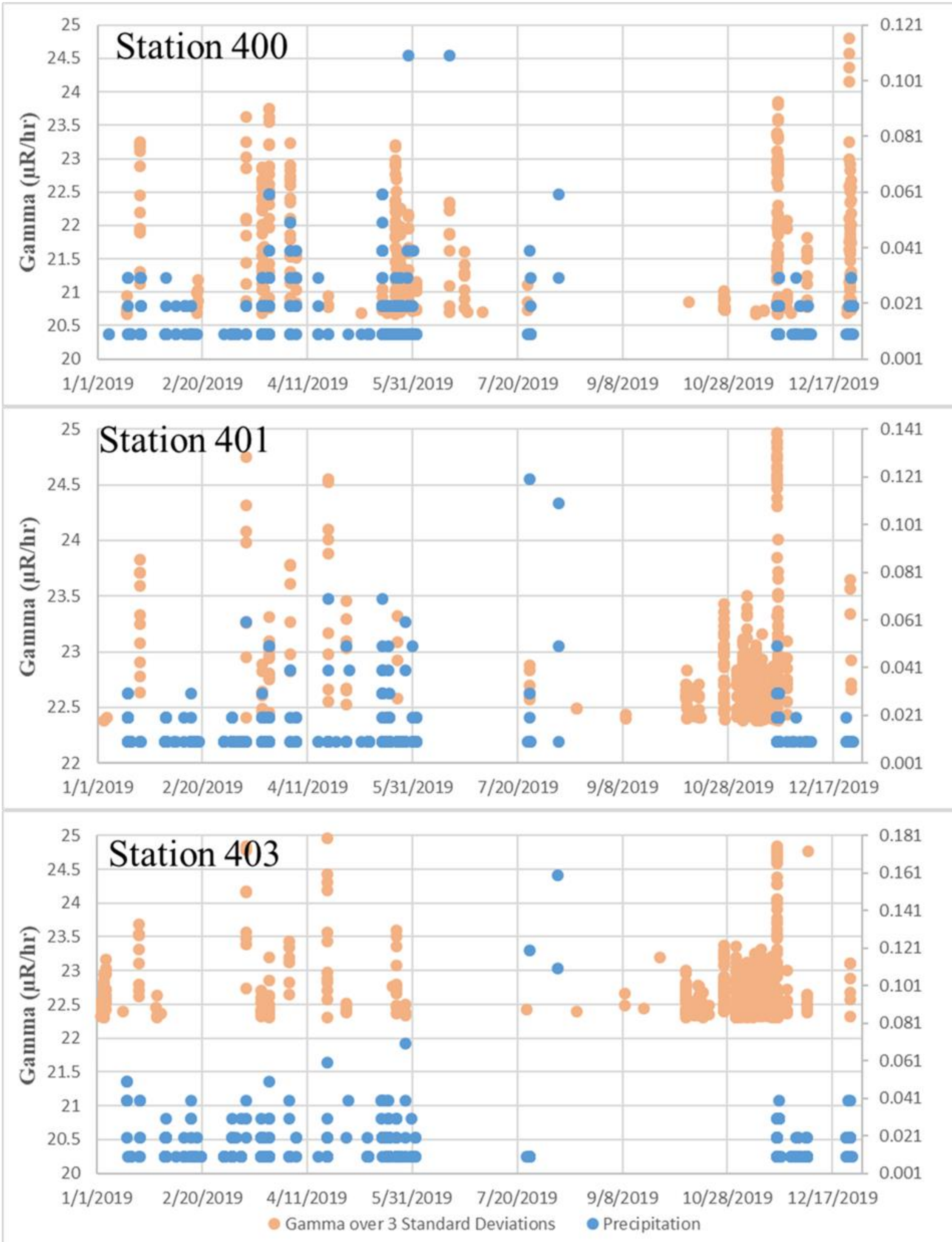


Figure 34. The CY2019 PIC gamma data (orange) showing only those values greater than the mean plus three standard deviations and 10-minute precipitation data (blue).

From the early summer in 2019 until mid-November of the same year, there was a shift to higher gamma rate observations at all three stations with PICs (Figure 32), but most particularly for Stations 401 and 403. At these two stations, a cluster of measurements greater than the mean plus three standard deviations occurs in October and early November without any coincident precipitation (Figure 34). This is after the completion of remediation activities at Clean Slate III at the end of August 2019, but during the ripping and seeding of the revegetation process (Table 1). Coincident with the onset of rain events starting in mid-November, the gamma rate trends decrease below the annual mean.

## RADIOLOGICAL ASSESSMENT OF SALTATION MATERIAL

Radiological analyses were performed for $^{238}$Pu, $^{239+240}$Pu, and $^{241}$Am (Table 19) for all BSNE samples. The particle size fraction is an important factor because there is a strong correlation between smaller particles and higher radionuclide concentrations (Figures 35 through 37). For most of the sample sets, the highest radionuclide concentration occurred for the size fraction below 63 µm and the lowest concentrations tended to be associated with the size fraction larger than 250 µm. There are exceptions to these general trends, most notably for the traps facing away from Clean Slate III at Station 403 that for the time period of February to September 2019 collected the highest $^{239+240}$Pu, $^{241}$Am, and $^{238}$Pu concentrations in the size fraction larger than 250 µm. The same was observed for the sample collected between September 2017 and January 2018 at this location.

It was anticipated that sand traps with the sample inlets oriented toward the contaminated area would collect higher concentrations of radionuclides than the corresponding traps oriented away from the areas. This relationship was observed for the majority of sample sets, but higher concentrations were observed for some of the traps collecting material moving toward the contaminated areas. For example, the smallest size fraction collected from the traps at Station 404 between February and September 2019, had higher concentrations of the plutonium isotopes in the traps facing away from the contamination area. Higher concentrations were also found in traps facing away from the contamination areas for the larger particle size fractions at Station 403 (as described above), at Station 401 for the September 2018 to February 2019 sample, and at Station 405 for the February to September 2019 sample.

Table 19. Alpha spectrometry analytical results for samples collected in saltation traps.

| Location | Date | Traps | Particle Size (µm) | $^{241}$Am (pCi/g) Result | Error | DL | $^{238}$Pu (pCi/g) Result | Error | DL | $^{239+240}$Pu (pCi/g) Result | Error | DL |
|---|---|---|---|---|---|---|---|---|---|---|---|---|
| CSII - 404 | 9/26/2018 2/12/2019 | 61, 63, 65 | <63 | 16.6 | 3.74 | 0.754 | 2.34 | 1.07 | 0.765 | 316 | 43.8 | 0.942 |
| | | | 63-250 | 5.30 | 1.18 | 0.248 | 0.402 | 0.265 | 0.386 | 92.8 | 13.2 | 0.225 |
| | | | >250 | 1.02 | 0.55 | 0.694 | 0.054 | 0.152 | 0.411 | 8.74 | 1.81 | 0.376 |
| CSII - 404 | 9/26/2018 2/12/2019 | 62, 64, 66 | <63 | 5.21 | 1.66 | 0.672 | 0.606 | 0.54 | 0.773 | 36.6 | 6.19 | 0.769 |
| | | | 63-250 | 1.11 | 0.538 | 0.558 | 0.169 | 0.226 | 0.43 | 7.06 | 1.58 | 0.428 |
| | | | >250 | 0.850 | 0.629 | 0.893 | 0.264 | 0.496 | 1.15 | 8.03 | 2.35 | 1.01 |
| CSII - 405 | 9/26/2018 2/12/2019 | 67, 69, 71 | <63 | 2.56 | 0.877 | 0.396 | 0.030 | 0.248 | 0.721 | 32.4 | 5.21 | 0.458 |
| | | | 63-250 | 1.16 | 0.59 | 0.68 | 0.029 | 0.189 | 0.568 | 11.4 | 2.24 | 0.398 |
| | | | >250 | 1.95 | 0.95 | 0.746 | 0.204 | 0.355 | 0.782 | 16.5 | 3.4 | 0.778 |
| CSII - 405 | 9/26/2018 2/12/2019 | 68, 70, 72 | <63 | 1.02 | 0.845 | 1.12 | 0.082 | 0.546 | 1.64 | 9.43 | 2.8 | 1.15 |
| | | | 63-250 | 0.137 | 0.199 | 0.386 | 0.080 | 0.16 | 0.374 | 3.20 | 0.933 | 0.372 |
| | | | >250 | 0.380 | 0.541 | 1.1 | -0.276 | 0.392 | 1.53 | 2.34 | 1.21 | 1.05 |
| CSIII - 401 | 9/26/2018 2/12/2019 | 13, 15, 17 | <63 | 22.3 | 3.88 | 0.092 | 2.37 | 0.489 | 0.097 | 382 | 53 | 0.105 |
| | | | 63-250 | 2.89 | 0.748 | 0.211 | 0.251 | 0.185 | 0.264 | 20.9 | 3.21 | 0.185 |
| | | | >250 | 1.28 | 0.348 | 0.126 | 0.047 | 0.076 | 0.172 | 6.99 | 1.16 | 0.118 |
| CSIII - 401 | 9/26/2018 2/12/2019 | 14, 16, 18 | <63 | 9.64 | 1.82 | 0.247 | 1.13 | 0.348 | 0.161 | 157 | 21.8 | 0.147 |
| | | | 63-250 | 1.85 | 0.558 | 0.278 | 0.076 | 0.108 | 0.221 | 12.9 | 2.1 | 0.177 |
| | | | >250 | 0.981 | 0.403 | 0.321 | 0.168 | 0.155 | 0.215 | 11.4 | 1.95 | 0.233 |
| CSIII - 403 | 9/26/2018 2/12/2019 | 19, 21, 23 | <63 | 10.5 | 2.27 | 0.442 | 0.815 | 0.493 | 0.675 | 108 | 15.5 | 0.393 |
| | | | 63-250 | 3.36 | 1.07 | 0.732 | 0.170 | 0.228 | 0.434 | 22.3 | 3.78 | 0.397 |
| | | | >250 | 2.67 | 0.931 | 0.431 | 0.312 | 0.278 | 0.398 | 18.8 | 3.21 | 0.396 |
| CSIII - 403 | 9/26/2018 2/12/2019 | 20, 22, 24 | <63 | 6.65 | 1.96 | 0.85 | 0.344 | 0.564 | 1.27 | 71.7 | 11.3 | 0.874 |
| | | | 63-250 | 2.56 | 0.896 | 0.629 | 0.080 | 0.208 | 0.534 | 10.6 | 2.07 | 0.375 |
| | | | >250 | 2.08 | 1.5 | 1.77 | -0.133 | 0.594 | 1.87 | 14.5 | 4.42 | 2.3 |

Shaded values are less than the analytical detection limit (DL).

Table 19. Alpha spectroscopy analytical results for samples collected in saltation traps (continued).

| Location | Date | Traps | Particle Size (µm) | $^{241}$Am (pCi/g) Result | Error | DL | $^{238}$Pu (pCi/g) Result | Error | DL | $^{239+240}$Pu (pCi/g) Result | Error | DL |
|---|---|---|---|---|---|---|---|---|---|---|---|---|
| CSII - 404 | 2/13/2019 9/25/2019 | 49, 51, 53 | <63 | 10.1 | 2.04 | 0.275 | 1.17 | 0.421 | 0.356 | 180 | 24.8 | 0.227 |
| | | | 63-250 | 1.47 | 0.388 | 0.106 | 0.103 | 0.087 | 0.137 | 16.7 | 2.44 | 0.105 |
| | | | >250 | 1.02 | 0.548 | 0.664 | 0.082 | 0.165 | 0.385 | 15.4 | 2.76 | 0.419 |
| CSII - 404 | 2/13/2019 9/25/2019 | 50, 52, 54 | <63 | 9.97 | 1.97 | 0.198 | 1.58 | 0.478 | 0.279 | 225 | 30.8 | 0.214 |
| | | | 63-250 | 0.689 | 0.234 | 0.128 | -0.007 | 0.038 | 0.144 | 6.51 | 1.07 | 0.126 |
| | | | >250 | 0.854 | 0.394 | 0.323 | -0.020 | 0.105 | 0.395 | 4.24 | 0.998 | 0.303 |
| CSII - 405 | 2/13/2019 9/25/2019 | 55, 57, 59 | <63 | 5.28 | 1.13 | 0.242 | 7.60 | 0.276 | 0.173 | 89.7 | 12.3 | 0.245 |
| | | | 63-250 | 0.507 | 0.185 | 0.163 | 0.031 | 0.038 | 0.087 | 6.56 | 1.06 | 0.108 |
| | | | >250 | 0.198 | 0.203 | 0.359 | 0.000 | 0.133 | 0.425 | 4.69 | 1.06 | 0.294 |
| CSII - 405 | 2/13/2019 9/25/2019 | 56, 58, 60 | <63 | 1.27 | 0.564 | 0.496 | 0.106 | 0.237 | 0.584 | 19.4 | 3.28 | 0.371 |
| | | | 63-250 | 0.497 | 0.283 | 0.376 | 0.085 | 0.114 | 0.217 | 11.8 | 1.97 | 0.217 |
| | | | >250 | 0.499 | 0.512 | 0.906 | 0.092 | 0.292 | 0.802 | 8.35 | 2.09 | 0.648 |
| CSIII - 401 | 2/13/2019 9/25/2019 | 1, 3, 5 | <63 | 21.7 | 3.78 | 0.123 | 2.02 | 0.415 | 0.104 | 339 | 46.1 | 0.091 |
| | | | 63-250 | 4.14 | 0.804 | 0.106 | 0.391 | 0.154 | 0.124 | 59.5 | 8.29 | 0.087 |
| | | | >250 | 0.543 | 0.212 | 0.184 | 0.015 | 0.046 | 0.126 | 7.09 | 1.16 | 0.126 |
| CSIII - 401 | 2/13/2019 9/25/2019 | 2, 4, 6 | <63 | 4.40 | 1.25 | 0.491 | 0.242 | 0.248 | 0.377 | 55.2 | 8.17 | 0.377 |
| | | | 63-250 | 0.945 | 0.277 | 0.094 | 0.081 | 0.074 | 0.128 | 10.6 | 1.59 | 0.089 |
| | | | >250 | 0.453 | 0.268 | 0.351 | 0.127 | 0.126 | 0.195 | 6.75 | 1.24 | 0.195 |
| CSIII - 403 | 2/13/2019 9/25/2019 | 7, 9, 11 | <63 | 15.3 | 2.88 | 0.25 | 1.23 | 0.431 | 0.331 | 234 | 32.2 | 0.26 |
| | | | 63-250 | 1.11 | 0.312 | 0.136 | 0.050 | 0.069 | 0.143 | 15.7 | 2.35 | 0.11 |
| | | | >250 | 0.293 | 0.186 | 0.275 | 0.104 | 0.103 | 0.159 | 6.13 | 1.09 | 0.146 |
| CSIII - 403 | 2/13/2019 9/25/2019 | 8, 10, 12 | <63 | 5.76 | 1.25 | 0.28 | 0.733 | 0.338 | 0.29 | 106 | 14.8 | 0.29 |
| | | | 63-250 | 0.193 | 0.198 | 0.351 | -0.017 | 0.074 | 0.234 | 2.62 | 0.695 | 0.289 |
| | | | >250 | 18.1 | 3.27 | 0.31 | 2.15 | 0.577 | 0.305 | 349 | 47.8 | 0.211 |

Shaded values are less than the analytical detection limit (DL).

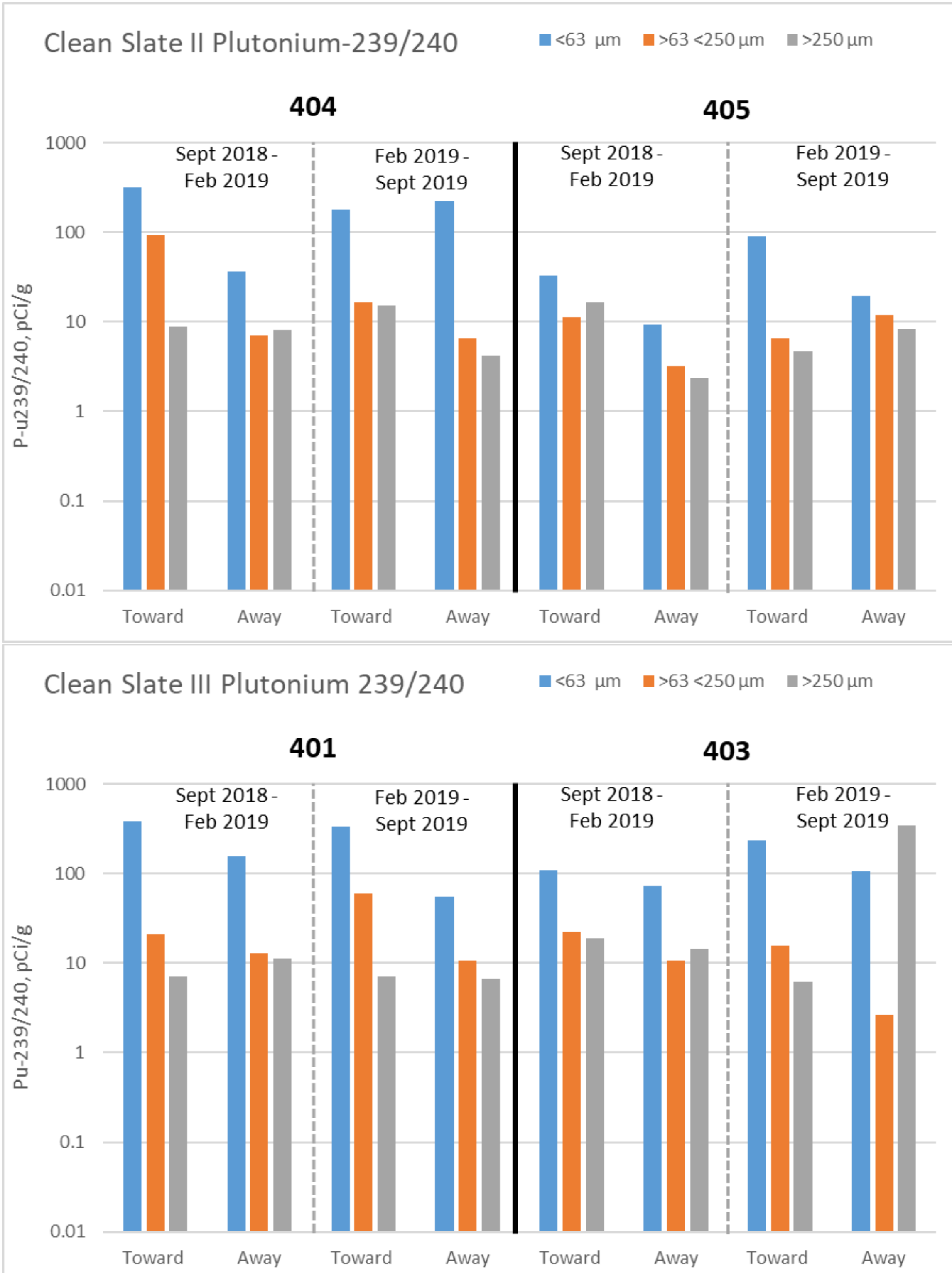


Figure 35. $^{239+240}$Pu concentrations in samples from the TTR saltation traps.

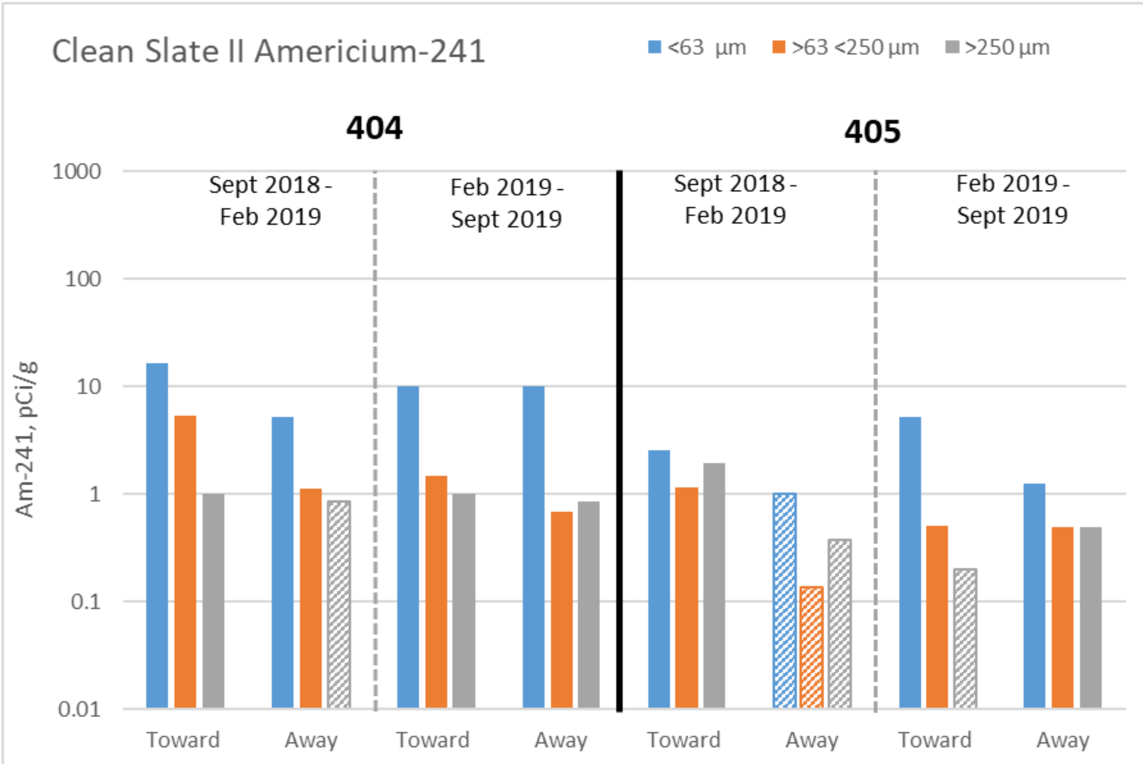


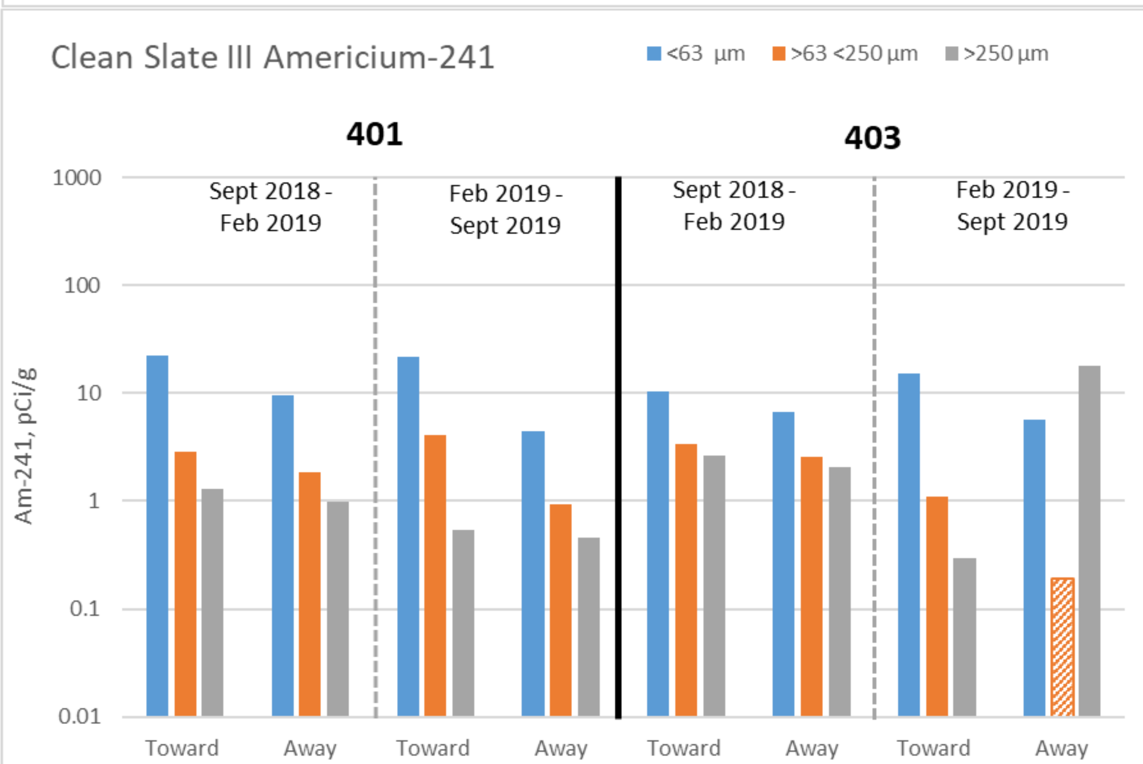


Figure 36. $^{241}$Am concentrations in samples from the saltation traps. The hachured pattern indicates a value below the analytical detection limit.

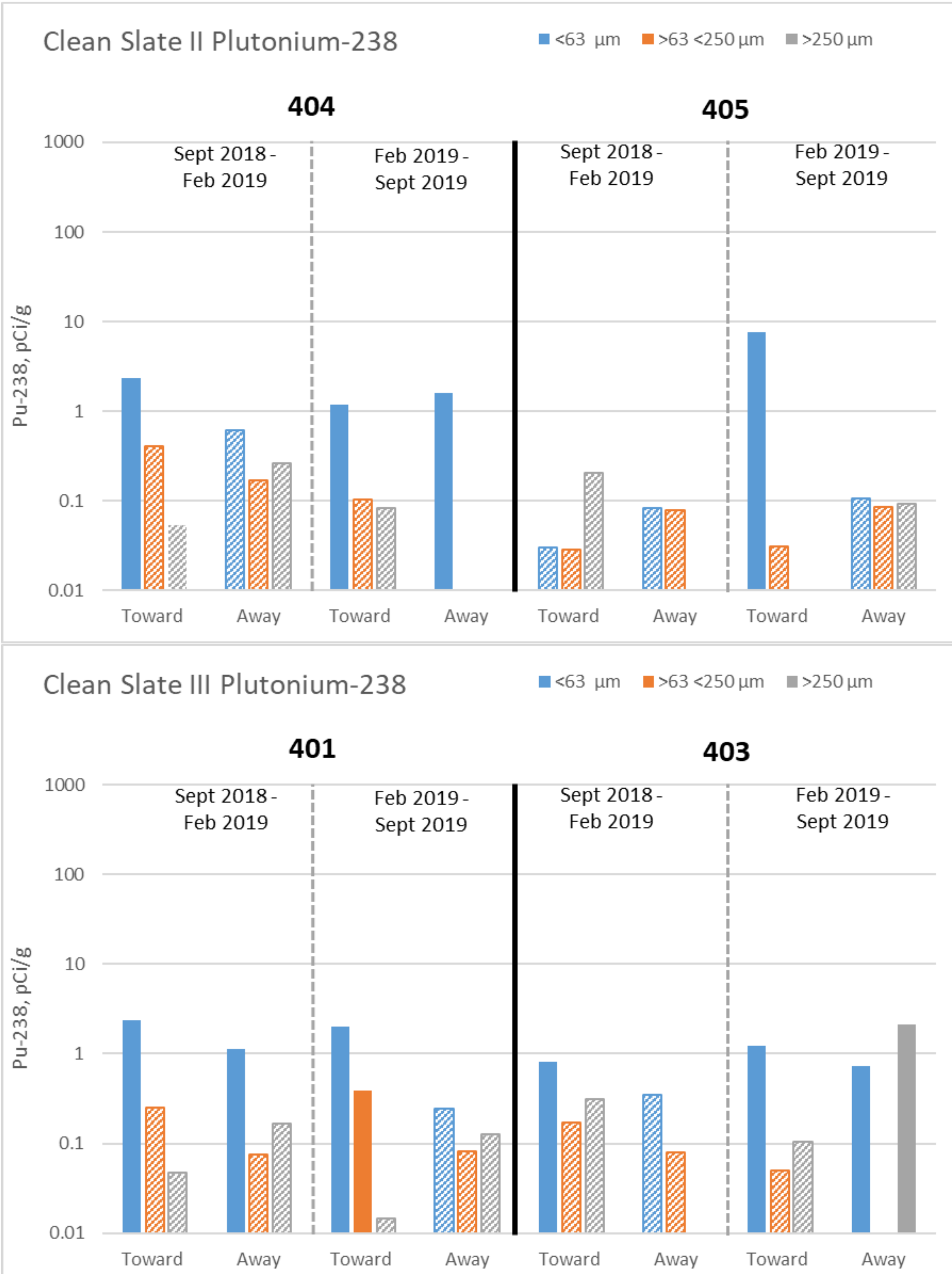


Figure 37. $^{238}Pu$ concentrations in samples from the TTR saltation traps. The hachured pattern indicates a value below the analytical detection limit.

Concentrations of radionuclides collected in the traps adjacent to Clean Slate II significantly declined in 2019 compared with those measured in 2018, during the site remediation activities. In some case, the concentration of $^{239+240}$Pu is more than an order of magnitude less than last year. Conversely, the radionuclide concentrations in the traps positioned near Clean Slate III tend to be higher in 2019 than in 2018. Within the 2019 reporting period itself, there are no consistent temporal trends between radionuclide concentrations measured during the first BSNE collection (September 2018 to February 2019) and those measured during the second collection (February 2019 to September 2019). Considering only the smallest size fraction sample, concentrations of $^{239+240}$Pu increased from the first to second collection for both the sampler facing away and facing toward the contamination areas at Stations 403 and 405, declined at both samplers at Station 401, and declined at the Station 404 sampler facing the contamination area but increased for the sampler facing away.

In general, the stations closer to the detonation point have higher radionuclide concentrations than the stations farther away. Station 401 is within 200 m (650 ft) of the Clean Slate III detonation point, whereas Station 403 is over 1,000 m (3,280 ft) distant from that point. Station 404 is 250 m (820 ft) from the Clean Slate II detonation point and Station 405 is 600 m (1,970 ft) distant from that point. In most cases, the radionuclide concentrations for a particular size fraction were higher at Station 401 than Station 403 and higher at Station 404 than Station 405. The greatest exception to this in 2019 was for the largest size fraction collected between February and September 2019 at Station 403, with much higher concentrations of all the measured radionuclides than found at Station 401, which is closer to the contamination area.

The $^{239+240}$Pu concentrations for all of the composited saltation samples were on the order of 150 to 27,000 times higher than background (which is assumed to be 0.014 pCi/g per Turner *et al.* [2003]), but 10 to 1,800 times lower than the 25 millirem per year action level established for environmental restoration of Soil Activity sites (which is equivalent to a $^{239+240}$Pu concentration of 4,120 pCi/g for an industrial area worker scenario) (U.S. DOE, 2014). The $^{239+240}$Pu/$^{238}$Pu ratio was also 4.4 to 7.7 times higher than that from atmospheric weapons testing fallout in the northern hemisphere (based on a fallout ratio of 30 from Turner *et al.* [2003]) for seven of the eight samples with $^{238}$Pu above the analytical detection limit of the samples, with the eighth sample being less than half the fallout ratio. The higher $^{239+240}$Pu/$^{238}$Pu ratio indicates a source for plutonium isotopes other than fallout and is consistent with the location adjacent to the Clean Slate plutonium dispersal tests.

## DISCUSSION

The EM NV began a final phase of remediation activities at TTR in late CY2017 that continued into CY2019. The activities included the removal of contaminated soil and debris, and the transport of that material to the NNSS where it was placed in radioactive waste management facilities. Soil disturbing activities in the Contamination Area at Clean Slate II began on October 31, 2017, and were completed on July 26, 2018 (Table 1). Approximately 0.036 km$^2$ (nine acres) were under remediation. Soil disturbing work at Clean Slate III began on September 5, 2018, and was completed on August 29, 2019, with a hiatus from December 20, 2018, until January 8, 2019. Approximately 0.04 km$^2$ (10 acres) were remediated at Clean Slate III. Revegetation activities, including ripping the soil and seeding, occurred between October 7 to 24, 2019, and December 9 to 18, 2019, at Clean Slate II and between October 1 and December 3, 2019, at Clean Slate III (Table 1). Monitoring results from CY2018 at the stations adjacent to the Clean Slate sites identified that the land disturbance associated with remediation activities caused a significant increase in the airborne transport of radionuclides (Chapman *et al*., 2019).

The sections below describe the CY2019 observations at Stations 401 and 403 during the remediation of Clean Slate III, and at Stations 404 and 405 after remediation at Clean Slate II. Station 400 at the ROC, which is the closest regularly staffed work location to the Clean Slate sites, was also operational throughout the year. The ROC is northwest of the Clean Slate sites, and therefore downwind of the contamination areas when winds are from the southeast (Figure 2). The mean gross alpha concentration at Station 400 was lower in 2019 than 2018 ($1.75 \times 10^{-15}$ µCi/mL and $2.51 \times 10^{-15}$ µCi/mL, respectively). Two filters collected during the first quarter of the year had gross alpha concentrations higher than the long-term annual mean plus standard deviation (a summation to $2.86 \times 10^{-15}$ µCi/mL) (Figure 38). Neither $^{238}Pu$ nor $^{239+240}Pu$ were above the detection limit concentration on any of the eight filters analyzed by alpha spectroscopy (Appendix E).

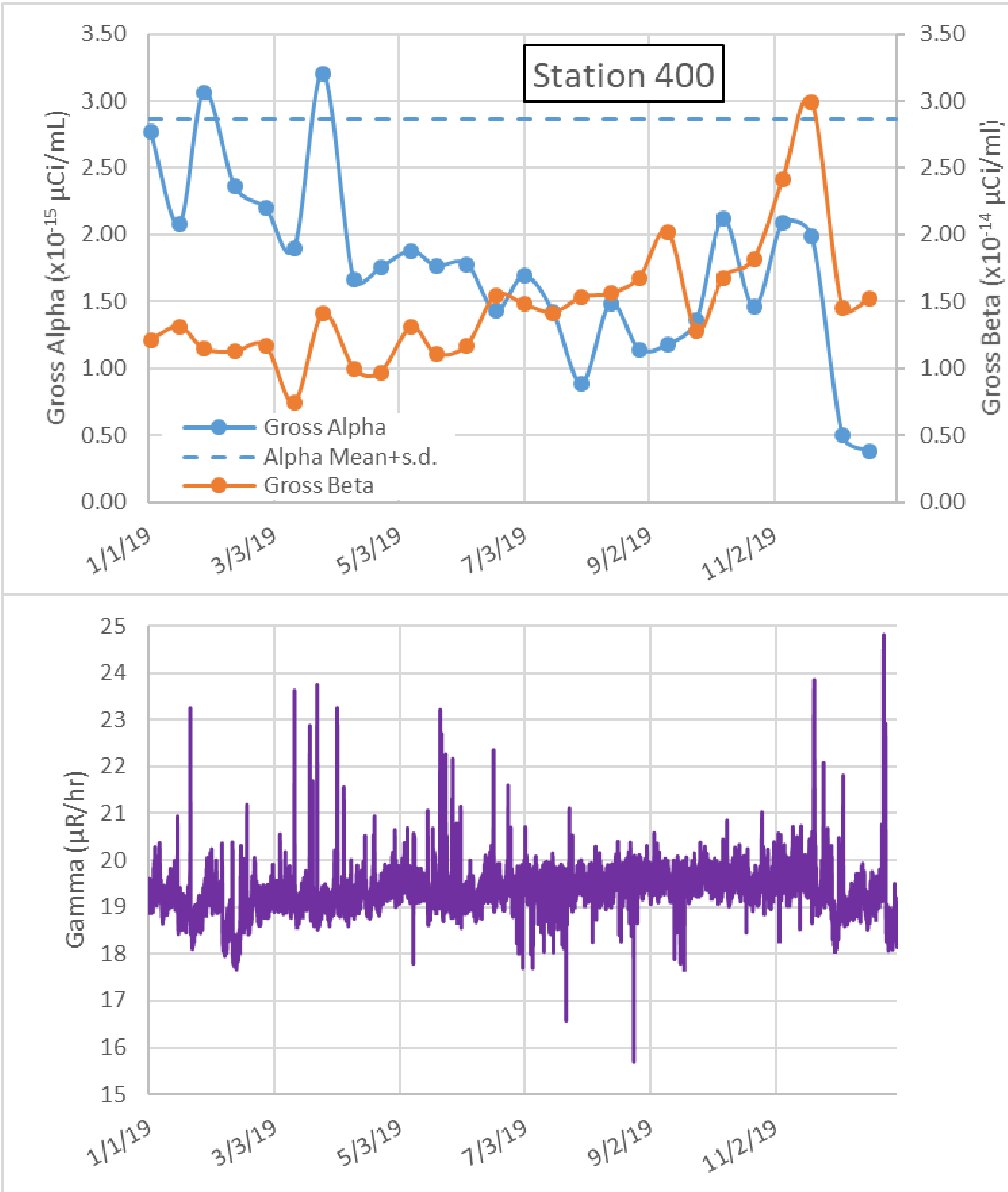


Figure 38. Gross alpha and beta (top), and gamma rate (bottom) measurements at Station 400 during CY2019. The mean and standard deviation for gross alpha are calculated for the 2014 to 2019 time period.

## Monitoring Observations during Remediation Activities in CY2019

During CY2019, Stations 401 and 403 at Clean Slate III were the monitoring locations closest to remediation activity (Figure 7). Station 401 is north of the Clean Slate III contamination area and receives dust from the area when winds are from the south. Station 403 is located to the southeast and receives dust from the contamination area when winds are from the north and northwest.

The mean gross alpha for Station 401 was $4.39 \times 10^{-15}$ µCi/mL in CY2019, which is an increase from the mean of $2.59 \times 10^{-15}$ µCi/mL in CY2018. Station 401 is the monitoring station with the longest record of gross alpha concentrations for filters collected prior to remediation activities, with a total of 254 pre-remediation filter analyses. The measurement exceeds the pre-remediation mean ($1.84 \times 10^{-15}$ µCi/mL**)** plus standard deviation ($1.19 \times 10^{-15}$ µCi/mL) for 11 of the 23 samples collected during CY2019 at Station 401 (Table 13 and Figure 39). These 11 samples are spread throughout the year, occurring in every sampled month except December (sampler problems prevented collection during July).

Four filters collected from Station 401 during CY2019 also detected $^{241}$Am during gamma spectroscopy analysis. This was the highest number of gamma spectroscopy $^{241}$Am detections in any single year of monitoring at the Clean Slate sites. The $^{241}$Am detections coincided with the highest three $^{239+240}$Pu concentrations and the only $^{238}$Pu concentrations above the detection limit. These all occurred in the first half of CY2019, whereas the fourth $^{241}$Am detection occurred in late October/early November after remediation work at Clean Slate III was completed but during revegetation activities. Revegetation activities of soil preparation (ripping) and reseeding occurred from October 7 to December 18, 2019, at Clean Slate III (Table 1).

All eight filters analyzed by alpha spectroscopy from Station 401 at Clean Slate III measured $^{239+240}$Pu above the detection limit (Appendix E). The highest $^{239+240}$Pu concentration of any station in 2019, a value of $301.75 \times 10^{-16}$ µCi/ml, was collected from late February to mid-March 2019 at this station. This sample also contained the highest concentration of $^{238}$Pu measured by the network in 2019 ($1.94 \times 10^{-16}$ µCi/ml). The other $^{238}$Pu detections at Station 401 occurred for samples collected in mid-February and late April to early May. Samples collected from early June 2019 onward were below the detection limit for $^{238}$Pu. After a decrease in $^{239+240}$Pu concentrations in samples collected in August and September, concentrations were observed to increase in the autumn.

In CY2019, six of the eight filters from Station 403 analyzed by alpha spectroscopy measured $^{239+240}$Pu above the detection limit, and one measured $^{238}$Pu above the detection limit (Appendix E). The highest $^{239+240}$Pu concentration of $102.73 \times 10^{-16}$ µCi/ml was measured on a filter collected in late March to early April (Figure 40). The second highest concentration ($83.78 \times 10^{-16}$ µCi/ml) occurred for a filter collected in late October to early November.

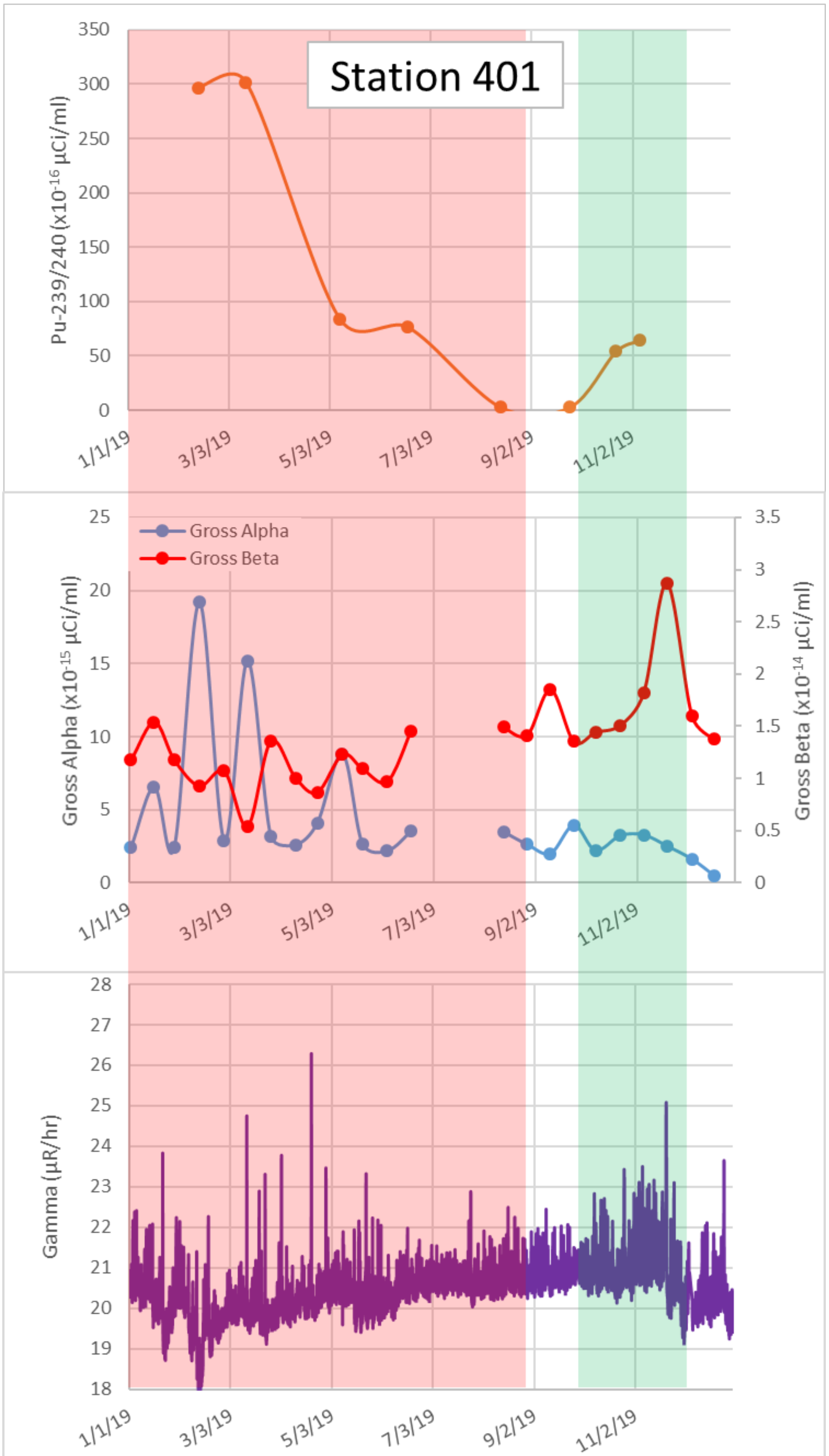


Figure 39. Radiologic data collected at Station 401 during CY2019. The red band denotes the time period of remediation work at Clean Slate III, and the green band aligns with the reseeding activities at the site.

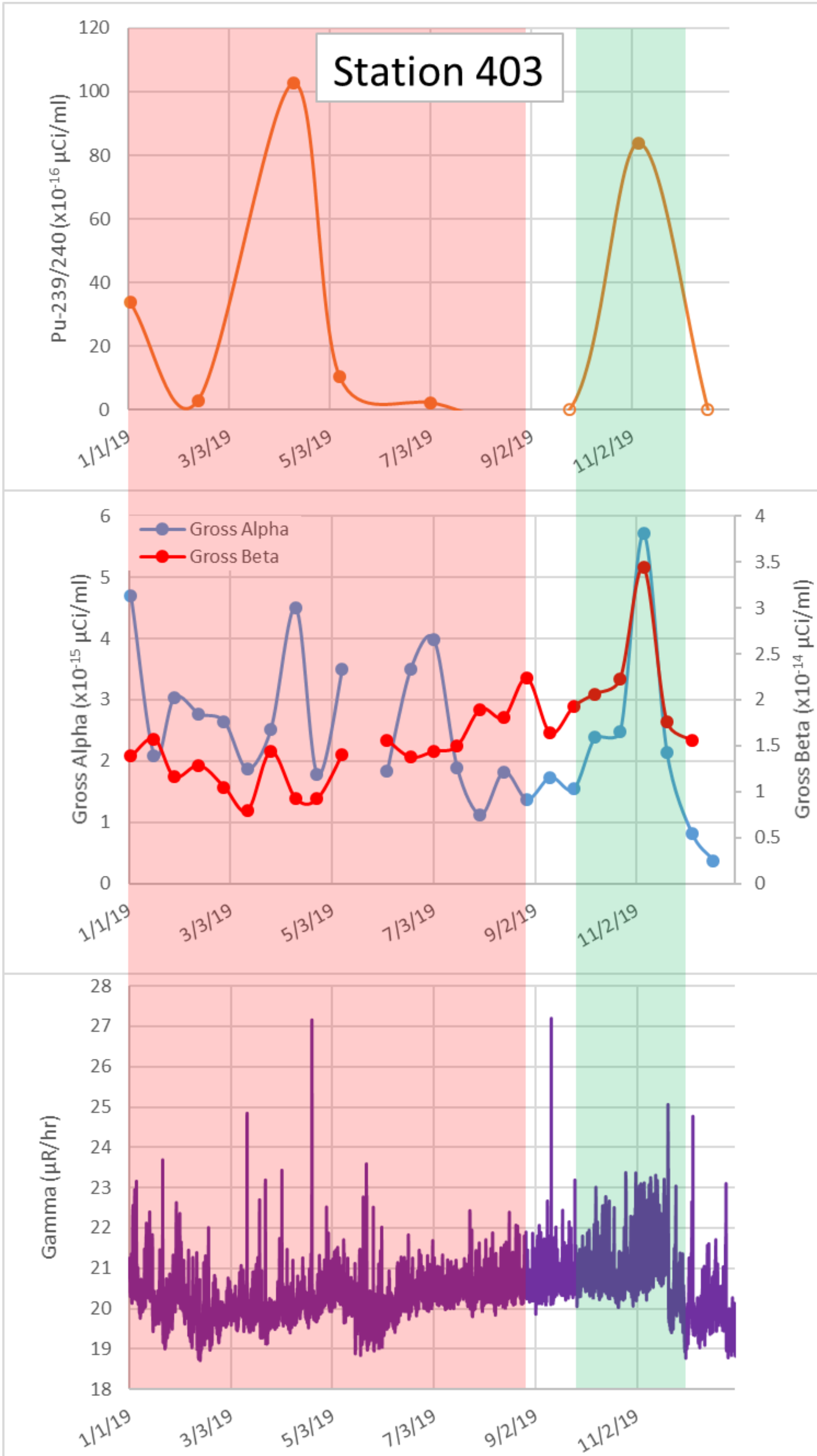


Figure 40. Radiologic data collected at Station 403 during CY2019. Open symbols indicate data below the analytical detection limit. The red band denotes the time period of remediation work at Clean Slate III, and the green band aligns with the reseeding activities at the site.

Station 403 had three filters with gross alpha concentrations higher than the pre-remediation mean plus standard deviation for this station (measured on the 34 filters collected at Station 403 prior to remediation; mean of $2.76 \times 10^{-15}$ µCi/mL and standard deviation of $1.62 \times 10^{-15}$ µCi/mL**)** (Table 13 and Figure 40). These three occurrences are spread throughout the year, with one on a filter sampling from December 19, 2018, to January 2, 2019 (during the hiatus in remediation work); one from March 27, 2019, to April 11, 2019; and one from October 23, 2019, to November 6, 2019 (the same time interval when $^{241}$Am was detected on the filter from Station 401). The first two detections occurred during filter collection periods where the filters at Station 401 were lower than the mean plus standard deviation of pre-remediation gross alpha concentration. Consistent with that observation, the winds during those sample intervals were predominantly from the northwest (Figure 41), such that Station 401 was upwind of the contamination area and Station 403 was downwind.

Evaluating the radiochemical results, dust loading on the sample filters, and the meteorological data reveal individual wind events leading to radionuclide transport. Several wind events are described below, selected based on their high $PM_{10}$ measurements, which occurred on January 5th, February 4th, March 12th, October 29th, and November 25th of 2019.

The filter collection period between January 2 and 16, 2019, has gross alpha readings of $6.55 \times 10^{-15}$ and $2.09 \times 10^{-15}$ µCi/mL at Stations 401 and 403, respectively, and filter mass loadings of 0.0221 g and 0.0054 g, respectively. The most significant wind episode during these two weeks was on January 5, 2019, when winds came consistently from the south and there were sustained wind speeds in excess of 40 km/hr (25 mph) (Figure 42). The $PM_{10}$ concentration at Station 401 reached a maximum of 5,247 µg/m$^3$, whereas the $PM_{10}$ concentration at Station 403 during the same period reached a maximum of 111 µg/m$^3$. The data are consistent with a significant increase in $PM_{10}$ as strong winds from the south blew across the Clean Slate III remediation area, suspending dust that caused a more than 300 percent increase in filter mass loading at Station 401 compared with Station 403. The gross alpha measured on the filter from Station 401 was more than three times higher compared with the filter from Station 403 during the same time period, which is consistent with Clean Slate III as the source of the dust. This event occurred when active remediation was on hiatus, so the observed suspended dust was entrained as strong winds blew across the Clean Slate III site and were not lofted by on-site activity.

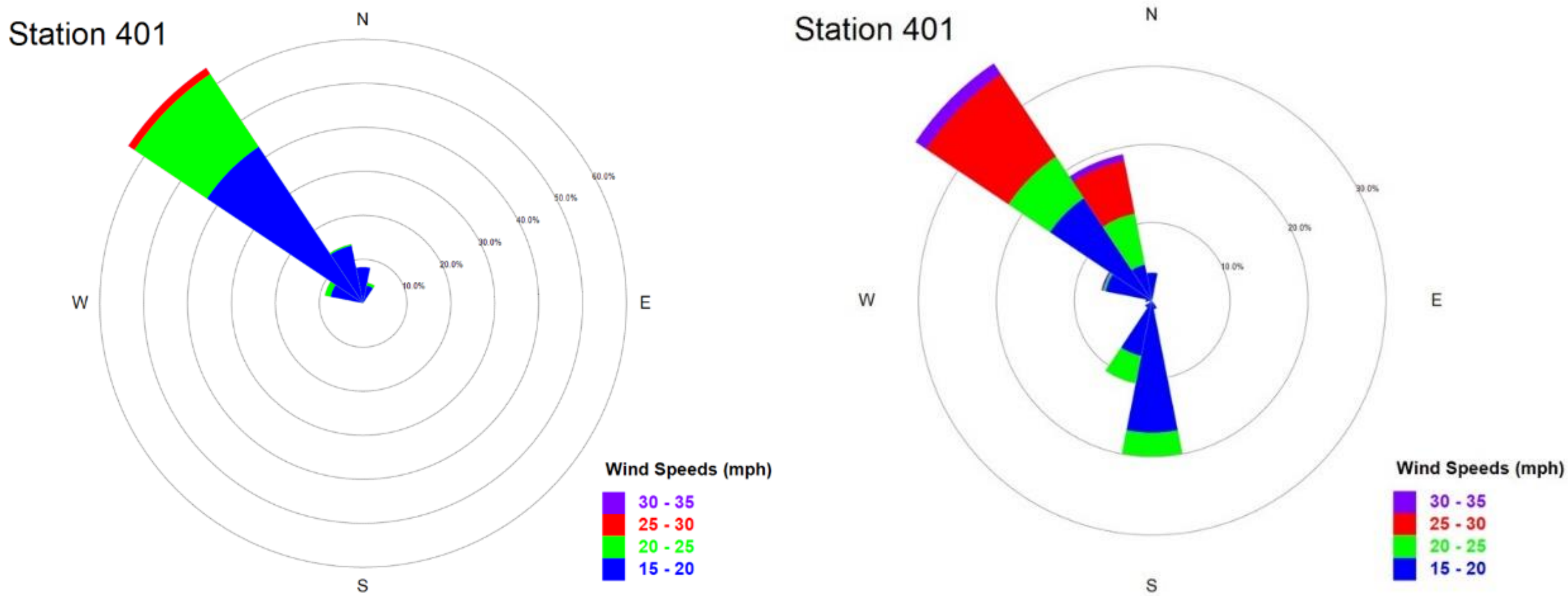


Figure 41. Wind roses for Station 401 winds greater than 24 km/hr (15 mph) for the time periods of December 19, 2018, to January 2, 2019 (left), and March 27, 2019, to April 11, 2019 (right).

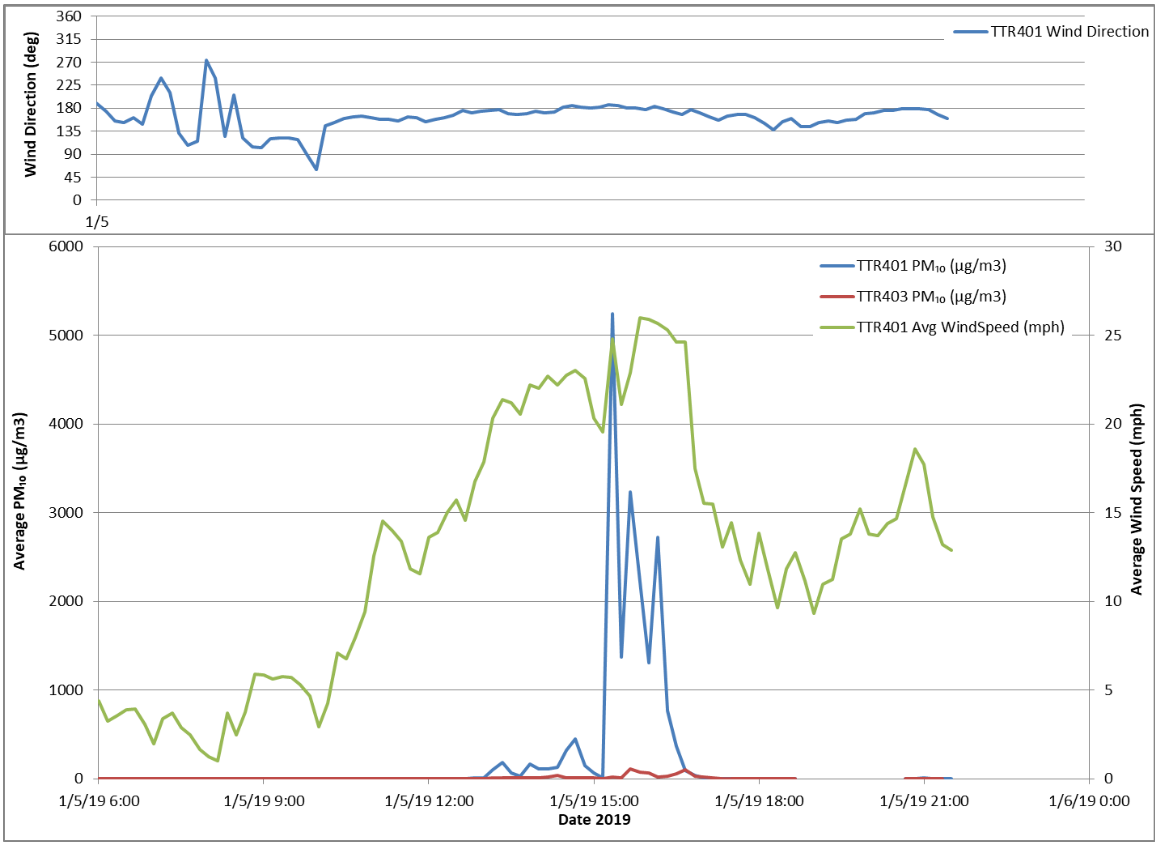


Figure 42. Dust transport episode at Clean Slate III on January 5, 2019.

Another example of dust and radionuclide transport by southerly winds across the Clean Slate III site occurred during the filter collection period between January 28 and February 12, 2019. The gross alpha measurements for the filters from Stations 401 and 403 were $19.2 \times 10^{-15}$ and $2.77 \times 10^{-15}$ µCi/mL, respectively, with filter mass loadings of 0.0208 g and 0.0034 g, respectively. Gross alpha was almost seven times higher and mass loading was six times greater at Station 401 compared with Station 403. Gamma spectroscopy of the filter from Station 401 identified $^{241}$Am, and alpha spectroscopy detected $^{238}$Pu and the second highest $^{239+240}$Pu concentrations measured on a filter during 2019. The most significant dust transport episode in this period, according to the $PM_{10}$ data, occurred on February 4, 2019, between 1300 and 1700 hours Pacific Standard Time (PST) during which sustained winds reached approximately 50 km/hr (31 mph) (Figure 43). The maximum hourly mean $PM_{10}$ of 2087 µg/m$^3$ at Station 401 coincided with maximum winds at 1500 hours PST. Station 403 recorded a much lower maximum $PM_{10}$ of 15 µg/m$^3$ over the same time period. Winds were blowing consistently from the south so that Station 401 was again downwind of Clean Slate III, with the contamination area presumed as a dust source. It is possible that the ongoing remediation activities contributed to suspension of $PM_{10}$. For example, during a maintenance trip to the Clean Slate III stations in February 2019, heavy machinery operation was observed during windy conditions to directly suspend dust that was then transported by wind.

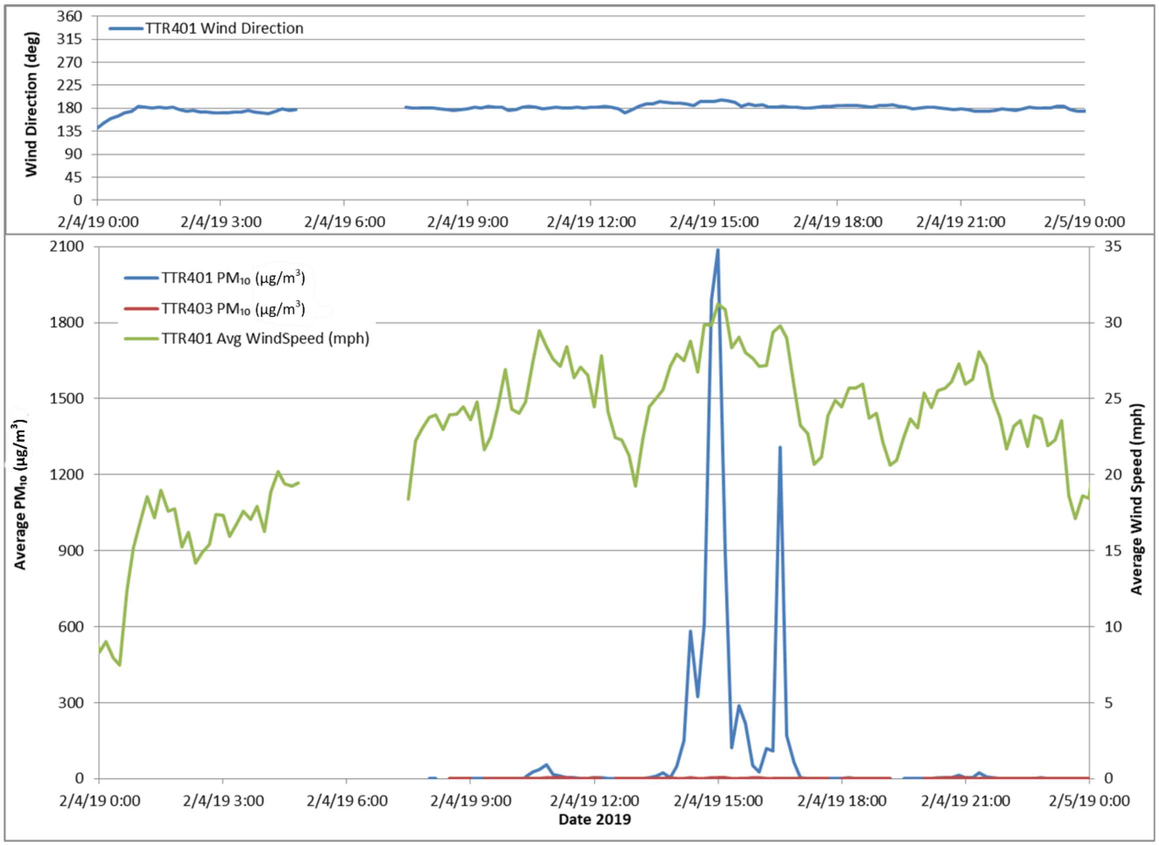


Figure 43. Dust transport episode at Clean Slate III on February 4, 2019.

The filter collection period between February 27 and March 13, 2019, resulted in gross alpha readings of $15.2 \times 10^{-15}$ and $1.87 \times 10^{-15}$ µCi/mL at TTR Stations 401 and 403, respectively, and filter mass loadings of 0.0077 g and 0.0040 g, respectively. Gross alpha readings were approximately eight times higher and mass loading was approximately 1.75 times greater at Station 401 compared with Station 403. The most significant dust transport episode in this time period occurred on March 12, 2019, between 1730 and 1900 hours PST, with sustained winds of 45 km/hr (28 mph) (Figure 44). The maximum $PM_{10}$ of 225 µg/m$^3$ at Station 401 coincided with maximum winds at 1810 hours PST. Station 403 recorded a maximum $PM_{10}$ of only 77 µg/m$^3$ over the same time period. Winds were initially blowing from the south as the wind speed increased to over 32 km/hr (20 mph), and then shifted to the northwest. Although wind speed and $PM_{10}$ concentration were not as high as the previously described wind episodes, the filter sample from this specific interval had the second highest gross alpha concentration, $^{241}$Am was detected, and it had the highest $^{239+240}$Pu concentration measured on a filter in 2019.

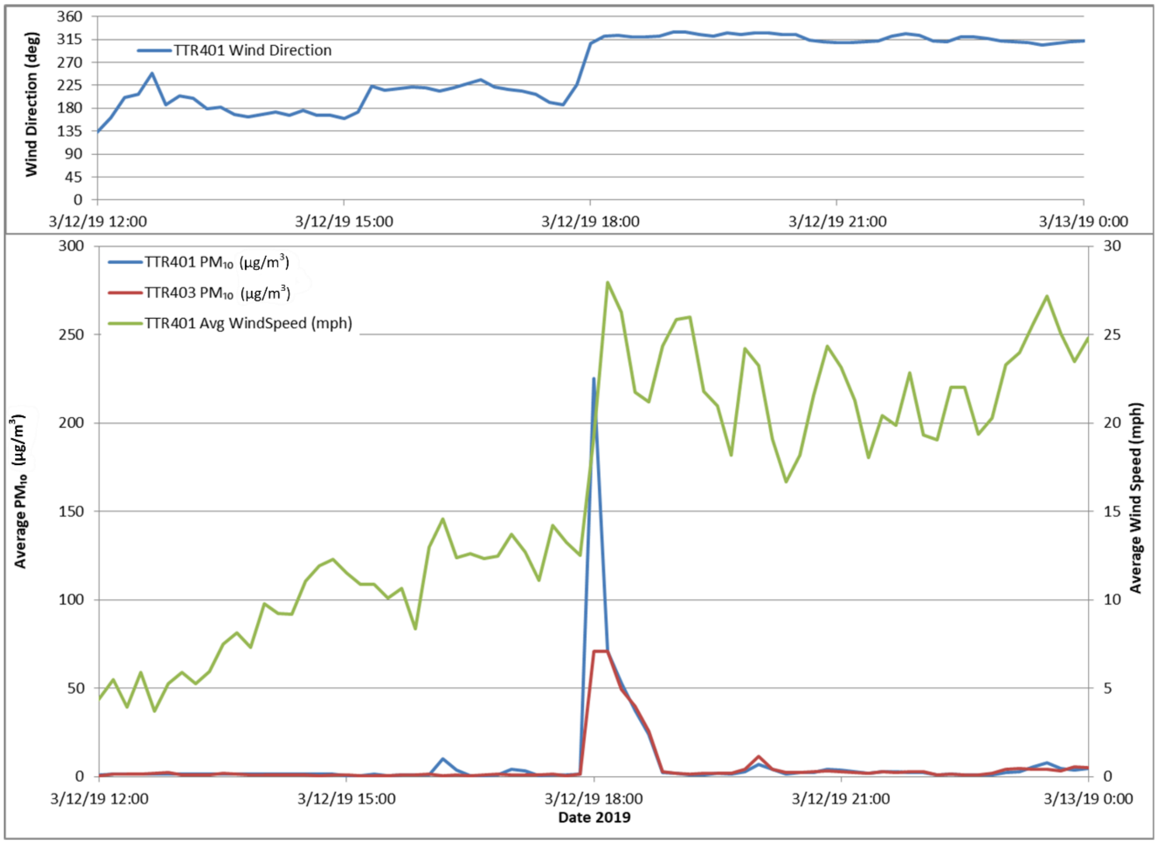


Figure 44. Dust transport episode Clean Slate III on March 12, 2019.

The filter collection period between October 23 and November 6, 2019, occurred after the remediation work at Clean Slate III ended, but was during the time period when reseeding of the site was taking place (which included ripping the soil). The gross alpha measured on the filters were $3.27 \times 10^{-15}$ and $5.71 \times 10^{-15}$ µCi/mL at Stations 401 and 403, respectively, the $^{239+240}$Pu concentrations were $64 \times 10^{-16}$ and $84 \times 10^{-16}$ µCi/mL, respectively, and $^{241}$Am was detected on the Station 401 filter. The filter mass loading was 0.0965 g at Station 401 and 0.0282 g at Station 403. During this two-week period, the most significant dust transport episode occurred on October 29, 2019, between 0600 and 1530 hours PST when sustained winds reached 50.7 km/hr (31.5 mph) (Figure 45). The maximum $PM_{10}$ of 4,534 µg/m$^3$ at Station 401 coincided closely with the maximum winds of 49.1 km/hr (30.5 mph) at 1050 hours PST. Station 403 recorded a maximum $PM_{10}$ of 1,080 µg/m$^3$ at the same time period. During this episode, winds were primarily from the northwest as the wind speed quickly increased to over 32 km/hr (20 mph), placing Station 403 downwind of the contamination area. This orientation relative to the wind accounts for the higher gross alpha and $^{239+240}$Pu concentrations at Station 403 compared with Station 401, despite Station 403 being farther from the contamination area. Nonetheless, Station 401 had a higher $PM_{10}$ concentration and a higher mass loading than observed at Station 403, and the radionuclides detected in the Station 401 filter were consistent with Clean Slate III, despite the absence of winds in excess of 24 km/hr (15 mph) from the south during the two-week period (Figure 46). These monitoring results suggest that activities at a waste staging area located immediately northwest of Station 401 could be the source of some portion of the dust detected at Station 401, and that there was resuspension of contaminants dispersed north-northwest of Clean Slate III. The timing of the contaminant dispersal to the north of the site is unknown. It could have occurred at the time of the Clean Slate III experiment, during the intervening decades in response to southerly wind events, during the remediation activity in response to southerly winds, or as part of the waste staging activities.

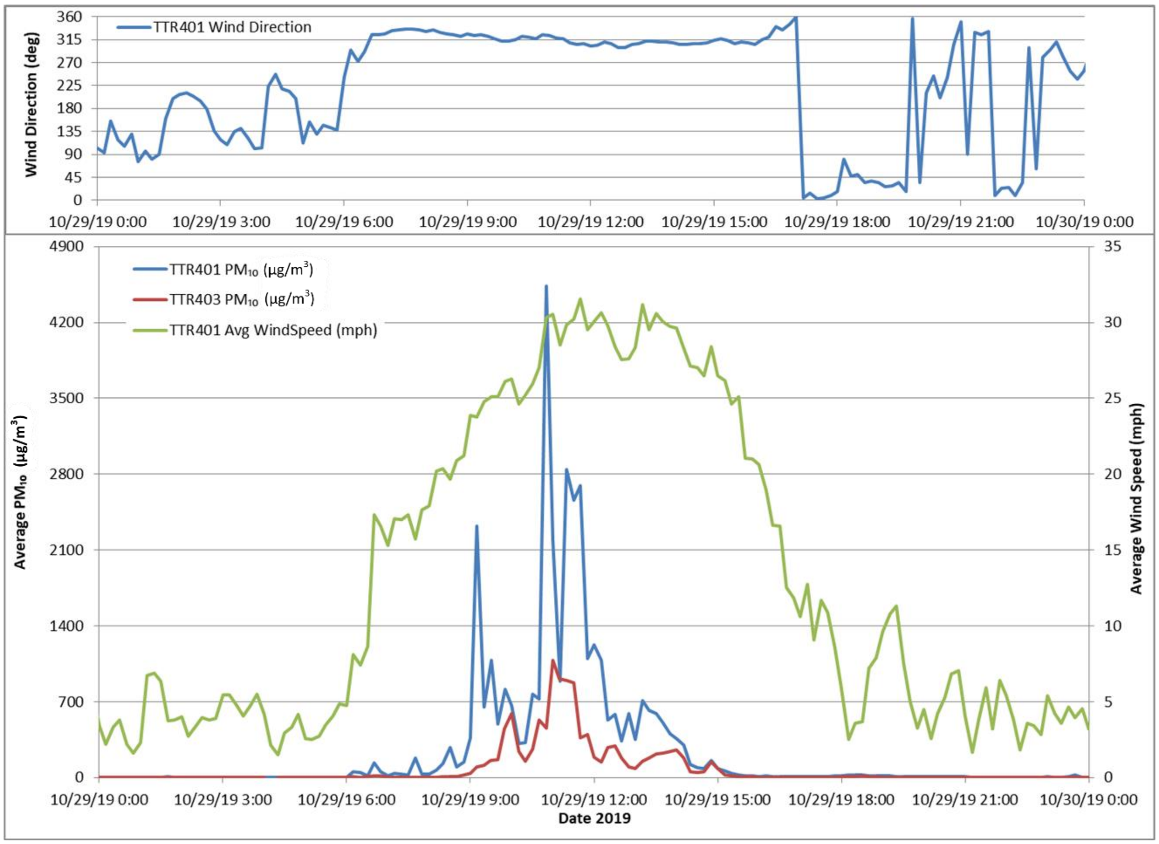


Figure 45. Dust transport episode at Clean Slate III on October 29, 2019.

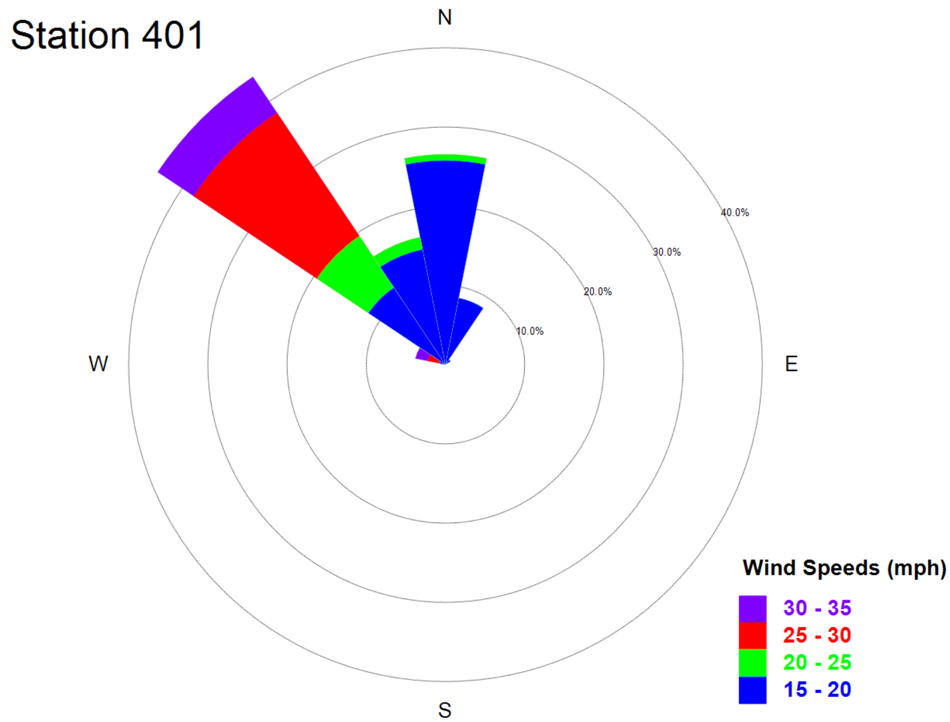


Figure 46. Wind rose for Station 401 for winds greater than 24 km/hr (15 mph) during October 23 through November 6, 2019.

A subsequent wind event from the north-northwest occurred on November 25, 2019, during the filter collection period between November 20 and December 5, 2019. Between 0910 and 1430 hours PST of that day, there were sustained winds as high as 51.5 km/hr (32 mph) (Figure 47). As with the late October event, the maximum $PM_{10}$ was recorded at Station 401 (1,795 μg/$m^3$) upwind during the event from Clean Slate III rather than at downwind Station 403 ($PM_{10}$ of 232 μg/$m^3$), and the larger mass loading was on the Station 401 filter for the sample period compared with that on the Station 403 filter (0.0448 g and 0.00592 g, respectively). However, the gross alpha concentrations for filters from both stations were within the pre-remediation mean plus one standard deviation of each site, indicating contaminant transport conditions similar to those observed prior to the disturbance of remediation activities. No alpha spectrometry was performed for this filter collection period.

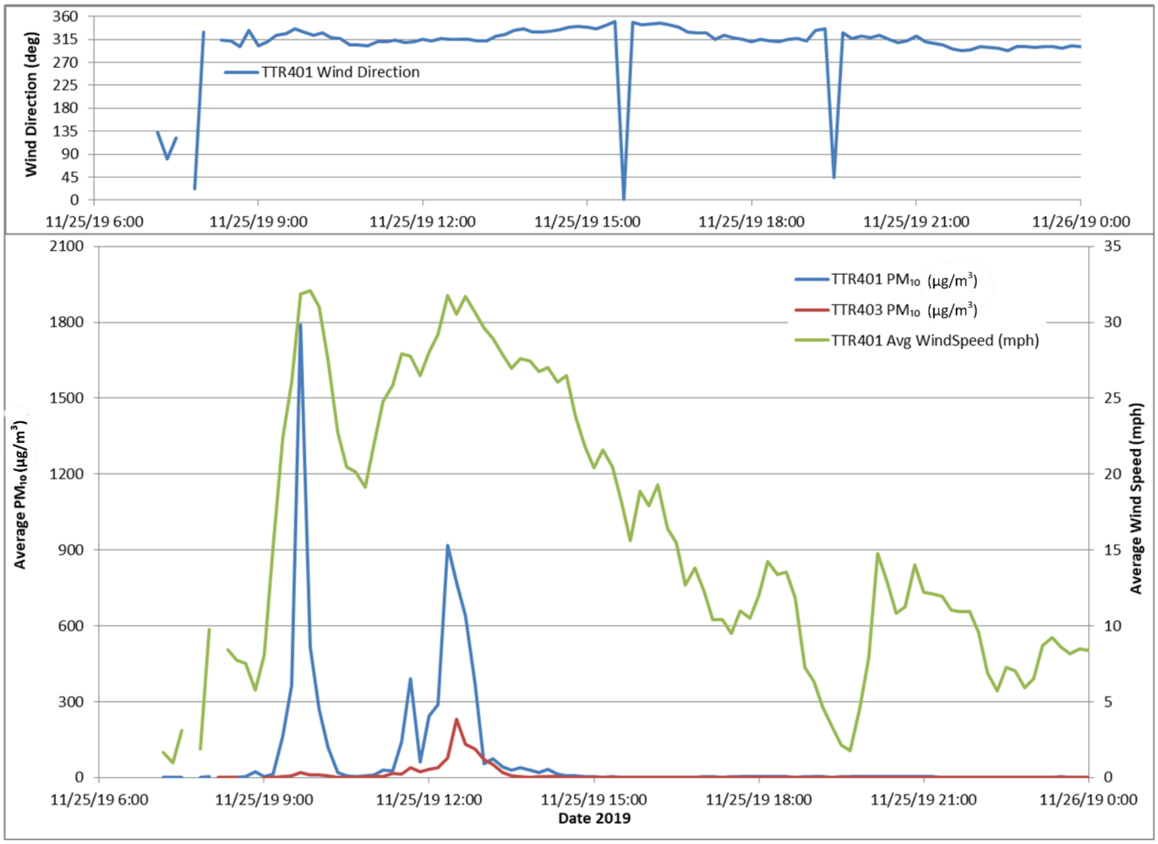


Figure 47. Dust transport episode Clean Slate III on November 25, 2019.

Saltation samples were collected over multimonth time frames. The collection periods in 2019 generally align with the remediation work at Clean Slate III. At Station 403, there was a large increase in the $^{239+240}$Pu activity of saltation material captured in traps facing both toward and away from the contaminated area during the remediation time frame (Figure 48). The same observation is true for the traps facing the contamination area at Station 401, with an order of magnitude increase in $^{238+239}$Pu concentrations for the smallest particle size material. The Station 401 traps facing away from the contamination area had lower radionuclide concentrations than the prior collection in 2018, but these concentrations were generally of the same magnitude of those measured at Station 403. The higher concentrations at Station 401 are consistent with the closer proximity of the station to the contaminated area.

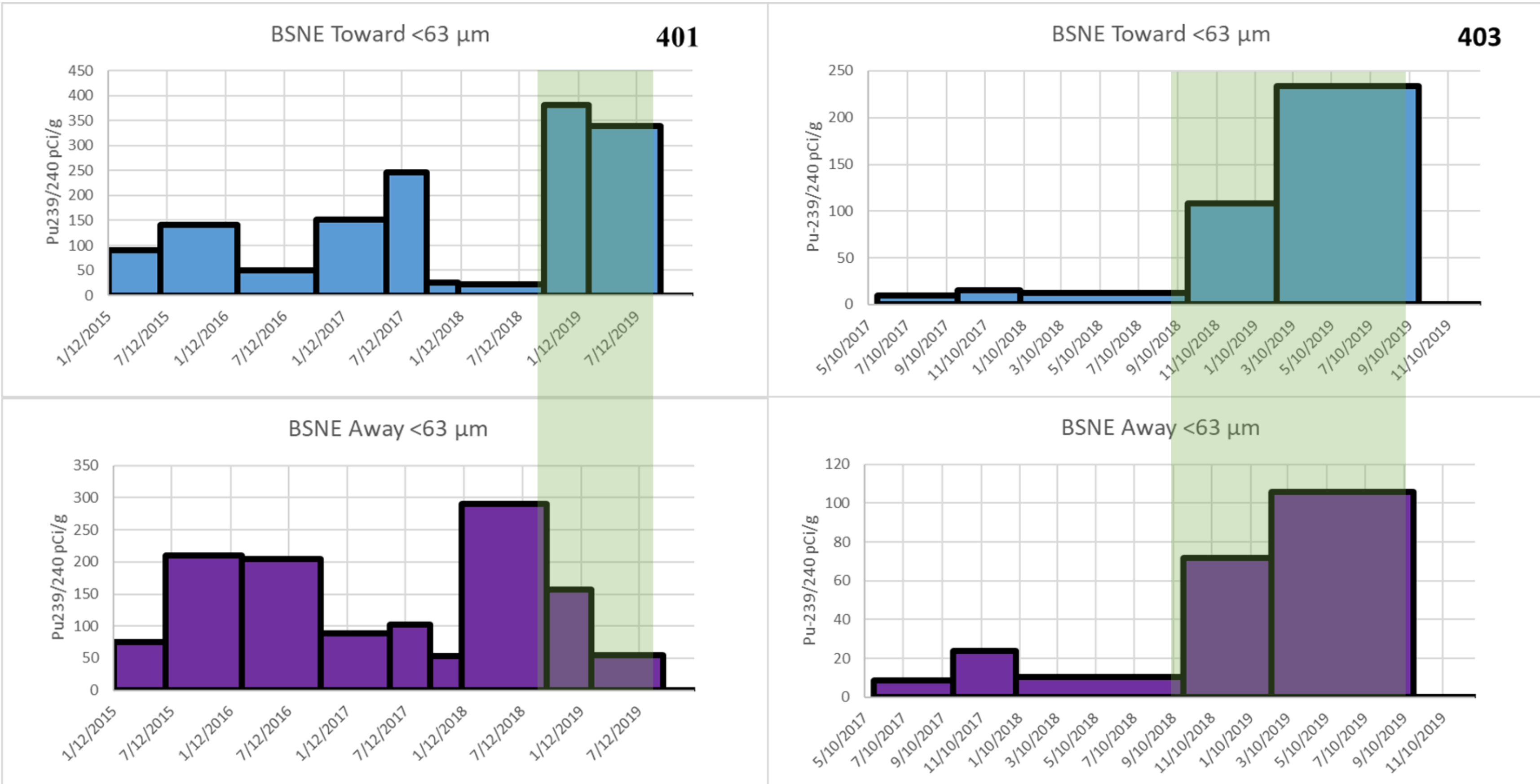


Figure 48. $^{239+240}$Pu concentrations in saltation samples from BSNE traps at Clean Slate III stations. The remediation activities at the site occurred during the time interval indicated by the shaded area.

**Monitoring Observations Post-remediation at Clean Slate II in 2019**

Only a limited number of pre-remediation gross alpha analyses are available for Station 404 (13 samples; mean of $2.65 \times 10^{-15}$ µCi/mL and standard deviation of $1.22 \times 10^{-15}$ µCi/mL) and Station 405 (nine samples; mean of $2.63 \times 10^{-15}$ µCi/mL and standard deviation of $0.97 \times 10^{-15}$ µCi/mL), but all of the CY2019 gross alpha concentrations at these stations were lower than the pre-remediation mean plus standard deviation (Figure 49). The filter collected from Station 404 for the period of March 13 to March 27, 2019, was very close to that threshold.

Six of the eight filters analyzed by alpha spectroscopy for Stations 404 and 405 measured $^{239+240}$Pu above the detection limit (Figure 49 and Appendix E). The two samples that were below the detection limit for $^{239+240}$Pu were collected during the summer months for both stations. The highest $^{239+240}$Pu concentrations at Stations 404 and 405 ($17.62 \times 10^{-16}$ µCi/ml and $5.09 \times 10^{-16}$ µCi/ml, respectively) occurred for the filter deployed between May 9 and 21, 2019. Nine of the 13 days in that period experienced winds greater than 24 km/hr (15 mph) and five of the days exceeded 32 km/hr (20 mph) winds, with two occurrences at each station of $PM_{10}$ in excess of 100 µg/m$^3$. For wind speeds in excess of 24 km/hr (15 mph), a direction from the south was most prevalent (Figure 50), which is consistent with the higher $^{239+240}$Pu concentration measured at Station 404, although winds that speed also occurred from the northwest, placing Station 405 downwind from the contamination area at those times.

Only one filter, collected in early May from Station 405, had $^{238}$Pu above the detection limit. The reseeding activities in the autumn (Table 1) coincided with a small uptick in $^{239+240}$Pu concentrations at Stations 404 and 405 (from concentrations below the analytical detection limit in the summer to detections of $^{239+240}$Pu of 0.7 to 2.3 µCi/ml $\times 10^{-16}$ during revegetation), although an increase was not indicated by the less sensitive gross alpha measurements.

The saltation material collected in 2019 from the Station 404 traps facing toward the contamination area returned to pre-remediation radionuclide concentrations (Figure 51). Concentrations were also low for the first 2019 collection from the traps facing away from the contamination area at Station 404, but the second collection returned to a concentration in excess of 200 pCi/g. The first 2019 collection period for the saltation traps at Station 405 had lower radionuclide concentrations than the prior collection, followed by higher concentrations during the second period (Figure 51).

The combined radionuclide results for CY2019 from the Clean Slate II stations indicate less suspension of radionuclide material from the contamination area compared with CY2018 during remediation activities, although suspended plutonium continues to be detected in most filters analyzed by alpha spectroscopy during the year, with the highest concentrations in May. Revegetation of the site occurred during October and December 2019, and that process increased suspended $^{239+240}$Pu compared with previous samples, but not to the degree observed at Clean Slate III.

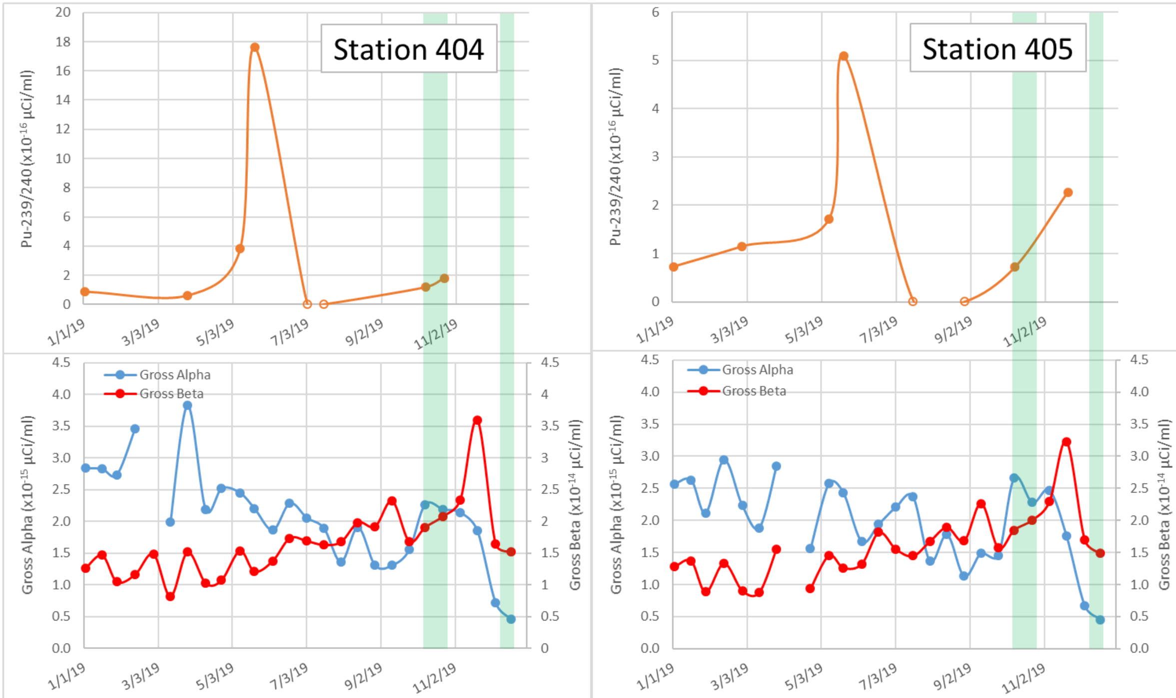


Figure 49. Radiologic data collected from Stations 404 and 405 during CY2019. Open symbols indicate data below the analytical detection limit. The green shaded areas indicate the time periods of reseeding activities at Clean Slate II.

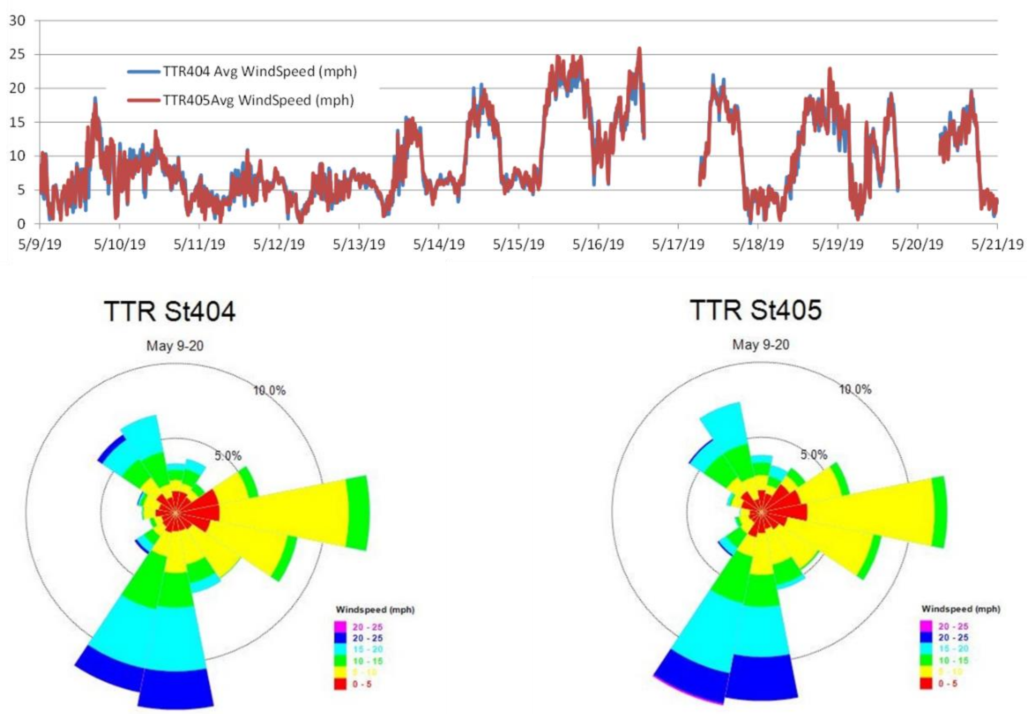


Figure 50. Wind speed and direction at Clean Slate II Stations 404 and 405 for the filter collection period of May 9 to 21, 2019.

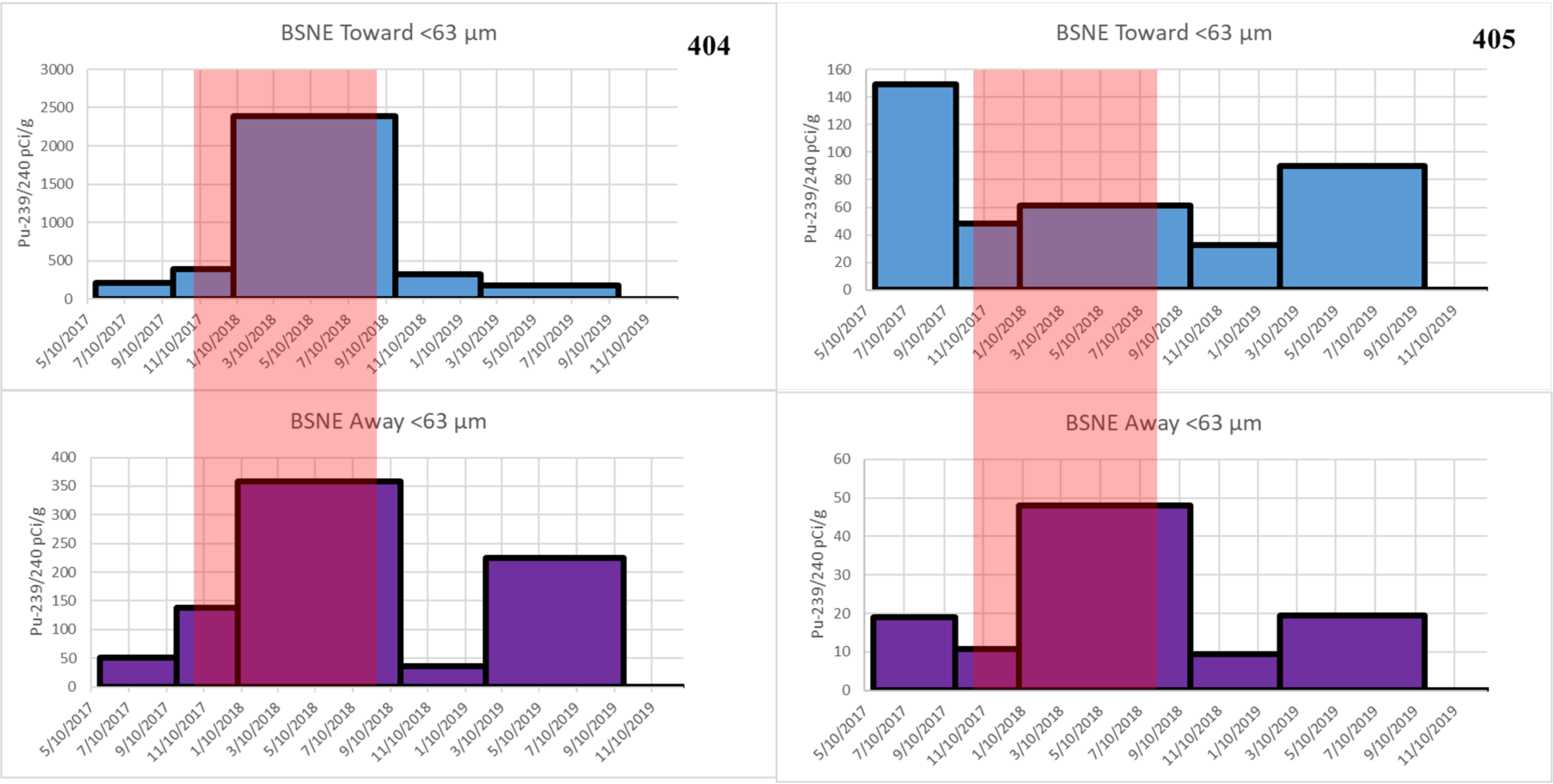


Figure 51. $^{239+240}$Pu concentrations in saltation samples from BSNE traps at the Clean Slate II stations (note that the graphs use different scales). The remediation activities occurred in the shaded time interval.

## Long-term Radionuclide Transport Trends

Pre-remediation radionuclide concentrations measured at the Clean Slate monitoring stations provide perspective on baseline conditions for suspended radionuclides prior to ground disturbance, but they do not represent natural background. For filters collected at Clean Slate II and III with measurements above the detection limit, the concentrations of $^{239+240}Pu$ exceeded the background concentration of $9.5 \times 10^{-19}$ µCi/ml (determined during continuous air monitoring at the TTR airport, northwest of the ROC, in 1996 and 1997 [SNL, 1998]). The background value was routinely exceeded by two orders of magnitude for air filters collected at the Clean Slate stations analyzed by alpha spectrometry (Appendix E), and background was exceeded by up to four orders of magnitude during the remediation activities.

Monitoring data collected prior to the site remediation activities (e.g., Chapman *et al*. [2018]) demonstrated that winds were moving plutonium-bearing particles in the environment by both suspension and saltation adjacent to the Clean Slate sites. Suspended dust with contamination above background was collected on air filters outside of the fenced contamination areas. Data from the saltation traps collected radionuclides moving toward, as well as away from, the contamination areas. These findings are consistent with site radiologic surveys that note the existence of "substantial areas of contamination…outside the fence" (EG&G, 1979).

The radionuclide concentrations of material collected during the remediation activities from 2017 to 2019 (Table 1) reveal increased migration and dispersal of plutonium-bearing dust as a consequence of land disturbing activities at the sites. The difference in gross alpha on filters from stations upwind and downwind during specific wind events indicates that the particulate matter suspended as wind moved across the remediation zone was more contaminated than dust from the surrounding area. These data also clearly demonstrate that the upwind or downwind position of the stations relative to the remediation areas shifted regularly because of the two dominant wind directions of northwesterly and southerly.

The time series of airborne particle counts and air filter and saltation trap radiological analytical results for the sites prior to remediation, during remediation, and after completion of remediation work can be used to evaluate restabilization of the areas. The stabilization metrics for $PM_{10}$ and $^{239+240}Pu$ concentrations are qualitative rather than quantitative. The $PM_{10}$ record is erratic because of the dependence on unpredictable wind events, but the remediation and reseeding time periods are characterized by concentration spikes that are larger and more frequent than the spikes generally observed outside of those times. The background concentration of $^{239+240}Pu$ should be below the analytical detection limit of the alpha spectroscopy analysis, as evidenced by the below detection limit concentrations for Station 400 (Appendix E). Above-detection concentrations have been routinely determined for air samples collected at Clean Slate II and III, but determining a quantitative pre-remediation baseline concentration for $^{239+240}Pu$ at Clean Slate II and III is hampered by the small number of analyses before the remediation activities. Although a less sensitive measurement than alpha spectroscopy, gross alpha can provide a quantitative metric in the mean plus one standard deviation measured at each site for gross alpha prior to remediation activities as an indicator of return to a generally stable soil surface condition.

Considering the combined measures of $PM_{10}$, gross alpha, and $^{239+240}Pu$ concentrations, the soil surface at Clean Slate II returned to a relatively stable condition approximately three months after remediation activities concluded (Figures 52 and 53). Nonetheless, suspension and saltation of radionuclides from the site continues to be observed in response to wind and ground disturbing events (reseeding), although at much lower concentrations than recorded during remediation activities.

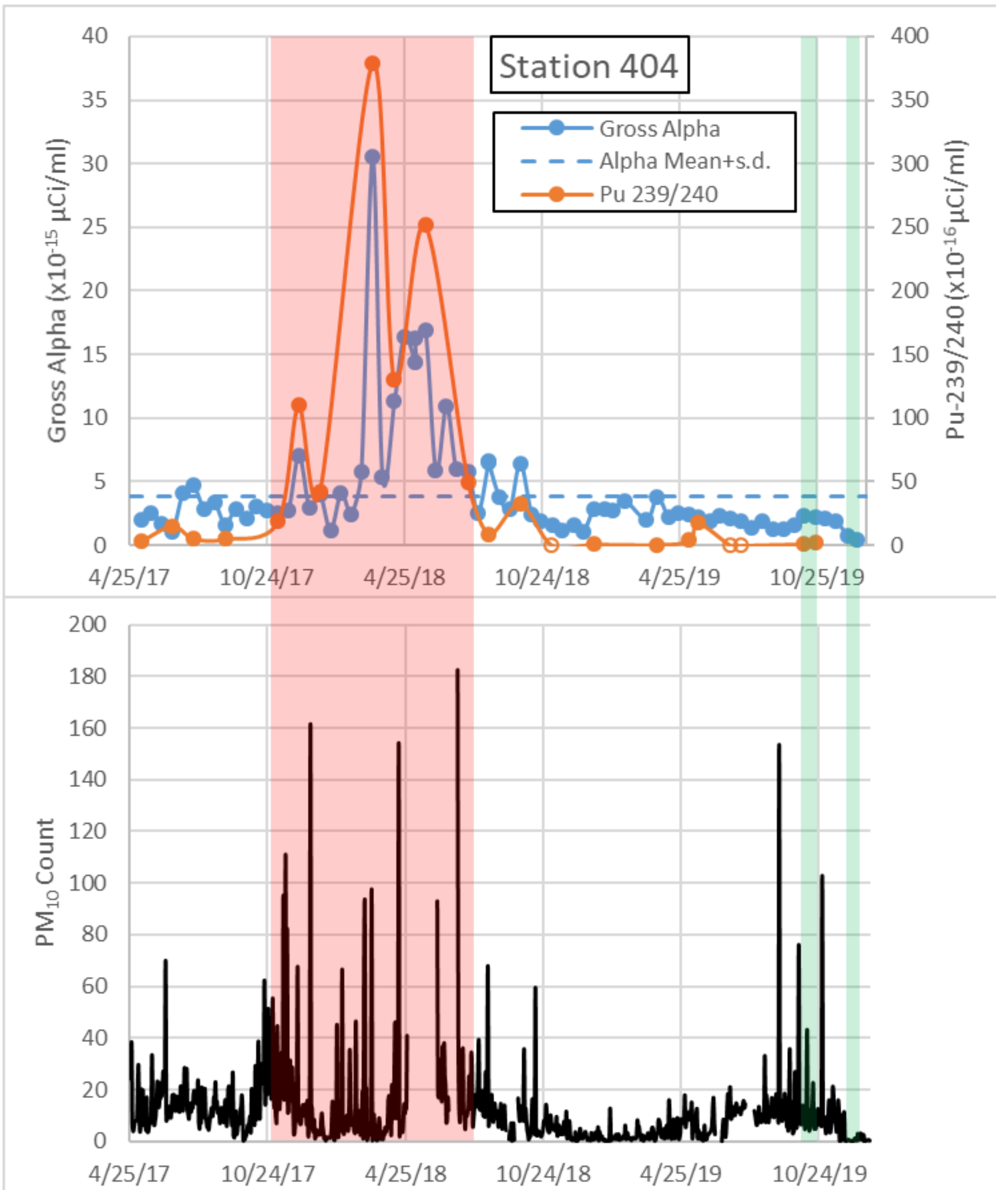


Figure 52. Gross alpha, $^{239+240}Pu$, and daily average $PM_{10}$ concentrations at Station 404 measured before, during, and after remediation activities at Clean Slate II (red band) and reseeding (green bands). Open symbols indicate data below the analytical detection limit. Gross alpha mean and standard deviation are calculated using pre-remediation data only.

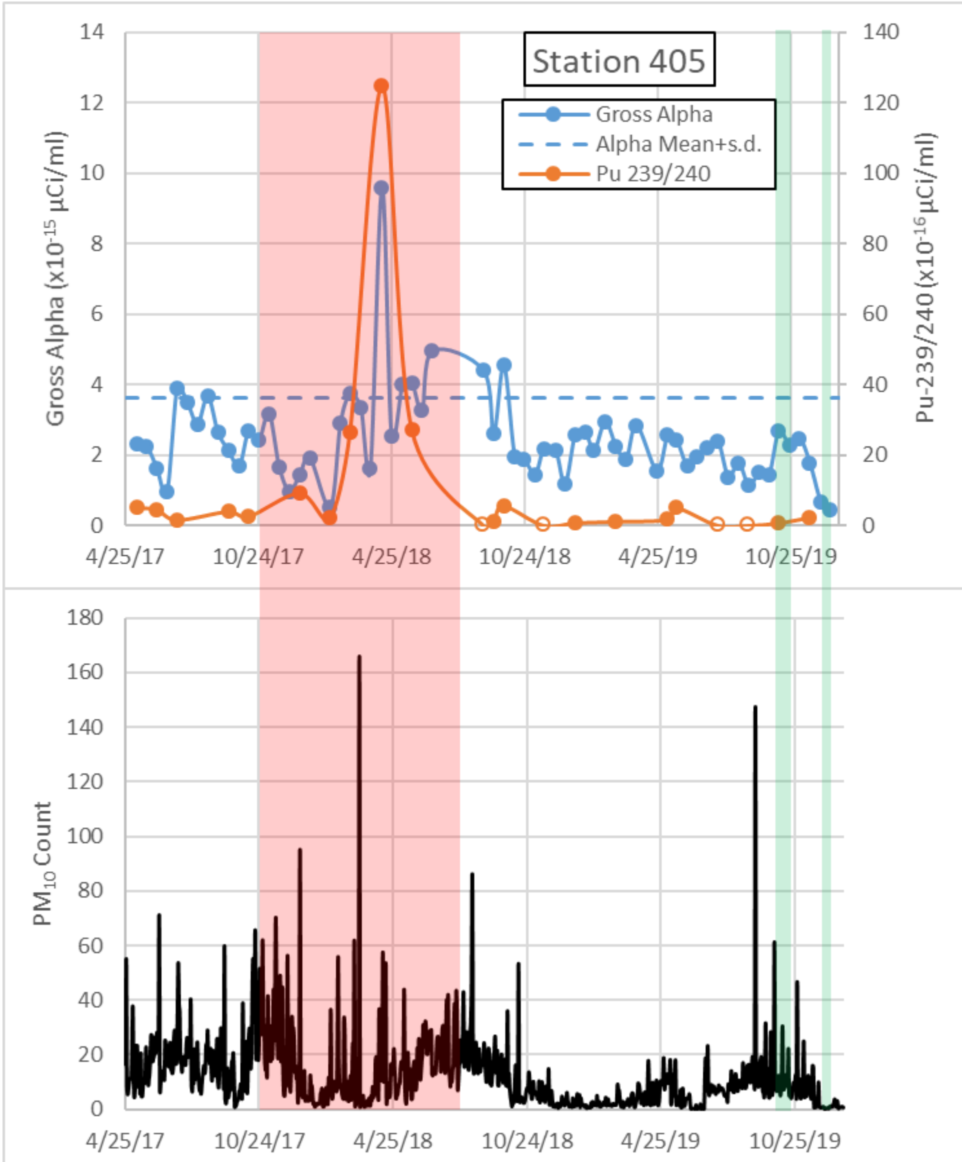


Figure 53. Gross alpha, $^{239+240}$Pu, and daily average $PM_{10}$ concentrations at Station 405 measured before, during, and after remediation activities at Clean Slate II (red band) and reseeding (green bands). Open symbols indicate data below the analytical detection limit. Gross alpha mean and standard deviation are calculated using pre-remediation data only.

At Clean Slate III, there are four months in CY2019 after remediation ended in late August, but three of these months included revegetation activities on and around the site (Table 1). Consequently, dust generation has remained high, particularly at Station 401 (Figure 54). The revegetation activities are coincident with higher-than-baseline concentrations of both gross alpha and $^{239+240}$Pu (Figures 54 and 55). The difference in the magnitude of the effect of revegetation activities on radionuclide transport at Clean Slate II and III may be related to the timing of that work. At Clean Slate II, the surface had been undisturbed for a year prior to the ripping and reseeding, whereas at Clean Slate III, those activities began a month after remediation concluded.

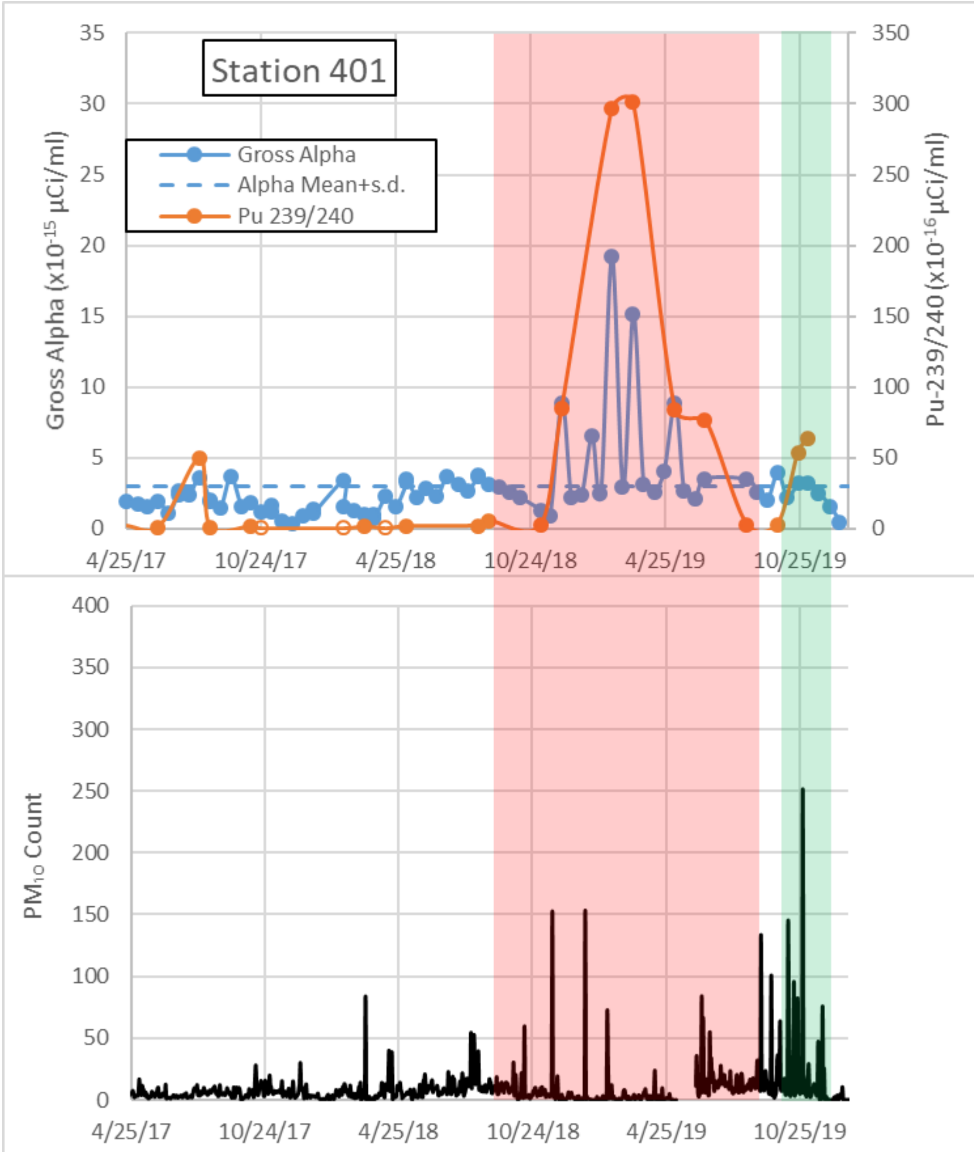


Figure 54. Gross alpha, $^{239+240}Pu$, and $PM_{10}$ concentrations at Station 401 measured before, during, and after remediation activities at Clean Slate III (red band) and reseeding (green band). Open symbols indicate data below the analytical detection limit. Gross alpha mean and standard deviation are calculated using pre-remediation data only.

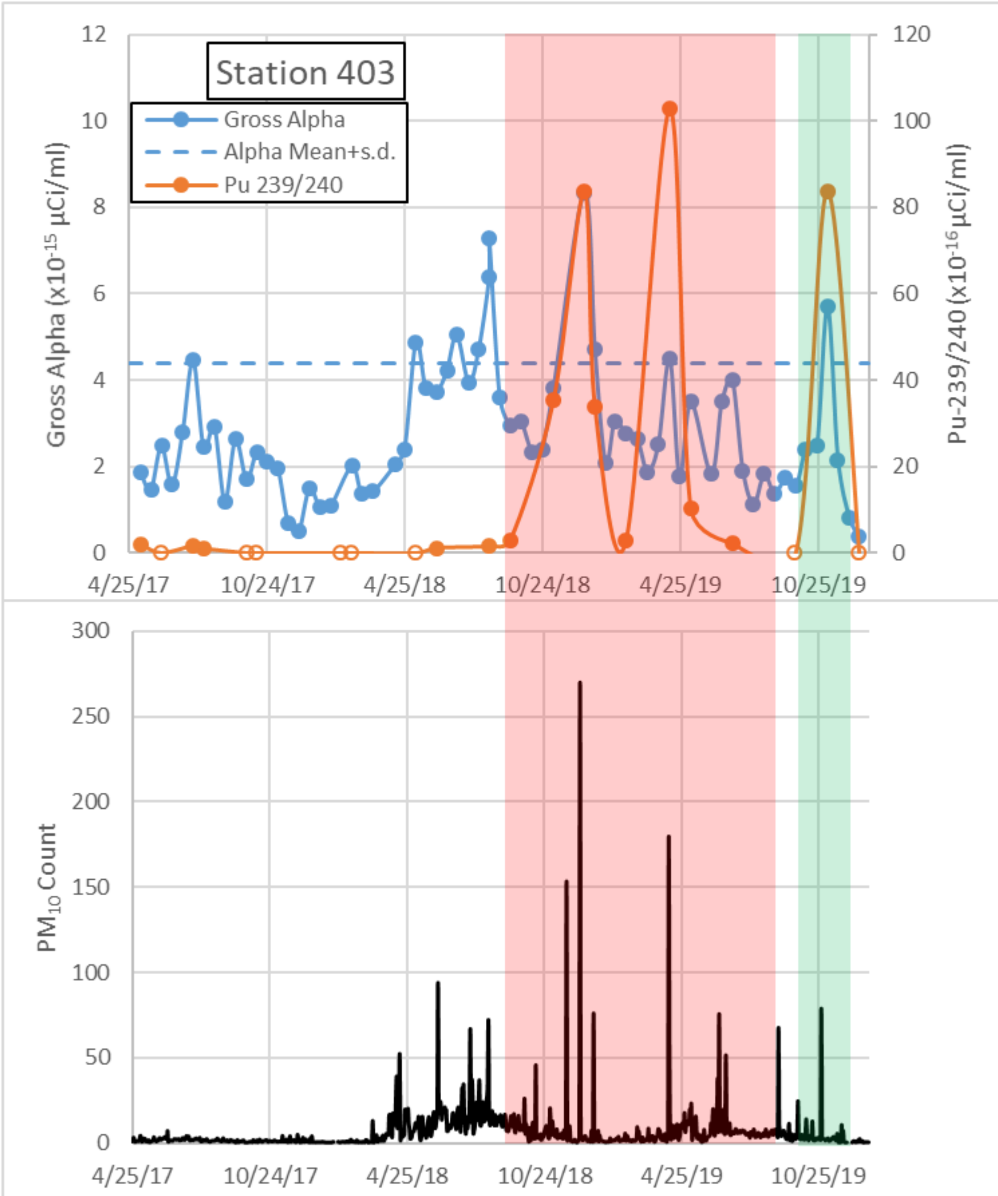


Figure 55. Gross alpha, $^{239+240}$Pu, and $PM_{10}$ concentrations at Station 403 measured before, during, and after remediation activities at Clean Slate III (red band) and reseeding (green band). Open symbols indicate data below the analytical detection limit. Gross alpha mean and standard deviation are calculated using pre-remediation data only.

## CONCLUSIONS

Conditions supporting wind-borne contaminant migration by both suspension and saltation are observed in the monitoring data from the Clean Slate sites. Contaminant transport occurs during high winds when the sites are undisturbed, but land disturbance from remediation activities at both the Clean Slate II and Clean Slate III sites significantly increased contaminant transport. Restabilization of the land disturbed by remediation may be indicated by lower radionuclide concentrations in samples collected in CY2019 from the monitoring stations at Clean Slate II compared with samples collected during the remediation activities in the previous two years. An additional year of monitoring during CY2020 will confirm site stabilization. Radionuclide transport was greater at the Clean Slate III site compared with previous years because of remediation and reseeding activities throughout CY2019.

Atmospheric conditions were generally similar to conditions observed in previous years. Predominant wind directions remained out of the northwest and south, with winds in excess of 24 km/hr (15 mph) accounting for the majority of dust/soil transport. Conclusions from the CY2019 monitoring results are as follows:

- Remediation activities caused a significant increase in the airborne transport of radionuclides from the Clean Slate III site. This increase is attributable to the disturbance of the soil surface, not only the direct activity of machinery, as indicated by radionuclide concentrations measured during a two-week hiatus in remediation work. Increased radionuclide transport occurs by both wind-driven suspension and saltation following disturbance.
- Radionuclide transport was observed to originate from the area north of Clean Slate III, which resulted in elevated gross alpha and $^{239+240}$Pu concentrations measured at Station 401 caused by winds that had not crossed the site. Contamination in the area north of Station 401 could be related to the use of that area for staging equipment during remediation activities or may have occurred at the time of the Clean Slate III experiment or by wind driven dispersion during subsequent years. The movement of $^{239+240}$Pu outside the fenced area is routinely observed in the saltation traps at all Clean Slate monitoring stations.
- The surface of the Clean Slate II site may have begun to restabilize after remediation work at that site concluded in late July 2018. Gross alpha and $^{239+240}$Pu concentrations in samples from the Clean Slate II monitoring stations were generally comparable in CY2019 to those measured prior to the remediation activity, although suspension and saltation of radionuclides continues to be observed from the site.
- The ripping and reseeding conducted in late CY2019 to promote revegetation had different effects on each site. At Clean Slate II, dust generation increased during the reseeding, but increases in contaminant concentrations were relatively small. At Clean Slate III, both dust and radionuclide concentrations were significantly increased during reseeding. The difference may relate to the different timing of the reseeding relative to the completion of remediation, with a year passing at Clean Slate II, whereas the reseeding occurred a month following remediation at Clean Slate III.
- Downwind and upwind directions relative to the contaminated areas shifted regularly between the two predominant wind directions, such that dispersion should be expected to be significant in both the north and south directions.

## RECOMMENDATIONS

The effect of land disturbance on contaminant transport during the remediation and reseeding activities was captured by the monitoring station data. The post-remediation period now provides an opportunity to identify how rapidly the sites return to pre-disturbance wind-driven contaminant transport rates and to determine if there are longer-lasting effects in terms of increased contaminant migration. Although the CY2019 data suggests the Clean Slate II site has begun to restabilize, a longer-term monitoring record there combined with post-remediation monitoring of Clean Slate III will help develop appropriate response plans for future site disruption events.

A record of gamma exposure rate for the pre-, during, and post-remediation periods is now complete for Clean Slate II and III. It is recommended that the PICs be removed from Stations 401 and 403. The PICs were ineffective at detecting the increase in airborne contaminant movement caused by the remediation work at either site and cannot be expected to identify any subsequent radionuclide transport. Similarly, the PIC at Station 400 is unlikely to serve any practical function in terms of meaningful monitoring of contaminant movement from the Clean Slate sites. Given that Station 400 is located at a personnel work area, discussions with the U.S. Air Force are recommended prior to the removal of the Station 400 PIC.

## REFERENCES

Chapman, J., G. Nikolich, C. Shadel, G. McCurdy, V. Etyemezian, J. Miller, and S. Mizell, 2017. Tonopah Test Range Air Monitoring: CY2016 Meteorological, Radiological, and Wind Transported Particulate Observations. Desert Research Institute Publication No. 45279, DOE/NV/0003590-05.

Dick, J.L., J.D. Shreve, and J.S. Iveson, 1963. Operation Roller Coaster, Interim Summary Report (II). POIR-2500 (Volume 1) Defense Atomic Support Agency predecessor to Defense Threat Reduction Agency, Washington, D.C.

Duncan, D., W. Forston, and R. Sanchez, 2000. 1999 Annual Site Environmental Report Tonopah Test Range, Nevada. SAND2000-2229, Sandia National Laboratories, Albuquerque, NM.

EG&G, 1979. An Aerial Radiological Survey of Clean Slates 1, 2, and 3, and Double Track, Test Range. EGG-1183-1737, Energy Measurement Group, EG&G, Las Vegas, NV.

Engelbrecht, J.P., I.G. Kavouras, D. Campbell, S.A. Campbell, S. Kohl, D. Shafer, 2008. Yucca Mountain Environmental Monitoring System Initiative, Air Quality Scoping Study for Tonopah Airport, Nye County, Nevada, Letter Report DOE/NV/26383-LTR2008-04.

Johnson, W.G., and S.R. Edwards, 1996. A historical evaluation of Operation Roller Coaster, Stonewall and Cactus Flats, Nellis Air Force Range and Tonopah Test Range, Nye County, Nevada. NTS Project #9649MA, Historic Evaluation Short Report #SR090996-1, prepared by Desert Research Institute for U.S. Department of Energy, Nevada Operations Office, Las Vegas, Nevada.

Mizell, S.A., V. Etyemezian, G. McCurdy, G. Nikolich, C. Shadel, and J. Miller, 2014. Radiological and environmental monitoring at the Clean Slate I and III Sites, Tonopah Test Range, Nevada, with emphasis on the implications for off-site transport. Desert Research Institute Publication No. 45257, DOE/NV/0000939-19.

Moosmüller, H., W.P. Arnott, C.F. Rogers, J.L. Bowen, J.A. Gillies, W.R. Pierson, JF. Collins, T.D. Durbin, and J.M. Norbeck, 2001. Time resolved characterization of diesel particulate emissions. 1. Instruments for particle mass measurements. *Environmental Science and Technology*, 35:781-787, http://dx.doi.org/10.1021/es0013935.

National Academy of Sciences, 1980. The Effects on Populations of Exposure to Low Levels of Ionizing Radiation, BEIR III. Washington, D.C.

Nikolich, G., C. Shadel, J. Chapman, S. Mizell, G. McCurdy, V. Etyemezian, and J. Miller, 2015. Tonopah Test Range Air Monitoring: CY2014 Meteorological, Radiological, and Airborne Particulate Observations. Desert Research Institute Publication No. 45271, DOE/NV/0000939-37.

Nikolich, G., C. Shadel, J. Chapman, G. McCurdy, V. Etyemezian, J. Miller and S. Mizell, 2016. Tonopah Test Range Air Monitoring: CY2015 Meteorological, Radiological, and Airborne Particulate Observations. Desert Research Institute Publication No. 45263, DOE/NV/0000939-26.

NSTec, 2013. Nevada National Security Site Environmental Report 2012. DOE/NV/25946-1856, prepared by National Security Technologies, LLC for the US Department of Energy, National Nuclear Security Administration, Nevada Site Office.

Proctor, A.E., and T.J. Hendricks, 1995. An aerial radiological survey of the Tonopah Test Range including Clean Slate 1, 2, 3, Roller Coaster, Decontamination area Cactus Springs Ranch Target areas Central Nevada. EGG 11265-1145, The Remote Sensing Laboratory, EG&G Energy Measurements prepared for the US Department of Energy.

Sandia National Laboratory (SNL), 2012. Calendar Year 2011 Annual Site Environmental Report for Tonopah Test Range, Nevada and Kauai Test Facility, Hawaii. SAND2012-7341P, Sandia National Laboratories, Albuquerque, NM.

Sandia National Laboratory (SNL), 1998. 1997 Annual Site Environmental Report, Tonopah Test Range, Nevada. SAND98-1832, Sandia National Laboratories, Albuquerque, NM.

Thakur, P., H. Khaing, and S. Salminen-Paatero, 2017. Plutonium in the atmosphere: a global perspective. *Journal of Environmental Radioactivity*, v.175-176, pp. 39-51.

Turner, M., M. Rudin, J. Cizdziel, and V. Hodge, 2003. Excess Plutonium in Soil near the Nevada Test Site, USA. *Environmental Pollution*, v. 125, pp. 193-203.

UNSCEAR, 2000. Sources and effects of ionizing radiation, Annex B: Exposures from natural radiation sources. United Nations Scientific Committee on the Effects of atomic Radiation. Available May 6, 2013 at: http://www.unscear.org/unscear/publications/2000_1.html.

U.S. Department of Energy, 2014. Soils Risk-Based Corrective Action Evaluation Process. Nevada Field Office, DOE/NV--1475-REV.1.

U.S. Department of Energy, 1996. Clean Slate Corrective Action Investigation Plan. Nevada Operations Office, DOE/NV--456.

Wang, X., G. Chancellor, J. Evenstad, J.E. Farnsworth, A. Hase, G.M. Olson, A. Sreenath, and J.K. Agarwal, 2009. A novel optical instrument for estimating size segregated aerosol mass concentration in real time. *Aerosol Science and Technology*, 43:939-950, http://dx.doi.org/10.1080/02786820903045141.

## APPENDIX A. QUALITY ASSURANCE PROGRAM

Although the current data collected for the Tonopah Test Range (TTR) air monitoring study are considered for informational purposes to support conceptual models or guide investigations, the U.S. Department of Energy, Environmental Management Nevada Program (DOE EM NV), Soils Activity Quality Assurance Plan (QAP) (2012) was used as a guideline to collect and analyze radiological data presented in the "Radiological Assessment of Wind Transported Material" section of this report. This QAP and the Desert Research Institute (DRI) Quality Assurance Program Manual for the TREDS Program (2017) ensures compliance with U.S. Department of Energy Order DOE O 414.1D, "Quality Assurance," which implements a quality management system to ensure the generation and use of quality data. The following items are addressed by the aforementioned quality assurance (QA) documents:

- Data quality objectives (DQOs)
- Sampling plan development appropriate to satisfy the DQOs
- Environmental health and safety
- Sampling plan execution
- Sample analyses
- Data review
- Continuous improvement

### Data Quality Objectives (DQOs)

The DQO process is a strategic planning approach that is used to plan data collection activities. It provides a systematic process for defining the criteria that a data collection design plan should satisfy. These criteria include when and where samples should be collected, how many samples to collect, and the tolerable level of decision errors for the study. The DQOs are unique to the specific data collection or monitoring activity and their defined level of use (in this case, informational purposes).

### Measurement Quality Objectives (MQOs)

The MQOs are equivalent to DQOs for analytical processes. The MQOs provide direction to the laboratory concerning performance objectives or requirements for specific method performance characteristics. Default MQOs are established in the subcontract with the laboratory but can be altered to satisfy changes in the DQOs. The MQOs for the TTR air monitoring study are described in terms of precision, accuracy, representativeness, completeness, and comparability requirements. These terms are defined and discussed in the DOE EM NV QAP.

### Sampling Quality Assurance Program

Quality assurance in field operations for the TTR air monitoring study includes sampling assessment, surveillance, and oversight of the following supporting elements:

- The sampling plan, DQOs, and field data sheets accompanying the sample package.

- Database support for field and laboratory results, including systems for long-term storage and retrieval.
- Qualified personnel able and available to perform the required tasks.

Sample packages include the following items:

- Field notes confirming all observable information pertinent to sample collection.
- An "Air Surveillance Network Sample Data" form documenting air sampler parameters, collection dates and times, and total sample volumes collected.
- Chain-of-custody forms that also include some of the elements of the field notes.

This managed approach to sampling ensures that the sampling is traceable and enhances the value of the final data available to the project manager. The sample package also ensures that the field personnel responsible for sample collection have followed proper procedures for sample collection.

Data obtained in the course of executing field operations are entered in the documentation accompanying the sample package during sample collection and in the TTR Study database along with analytical results on their receipt and evaluation.

Hard copies of the completed sample packages are kept in the archived files. The analytical reports are kept in dedicated and secure archival systems that are protected and maintained in accordance with the DRI's Computer Protection Program and hard copies are kept in the file archives.

**Laboratory QA Oversight**

Although the data for the TTR air monitoring study are for informational purposes, the main aspects of the DOE O 414.1D requirements are used as guidelines to evaluate laboratory services through review of the vendor laboratory policies formalized in a Laboratory Quality Assurance Plan (LQAP). The TTR study is assured of obtaining quality data from laboratory services through a multifaceted approach that involves specific procurement protocols, the conduct of quality assessments, and requirements for selected laboratories to have an acceptable QA Program. These elements are discussed below.

**Procurement**

Laboratory services are procured through subcontracts that establish the technical specifications required of the laboratory to provide the basis for determining compliance with those requirements and for evaluating overall performance. A subcontract is usually awarded on a "best value" basis determined by pre-award audits, but because of the specific requirement requested for gamma spectroscopy analysis (24-hour count duration) for the TTR study, the laboratory was procured on a sole proprietor basis. The laboratory was required to provide a review package that included the following items:

- All procedures pertinent to subcontract scope
- Environment, Health, and Safety Plan
- LQAP
- Example deliverables (hard copy and/or electronic)
- Proficiency testing (PT) results from the previous year from recognized PT programs

- Résumés
- Accreditations and certifications
- Licenses

**Continuing Assessment**

A continuing assessment of the selected laboratory involves ongoing monitoring of the laboratory's performance against the contract terms and conditions, part of which are the technical specifications. The following tasks support continuing assessment:

- Tracking schedule compliance.
- Reviewing analytical data deliverables.
- Monitoring the laboratory's adherence to the LQAP.
- Monitoring for continued successful participation in approved PT programs.

**Data Review**

Essential components of process-based QA are data checks, verification, validation, and data quality assessment to evaluate data quality and usability.

**Data checks:** Data checks are conducted to ensure accuracy and consistency of field data collection operations prior to and upon data entry into the TTR databases and data management systems.

**Data verification:** Data verification is defined as a compliance and completeness review to ensure that all laboratory data and sample documentation are present and complete. Sample preservation, chain-of-custody, and other field sampling documentation shall be reviewed during the verification process. Data verification ensures that the reported results entered in the TTR databases correctly represent the sampling and/or analyses performed and includes evaluation of quality control (QC) sample results.

**Data validation:** Data validation is the process of reviewing a body of analytical data to determine if it meets the data quality criteria defined in operating instructions. Data validation ensures that the reported results correctly represent the sampling and/or analyses performed, determines the validity of the reported results, and assigns data qualifiers (or "flags") if required. The process of data validation consists of the following:

- Evaluating the quality of the data to ensure that all project requirements are met.
- Determining the effect of not meeting those requirements on data quality.
- Verifying compliance with QA requirements.
- Checking QC values against defined limits.
- Applying qualifiers to analytical results in the TTR databases for the purposes of defining the limitations in the use of the reviewed data.

Operating instructions, procedures, applicable project-specific work plans, field sampling plans, QA plans, analytical method references, and laboratory statements of work may all be used in the data validation process. Documentation of data validation includes checklists, qualifier assignments, and summary forms.

**Data quality assessment (DQA):** The DQA is the scientific evaluation of data to determine if the data obtained from environmental data operations are of the right type, quality, and quantity to support their intended use. The DQA review is a systematic review against pre-established criteria to verify that the data are valid for their intended use.

## 2019 Sample QA Results

Assessments of QA were performed as part of the TTR air monitoring study, including the laboratories responsible for sample analyses. These assessments ensure that sample collection procedures, analytical techniques, and data provided by the subcontracted laboratories comply with TTR study requirements. Data were provided by the University of Nevada, Las Vegas, Radioanalytical Services Laboratory (RSL) for gross alpha, gross beta, and gamma spectroscopy analyses and Eurofins TestAmerica Laboratories, Inc., for alpha spectrometry analyses. A brief discussion of the 2019 results for laboratory duplicates, control samples, blank analyses, and interlaboratory comparison studies is provided along with summary tables in this section.

## Laboratory Duplicates (Precision)

A laboratory duplicate is a sample that is handled and analyzed following the same procedures as the primary analysis. The relative percent difference (RPD) between the initial result and the corresponding duplicate result is a measure of the variability in the analytical process of the laboratory, mainly overall measurement uncertainty. The average absolute RPD was determined for calendar year (CY) 2019 samples and is listed in Table A-1. An RPD of zero indicates a perfect duplication of results of the duplicate pair, whereas an RPD greater than 100 percent generally indicates that a duplicate pair falls beyond acceptable QA requirements and is not considered valid for use in data interpretation. These samples are further evaluated to determine the reason for QA failure and if any corrective actions are required. Overall, the RPD values for all analyses indicate very good results with no samples exceeding an RPD of 100 percent.

Table A-1. Summary of laboratory duplicate samples for the TTR air monitoring study in 2019.

| Analysis | Matrix | Number of Samples Reported[(a)] | Number of Samples Reported Above MDC[(b)] | Average Absolute RPD of Those Above MDC (%)[(c)] |
|---|---|---|---|---|
| Gross Alpha | Air | 26 | 25 | 14.1 |
| Gross Beta | Air | 26 | 26 | 4.6 |
| Gamma – Beryllium-7 | Air | 25 | 23 | 15.7 |
| Gamma – Lead-210 | Air | 25 | 17 | 19.2 |
| Alpha spectrometry – $^{238}$Pu | Air | 3 | 3 | 9.5 |
| Alpha spectrometry – $^{239+240}$Pu | Air | 3 | 3 | 4.8 |

(a) Represents the number of laboratory duplicates reported for the purpose of monitoring precision.
(b) Represents the number of laboratory duplicate result sets reported above the minimum detectable concentration (MDC). If either the original laboratory analysis or its duplicate was reported below the detection limit, the precision was not determined.
(c) Reflects the average absolute RPD calculated for those field duplicates reported above the MDC.

The absolute RPD calculation is as follows:

$$Absolute\ RPD = \frac{|LD - LS|}{(LD + LS)/2}\ X\ 100\% \tag{1}$$

where: LD = Laboratory duplicate result

LS = Laboratory sample result

**Laboratory Control Samples (Accuracy)**

Laboratory control samples (LCSs) are performed by the subcontract laboratories to evaluate analytical accuracy, which is the degree of agreement of a measured value with the true or expected value. Samples of known activity are analyzed using the same methods used for the project samples. The results are determined as the measured value divided by the true value, expressed as a percentage. To be considered valid, the results must fall within established control limits (or percentage ranges). Table A-2 summarizes the LCS results obtained for 2019. The LCS results were satisfactory, with all sample results falling within control parameters for the air sample matrix.

Table A-2. Summary of laboratory control samples for the TTR air monitoring study in 2019.

| Analysis | Matrix | Number of LCS Results Reported | Number Within Control Limits[a] |
|---|---|---|---|
| Gross Alpha | Air | 34 | 34 |
| Gross Beta | Air | 34 | 34 |
| Gamma Spectroscopy | Air | 4 | 4 |
| Alpha Spectrometry | Air | 3 | 3 |

(a) Control limits are as follows: 75% to 125% for gross alpha, 75% to 125% for gross beta, 80% to 125% for $^{238}$plutonium (alpha spec), and 81% to 125% for $^{239/240}$plutonium (alpha spec).

**Laboratory Blank Analyses**

Laboratory blank sample analyses are essentially the opposite of the LCSs discussed above. These samples do not contain any of the analyte of interest. Results of these analyses are expected to be “zero,” or more specifically, below the MDC of a specific analytical procedure. Blank analysis and control samples are used to evaluate overall laboratory procedures, including sample preparation and instrument performance. Table A-3 summarizes the laboratory blank sample results obtained for 2019. The laboratory blank results were satisfactory with all samples falling within control parameters for the air sample matrix.

Table A-3. Summary of laboratory blank samples for the TTR air monitoring study in 2019.

| **Analysis** | **Matrix** | **Number of Blank Results Reported** | **Number within Control Limits(a)** |
|---|---|---|---|
| Gross Alpha | Air | 18 | 18 |
| Gross Beta | Air | 18 | 18 |
| Gamma Spectroscopy | Air | 14 | 14 |
| Alpha Spectrometry | Air | 3 | 3 |

(a) Control limit is less than the MDC.

## Interlaboratory Comparison Studies

Interlaboratory comparison studies are conducted by the subcontracted laboratories to evaluate their performance relative to other laboratories providing the same service. These types of samples are commonly known as "blind" samples, in which the expected values are known only to the program conducting the study. The analyses are evaluated and if found satisfactory, the laboratory is certified that its procedures produce reliable results. Table A-4 summarizes the interlaboratory comparison sample results obtained for 2019.

Table A-4 shows the summary of interlaboratory comparison sample results for the subcontract radiochemistry laboratory. The laboratories participated in the QA Program administered by the Mixed Analyte Performance Evaluation Program (MAPEP) for gamma analyses and Environmental Research Associates (ERA) for alpha spectrometry analyses. The subcontracted laboratories performed acceptably for the parameters analyzed.

Table A-4. Summary of interlaboratory comparison samples of the radiochemistry laboratory for the TTR air monitoring study in 2019.

| **Analysis** | **Matrix** | **MAPEP and ERA Results** | |
|---|---|---|---|
| | | **Number of Results Reported** | **Number Within Control Limits(a)** |
| Gross Alpha | Air | 2 | 2 |
| Gross Beta | Air | 2 | 2 |
| Gamma Spectroscopy | Air | 2 | 2 |
| Alpha spectrometry | Air | 2 | 2 |

(a) Control limits are determined by the individual interlaboratory comparison study.

## REFERENCES

Desert Research Institute, 2017. Desert Research Institute Quality Assurance Program Manual for the TREDS Program. August 2017.

U.S. Department of Energy, 2011. Quality Assurance. DOE O 414.1D.

U.S. Department of Energy, 2017. Soils Activity Quality Assurance Plan. Environmental Management Nevada Program report DOE/NV—1478-REV.1.

## APPENDIX B. STATION PHOTOGRAPHS AND EQUIPMENT LAYOUT

**(Station 400 is shown within the body of the report)**

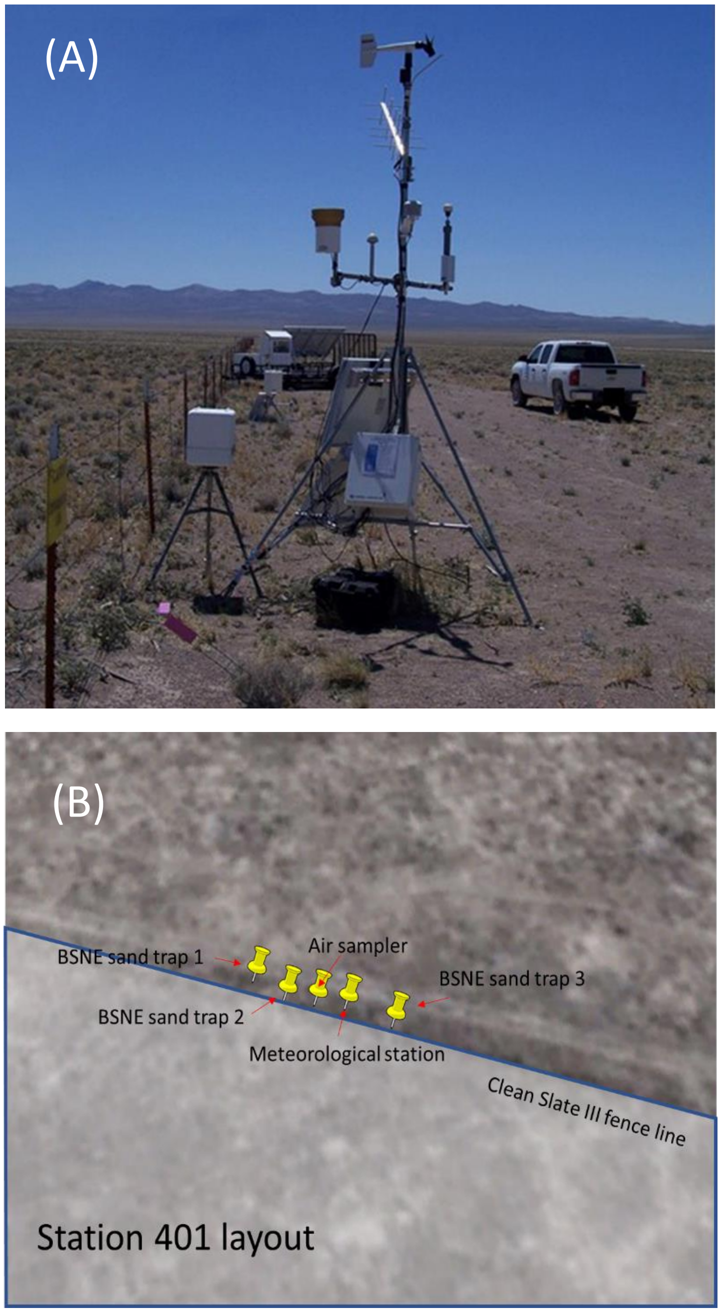


Figure B-1. (A) The solar-powered air sampler, saltation sensor, and meteorological tower (background, center, and foreground, respectively) at Station 401 are located along the north fence that bounds the Clean Slate III contamination area. (B) Aerial view of equipment locations after the site was relocated in early June 2018. An aerial view of the previous equipment locations can be found in Chapman *et at*. (2018).

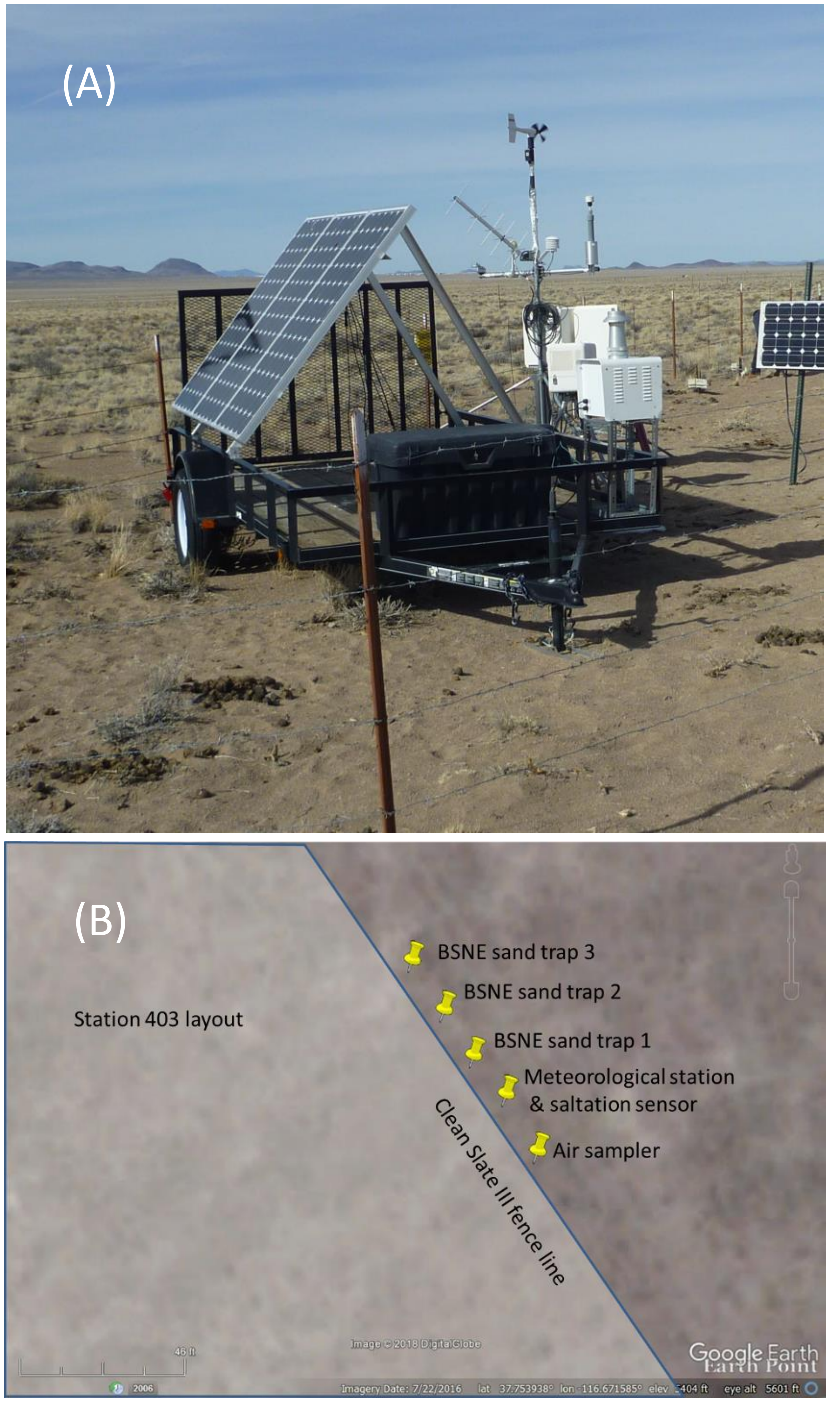


Figure B-2. (A) The solar-powered air sampler, saltation sensor, and meteorological tower (front to rear, respectively, and to the right of the large solar panel) at Station 403 are located along the south fence that bounds the Clean Slate III contamination area. (B) Aerial view of equipment locations.

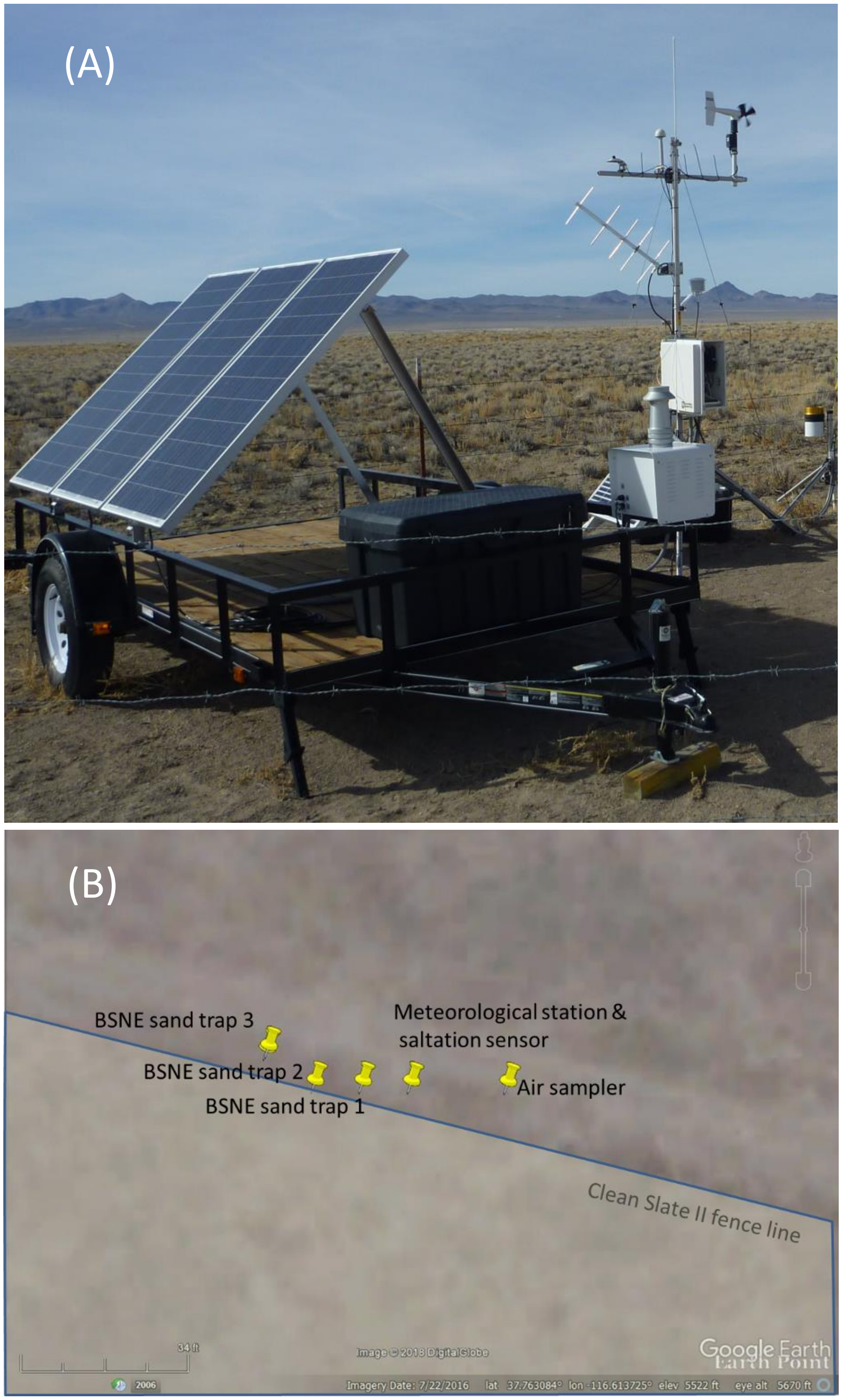


Figure B-3. (A) The solar-powered air sampler, saltation sensor, and meteorological tower (front to rear, respectively, to right of solar panel) at Station 404 are located along the north fence that bounds the Clean Slate II contamination area. (B) Aerial view of equipment locations.

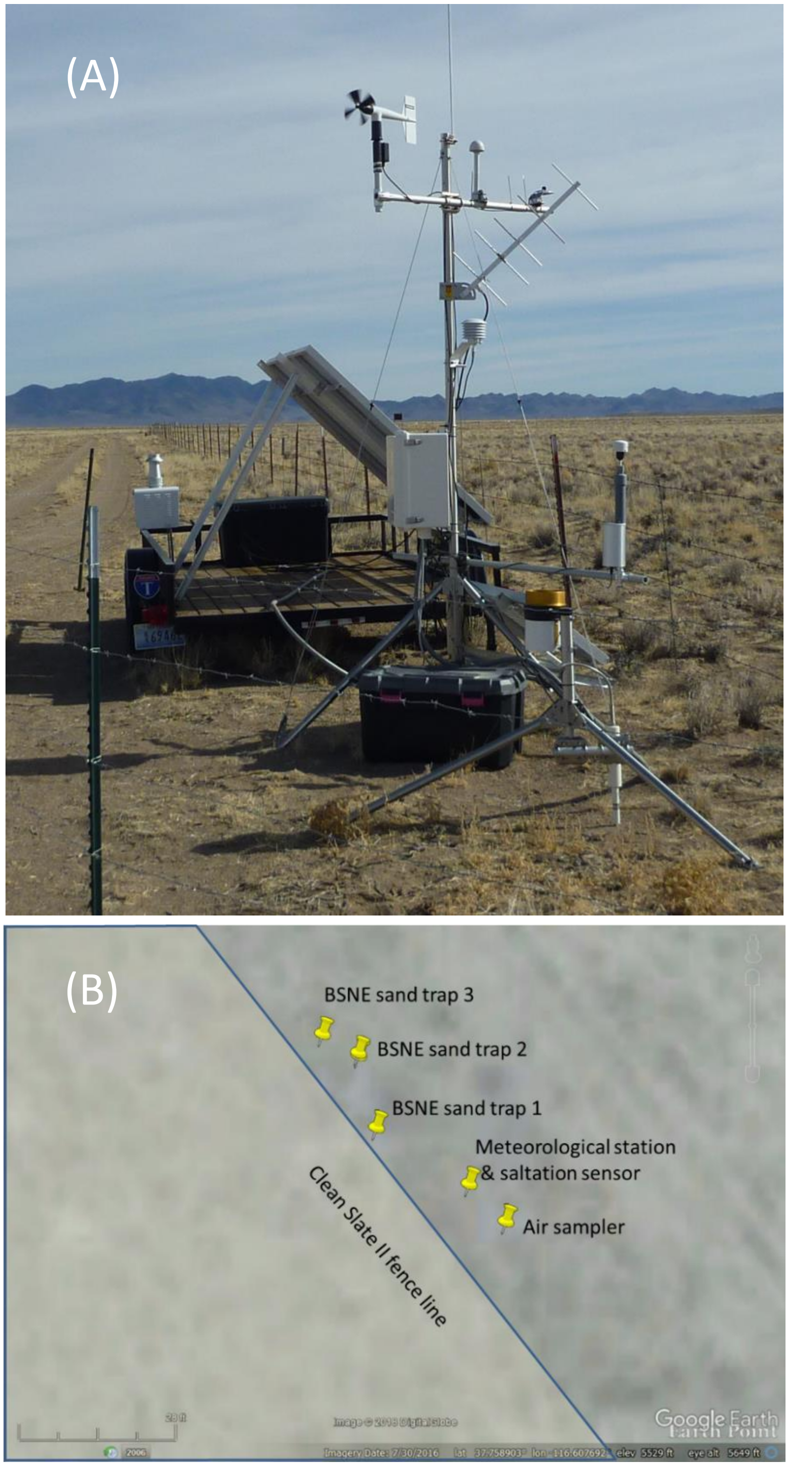


Figure B-4. (A) The solar-powered air sampler (back of trailer), saltation sensor, and meteorological tower (center front of trailer) at Station 405 are located along the south fence that bounds the Clean Slate II contamination area. (B) Aerial view of equipment locations.

# APPENDIX C. METEOROLOGICAL DATA SUMMARY

Table C-1. Station 400 summary of monthly and annual meteorological data from CY2019.

| Month | Jan | Feb | Mar | Apr | May | June | Jul | Aug | Sep | Oct | Nov | Dec | Annual | Value |
|---|---|---|---|---|---|---|---|---|---|---|---|---|---|---|
| **Wind Speed Avg (mph)** | 7.15 | 10.42 | 7.99 | 7.72 | 7.79 | 7.04 | 7.69 | 7.18 | 7.63 | 6.57 | 5.12 | 5.89 | **AVG** | 7.35 |
| **Wind Speed Max (mph)** | 31.56 | 28.98 | 28.40 | 27.54 | 28.19 | 26.39 | 22.60 | 22.77 | 25.27 | 30.62 | 29.95 | 26.98 | **MAX** | 31.56 |
| **Wind Speed Gust (mph)** | 42.45 | 43.26 | 42.45 | 42.74 | 41.57 | 49.98 | 42.23 | 35.15 | 37.19 | 45.52 | 45.81 | 37.92 | **MAX** | 49.98 |
| **Wind Freq from S*** | 35.79% | 51.04% | 44.42% | 31.76% | 39.86% | 43.17% | 64.24% | 69.78% | 46.12% | 24.57% | 30.10% | 33.86% | **AVG** | 42.89% |
| **Wind Freq from NW**** | 43.69% | 30.36% | 36.45% | 50.63% | 41.10% | 38.15% | 15.73% | 11.68% | 38.49% | 60.71% | 53.20% | 43.72% | **AVG** | 38.66% |
| **Air Temperature Avg (deg F)** | 35.09 | 29.84 | 41.64 | 52.64 | 52.64 | 68.41 | 76.28 | 75.94 | 64.69 | 48.38 | 41.49 | 32.66 | **AVG** | 51.64 |
| **Air Temperature Min (deg F)** | 11.52 | -3.315 | 18.96 | 28.21 | 30.77 | 42.43 | 51.98 | 50.22 | 28.64 | 13.71 | 5.954 | 8.24 | **MIN** | -3.32 |
| **Air Temperature Max (deg F)** | 58.51 | 59.36 | 63.72 | 81.30 | 80.26 | 90.43 | 96.12 | 95.54 | 93.56 | 79.41 | 72.36 | 57.61 | **MAX** | 96.12 |
| **Relative Humidity Avg (%)** | 65.51 | 66.04 | 54.97 | 43.14 | 48.82 | 28.11 | 21.51 | 18.25 | 28.07 | 20.83 | 43.90 | 71.27 | **AVG** | 42.54 |
| **Relative Humidity Min (%)** | 14.74 | 20.10 | 10.80 | 8.12 | 7.58 | 5.11 | 4.16 | 4.94 | 4.50 | 3.25 | 5.12 | 11.89 | **MIN** | 3.25 |
| **Relative Humidity Max (%)** | 100.00 | 98.30 | 100.00 | 97.90 | 100.00 | 92.30 | 95.30 | 84.20 | 79.04 | 65.58 | 100.00 | 100.00 | **MAX** | 100 |
| **Total Precipitation (inch)** | 0.34 | 0.49 | 1.14 | 0.50 | 2.05 | 0.14 | 0.15 | 0.09 | 0.00 | 0.00 | 0.49 | 0.62 | **TOTAL** | 6.01 |
| **Max Daily Precipitation (inch)** | 0.19 | 0.25 | 0.42 | 0.25 | 0.50 | 0.11 | 0.13 | 0.09 | 0.00 | 0.00 | 0.29 | 0.20 | **MAX** | 0.50 |
| **Soil Temperature Avg (deg F)** | 38.00 | 35.20 | 47.37 | 59.42 | 61.01 | 76.12 | 84.71 | 85.25 | 75.97 | 59.55 | 48.58 | 36.80 | **AVG** | 59.00 |
| **Soil Temperature Min (deg F)** | 27.53 | 27.08 | 34.30 | 42.58 | 43.21 | 50.68 | 71.46 | 70.92 | 57.22 | 37.61 | 33.76 | 31.36 | **MIN** | 27.08 |
| **Soil Temperature Max (deg F)** | 51.60 | 53.62 | 65.21 | 82.06 | 82.85 | 92.16 | 97.47 | 98.28 | 94.57 | 77.41 | 62.64 | 48.79 | **MAX** | 98.28 |
| **Soil Vol. Water Content Avg** | 0.15 | 0.16 | 0.17 | 0.16 | 0.17 | 0.18 | 0.15 | 0.14 | 0.12 | 0.11 | 0.12 | 0.16 | **AVG** | 0.15 |
| **Soil Vol. Water Content Min** | 0.10 | 0.10 | 0.14 | 0.14 | 0.13 | 0.15 | 0.13 | 0.12 | 0.11 | 0.10 | 0.10 | 0.11 | **MIN** | 0.10 |
| **Soil Vol. Water Content Max** | 0.21 | 0.25 | 0.24 | 0.21 | 0.27 | 0.22 | 0.17 | 0.15 | 0.13 | 0.13 | 0.18 | 0.21 | **MAX** | 0.27 |
| **Solar Radiation Avg (ly/day)** | 116 | 167 | 230 | 288 | 301 | 381 | 377 | 351 | 374 | 288 | 143 | 97 | **AVG** | 259.42 |
| **Solar Radiation Max (ly/day)** | 158 | 235 | 323 | 369 | 397 | 428 | 424 | 391 | 344 | 269 | 199 | 136 | **MAX** | 428 |
| **Barometric P. Avg (in Hg)** | 24.62 | 24.41 | 24.54 | 24.53 | 24.43 | 24.57 | 24.61 | 24.62 | 24.57 | 24.61 | 24.56 | 24.57 | **AVG** | 24.55 |
| **Barometric P. Min (in Hg)** | 24.19 | 24.03 | 24.10 | 24.24 | 24.19 | 24.32 | 24.40 | 24.44 | 24.10 | 24.27 | 23.94 | 24.26 | **MIN** | 23.94 |
| **Barometric P. Max (in Hg)** | 24.92 | 24.73 | 24.81 | 24.84 | 24.61 | 24.84 | 24.80 | 24.76 | 24.81 | 24.87 | 24.87 | 24.90 | **MAX** | 24.92 |
| **$PM_{2.5}$ Avg Concentration (μg/m$^3$)** | 0.45 | 0.72 | 1.25 | 1.89 | 2.30 | 2.92 | 0.59 | 0.51 | 1.17 | 1.44 | 1.16 | 0.49 | **AVG** | 1.24 |
| **$PM_{2.5}$ Max Concentration (μg/m$^3$)** | 5.38 | 14.59 | 85.64 | 91.50 | 57.40 | 365.00 | 25.45 | 12.64 | 37.41 | 44.32 | 15.19 | 5.23 | **MAX** | 365.00 |
| **$PM_{10}$ Avg Concentration (μg/m$^3$)** | 2.43 | 2.70 | 4.61 | 5.78 | 4.46 | 8.33 | 3.21 | 3.26 | 5.11 | 5.27 | 3.09 | 1.09 | **AVG** | 4.11 |
| **$PM_{10}$ Max Concentration (μg/m$^3$)** | 104.98 | 114.64 | 1,725.42 | 595.49 | 221.85 | 2517.91 | 144.09 | 145.23 | 169.30 | 308.62 | 111.07 | 39.11 | **MAX** | 2,517.91 |

*Wind Freq from S (indicates aggregate frequency for winds over 5 mph coming from south direction).

**Wind Freq from NW (indicates aggregate frequency for winds over 5 mph coming from northwest direction).

Table C-2. Station 401 summary of monthly and annual meteorological data from CY2019. Solar radiation and barometric pressure are not measured at this station. Highlighted values indicate the month is missing five or more days of measurements.

| Month | Jan | Feb | Mar | Apr | May | June | Jul | Aug | Sep | Oct | Nov | Dec | Annual | Value |
|---|---|---|---|---|---|---|---|---|---|---|---|---|---|---|
| **Wind Speed Avg (mph)** | 6.63 | 10.07 | 7.72 | 8.13 | 8.10 | 7.36 | 7.41 | 6.73 | 7.26 | 6.26 | 4.40 | 5.41 | **AVG** | 7.12 |
| **Wind Speed Max (mph)** | 28.42 | 31.65 | 27.94 | 31.77 | 29.56 | 31.76 | 22.12 | 24.44 | 26.38 | 31.55 | 32.06 | 28.65 | **MAX** | 32.06 |
| **Wind Speed Gust (mph)** | 39.09 | 43.04 | 38.94 | 44.42 | 40.11 | 45.67 | 34.71 | 38.29 | 39.75 | 42.45 | 43.77 | 37.70 | **MAX** | 45.67 |
| **Wind Freq from S*** | 39.71% | 56.02% | 45.90% | 26.88% | 35.75% | 36.08% | 60.96% | 60.52% | 43.03% | 17.88% | 34.76% | 27.97% | **AVG** | 40.46% |
| **Wind Freq from NW**** | 42.21% | 28.79% | 33.75% | 46.64% | 35.21% | 37.03% | 13.86% | 11.11% | 37.68% | 59.70% | 49.04% | 54.83% | **AVG** | 37.49% |
| **Air Temperature Avg (deg F)** | 33.77 | 29.59 | 41.42 | 52.33 | 53.35 | 68.06 | 76.00 | 75.21 | 64.05 | 45.71 | 38.21 | 31.59 | **AVG** | 50.77 |
| **Air Temperature Min (deg F)** | 5.58 | -8.68 | 18.07 | 25.88 | 28.20 | 39.72 | 47.79 | 43.88 | 25.12 | -2.78 | -2.36 | 4.93 | **MIN** | -8.68 |
| **Air Temperature Max (deg F)** | 57.76 | 60.42 | 65.03 | 83.14 | 80.91 | 92.70 | 97.59 | 97.66 | 96.51 | 80.06 | 73.76 | 58.78 | **MAX** | 97.66 |
| **Relative Humidity Avg (%)** | 68.82 | 69.89 | 59.92 | 46.84 | 49.57 | 30.32 | 22.29 | 19.06 | 28.64 | 21.24 | 45.06 | 73.45 | **AVG** | 44.59 |
| **Relative Humidity Min (%)** | 16.66 | 25.57 | 10.88 | 8.21 | 6.97 | 3.90 | 3.13 | 4.00 | 3.79 | 2.06 | 5.56 | 12.54 | **MIN** | 2.06 |
| **Relative Humidity Max (%)** | 100.00 | 97.70 | 99.90 | 99.40 | 99.40 | 98.40 | 95.90 | 91.40 | 83.40 | 73.60 | 100.00 | 100.00 | **MAX** | 100 |
| **Total Precipitation (inch)** | 0.27 | 0.56 | 1.17 | 0.52 | 1.48 | 0.07 | 0.23 | 0.17 | 0.00 | 0.00 | 0.70 | 0.17 | **TOTAL** | 5.34 |
| **Max Daily Precipitation (inch)** | 0.21 | 0.32 | 0.40 | 0.18 | 0.61 | 0.07 | 0.22 | 0.17 | 0.00 | 0.00 | 0.36 | 0.07 | **MAX** | 0.61 |
| **Soil Temperature Avg (deg F)** | 35.06 | 32.75 | 45.45 | 57.71 | 59.78 | 78.15 | 85.61 | 83.33 | 71.43 | 51.86 | 41.93 | 32.93 | **AVG** | 56.33 |
| **Soil Temperature Min (deg F)** | 10.11 | 10.26 | 23.90 | 30.26 | 31.87 | 42.00 | 51.53 | 49.46 | 30.17 | 5.05 | 14.92 | 16.09 | **MIN** | 5.05 |
| **Soil Temperature Max (deg F)** | 66.56 | 71.69 | 81.48 | 108.30 | 112.40 | 128.20 | 133.10 | 130.20 | 125.80 | 104.00 | 83.16 | 57.56 | **MAX** | 133.10 |
| **Soil Vol. Water Content Avg** | 0.17 | 0.21 | 0.24 | 0.21 | 0.21 | 0.19 | 0.13 | 0.13 | 0.11 | 0.10 | 0.14 | 0.22 | **AVG** | 0.17 |
| **Soil Vol. Water Content Min** | 0.12 | 0.14 | 0.21 | 0.179 | 0.126 | 0.138 | 0.118 | 0.114 | 0.101 | 0.088 | 0.09 | 0.151 | **MIN** | 0.088 |
| **Soil Vol. Water Content Max** | 0.22 | 0.312 | 0.286 | 0.25 | 0.294 | 0.272 | 0.165 | 0.157 | 0.122 | 0.112 | 0.251 | 0.276 | **MAX** | 0.312 |
| **Solar Radiation Avg (ly/day)** | -- | -- | -- | -- | -- | -- | -- | -- | -- | -- | -- | -- | **AVG** | -- |
| **Solar Radiation Max (ly/day)** | -- | -- | -- | -- | -- | -- | -- | -- | -- | -- | -- | -- | **MAX** | -- |
| **Barometric P. Avg (in Hg)** | -- | -- | -- | -- | -- | -- | -- | -- | -- | -- | -- | -- | **AVG** | -- |
| **Barometric P. Min (in Hg)** | -- | -- | -- | -- | -- | -- | -- | -- | -- | -- | -- | -- | **MIN** | -- |
| **Barometric P. Max (in Hg)** | -- | -- | -- | -- | -- | -- | -- | -- | -- | -- | -- | -- | **MAX** | -- |
| **$PM_{2.5}$ Avg Concentration (µg/m$^3$)** | 1.57 | 1.51 | 1.48 | 1.18 | 0.57 | 2.70 | 1.93 | 1.85 | 3.49 | 3.34 | 1.60 | 0.42 | **AVG** | 1.80 |
| **$PM_{2.5}$ Max Concentration (µg/m$^3$)** | 909.24 | 316.70 | 105.08 | 422.63 | 5.36 | 595.12 | 43.48 | 92.65 | 235.49 | 393.88 | 210.11 | 122.23 | **MAX** | 909.24 |
| **$PM_{10}$ Avg Concentration (µg/m$^3$)** | 6.46 | 6.09 | 2.76 | 3.22 | 1.05 | 20.17 | 13.61 | 12.97 | 21.14 | 30.46 | 12.03 | 2.07 | **AVG** | 11.00 |
| **$PM_{10}$ Max Concentration (µg/m$^3$)** | 5,247.72 | 2087.61 | 464.96 | 1,021.48 | 27.03 | 5,308.79 | 496.37 | 860.85 | 1,938.12 | 4,534.72 | 1,790.95 | 814.87 | **MAX** | 5,308.79 |

*Wind Freq from S (indicates aggregate frequency for winds over 5 mph coming from south direction).

**Wind Freq from NW (indicates aggregate frequency for winds over 5 mph coming from northwest direction).

Table C-3. Station 403 summary of monthly and annual meteorological data from CY2019.

| Month | Jan | Feb | Mar | Apr | May | June | Jul | Aug | Sep | Oct | Nov | Dec | Annual | Value |
|---|---|---|---|---|---|---|---|---|---|---|---|---|---|---|
| **Wind Speed Avg (mph)** | 5.80 | 8.74 | 6.86 | 7.48 | 7.36 | 6.83 | 6.76 | 6.13 | 6.65 | 5.70 | 3.92 | 4.62 | **AVG** | 6.40 |
| **Wind Speed Max (mph)** | 27.70 | 28.63 | 25.71 | 29.18 | 27.82 | 28.56 | 21.07 | 22.78 | 25.07 | 28.50 | 28.96 | 25.52 | **MAX** | 29.18 |
| **Wind Speed Gust (mph)** | 38.14 | 44.72 | 38.94 | 42.82 | 39.6 | 40.48 | 37.56 | 39.97 | 37.26 | 40.63 | 40.84 | 34.78 | **MAX** | 44.72 |
| **Wind Freq from S*** | 44.58% | 60.17% | 48.64% | 23.69% | 33.95% | 35.76% | 60.90% | 59.12% | 44.69% | 16.62% | 40.31% | 49.75% | **AVG** | 43.18% |
| **Wind Freq from NW**** | 40.07% | 26.94% | 33.96% | 42.04% | 36.09% | 33.08% | 14.30% | 10.84% | 35.78% | 57.85% | 44.92% | 63.40% | **AVG** | 36.61% |
| **Air Temperature Avg (deg F)** | 33.55 | 29.58 | 41.28 | 52.16 | 52.62 | 67.82 | 75.88 | 75.04 | 63.80 | 45.50 | 38.07 | 32.85 | **AVG** | 50.68 |
| **Air Temperature Min (deg F)** | 5.52 | -8.54 | 17.63 | 24.22 | 26.18 | 38.85 | 46.58 | 43.87 | 24.61 | -4.22 | -0.53 | 3.87 | **MIN** | -8.54 |
| **Air Temperature Max (deg F)** | 58.12 | 61.36 | 66.02 | 83.79 | 83.05 | 92.70 | 99.07 | 97.68 | 97.09 | 80.51 | 73.81 | 58.86 | **MAX** | 99.07 |
| **Relative Humidity Avg (%)** | 70.25 | 71.25 | 61.55 | 48.50 | 52.49 | 31.84 | 23.32 | 20.12 | 29.91 | 21.93 | 45.69 | 77.35 | **AVG** | 46.18 |
| **Relative Humidity Min (%)** | 17.31 | 26.96 | 12.32 | 9.06 | 7.45 | 3.76 | 2.95 | 3.80 | 3.40 | 1.44 | 4.96 | 13.19 | **MIN** | 1.44 |
| **Relative Humidity Max (%)** | 99.70 | 100.00 | 100.00 | 99.30 | 99.30 | 98.90 | 95.70 | 93.00 | 86.20 | 77.48 | 100.00 | 100.00 | **MAX** | 100 |
| **Total Precipitation (inch)** | 0.38 | 0.66 | 1.16 | 0.42 | 1.63 | 0.06 | 0.19 | 0.27 | 0.00 | 0.00 | 0.74 | 0.75 | **TOTAL** | 6.26 |
| **Max Daily Precipitation (inch)** | 0.21 | 0.31 | 0.42 | 0.19 | 0.51 | 0.06 | 0.18 | 0.27 | 0.00 | 0.00 | 0.31 | 0.41 | **MAX** | 0.51 |
| **Soil Temperature Avg (deg F)** | 34.46 | 32.89 | 44.00 | 57.68 | 58.65 | 76.02 | 83.77 | 82.12 | 70.62 | 50.83 | 41.42 | 33.39 | **AVG** | 55.49 |
| **Soil Temperature Min (deg F)** | 14.83 | 18.33 | 26.36 | 33.79 | 34.71 | 43.82 | 55.31 | 55.45 | 33.88 | 8.94 | 17.87 | 17.47 | **MIN** | 8.94 |
| **Soil Temperature Max (deg F)** | 56.50 | 63.54 | 74.30 | 97.65 | 102.30 | 117.80 | 122.80 | 118.70 | 114.90 | 92.32 | 75.76 | 54.50 | **MAX** | 122.80 |
| **Soil Vol. Water Content Avg** | 0.16 | 0.19 | 0.23 | 0.23 | 0.23 | 0.22 | 0.17 | 0.18 | 0.15 | 0.13 | 0.13 | 0.19 | **AVG** | 0.18 |
| **Soil Vol. Water Content Min** | 0.13 | 0.16 | 0.20 | 0.21 | 0.19 | 0.18 | 0.15 | 0.15 | 0.13 | 0.11 | 0.11 | 0.15 | **MIN** | 0.11 |
| **Soil Vol. Water Content Max** | 0.18 | 0.24 | 0.26 | 0.25 | 0.31 | 0.28 | 0.19 | 0.20 | 0.17 | 0.14 | 0.16 | 0.21 | **MAX** | 0.31 |
| **Solar Radiation Avg (ly/day)** | 233 | 316 | 421 | 543 | 568 | 715 | 699 | 671 | 506 | 447 | 295 | 203 | **AVG** | 468.08 |
| **Solar Radiation Max (ly/day)** | 316 | 445 | 602 | 710 | 782 | 824 | 803 | 748 | 637 | 519 | 389 | 284 | **MAX** | 824 |
| **Barometric P. Avg (in Hg)** | 24.74 | 24.51 | 24.64 | 24.63 | 24.55 | 24.69 | 24.72 | 24.73 | 24.68 | 24.73 | 24.70 | 24.71 | **AVG** | 24.67 |
| **Barometric P. Min (in Hg)** | 24.32 | 24.16 | 24.20 | 24.33 | 24.31 | 24.43 | 24.52 | 24.55 | 24.21 | 24.38 | 24.10 | 24.40 | **MIN** | 24.1 |
| **Barometric P. Max (in Hg)** | 25.04 | 24.82 | 24.90 | 24.94 | 24.71 | 24.96 | 24.90 | 24.87 | 24.93 | 24.99 | 24.99 | 25.04 | **MAX** | 25.04 |
| **$PM_{2.5}$ Avg Concentration (µg/$m^3$)** | 0.26 | 0.49 | 0.84 | 2.10 | 1.48 | 2.20 | 0.82 | 0.73 | 1.24 | 1.08 | 0.47 | 0.12 | **AVG** | 0.99 |
| **$PM^{2.5}$ Max Concentration (µg/$m^3$)** | 11.99 | 10.86 | 29.28 | 992.91 | 45.64 | 873.58 | 11.96 | 25.26 | 55.39 | 206.69 | 35.34 | 2.69 | **MAX** | 992.91 |
| **$PM_{10}$ Avg Concentration (µg/$m^3$)** | 1.44 | 2.28 | 2.82 | 13.20 | 6.58 | 13.55 | 5.75 | 5.06 | 7.05 | 5.67 | 2.25 | 0.57 | **AVG** | 5.52 |
| **$PM_{10}$ Max Concentration (µg/$m^3$)** | 111.42 | 84.80 | 133.80 | 8,552.26 | 269.19 | 5919.87 | 73.37 | 125.08 | 365.72 | 1,081.40 | 232.30 | 44.25 | **MAX** | 8,552.26 |

*Wind Freq from S (indicates aggregate frequency for winds over 5 mph coming from south direction).

**Wind Freq from NW (indicates aggregate frequency for winds over 5 mph coming from northwest direction).

Table C-4. Station 404 summary of monthly and annual meteorological data from CY2019. Highlighted values indicate the month is missing five or more days of measurements.

| Month | Jan | Feb | Mar | Apr | May | June | Jul | Aug | Sep | Oct | Nov | Dec | Annual | Value |
|---|---|---|---|---|---|---|---|---|---|---|---|---|---|---|
| **Wind Speed Avg (mph)** | 6.36 | 9.16 | 7.23 | 7.82 | 7.96 | 6.95 | 7.27 | 6.83 | 6.86 | 6.16 | 4.66 | 5.13 | **AVG** | 6.86 |
| **Wind Speed Max (mph)** | 28.97 | 29.62 | 27.12 | 30.05 | 27.65 | 28.11 | 20.91 | 24.48 | 25.10 | 29.52 | 28.89 | 28.88 | **MAX** | 30.05 |
| **Wind Speed Gust (mph)** | 41.14 | 43.04 | 38.07 | 42.31 | 39.53 | 40.48 | 42.45 | 34.78 | 38.58 | 39.38 | 40.04 | 38.36 | **MAX** | 43.04 |
| **Wind Freq from S*** | 39.09% | 55.11% | 44.20% | 22.78% | 31.98% | 33.75% | 51.71% | 46.40% | 39.10% | 13.92% | 28.76% | 34.38% | **AVG** | 36.76% |
| **Wind Freq from NW**** | 33.69% | 21.37% | 25.04% | 34.24% | 29.02% | 28.99% | 10.80% | 7.79% | 29.06% | 40.68% | 30.85% | 42.48% | **AVG** | 27.83% |
| **Air Temperature Avg (deg F)** | 33.23 | 28.92 | 40.18 | 50.79 | 51.33 | 66.34 | 74.52 | 74.18 | 62.61 | 45.61 | 38.69 | 31.57 | **AVG** | 49.83 |
| **Air Temperature Min (deg F)** | 6.19 | -4.13 | 17.56 | 21.54 | 23.42 | 37.67 | 45.97 | 43.06 | 25.48 | -1.59 | 2.80 | 5.63 | **MIN** | -4.13 |
| **Air Temperature Max (deg F)** | 56.50 | 59.25 | 64.51 | 81.25 | 80.01 | 90.41 | 96.03 | 95.97 | 95.11 | 78.94 | 71.31 | 57.54 | **MAX** | 96.03 |
| **Relative Humidity Avg (%)** | 68.80 | 70.02 | 60.73 | 48.00 | 51.82 | 31.54 | 23.33 | 19.73 | 30.23 | 22.17 | 45.67 | 73.38 | **AVG** | 45.45 |
| **Relative Humidity Min (%)** | 17.50 | 27.06 | 11.80 | 9.68 | 8.15 | 4.39 | 3.04 | 4.64 | 4.73 | 2.01 | 5.96 | 11.54 | **MIN** | 2.01 |
| **Relative Humidity Max (%)** | 99.20 | 97.60 | 99.20 | 99.40 | 99.50 | 97.20 | 98.00 | 92.30 | 84.60 | 70.45 | 100.00 | 100.00 | **MAX** | 100 |
| **Total Precipitation (inch)** | 0.36 | 0.73 | 1.38 | 0.41 | 1.62 | 0.08 | 0.22 | 0.09 | 0.03 | 0.00 | 0.73 | 0.74 | **TOTAL** | 6.39 |
| **Max Daily Precipitation (inch)** | 0.20 | 0.35 | 0.38 | 0.18 | 0.46 | 0.08 | 0.12 | 0.09 | 0.02 | 0.00 | 0.32 | 0.42 | **MAX** | 0.46 |
| **Soil Temperature Avg (deg F)** | 36.88 | 34.36 | 45.02 | 56.56 | 58.72 | 74.92 | 84.06 | 84.08 | 73.75 | 56.79 | 46.66 | 35.47 | **AVG** | 57.27 |
| **Soil Temperature Min (deg F)** | 18.08 | 22.21 | 31.19 | 36.90 | 37.81 | 47.37 | 64.22 | 61.50 | 44.96 | 22.13 | 29.18 | 25.83 | **MIN** | 18.08 |
| **Soil Temperature Max (deg F)** | 56.80 | 57.76 | 68.63 | 88.00 | 93.11 | 104.60 | 112.90 | 113.50 | 108.60 | 89.80 | 73.78 | 51.82 | **MAX** | 113.50 |
| **Soil Vol. Water Content Avg** | 0.08 | 0.12 | 0.16 | 0.15 | 0.13 | 0.12 | 0.09 | 0.08 | 0.07 | 0.05 | 0.05 | 0.12 | **AVG** | 0.10 |
| **Soil Vol. Water Content Min** | 0.06 | 0.08 | 0.14 | 0.12 | 0.10 | 0.10 | 0.08 | 0.07 | 0.06 | 0.05 | 0.05 | 0.06 | **MIN** | 0.05 |
| **Soil Vol. Water Content Max** | 0.09 | 0.16 | 0.20 | 0.18 | 0.17 | 0.16 | 0.10 | 0.09 | 0.07 | 0.06 | 0.07 | 0.14 | **MAX** | 0.20 |
| **Solar Radiation Avg (ly/day)** | 223 | 308 | 409 | 531 | 546 | 701 | 692 | 640 | 500 | 410 | 267 | 188 | **AVG** | 451.25 |
| **Solar Radiation Max (ly/day)** | 309 | 417 | 585 | 680 | 722 | 783 | 771 | 709 | 619 | 484 | 349 | 252 | **MAX** | 783 |
| **Barometric P. Avg (in Hg)** | 24.73 | 24.50 | 24.64 | 24.60 | 24.50 | 24.61 | 24.62 | 24.62 | 24.57 | 24.61 | 24.61 | 24.70 | **AVG** | 24.61 |
| **Barometric P. Min (in Hg)** | 24.31 | 24.12 | 24.15 | 24.29 | 24.21 | 24.32 | 24.40 | 24.44 | 24.13 | 24.27 | 24.08 | 24.41 | **MIN** | 24.08 |
| **Barometric P. Max (in Hg)** | 25.04 | 24.80 | 24.92 | 24.93 | 24.71 | 24.86 | 24.90 | 24.76 | 24.82 | 24.87 | 24.92 | 25.02 | **MAX** | 25.04 |
| **$PM_{2.5}$ Avg Concentration (μg/m$^3$)** | 0.32 | 0.60 | 1.03 | 1.07 | 1.19 | 1.74 | 1.88 | 1.86 | 3.45 | 2.17 | 1.52 | 0.28 | **AVG** | 1.43 |
| **$PM_{2.5}$ Max Concentration (μg/m$^3$)** | 16.93 | 10.96 | 30.15 | 48.79 | 12.28 | 30.15 | 42.28 | 70.95 | 163.74 | 106.49 | 123.29 | 7.27 | **MAX** | 163.74 |
| **$PM_{10}$ Avg Concentration (μg/m$^3$)** | 1.78 | 2.36 | 2.92 | 5.40 | 5.65 | 9.19 | 12.64 | 11.35 | 18.59 | 13.43 | 8.05 | 1.26 | **AVG** | 7.72 |
| **$PM_{10}$ Max Concentration (μg/m$^3$)** | 157.64 | 81.38 | 150.64 | 296.45 | 252.23 | 173.09 | 182.09 | 294.26 | 858.15 | 997.53 | 1,006.32 | 109.06 | **MAX** | 1,006.32 |

*Wind Freq from S (indicates aggregate frequency for winds over 5 mph coming from south direction).

**Wind Freq from NW (indicates aggregate frequency for winds over 5 mph coming from northwest direction).

Table C-5. Station 405 summary of monthly and annual meteorological data from CY2019. Highlighted values indicate the month is missing five or more days of measurements.

| Month | Jan | Feb | Mar | Apr | May | June | Jul | Aug | Sep | Oct | Nov | Dec | Annual | Value |
|---|---|---|---|---|---|---|---|---|---|---|---|---|---|---|
| **Wind Speed Avg (mph)** | 6.12 | 8.77 | 6.94 | 7.58 | 7.93 | 7.13 | 7.58 | 7.16 | 7.12 | 6.28 | 4.78 | 5.30 | **AVG** | 6.89 |
| **Wind Speed Max (mph)** | 27.10 | 28.83 | 24.30 | 28.27 | 29.66 | 28.16 | 22.78 | 24.55 | 27.52 | 28.85 | 28.92 | 28.22 | **MAX** | 29.66 |
| **Wind Speed Gust (mph)** | 38.43 | 40.33 | 35.62 | 42.01 | 40.48 | 50.20 | 41.87 | 35.58 | 39.09 | 42.96 | 39.68 | 38.29 | **MAX** | 50.20 |
| **Wind Freq from S*** | 36.25% | 55.61% | 44.60% | 21.09% | 31.32% | 32.37% | 48.78% | 42.53% | 36.22% | 13.52% | 27.29% | 29.76% | **AVG** | 34.94% |
| **Wind Freq from NW**** | 36.35% | 21.30% | 24.94% | 34.61% | 28.84% | 26.58% | 10.85% | 7.57% | 28.02% | 38.53% | 28.64% | 37.79% | **AVG** | 27.00% |
| **Air Temperature Avg (deg F)** | 32.78 | 28.34 | 39.78 | 50.60 | 51.14 | 66.27 | 74.59 | 74.21 | 62.44 | 44.88 | 37.92 | 30.52 | **AVG** | 49.46 |
| **Air Temperature Min (deg F)** | 3.92 | -4.67 | 15.44 | 20.19 | 21.98 | 36.47 | 44.34 | 40.78 | 22.78 | -4.31 | 1.63 | 4.93 | **MIN** | -4.67 |
| **Air Temperature Max (deg F)** | 56.84 | 59.02 | 64.90 | 82.18 | 80.83 | 91.18 | 96.40 | 96.89 | 95.02 | 79.11 | 72.91 | 58.05 | **MAX** | 96.89 |
| **Relative Humidity Avg (%)** | 67.83 | 70.52 | 61.27 | 48.15 | 51.96 | 31.78 | 23.51 | 19.94 | 30.42 | 22.62 | 46.17 | 73.69 | **AVG** | 45.66 |
| **Relative Humidity Min (%)** | 17.65 | 26.69 | 11.61 | 9.74 | 8.25 | 3.96 | 2.86 | 4.66 | 5.10 | 2.25 | 6.24 | 11.68 | **MIN** | 2.25 |
| **Relative Humidity Max (%)** | 98.90 | 100.00 | 99.20 | 99.60 | 99.70 | 97.70 | 98.60 | 93.40 | 85.70 | 72.13 | 100.00 | 99.70 | **MAX** | 100 |
| **Total Precipitation (inch)** | 0.15 | 0.79 | 1.36 | 0.47 | 1.84 | 0.14 | 0.11 | 0.11 | 0.01 | 0.00 | 0.68 | 0.70 | **TOTAL** | 6.36 |
| **Max Daily Precipitation (inch)** | 0.06 | 0.31 | 0.38 | 0.17 | 0.48 | 0.07 | 0.10 | 0.11 | 0.01 | 0.00 | 0.29 | 0.39 | **MAX** | 0.48 |
| **Soil Temperature Avg (deg F)** | 37.25 | 33.88 | 45.03 | 59.39 | 62.33 | 80.78 | 90.03 | 88.67 | 74.60 | 54.92 | 45.29 | 35.19 | **AVG** | 58.95 |
| **Soil Temperature Min (deg F)** | 16.07 | 17.28 | 31.46 | 37.66 | 38.69 | 47.73 | 66.06 | 61.38 | 43.97 | 19.59 | 27.10 | 23.82 | **MIN** | 16.07 |
| **Soil Temperature Max (deg F)** | 58.17 | 56.91 | 70.20 | 91.80 | 99.10 | 110.60 | 120.00 | 117.50 | 112.00 | 88.34 | 71.78 | 51.51 | **MAX** | 120.00 |
| **Soil Vol. Water Content Avg** | 0.10 | 0.14 | 0.22 | 0.26 | 0.23 | 0.22 | 0.18 | 0.16 | 0.13 | 0.11 | 0.11 | 0.16 | **AVG** | 0.17 |
| **Soil Vol. Water Content Min** | 0.09 | 0.10 | 0.18 | 0.23 | 0.19 | 0.18 | 0.16 | 0.15 | 0.12 | 0.10 | 0.10 | 0.11 | **MIN** | 0.09 |
| **Soil Vol. Water Content Max** | 0.12 | 0.19 | 0.29 | 0.29 | 0.26 | 0.26 | 0.19 | 0.17 | 0.15 | 0.12 | 0.12 | 0.18 | **MAX** | 0.29 |
| **Solar Radiation Avg (ly/day)** | 258 | 333 | 437 | 541 | 545 | 698 | 692 | 656 | 522 | 443 | 297 | 208 | **AVG** | 469.17 |
| **Solar Radiation Max (ly/day)** | 340 | 459 | 614 | 688 | 733 | 788 | 774 | 721 | 643 | 517 | 388 | 289 | **MAX** | 788 |
| **Barometric P. Avg (in Hg)** | 24.60 | 24.37 | 24.50 | 24.50 | 24.41 | 24.55 | 24.59 | 24.60 | 24.54 | 24.59 | 24.55 | 24.55 | **AVG** | 24.53 |
| **Barometric P. Min (in Hg)** | 24.18 | 24.03 | 24.07 | 24.20 | 24.17 | 24.30 | 24.39 | 24.42 | 24.08 | 24.24 | 23.94 | 24.25 | **MIN** | 23.94 |
| **Barometric P. Max (in Hg)** | 24.90 | 24.67 | 24.76 | 24.80 | 24.58 | 24.82 | 24.76 | 24.74 | 24.79 | 24.85 | 24.85 | 24.87 | **MAX** | 24.90 |
| **$PM_{2.5}$ Avg Concentration (µg/m$^3$)** | 0.29 | 0.55 | 1.01 | 1.08 | 1.21 | 1.65 | 1.17 | 1.51 | 2.81 | 1.61 | 1.15 | 0.21 | **AVG** | 1.19 |
| **$PM_{2.5}$ Max Concentration (µg/m$^3$)** | 7.54 | 7.11 | 29.03 | 48.29 | 9.20 | 26.80 | 14.61 | 53.14 | 122.68 | 65.58 | 51.24 | 4.23 | **MAX** | 122.68 |
| **$PM_{10}$ Avg Concentration (µg/m$^3$)** | 1.82 | 2.39 | 3.21 | 6.15 | 6.70 | 10.05 | 6.89 | 10.82 | 17.68 | 10.86 | 7.28 | 1.13 | **AVG** | 7.08 |
| **$PM_{10}$ Max Concentration (µg/m$^3$)** | 360.22 | 73.18 | 93.12 | 257.79 | 489.63 | 127.53 | 115.54 | 212.18 | 698.30 | 528.94 | 876.87 | 37.03 | **MAX** | 876.87 |

*Wind Freq from S (indicates aggregate frequency for winds over 5 mph coming from south direction).

**Wind Freq from NW (indicates aggregate frequency for winds over 5 mph coming from northwest direction).

# APPENDIX D. DAILY AVERAGE METEOROLOGICAL AND ENVIRONMENTAL DATA FOR TTR MONITORING STATIONS 400, 401, 403, 404, AND 405 DURING CY2019

## Tonopah Test Range Station 400, 2019

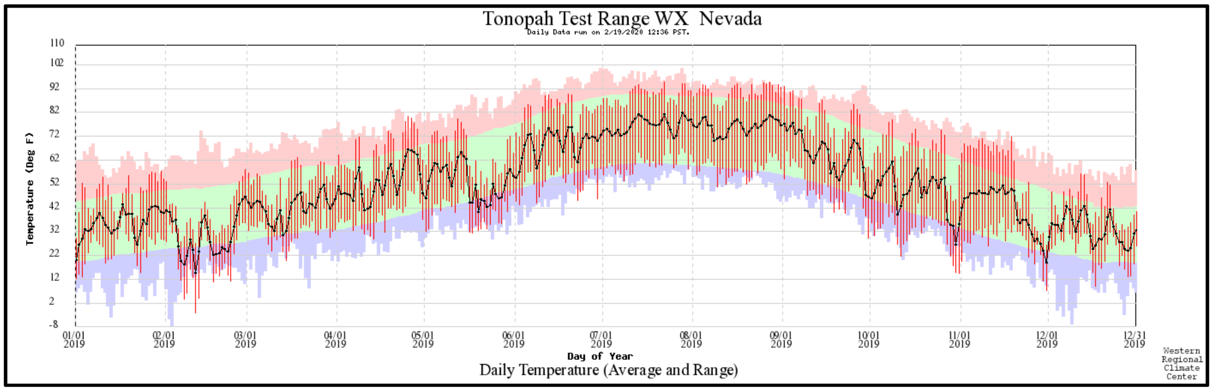


Figure D-1. Graphical summary of daily maximum and minimum (red bars) and average (black line) temperature data collected by the TTR 400 station from January 1, 2019, until December 31, 2019. Underlying pastel colors represent the period-of-record extremes (red and blue) and averages (green).

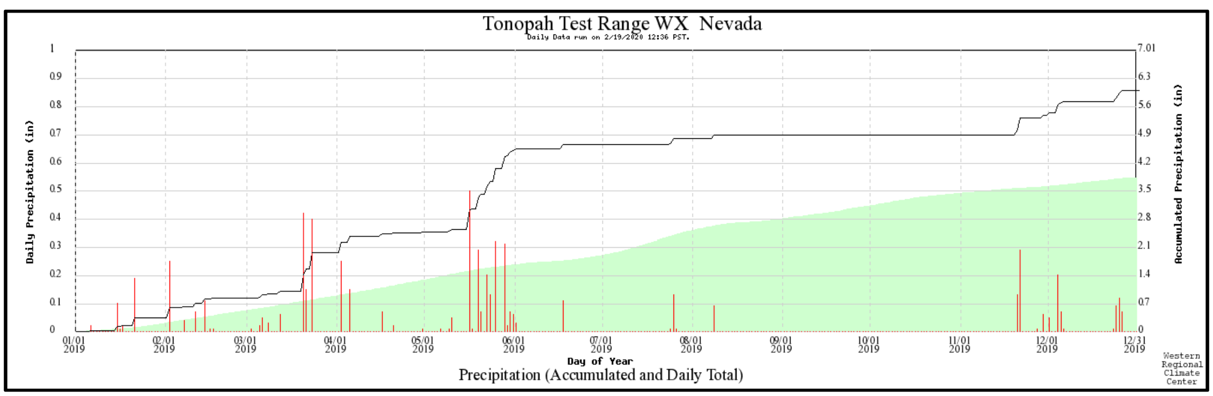


Figure D-2. Graphical summary of the daily total (red bars) and accumulated (black line) precipitation data collected by the TTR 400 station from January 1, 2019, until December 31, 2019. Underlying light green shaded area represents the station period-of-record average precipitation accumulation.

## Tonopah Test Range Station 400, 2019

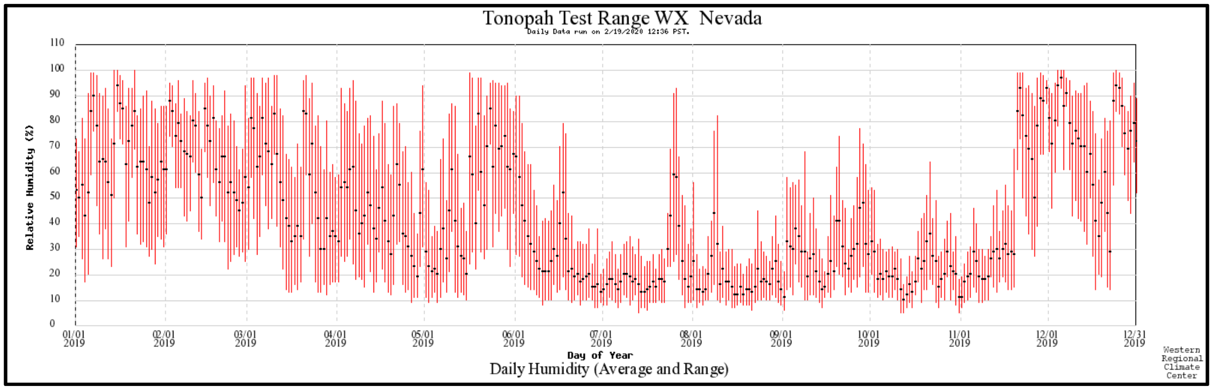


Figure D-3. Graphical summary of the daily maximum and minimum (red bars) and average (black marks) humidity data collected by the TTR 400 station from January 1, 2019, until December 31, 2019.

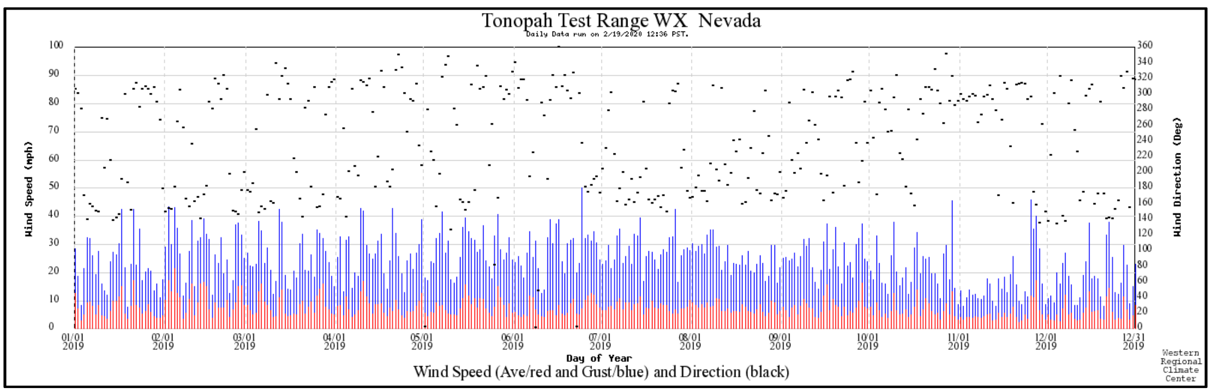


Figure D-4. Graphical summary of daily average (red lines) and daily peak gust (blue lines) wind speed and wind direction (black marks) data collected by the TTR 400 station from January 1, 2019, until December 31, 2019.

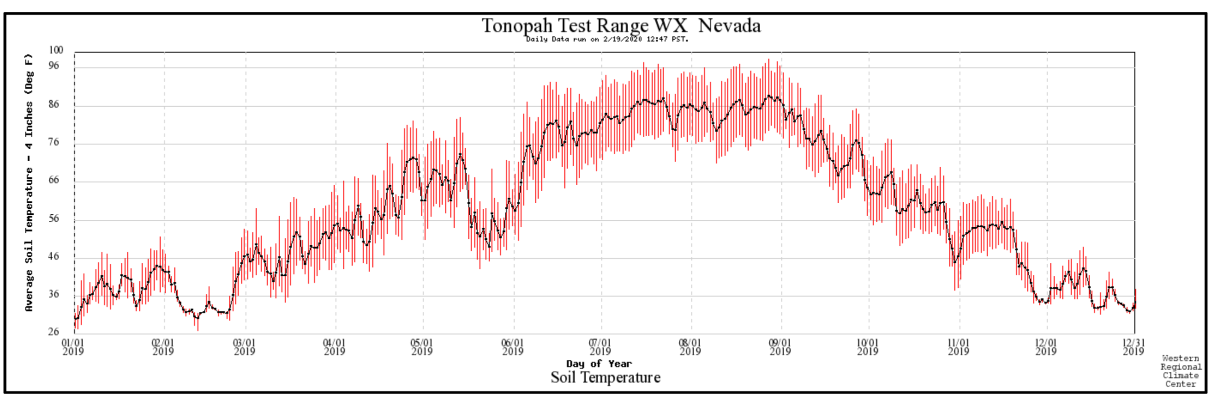


Figure D-5. Graphical summary of daily maximum and minimum (red bars) and average (black line) soil temperature data collected by the TTR 400 station from January 1, 2019, until December 31, 2019.

**Tonopah Test Range Station 400, 2019**

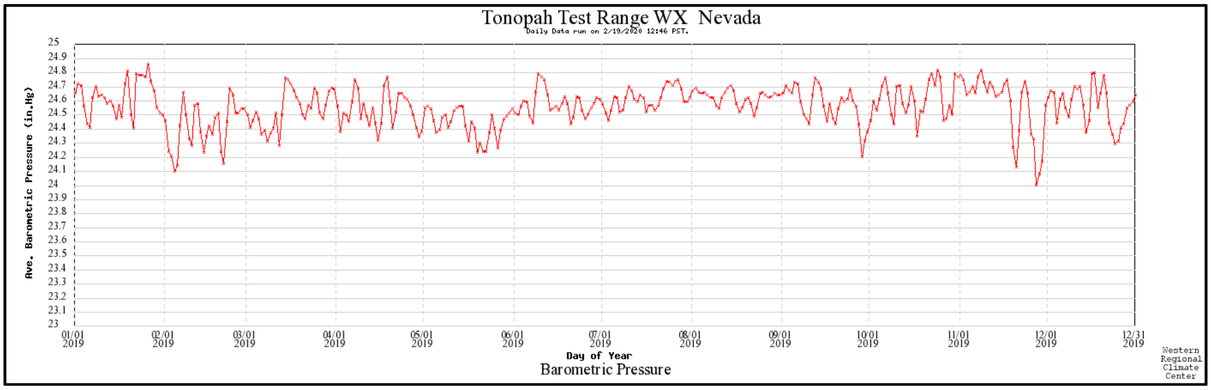


Figure D-6. Graphical summary of the daily average barometric pressure data collected by the TTR 400 station from January 1, 2019, until December 31, 2019.

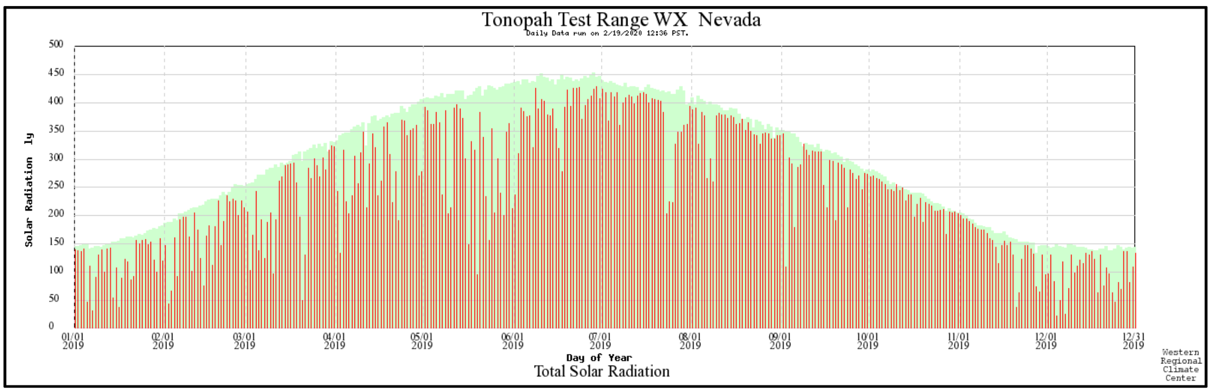


Figure D-7. Graphical summary of daily total solar radiation (red bar) data collected by the TTR 400 station from January 1, 2019, until December 31, 2019. Underlying light green shaded area represents the station period-of-record maximum daily solar radiation.

## Clean Slate III Station 401, 2019

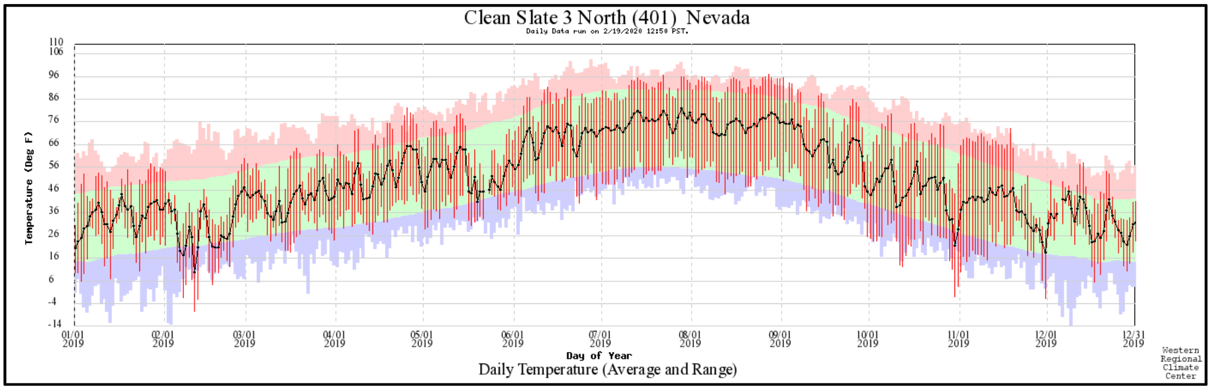


Figure D-8. Graphical summary of daily maximum and minimum (red bars) and average (black line) temperature data collected by the Clean Slate III station from January 1, 2019, until December 31, 2019. Underlying pastel colors represent the period-of-record extremes (red and blue) and averages (green).

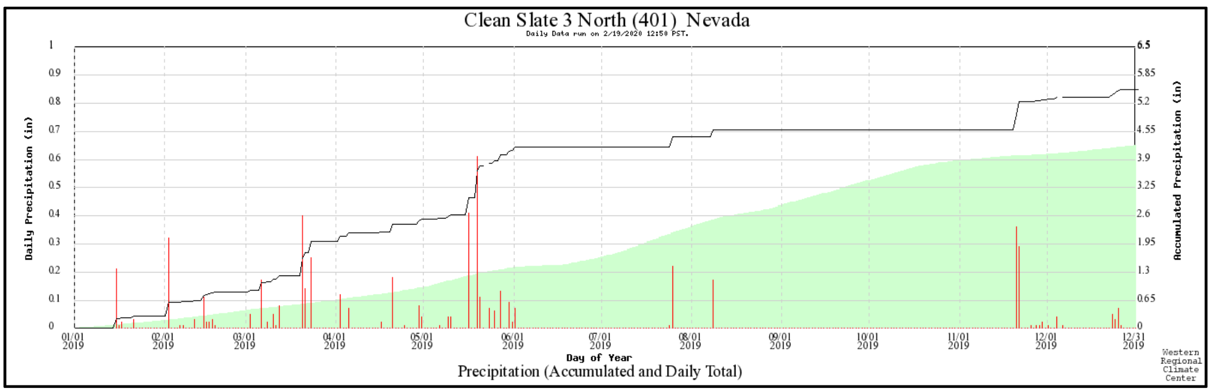


Figure D-9. Graphical summary of daily total (red bars) and accumulated (black line) precipitation data collected by the Clean Slate III station from January 1, 2019, until December 31, 2019. Underlying light green shaded area represents the station period-of-record average precipitation accumulation.

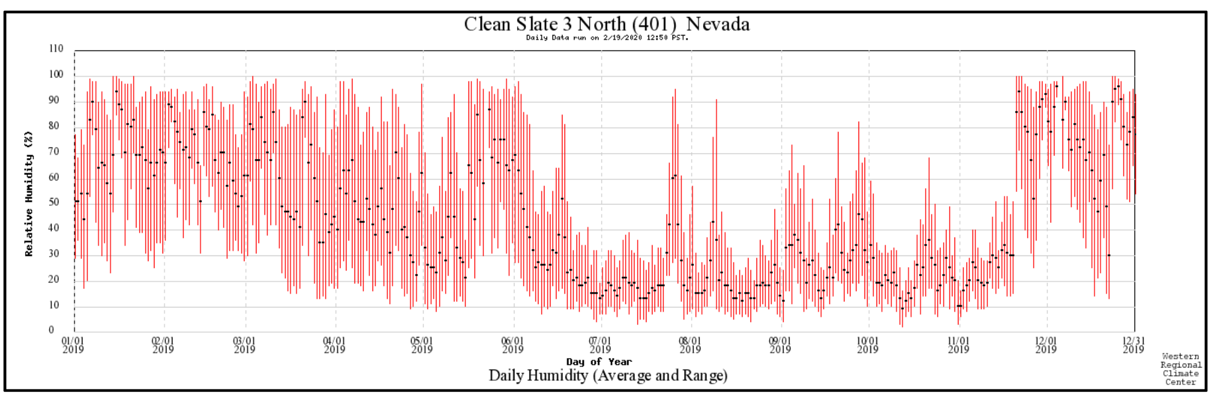


Figure D-10. Graphical summary of the daily maximum and minimum (red bars) and average (black marks) humidity data collected by the Clean Slate III station from January 1, 2019, until December 31, 2019.

## Clean Slate III Station 401, 2019

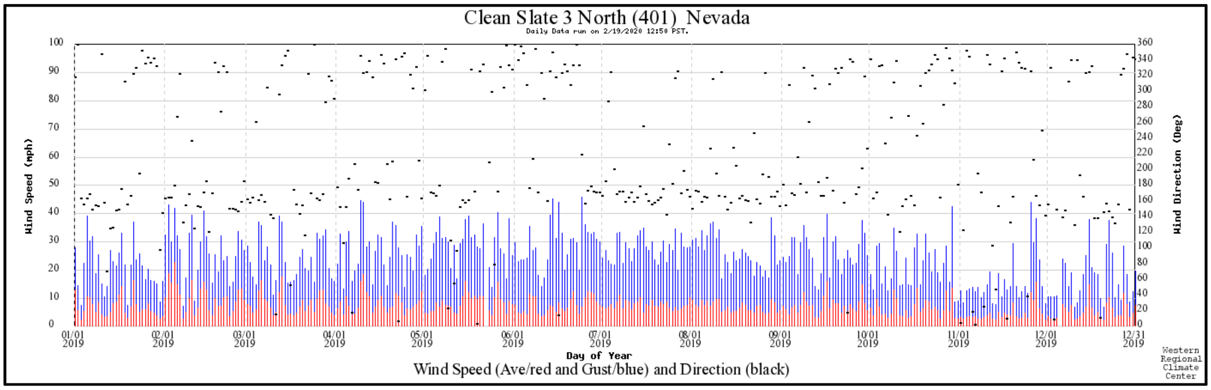


Figure D-11. Graphical summary of daily average (red bars) and daily peak gust (blue bars) wind speed and wind direction (black marks) data collected by the Clean Slate III station from January 1, 2019, until December 31, 2019.

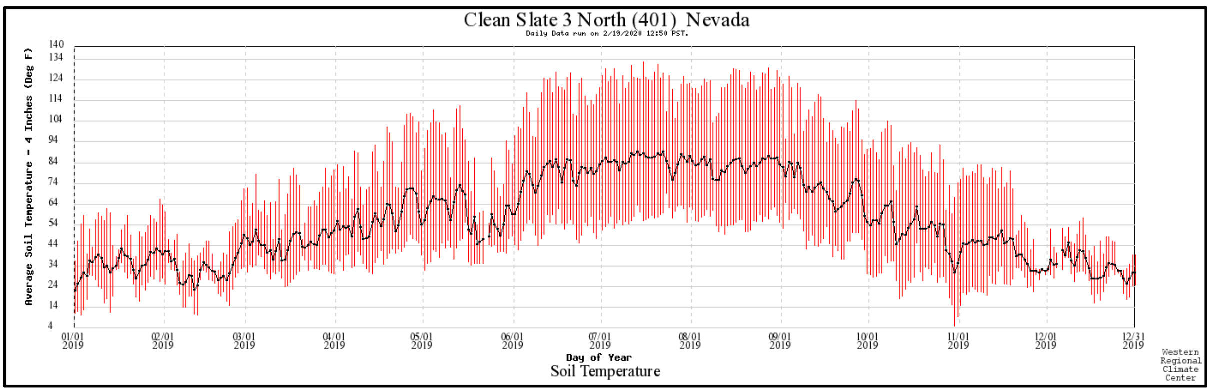


Figure D-12. Graphical summary of daily maximum and minimum (red bars) and average (black line) soil temperature data collected by the Clean Slate III station from January 1, 2019, until December 31, 2019.

## Clean Slate III Station 403, 2019

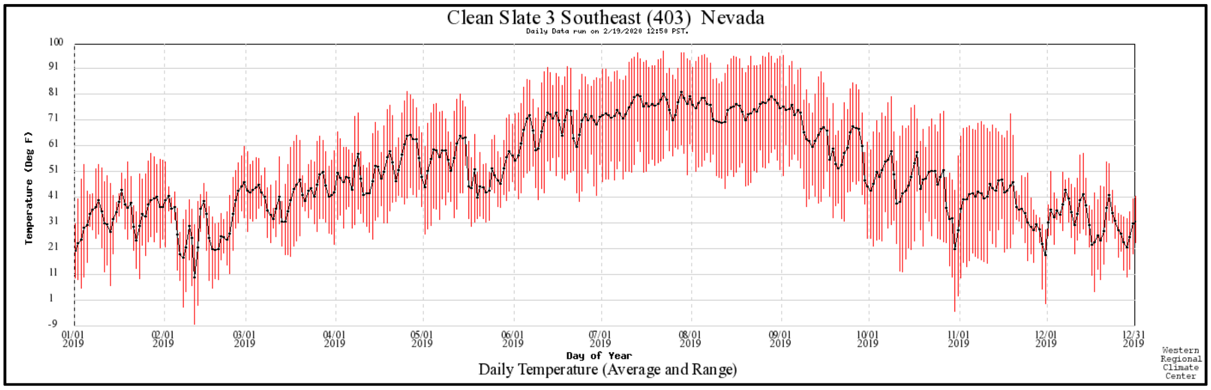


Figure D-13. Graphical summary of daily maximum and minimum (red bars) and average (black line) temperature data collected by the Clean Slate III station from January 1, 2019, until December 31, 2019.

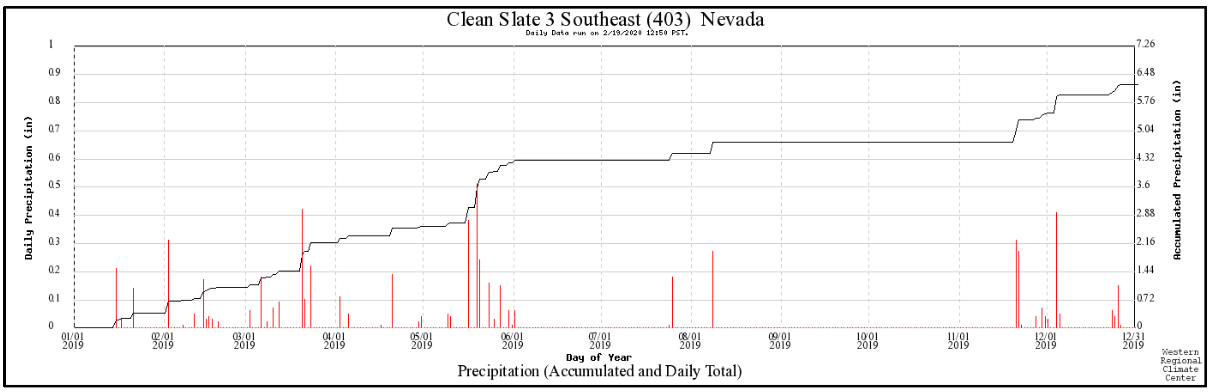


Figure D-14. Graphical summary of daily total (red bars) and accumulated (black line) precipitation data collected by the Clean Slate III station from January 1, 2019, until December 31, 2019.

## Clean Slate III Station 403, 2019

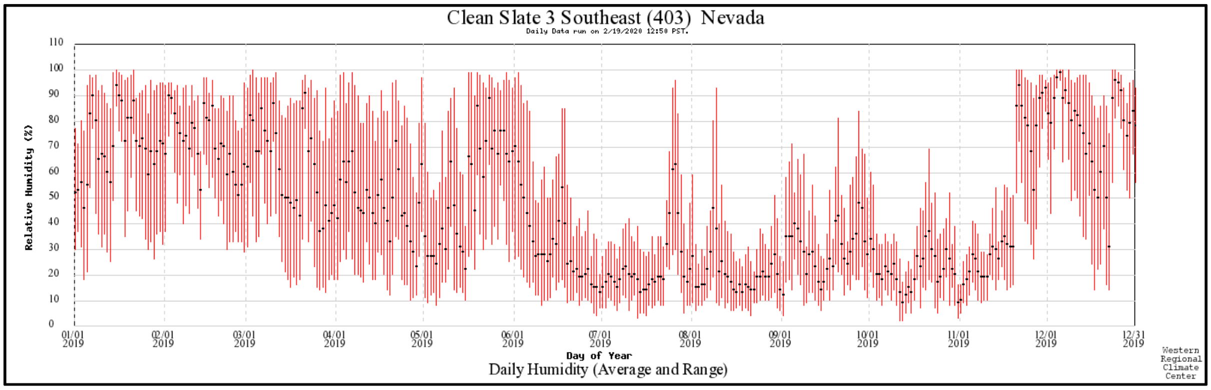


Figure D-15. Graphical summary of the daily maximum and minimum (red bars) and average (black marks) humidity data collected by the Clean Slate III station from January 1, 2019, until December 31, 2019.

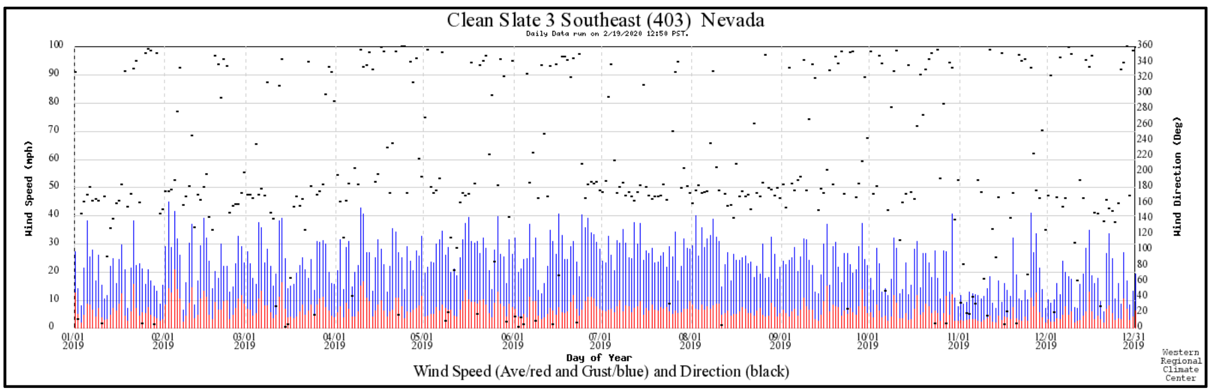


Figure D-16. Graphical summary of the daily average (red bars) and daily peak gust (blue bars) wind speed and wind direction (black marks) data collected by the Clean Slate III station from January 1, 2019, until December 31, 2019.

## Clean Slate III Station 403, 2019

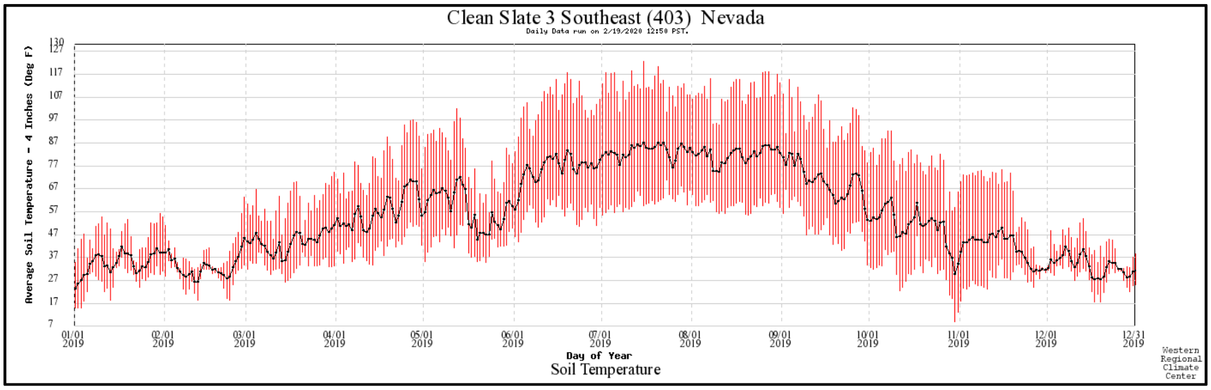


Figure D-17. Graphical summary of daily maximum and minimum (red bars) and average (black line) soil temperature data collected by the Clean Slate III station from January 1, 2019, until December 31, 2019.

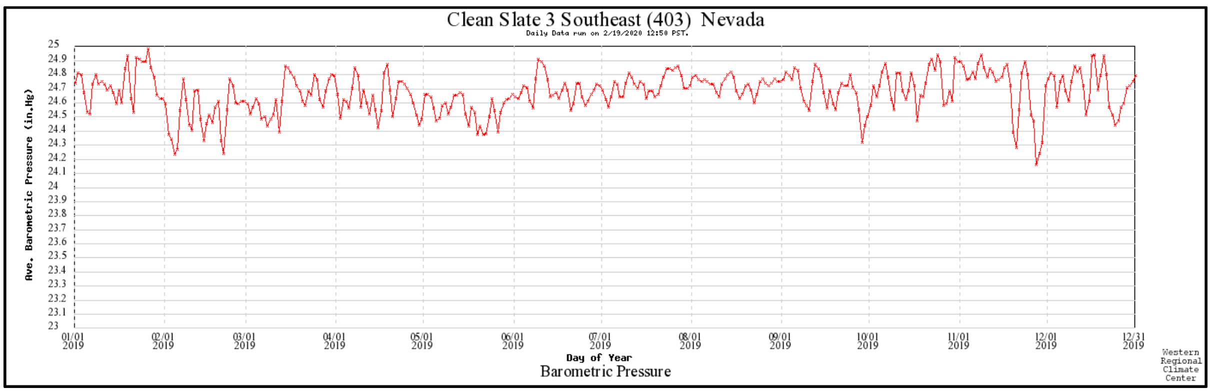


Figure D-18. Graphical summary of the daily average barometric pressure data collected by the Clean Slate III station from January 1, 2019, until December 31, 2019.

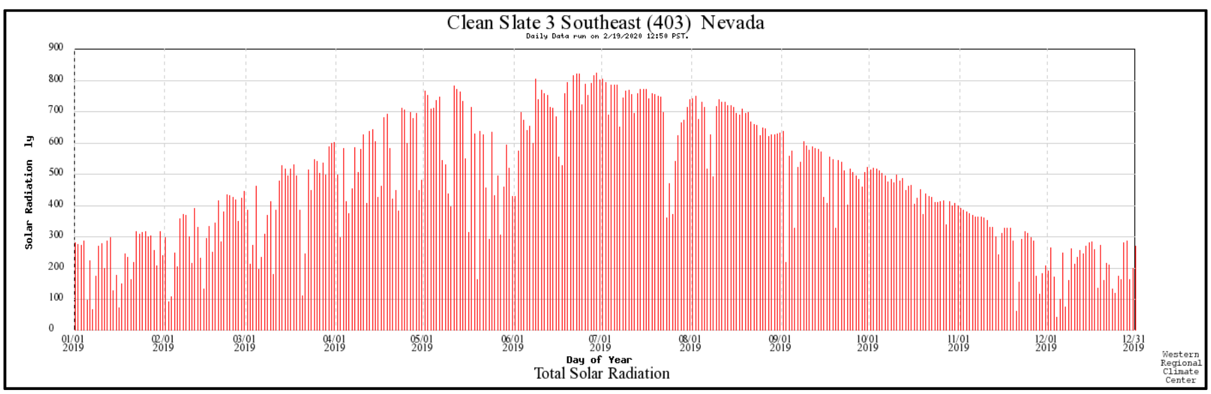


Figure D-19. Graphical summary of daily total solar radiation data collected by the Clean Slate III station from January 1, 2019, until December 31, 2019.

## Clean Slate II Station 404, 2019

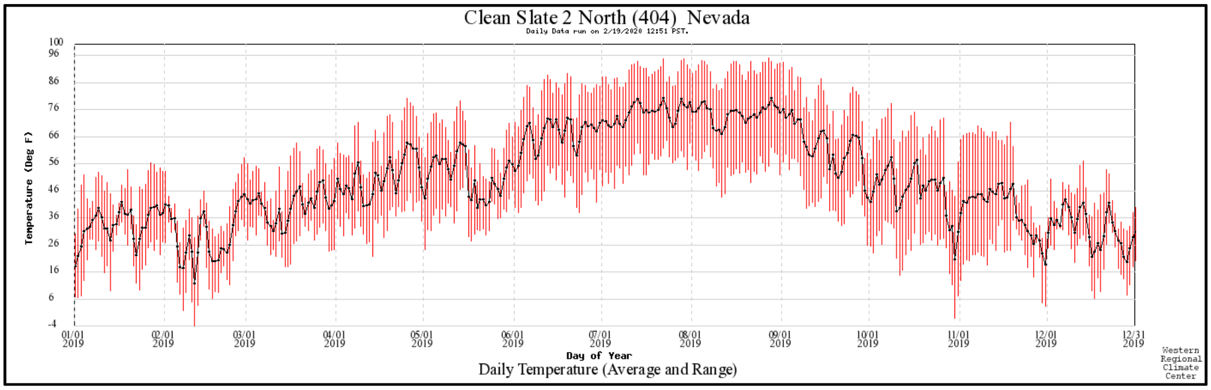


Figure D-20. Graphical summary of daily maximum and minimum (red bars) and average (black line) temperature data collected by the Clean Slate II station from January 1, 2019, until December 31, 2019.

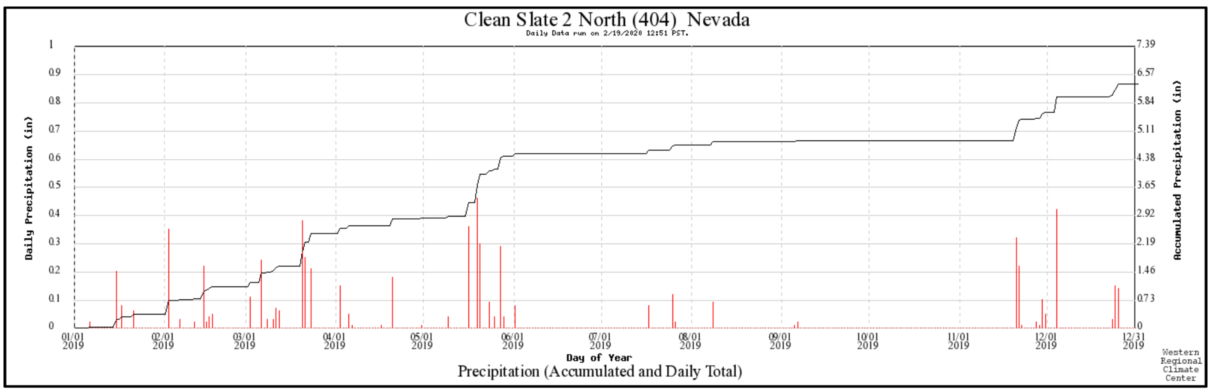


Figure D-21. Graphical summary of daily total (red bars) and accumulated (black line) precipitation data collected by the Clean Slate II station from January 1, 2019, until December 31, 2019.

## Clean Slate II Station 404, 2019

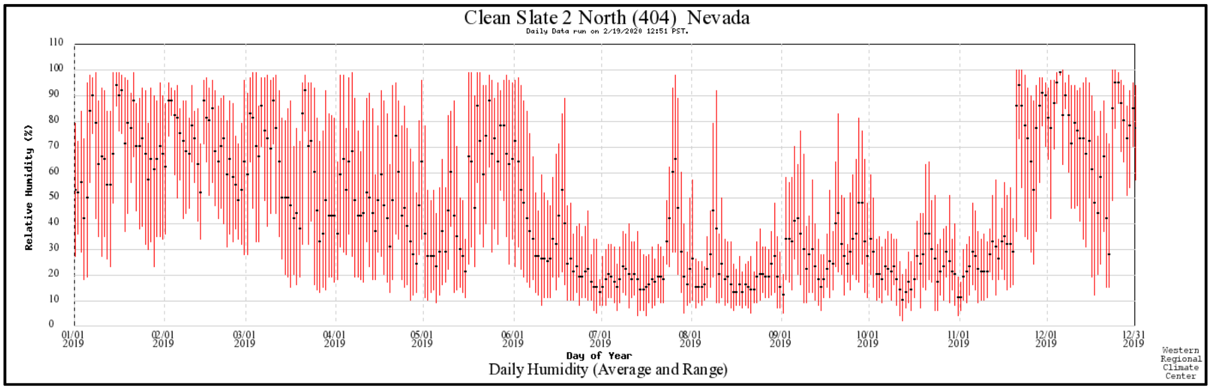


Figure D-22. Graphical summary of the daily maximum and minimum (red bars) and average (black marks) humidity data collected by the Clean Slate II station from January 1, 2019, until December 31, 2019.

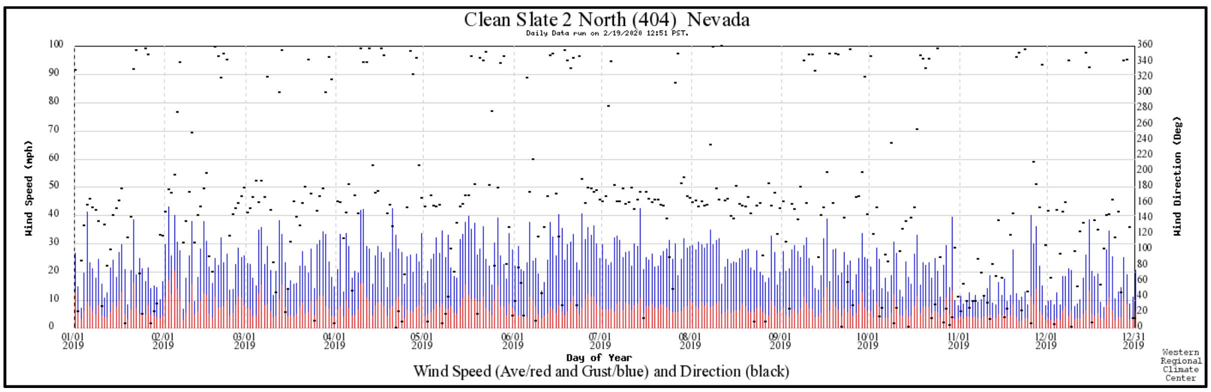


Figure D-23. Graphical summary of daily average (red bars) and daily peak gust (blue bars) wind speed and wind direction (black marks) data collected by the Clean Slate II station from January 1, 2019, until December 31, 2019.

## Clean Slate II Station 404, 2019

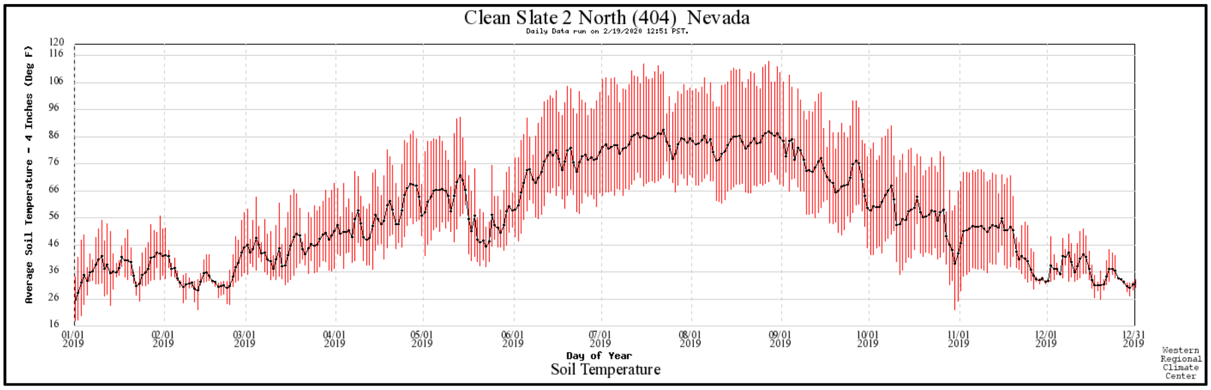


Figure D-24. Graphical summary of daily maximum and minimum (red bars) and average (black line) soil temperature data collected by the Clean Slate II station from January 1, 2019, until December 31, 2019.

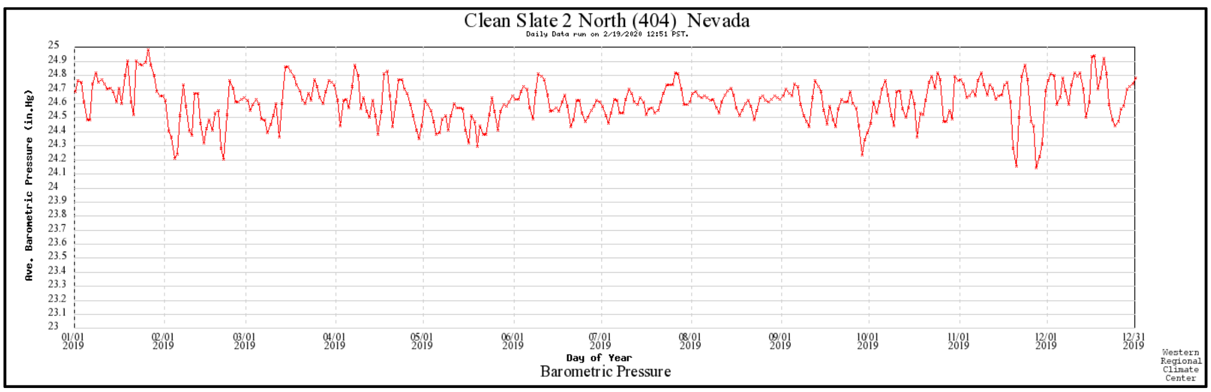


Figure D-25. Graphical summary of the daily average barometric pressure data collected by the Clean Slate II station from January 1, 2019, until December 31, 2019.

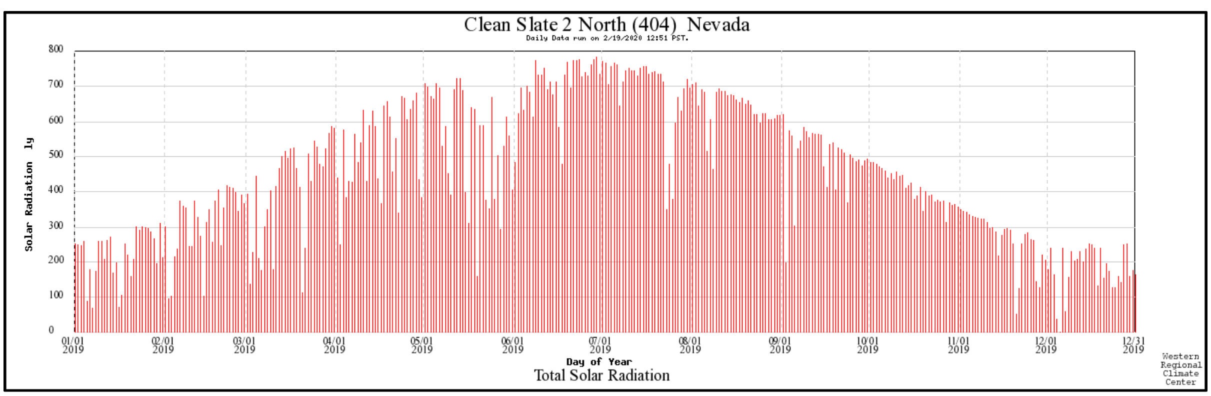


Figure D-26. Graphical summary of daily total solar radiation data collected by the Clean Slate II station from January 1, 2019, until December 31, 2019.

# Clean Slate II Station 405, 2019

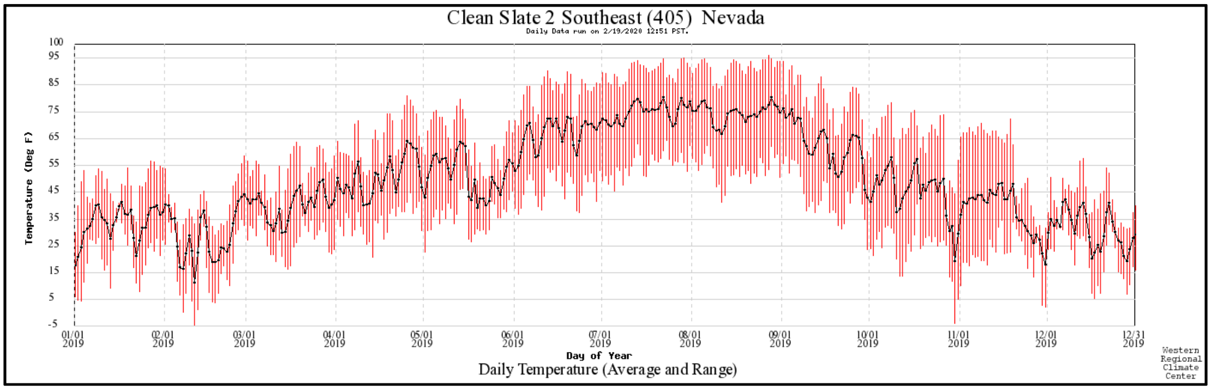


Figure D-27. Graphical summary of daily maximum and minimum (red bars) and average (black line) temperature data collected by the Clean Slate II station from January 1, 2019, until December 31, 2019.

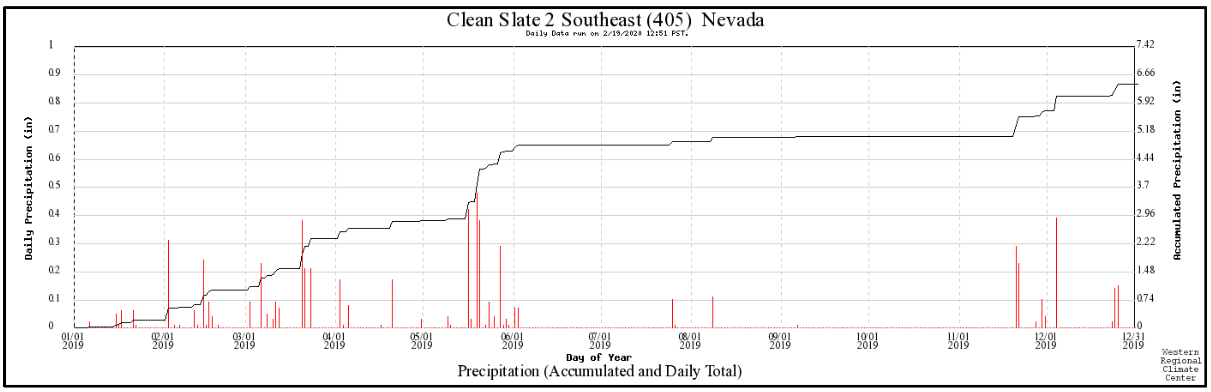


Figure D-28. Graphical summary of daily total (red bars) and accumulated (black line) precipitation data collected by the Clean Slate II station from January 1, 2019, until December 31, 2019.

## Clean Slate II Station 405, 2019

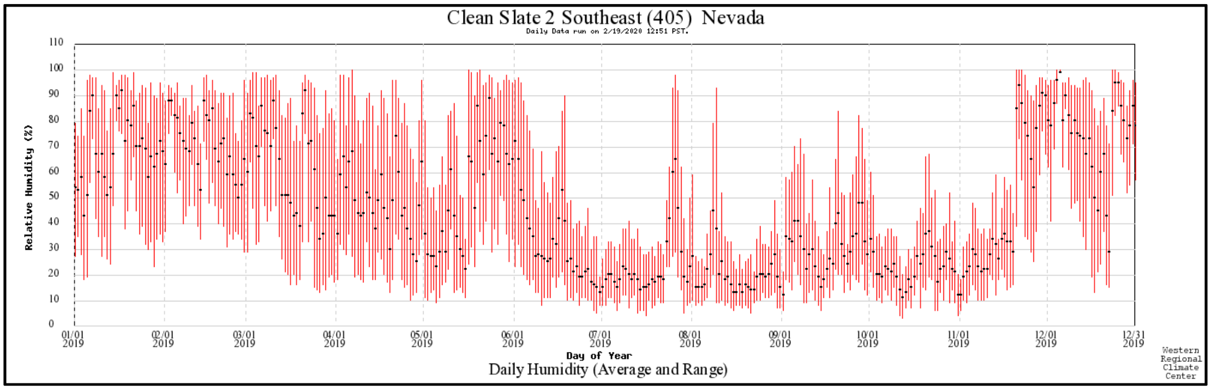


Figure D-29. Graphical summary of the daily maximum and minimum (red bars) and average (black marks) humidity data collected by the Clean Slate II station from January 1, 2019, until December 31, 2019.

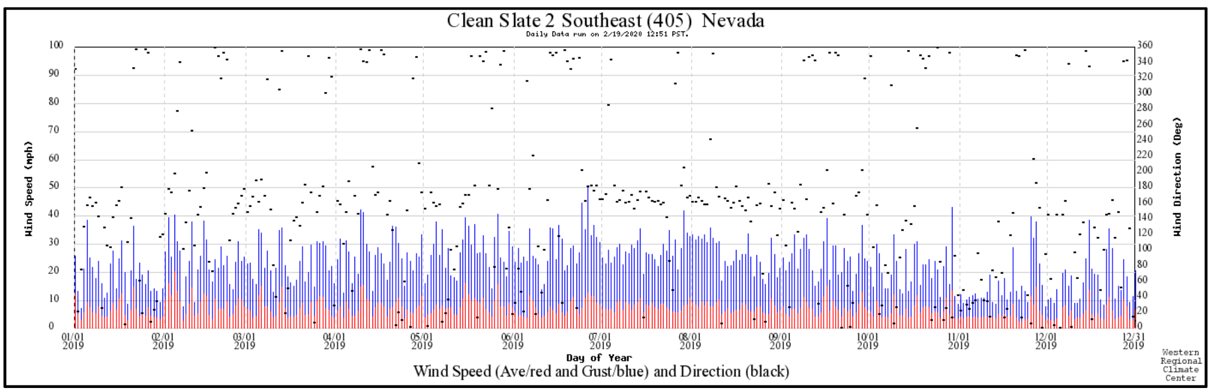


Figure D-30. Graphical summary of daily average (red bars) and daily peak gust (blue bars) wind speed and wind direction (black marks) data collected by the Clean Slate II station from January 1, 2019, until December 31, 2019.

## Clean Slate II Station 405, 2019

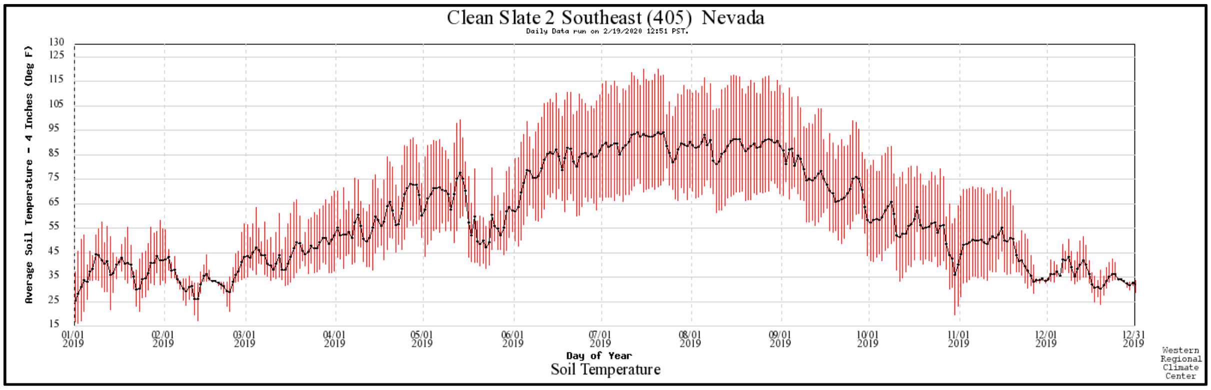


Figure D-31. Graphical summary of daily maximum and minimum (red bars) and average (black lines) soil temperature data collected by the Clean Slate II station from January 1, 2019, until December 31, 2019.

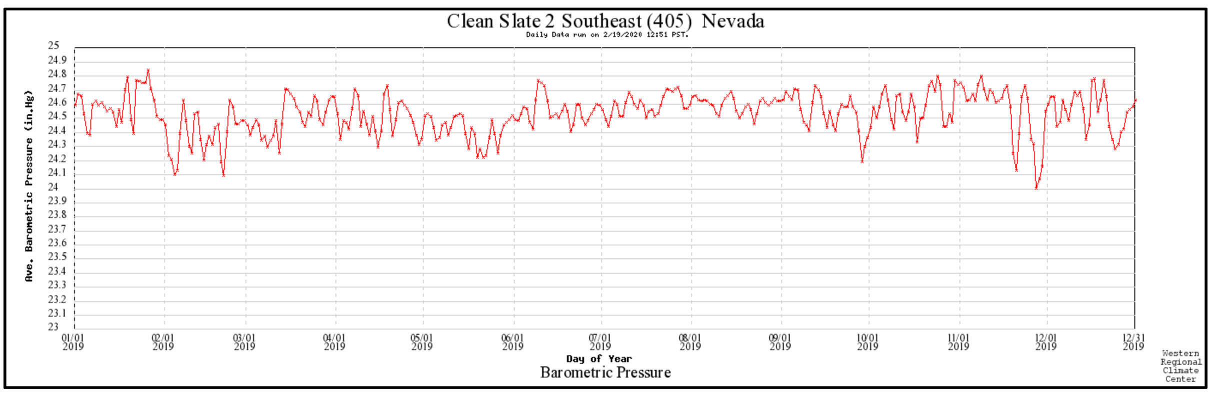


Figure D-32. Graphical summary of the daily average barometric pressure data collected by the Clean Slate II station from January 1, 2019, until December 31, 2019.

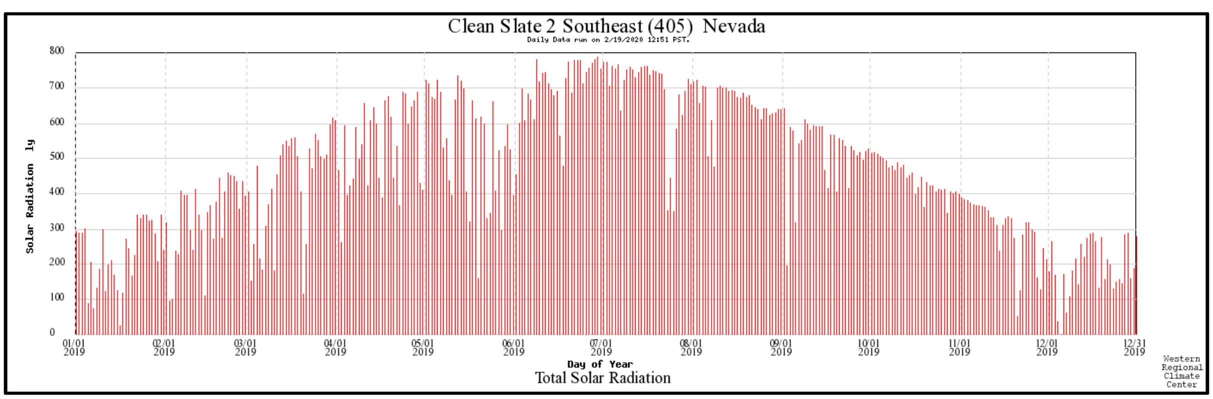


Figure D-33. Graphical summary of daily total solar radiation data collected by the Clean Slate II station from January 1, 2019, until December 31, 2019.

# APPENDIX E. ALPHA SPECTROMETRY RESULTS FOR INDIVIDUAL FILTERS SELECTED DURING CY2019

Table E-1. Alpha spectrometry results for individual filters selected from CY2019. Shaded boxes indicate values below the detection limit (DL).

| Station | Start Date | End Date | $^{239+240}$Pu (µCi/ml × $10^{-16}$) | | | $^{238}$Pu (µCi/ml × $10^{-16}$) | | |
|---|---|---|---|---|---|---|---|---|
| | | | Results | Error | DL | Results | Error | DL |
| 400 | 1/16/2019 | 1/28/2019 | 0.040 | 0.180 | 0.386 | 0.081 | 0.228 | 0.445 |
| | 3/13/2019 | 3/27/2019 | -0.041 | 0.182 | 0.450 | 0.122 | 0.215 | 0.390 |
| | 4/24/2019 | 5/9/2019 | 0.066 | 0.132 | 0.252 | 0.000 | 0.093 | 0.252 |
| | 5/21/2019 | 6/5/2019 | -0.142 | 0.143 | 0.438 | -0.107 | 0.159 | 0.438 |
| | 6/19/2019 | 7/3/2019 | 0.034 | 0.295 | 0.837 | -0.101 | 0.117 | 0.837 |
| | 8/28/2019 | 9/11/2019 | -0.033 | 0.299 | 0.928 | -0.033 | 0.065 | 0.632 |
| | 9/25/2019 | 10/8/2019 | 0.000 | 0.066 | 0.395 | -0.164 | 0.148 | 0.935 |
| | 11/20/2019 | 12/5/2019 | 0.097 | 0.269 | 0.630 | 0.000 | 0.065 | 0.390 |
| 401 | 1/28/2019 | 2/12/2019 | 296.495 | 25.817 | 0.391 | 1.916 | 0.582 | 0.122 |
| | 2/27/2019 | 3/13/2019 | 301.745 | 26.265 | 0.372 | 1.935 | 0.582 | 0.297 |
| | 4/24/2019 | 5/9/2019 | 84.017 | 7.851 | 0.106 | 0.817 | 0.362 | 0.272 |
| | 6/5/2019 | 6/19/2019 | 76.771 | 7.313 | 0.428 | 0.155 | 0.289 | 0.519 |
| | 7/31/2019 | 8/14/2019 | 3.139 | 1.464 | 0.901 | -0.121 | 0.386 | 1.262 |
| | 9/11/2019 | 9/25/2019 | 2.941 | 1.410 | 0.489 | 0.163 | 0.489 | 1.088 |
| | 10/8/2019 | 10/23/2019 | 53.954 | 7.178 | 0.957 | 0.465 | 0.587 | 0.887 |
| | 10/23/2019 | 11/6/2019 | 64.124 | 8.594 | 0.979 | 0.262 | 0.510 | 0.978 |
| 403 | 12/19/2018 | 1/2/2019 | 33.854 | 3.587 | 0.270 | 0.353 | 0.246 | 0.269 |
| | 1/28/2019 | 2/12/2019 | 2.739 | 0.716 | 0.380 | 0.119 | 0.177 | 0.303 |
| | 3/27/2019 | 4/11/2019 | 102.725 | 9.424 | 0.352 | 0.403 | 0.422 | 0.676 |
| | 4/24/2019 | 5/9/2019 | 10.287 | 1.506 | 0.279 | 0.073 | 0.179 | 0.349 |
| | 6/19/2019 | 7/3/2019 | 2.199 | 1.221 | 0.956 | -0.193 | 0.174 | 1.100 |
| | 9/11/2019 | 9/25/2019 | -0.166 | 0.167 | 1.104 | -0.166 | 0.167 | 1.104 |
| | 10/23/2019 | 11/6/2019 | 83.780 | 10.597 | 1.159 | 0.140 | 0.567 | 1.325 |
| | 12/5/2019 | 12/18/2019 | 0.664 | 0.817 | 1.259 | 0.044 | 0.385 | 1.093 |
| 404 | 12/19/2018 | 1/2/2019 | 0.860 | 0.365 | 0.263 | -0.034 | 0.069 | 0.263 |
| | 3/13/2019 | 3/27/2019 | 0.603 | 0.336 | 0.307 | 0.000 | 0.113 | 0.307 |
| | 4/24/2019 | 5/9/2019 | 3.816 | 0.827 | 0.286 | 0.112 | 0.167 | 0.285 |
| | 5/9/2019 | 5/21/2019 | 17.624 | 2.350 | 0.140 | 0.094 | 0.133 | 0.140 |
| | 6/19/2019 | 7/3/2019 | 0.286 | 0.558 | 1.072 | -0.144 | 0.165 | 1.176 |
| | 7/3/2019 | 7/17/2019 | 0.367 | 0.520 | 0.550 | 0.000 | 0.409 | 1.229 |
| | 9/25/2019 | 10/8/2019 | 1.175 | 0.929 | 0.999 | -0.040 | 0.370 | 1.143 |
| | 10/8/2019 | 10/23/2019 | 1.816 | 1.131 | 1.002 | 0.000 | 0.081 | 0.483 |
| 405 | 12/19/2018 | 1/2/2019 | 0.730 | 0.356 | 0.367 | -0.066 | 0.133 | 0.367 |
| | 2/12/2019 | 2/27/2019 | 1.147 | 0.577 | 0.487 | -0.064 | 0.220 | 0.610 |
| | 4/24/2019 | 5/9/2019 | 1.721 | 0.503 | 0.110 | 0.110 | 0.128 | 0.110 |
| | 5/9/2019 | 5/21/2019 | 5.089 | 1.112 | 0.479 | 0.050 | 0.100 | 0.149 |
| | 7/3/2019 | 7/17/2019 | 0.350 | 0.496 | 0.524 | 0.131 | 0.360 | 0.846 |
| | 8/14/2019 | 8/28/2019 | 0.000 | 0.090 | 0.538 | -0.089 | 0.127 | 1.003 |
| | 9/25/2019 | 10/8/2019 | 0.718 | 0.720 | 0.538 | 0.090 | 0.380 | 1.003 |
| | 11/6/2019 | 11/20/2019 | 2.265 | 1.270 | 0.522 | 0.260 | 0.507 | 0.974 |

## STANDING DISTRIBUTION LIST

Robert Boehlecke
EM NV Program Manager
Department of Energy
Environmental Management Nevada Program
100 N. City Parkway, Suite #1750
Las Vegas, NV 89106
Robert.Boehlecke@emcbc.doe.gov

Bill Wilborn
EM NV Deputy Program Manager, Operations
Department of Energy
Environmental Management Nevada Program
100 N. City Parkway, Suite #1750
Las Vegas, NV 89106
Bill.Wilborn@emcbc.doe.gov

Kevin Cabble
Soils Activity Lead
Department of Energy
Environmental Management Nevada Program
100 N. City Parkway, Suite #1750
Las Vegas, NV 89106
Kevin.Cabble@emcbc.doe.gov

Tiffany Gamero
Long-Term Monitoring Activity Lead
Department of Energy
Environmental Management Nevada Program
100 N. City Parkway, Suite #1750
Las Vegas, NV 89106
Tiffany.Gamero@emcbc.doe.gov

Jeff Berger
Nevada Field Office
National Nuclear Security Administration
U.S. Department of Energy
P.O. Box 98518
Las Vegas, NV 89193-8518
Jeff.Berger@nnsa.doe.gov

Patrick Sawyer
DOE Program Manager
Division of Hydrologic Sciences
Desert Research Institute
755 E. Flamingo Road
Las Vegas, NV 89119-7363
Patrick.Sawyer@dri.edu

Julianne Miller
DOE Soils Activity Manager
Division of Hydrologic Sciences
Desert Research Institute
755 E. Flamingo Road
Las Vegas, NV 89119-7363
Julie.Miller@dri.edu

Pat Matthews
Navarro, LLC
Department of Energy
Environmental Management Nevada Program
100 N. City Parkway, Suite #1750
Las Vegas, NV 89106
Patrick.Matthews@emnv.doe.gov

Alissa Silva
Mission Support and Test Services (MSTS)
P.O. Box 98521
M/S NLV082
Las Vegas, NV 89193-8521
silvasaj@nv.doe.gov

Nevada State Library and Archives
State Publications
100 North Stewart Street
Carson City, NV 89701-4285
NSLstatepubs@admin.nv.gov

Archives Getchell Library
University of Nevada, Reno
1664 N. Virginia St.
Reno, NV 89557
tradniecki@unr.edu

DeLaMare Library 262
University of Nevada, Reno
1664 N. Virginia St.
Reno, NV 89557
tradniecki@unr.edu

Document Section, Library
University of Nevada, Las Vegas
4505 Maryland Parkway
Las Vegas, NV 89154
sue.wainscott@unlv.edu

†Library
Southern Nevada Science Center
Desert Research Institute
755 E. Flamingo Road
Las Vegas, NV 89119-7363

‡Theodore Candalino
Nuclear Testing Archive
Mission Support and Test Services (MSTS)
Contractor for the Nevada National Security Site
Mail Stop 400
PO Box 98521
Las Vegas, NV 89193-8521
candaltg@nv.doe.gov
(2 CDs)

∫Office of Scientific and Technical Information
U.S. Department of Energy
P.O. Box 62
Oak Ridge, TN 37831-9939

***All on distribution list receive one electronic PDF copy, unless otherwise noted.***

---

† 2 paper copies; CD with pdf (from which to print)
‡ compact disc only
∫ electronic copy (pdf) only